Characterizing various aspects of the male genital tract barrier function and immunity

Dr. Cosnet Lerato Rametse

This thesis is submitted to the University of Cape Town in fulfilment of the requirements for the degree

DOCTOR OF PHILOSOPHY

In

Clinical Sciences and Immunology

In the Division of Immunology, Department of Pathology, Faculty of Health Sciences

Supervisor(s)	Professor M Clive Gray
	Professor Mashiko Setshedi (administrative)
Co-Supervisor	Dr Heather B Jaspan
Date of submission	

University of Cape Town

The copyright of this thesis vests in the author. No quotation from it or information derived from it is to be published without full acknowledgement of the source. The thesis is to be used for private study or non-commercial research purposes only.

Published by the University of Cape Town (UCT) in terms of the non-exclusive license granted to UCT by the author.

University of Cape Town

Plagiarism declaration

I, Dr. Cosnet Lerato Rametse, hereby declare that the work on which this dissertation is based is my original work (except where acknowledgements indicate otherwise) and that neither the whole work nor any part of it has been, is being, or is to be submitted for another degree in this or any other university.

I empower the university to reproduce for the purpose of research either the whole or any portion of the contents in any manner whatsoever.

Signature:
Date:

Inclusion of publications

I confirm that I have been granted permission by the University of Cape Town's Doctoral Degrees Board to include the following publication(s) in my PhD thesis, and where co-authorships are involved, my co-authors have agreed that I may include the publication(s):

1. **Ramese, CL et al.**, "A randomized clinical trial of on-demand oral pre-exposure prophylaxis does not modulate lymphoid/myeloid HIV target cell density in the foreskin." AIDS. 2023 Sep 1;37(11):1651-1659. doi: 10.1097/QAD.0000000000003619. Epub 2023 Jun 6. PMID: 37289572.

Signature:
Date:
Student Name: Dr Cosnet Lerato Rametse
Student Number: RMTCOS001

Key Presentations and seminars

1. **LINDAU NOBEL LAUREATE MEETING**. (Medicine & Physiology) June 2023. Next Generation Sessions Young Scientist Oral Presentation: Asymptomatic STIs and penile immune changes.
2. **GLOBAL YOUNG SCIENTISTS SUMMIT (GYSS) 2023 PARTICIPANT** (SINGAPORE 17-20 JAN 2023). Oral presentation: What renders the human penis susceptible to HIV?
3. **AIDS 2022 Conference**. Poster Presentation; Penile Barrier Integrity and a Mechanistic Search for the Effectiveness of Medical Male Circumcision in Preventing HIV Acquisition
4. **The Inaugural South African Clinicians Scientists Conference.** February 2021 Oral presentation: Barrier integrity & Understanding HIV susceptibility in the penis: A mechanistic search for medical male circumcision
5. **Conference on Retroviruses and Opportunistic Infections (CROI) International**. March 2020. Male Medical circumcision improves barrier integrity in various penile site: understanding HIV susceptibility in Poster presentation: Medical male circumcision disciplines the penis: understanding HIV Susceptibility
6. **Immunology Seminar, Institute Of Infectious Disease and Molecular Medicine (IDM**), Wed, 27 Nov 2019.Seminar title: The effect of asymptomatic sexually transmitted infections on HIV susceptibility in the penis
7. Annal 2019-2022 **Early Career Scientist Conference (South African Medical Research Council)** Oral presentation.

TABLE OF CONTENT

Plagiarism declaration 2

Inclusion of publications 2

Key Presentations and seminars 3

Acknowledgments 6

List of abbreviations 8

List of figures 9

List of tables 10

Abstract 12

CHAPTER 1 16

Sexually Transmitted Infections, Medical Male Circumcision, and the penile tract immunity 16

1. Epidemiology of STIs and HIV in men 17

2. Medical Male Circumcision as an HIV prevention strategy 29

3. Innate defense of the penile tract 31

4. Adaptive immune Defense of the penile tract 41

5. PrEP in males as an HIV prevention strategy 43

6. Problem statement 45

CHAPTER 2 47

Prevalence of asymptomatic sexually transmitted infections among men attending MMC recruitment site clinics 47

CHAPTER 3 64

Measurements of in vivo and ex vivo Penile Epithelial Barrier Function 64

CHAPTER 4 92

Histopathology and immune cell measurements in foreskins from asymptomatic STI positive and negative male participants 92

CHAPTER 5 113

Spatial Transcriptomic Profiling of foreskin Epithelial and Macrophage cells in STI positive and negative participants 113

CHAPTER 6 149

The impact of Pre-exposure Prophylaxis on immune cells in foreskins from HIV uninfected participants 149

CHAPTER 7 ..... *168*
Thesis Summary and Discussion *168*
REFERENCE LIST *174*
APPENDIX I *205*
APPENDIX II *223*
APPENDIX III *230*
APPENDIX IV *232*

Acknowledgments

This PhD is a true product of "it takes a village", obtaining it would not have been possible without many people. Firstly, I would like to thank my supervisor Professor Clive Gray. Where do I even begin? For me, you have been the definition of a "wholesome" mentor. Thank you for your dedication and intentional efforts towards my PhD journey. For teaching me the principles and heart of science, for challenging me to be my best always (as cliché as it may sound), and for engaging my curious mind. Thank you for creating a space for me in this journey, to feel safe enough to try, lead and manage, and persevere. I have also gone through life-threatening health challenges at some point and your support will forever be unmatched. Thank you. Dr Heather Jaspan, thank you for your availability. My thesis writing journey would have been incomplete without your presence. I have learned a lot from you in the process, thank you. To my mentor Prof Setsthedi, your guidance and mentorship throughout this journey (literally from day one), kept me together in many instances, thank you.

To the men who opted to participate in this study, from the local circumcision clinics, especially through Jhpiego NGO, this would not have been possible without your voluntary participation. On that note, to Michael Mziwoxolo Mndini, our study clinical coordinator, this recruitment would not have been as successful without your pivotal role. It has been such a delight working with you. To our study collaborators from Northwestern University, Professor Tom Hope, Gianguido C Cianci, Michael D McRaven, and Ramon Redondo. Michael, you have been extremely supportive whenever I needed to troubleshoot the Delta microscope, thank you. Ramon, thank you for assisting with the meter data analysis. Kyle O'hagan, thank you for orientating and teaching me how to use the microscope for the imaging.

Thank you to: National Health Laboratory Johannesburg for diligently running the STI PCR screenings for us throughout the years. Mikateko Mazinu and Nomonde Gwebushe at the MRC for assisting with the STI data analysis. Lerato Hlatshwayo for your support with the STI data analysis. Centre for Proteomic and Genomic Research (CPGR), for allowing me to personally use their facilities for my PCR work, with key support from Aubrey Shoko. Prof Riyaadh Roberts, specialist Anatomical Pathologist at NHLS UCT, who examined the H&E slides. Dr Nyaradzo Chigorimbo-Tsikiwa for teaching me the crawl assay for my cell isolation work and Dr Sonwabile Dzanibe for guiding me through flow cytometry analysis. Prof Chakraborty Rana, for hosting me in his lab at the Mayo Clinic to learn Digital Spatial Profiling (DSP) and

to complete that aspect of my PhD whilst there. Thanks to Dr Lal Sohan and Elizabeth Enninga for teaching me how to use the DSP. Elise Sintim-Aboagye and Sheila Farnan for making my trip to the Rana lab so worthwhile, and for supporting and assisting me through the lab work I did there for the DSP chapter! Cheers to life-long friendship ladies! Dr Jerid Robinson, from Nanostring Technologies, for your immense support and guidance throughout my DSP project and especially through troubleshooting. Thank you to Huy Quach and Kalonji Abondance for assisting with and guiding me through the DSP data analysis. Finally, for CHAPS clinical trial work, all the co-authors are listed in the manuscript, but thank you to Asiphe Besethi and Bongani Motaung for assisting in the lab and with image data analysis. Yacoeb Ganief, our clinical samples freezer manager, your great organization skills and willingness to help and go the extra mile was appreciated. Berenice Alinde, thank you for being such a mom of a lab-manager. You kept the lab in check and thus made experiments run smoothly. Thank you for the moral support as well.

To my PhD office gang, Claire, Saori, Tatenda, Millicent, Rachel, Adijat and Malika, the office has been such an important part of my journey. The laughs we shared, and encouragement we gave each other! To my friends, Jarryd Lunn, Matthew Amoni, Kamogelo Lebeko, Oyama Mjele-Diaho and Richmond, thank you for your support.

To my family: my mother Yvonne Rametse, what a rock you continue to be. My husband, Mpumelelo Sangweni, thank you for your support and patience with me. Thank you to the two of you for being my cheerleaders and strength in the hard times. Finally, to my newborn, first child, thesis baby, Enhle Sangweni, mommy wants to thank you for being so kind to me throughout this thesis writing journey. You are exactly 3 weeks old today as I submit this and I couldn’t be prouder of us my sweetheart. I dedicate this thesis to the three of you! I dedicate this thesis to the three of you! Finally, to God, my good and faithful shepherd. I am that I am because of Your grace and love. Ebenezer!

List of abbreviations

NGU nongonococcal urethritis

PID pelvic inflammatory disease

EB elementary body

RB reticulate body

MG *Mycoplasma genitalium*

TV *Trichomonas vaginalis*

VMMC Voluntary medical male circumcision

SC Stratum Corneum

TJs Tight Junctions

AJs adherens junction

SPRR small proline-rich proteins

TEWL Transepithelial water loss

SCH Stratum corneum hydration

CCR5 C-C chemokine receptor type 5

CD4 Clusters of differentiation 4

CD8 Clusters of differentiation 8

PrEP Pre-exposure prophylaxis

STI Sexually transmitted infections

DEGs Differentially expressed gene

PanCK Pancytokeratin

CD68 Clusters of differentiation 68

RPL ribosomal proteins

List of figures

Figure 1. 1 Biphasic life cycle of C. trachomatis in an epithelial cell. 21
Figure 1. 2 The foreskin histoanatomy.....34
Figure 1. 3 Schematic structures of major tight junction proteins. 37

Figure 3. 1 Mechanics of Skin Hydration & Meter machines measurement principles. 68
Figure 3. 2Barrier function meter measurements in males in South Africa (n=203) before MMC (normalised by hip) in various penile anatomical sites.....79
Figure 3. 3 Durable changes in penile barrier integrity months post-circumcision. 81
Figure 3. 4 aSTI infected men have increased SC moisture in their penile glans in vivo. 82
Figure 3. 5 Inner vs outer foreskin epithelial barrier proteins gene expressions in STI negative men.....84

Figure 3.6. A A Heatmap of epithelial barrier protein mRNA expression by aSTI status. 85
Figure 3.6. B Epithelial barrier protein mRNA expression by aSTI status.....86

Figure 3.7 1 Impact of aSTI status on differential epithelial barrier proteins.....86

Figure 4. 1Photomicrograph of hematoxylin and eosin-stained foreskin tissues with and without aSTIs. 100
Figure 4. 2 Photomicrograph of hematoxylin and eosin-stained foreskin. 105
Figure 4. 3 Foreskin lymphocyte infiltrate cells are predominantly CD4 and CD8 cells in aSTI negative men. 108

Figure 5. 1 Slide preparation for DSP analysis. Showing tissue placement and orientation per slide. (*Created by CL Rametse*) 120
Figure 5. 2 Spatially Resolved Transcriptomics with NanoString GeoMX Profiler.....123
Figure 5. 3 Differentially expressed genes (DEGs) in Foreskin CD68 cells (Macrophages) using NanoString GeoMX spatial transcriptomic profiling. 127
Figure 5. 4 Identification of differentially expressed genes and associated biological processes in macrophages of the inner and outer foreskin tissues of men infected versus uninfected with asymptomatic chlamydia infection. 130

Figure 5. 5 Identification of differentially expressed genes and associated biological processes in macrophages of the inner and outer foreskin tissues of men infected versus uninfected with asymptomatic chlamydia infection. 132
Figure 5. 6 Differentially expressed genes (DEGs) in Foreskin PanCK cells (Epithelial) using NanoString GeoMX spatial transcriptomic profiling. 134
Figure 5. 7 Identification of differentially expressed genes and associated biological processes in Epithelial cells of the inner and outer foreskin tissues of men infected versus uninfected with asymptomatic chlamydia infection. 136
Figure 5. 8 Identification of differentially expressed genes and associated biological processes in epithelial cells of the inner and outer foreskin tissues of men infected versus uninfected with asymptomatic chlamydia infection. (A and B). 139

Figure 5.9. A HIV-1 infection associated genes differential expression in macrophages of the inner and outer foreskin tissues of men infected versus uninfected with asymptomatic chlamydia infection. 141
Figure 5.9. B HIV-1 infection-associated genes differential expression in macrophages of the inner and outer foreskin tissues of men infected versus uninfected with asymptomatic chlamydia infection. 142

Figure 6. 1 Density of $CD4^+CCR5^+$ and CCR5 on $CD4^+$ cells in foreskins from the participants of the CHAPS trial. 157
Figure 6. 2 Density of $CD1a^+$ and claudin-1 expression in the foreskins of men in different trial arms. 161
Figure 6. 3 Forest plots of correlations of TVF-DP, FTC-TP and p24 (high and low dose) with log10 cell densities, distance from the epidermis, % claudin and eCD1a/iCD1a ratio. 165

Fgure 7. 1 Thesis results summary: *in vivo* and *ex vivo* molecular penile tract responses to asymptomatic STIs 172

List of tables

Table 2. 1 Socio-demographic characteristics of young men tested for Chlamydia trachomatis, Neisseria gonorrhea, Trichomonas vaginalis and Mycoplasm genitalium at two medical circumcision clinics in the Western Cape (WC), South Africa (n=320). 52

Table 2. 2 STI prevalence by Clinical site. 55

Table 2.3 0-a Patterns of STI infections among South African young men. 55
Table 2.3 0-b Patterns of STI infections among South African young men. 56

Table 2.4. Factors associated with prevalent STI (either Chlamydia trachomatis, Neisseria gonorrhoeae, Trichomonas vaginalis or Mycoplasm genitalium) (Univariate analysis). 58
Table 2. 5. Multivariate analysis of factors associated with prevalent STIs. 60

Table 4. 1 The prevalence and intensity of immune cell infiltration in the foreskins of STI^+ and STI^- men. 99
Table 4. 2 Immune cell density in the different locations in the foreskin tissues of STI^+ and STI^- men.....102
Table 4. 3 The prevalence of spongiosis in the foreskin tissues of $aSTI^+$ and $aSTI^-$ men.....104

Table 6. 1 Comparisons between trial arms for $CD4^+CCR5^+$, $CD1a^+$ cells, claudin-1 expression and ratio of eCD1a/iCD1a. 162

Abstract
Background

There has been significant progress in the management of Human Immunodeficiency Virus-1 (HIV-1) infection and prevention globally since the availability of antiretroviral drugs (ARVs). Due to a combination of ARV availability, increased HIV testing, and the introduction of a range of HIV prevention tools, HIV mortality in Africa has declined. However, HIV remains a global burden that still needs urgent attention, as there is still a high rate of new HIV infections globally and in South Africa. Effective control of this epidemic requires a complete understanding of the mechanisms of transmission and acquisition of this virus. HIV acquisition in men through penile exposure is one of the least studied modes of HIV transmission. Voluntary medical male circumcision (VMMC) is associated with a 60% reduced risk of HIV acquisition through heterosexual intercourse. However, uncircumcised men comprise approximately 70% of the male population worldwide, implying that although an effective prevention method has been shown, many men remain uncircumcised. Furthermore, it is not well understood why there remains a group of circumcised males who remain susceptible to infection. Understanding the immune milieu in the male genital tract may reveal additional HIV susceptibility mechanisms and factors that can be used as a foundation for alternative HIV preventative strategies.

This PhD thesis examines barrier function, the density of HIV target cells and various expressed epithelial barrier proteins and genes in different anatomical sites of the intact penis before VMMC and in foreskin tissue after surgical removal. How these measurements are impacted by asymptomatic STIs is explored. The central hypothesis is that the inner foreskin has a relatively reduced barrier function compared to the other penile sites, which is further reduced by the presence of asymptomatic STIs (aSTIs).

To test this hypothesis, the following aims were explored:

1. To describe the prevalence of aSTIs, including *Chlamydia trachomatis, Neisseria gonorrhoeae, Trichomonas vaginalis* and *Mycoplasma genitalium* at two medical circumcision clinics in the Western Cape, South Africa.
2. To characterize *in vivo* and *ex vivo* penile barrier function, represented by transepithelial water loss (TEWL), surface hydration and water content in the glans, foreskin and shaft and further examine how this is impacted by common aSTI and VMMC.
3. To evaluate inflammatory inner and outer foreskin changes associated with aSTIs.

4. To compare spatial transcriptomic patterns in macrophages and epithelial cells between the inner and outer foreskin in the presence of an aSTI.
5. To examine the impact of in vivo Oral Pre-Exposure Prophylaxis (PrEP) on claudin-1 expression and lymphoid/myeloid cells in the foreskin (Published manuscript chapter)

Methods

Male volunteers who were undergoing VMMC were recruited from community clinics in Retreat, TC-Newman and Mitchells Plain, Western Cape. Multiplex PCR testing was performed on first-pass urine samples collected from 320 HIV-negative male participants to screen for the prevalence of common curable aSTIs: *Chlamydia trachomatis,* Neisseria *gonorrhoeae, Trichomonas vaginalis* and *Mycoplasma genitalium.* Penile *in vivo* hydration (n=203) was measured using vapometers, moisture meters SC and D, epi-D to measure proxy barrier function in the absence and presence of an aSTI. Longitudinal measurements were made at 2, 12 (n=28) and 24 weeks (n=16) after VMMC. Foreskin (FS) tissue was collected from a subset of 96 males and examined using histological scoring and gene expression using RT-qPCR of Filaggrin, Involucrin, E-cadherin and Claudin. Spatially resolved gene expression in CD68+ macrophages and pan-cytokeratin epithelial cells was made from 8 foreskin tissue samples dissected into inner and outer tissue. Using a DeltaVision Elite microscope, the density of CD4+CCR5+, CD1a+ cells, and percent claudin-1 expression were analyzed in 144 male participant foreskin tissue samples from a randomized on-demand pre-exposure prophylactic clinical trial.

Results

The overall prevalence of asymptomatic STIs was 15.9%, where the highest prevalence was Chlamydia (12.2%) followed by *Mycoplasma genitalium* (4.38%,). Marital and educational status were significantly associated with a lower risk of any STI. *In vivo* measurements of the penile glans, inner foreskin and shaft barrier function show that the trans-epithelial water loss (TEWL) of the inner foreskin (median 27.6 g/hr/m^2) and glans (median 22.3 g/hr/m^2) of uncircumcised males was significantly higher compared to the shaft (median 16.2 g/hr/m^2) of the penis ($p<0.0001$). Analysis by aSTI status revealed that in the presence of an aSTI, stratum corneum surface hydration in the penile glans was significantly higher (97.4au vs 52.3au; p=0.038). Six months post-circumcision, TEWL in the glans was significantly decreased (p=0.011) from baseline (pre-VMMC), matching that of the shaft. Histological measurements show that total immune cell density was higher in $aSTI^+$ (n=38) vs aSTI- males (n=58), in the

epidermis (24.6 vs 10.4 cells /m2 p=0.002), papillary dermis (119.9 vs 61.4 cells/m^2, p=0.014) and reticular dermis (13.6 vs 6.5 cells/m^2, p=0.03). These were predominantly lymphocytic infiltrates that were largely in the papillary dermis. Claudin-1 percent expression was significantly decreased in the inner foreskin compared to the outer foreskin in the presence of an aSTI. This was matched by increased penile glans surface hydration in the presence of an aSTI (58.3 vs 105.6 au, p=0.003). Transcriptomic data showed that in the presence of asymptomatic chlamydia infection, macrophages, and epithelial cells of the inner foreskin showed predominant upregulation of immune-associated genes and pathways such as increased HLA-DQA1, HLA-DQB1 and HLA-DRB1, IL7R expression. Whereas the outer foreskin showed significant downregulation in protein synthesis genes. Examining the impact of ARV alone on the on foreskin immune and barrier function markers in a randomized PrEP study, showed no significant difference in the density of $CD4^+CCR5^+$ or $CD1a^+$ cells in foreskins between treatment arms compared with the control arm. Claudin-1 expression was 34% higher (p=0.003) relative to controls in the ARV arm, but after multiple comparisons was no longer statistically significant.

Conclusions

The difference in TEWL between those with and without an aSTI showed that the uncircumcised penis has a lower barrier function compared to the penis after VMMC. Additionally, the presence of an aSTI significantly increased inflammatory cells in the foreskin epidermis and dermis, with most infiltrates localizing within the papillary dermis. This is associated with decreased expression of Claudin in the inner foreskin (hence reduced barrier integrity) and increased moisture in the glans. These findings show that aSTI's alter gene expression in key immunological cells and in epithelia that have implications for potentially elevating the risk of HIV infection in uncircumcised males. This PhD is also the first to show that oral dosage and timing of on-demand PrEP have no effect on the numbers or anatomical location of lymphoid or myeloid HIV target cells in foreskin tissue. Overall, The high burden of chlamydia and concurrent STIs highlights the urgent need to improve the prevention, detection, and appropriate management of sexually-acquired infections in young men as they profoundly impact epithelial integrity and immunological events in the foreskin. Screening of aSTIs should be encouraged among young men.

Impact statement:

The association between urethral aSTIs (i.e., diagnosed in urine) and inflammatory changes in foreskin tissue is novel and an important contribution to the field. The observed changes in foreskin immunology are likely to result in increased susceptibility to HIV and provide evidence for public health policy change, from testing and treating only when symptoms are present to testing and treating all males who are sexually active. The barrier function studies data suggest that the inner foreskin and glans are more permeable than the shaft skin. Additionally, that the inner foreskin has significantly lower mRNA expression of many proteins involved in epithelial barrier function. Together, these data provide support for a novel explanation for how circumcision lowers HIV risk: the inner foreskin and glans of the uncircumcised penis are more permeable, and removal of the foreskin causes changes in the glans epithelium that decreases permeability. These findings could suggest alternative targets for rendering protection against HIV-1 in men in a less invasive way (such as VMMC), this could be through making gels that target the barrier of various penile anatomical sites. Lastly, this project demonstrates that short-term PrEP does not induce inflammation or change claudin-1 expression (a tight junction protein) in the foreskin. This data is important for providing evidence of the safety of using short-term PrEP for HIV prevention in men engaging in insertive sex.

CHAPTER 1

Sexually Transmitted Infections, Medical Male Circumcision, and the penile tract immunity

Table of Contents

1. Epidemiology of STIs and HIV in men 17

1.1 Common STIs 17

1.2 The interaction between STIs and HIV 27

1.3 STIs and HIV prevention trials 28

1.4 What are the gaps in knowledge? 29

2. Medical Male Circumcision as an HIV prevention strategy 29

2.1 The foreskin 30

2.2 What are the gaps in knowledge? 30

3. Innate defense of the penile tract 31

3.1 Innate immune cells – Langerhans cells, dendritic cells 31

3.2 Barrier Function 32

3.2.1 Barrier Proteins 35

3.2.1.1 Filaggrin (FLG) 35

3.2.1.2 Involucrin (IVL) 35

3.2.1.3 Junction Proteins (Tight and Adherens junctions) 36

3.3. What are the gaps in knowledge? 41

4. Adaptive immune Defense of the penile tract 41

4.1 T and B cells 41

4.2 The effect of STIs on foreskin immunity 42

4.3 What are the gaps in knowledge? 43

5. PrEP in males as an HIV prevention strategy 43

5.1 Pre-exposure prophylaxis 43

5.2 What are the gaps in knowledge? 44

6. Problem statement 45

6.1 Impact of STI on penile tract innate and adaptive immunity. 45

6.1.1 Aims and hypothesis 45

6.1.2 Objectives 45

Sexually transmitted infections(STIs) remain a global public health burden because of their adverse effects on reproduction and their bidirectional relation with HIV infection, especially in high endemic regions[1–6]. Apart from spreading acquired pathogens throughout sexually active population, STIs can have a debilitating effect on the individual, if untreated. For example, reproductive tract disease is one such outcome, which includes ectopic pregnancy, pelvic inflammatory disease (PID), chronic pelvic pain in women preterm delivery, hydrosalpinx, and tubal factor infertility (TFI). In men, it can lead to epididymitis, testicular pain, and infertility. Despite variable treatment therapies available to successfully treat diagnosed infections, asymptomatic infections are common[7,8]. Antibiotic interventions are not viable in the absence of obvious symptoms that prompt individuals to visit their primary care provider. The estimated rate of asymptomatic infections is at least 4.3 times higher than the rate of confirmed infections[8,9]. STIs are managed utilizing the syndromic approach in the public health sector of South Africa and other low- and middle-income countries (LMICs) [10]. According to guidelines, this empiric treatment of STIs is based on a cluster of urinary and or vaginal symptoms. This has resulted in either a significant under-treatment of asymptomatic infections or the overtreatment of people with non-specific symptoms[10,11]. Recent surveillance data following the COVID pandemic found a substantial increase in reported STIs , especially Chlamydia and syphilis in the United States between 2020 and 2021[12]. Moreover, research has conclusively shown that women possess a greater inherent susceptibility to acquiring sexually transmitted infections (STIs) and HIV compared to men, with a larger likelihood of transmission from men to women than the other way around. Consequently, there is a global lag in STI surveillance studies in men compared to that in women. The initial part of this chapter outlines some of the most common STIs and forms a backdrop to this PhD thesis.

1. Epidemiology of STIs and HIV in men

1.1 Common STIs

Sexually transmitted diseases (STDs) are the later stages of an STI when the infection progresses to disease. An STD would often be symptomatic, whereas many STIs may show no signs or symptoms. According to the World Health Organization (WHO) STI Report 2022, on a daily basis worldwide, more than 1 million sexually transmitted infections (STIs) are acquired, the majority of which are asymptomatic[13].More than thirty different bacteria, parasites, and viruses are known to be transmitted through sexual contact, including anal, vaginal, and oral sex[14]. Pathogens causing STIs can also be transmitted from mother-to-child during pregnancy and childbirth[15]. The most common STIs are caused by eight main

organisms[13], of which four of these are currently curable: *Treponema pallidum* (syphilis), *Neisseria gonorrhea*, *Chlamydia trachomatis,* and *Trichomonas vaginalis*. Common viral STIs include Human Immunodeficiency Virus (HIV), human papillomavirus (HPV), hepatitis B, and herpes simplex virus (HSV). An estimated 374 million new cases of one of the four curable STIs occur annually [13]. The 2017 Spectrum-STIs (SA) estimates confirmed the high burden of STIs in South Africa based on monitoring data STIs surveillance[16]. It was estimated that the prevalence of chlamydia among South African women was 14.7% (95% CI, 9.9-21%) and 6% in men (95%CI 3.8-10.4%). The overall prevalence for chlamydia (10.3%) and gonorrhoea (5.1%) are still among the highest in the world[17]. A combined total of 4.5 million new gonorrhoea infections were estimated to occur in 2017 (2.3 in women and 2.4 in men), no notable disparity in the occurrence rates between both sexes. It was estimated that there were around 5.7 million new chlamydia infections in both men and women, with men being nearly twice as likely to present with a new infection (2:1), despite the fact that chlamydia and gonorrhea are both more prevalent in women (14.7%)[17].

There has been significant progress in the management of HIV infection and prevention globally since the enrolment of ARVs. Due to a combination of antiretroviral (ARV) availability, increased HIV testing, and the introduction of a range of HIV prevention tools, HIV incidence and mortality in Africa has declined[18–22]. However, HIV remains a global burden that still needs urgent attention, there is still a high rate of new HIV infection globally and in South Africa. In 2021, 38.4 million individuals worldwide were living with HIV, of those, 20.6 million, are from Eastern and Southern Africa[18]. While the rates of new HIV infections have been recently reported to have been reduced by 54% since the peak in 1996 globally, in 2021, around 1.5 million people were newly infected with HIV[18]. In South Africa, the number of new HIV infections in 2021 (198 311) compared to 2010 (401 608), was reduced by 51%. However, South Africa failed to meet the 2010 global target of a 75% reduction in HIV cases by 2020-22. To meet the international goal of eradicating AIDS by 2030, South Africa must reduce the annual incidence of new HIV infections from 189,000 in 2022 to 40,000[18,23].

Types of STIs and Pathophysiology

There are three major causes of STIs, these are viral, parasitic and bacterial. Viral genomes can be dsDNA, ssDNA, or RNA, and must infect a host to survive and replicate. These include human papilloma virus (genital warts), Herpes A, B, C and D, Herpes type I and II, HIV, and Epstein Bar Virus (mononucleosis). STIs caused by parasites, which are organisms that live in

or on a host organism and live off the host, include trichomoniasis and pubic lice[18,24,25]. Bacteria are single-celled microorganisms. They can live in many different niches in the human body[18,24,25]. Examples include *Chlamydia, Mycoplasma genitalium*, gonorrhoea and syphilis

Bacterial STIs:

Chlamydia Trachomatis

Chlamydia is the leading cause of bacterial STIs globally. It is a gram-negative strict intracellular bacteria with a unique developmental biphasic cycle that infects genital, ocular, and respiratory tissues[26]. Strains are classified into three biovars and are further subtyped by serovar. *15 serovars (genovars) of C. trachomatis* are discernible according to antigenic variation in the main outer membrane protein (MOMP), which is encoded by ompA. Serovars D-K are frequently linked to urogenital infections, whereas serovars A-C are associated with trachoma. Trachoma biovar is the predominant bacterium responsible for non-congenital blindness in developing countries, while genital tract biovar (serovars D–K) is the most widely distributed sexually transmitted organism[27,28]. The majority of infections caused by various bacterial STIs are asymptomatic. In the case of chlamydia, symptomatic infections occur in only 11%–33% of men and 6%–17% of women[29–31]. When present, symptoms of a genital infection typically manifest one to three weeks following exposure. Abnormal vaginal discharge, pain during intercourse, lower abdominal pain, and post-coital and intermenstrual hemorrhage are all possible symptoms in females[32–34]. Additionally, the urethra can become infected with *C. trachomatis,* and certain individuals may exhibit indications of a urinary tract infection, such as increased frequency and dysuria. The infection may persist for years if left untreated[32]. 15%–40% of infections that affect women progress to the upper genital tract, where they can cause ectopic pregnancy, infertility, and pelvic inflammatory disease (PID), among other severe complications[35,36]. Although not widely accepted , long-term complication of *C. trachomatis* infection can also lead to cancer, primarily fallopian tube carcinomas in patients with PID[36–38]. *C. trachomatis* is the most common cause of nongonococcal urethritis (NGU) in men[35,36]. Symptoms may present with a watery/mucoid urethral discharge with dysuria. Discharge may be clear or scant or only be observed after milking the urethra[37]. Inflammation of the testes and epididymis may result from a *C. trachomatis infection,* which is one of the most prevalent causes of epididymitis in sexually active men younger than 35 years old. Controversy surrounds the possibility that this infection could result in chronic prostatitis, a complication that could have an adverse effect on male infertility [39]. The rate of *C. trachomatis* infection in young women can be predicted by a number of factors, such as smoking and related

indicators of socioeconomic status, having a new sex partner or concurrent partnerships, being single, bacterial vaginosis, having other STIs like gonorrhea, and having carcinogenic human papillomavirus[40–44]. Finally, *C. trachomatis* is the endemic cause of trachoma, a prominent cause of avoidable blindness worldwide, primarily in the Middle East and Africa[13,45]. In this case it is commonly spread through personal contact or by flies. It can also lead to neonatal conjunctivitis and pneumonia in newborns [46].

Pathogenesis

The life cycle of *C. trachomatis* consists of two distinct phases, as demonstrated in Figure 1.1 : the extracellular phase, characterized by the presence of the elementary body (EB), which is infectious but inactive, and the intracellular phase, characterized by the presence of the reticulate body (RB), which is non-infectious yet responsible for reproduction.[47]. Upon entering the host cell, the infectious elementary body (EB) becomes confined within a modified membrane-bound inclusion. There, it undergoes decondensation, transforming into the reticulate body (RB), which does not enable infectious replication. By commandeering host organelles and metabolites, *C. trachomatis* exploits the host cell from this particular compartment[48–50]. The RB can redifferentiate into the infectious EB form and extrude or lyse from epithelial host cells for dissemination two to three days after infection. While epithelial and endothelial cells are the optimal host for human pathogenic C. trachomatis replication, these cells remain in direct interaction with phagocytic cells such as macrophages, which are responsible for eliminating particles from tissues, including microorganisms and damaged cells[51]. *C. trachomatis* that has been liberated from their epithelial host cells are subsequently ingested by macrophages, a process that could potentially result in various ramifications. The phagolysosome has the potential to either eliminate the bacteria or, if it inhibits their maturation, allow them to survive, persist, or replicate. Chlamydia's replication failure is contingent upon its utilization of host cell machinery throughout invasion, formation of inclusions, and development. This, however, activates pro-inflammatory signaling pathways that facilitate the infiltration of innate cells via the release of cytokines and chemokines. A subgroup of women who have ascending infection develop tubal occlusion due to extensive immunopathology and fibrosis [49].

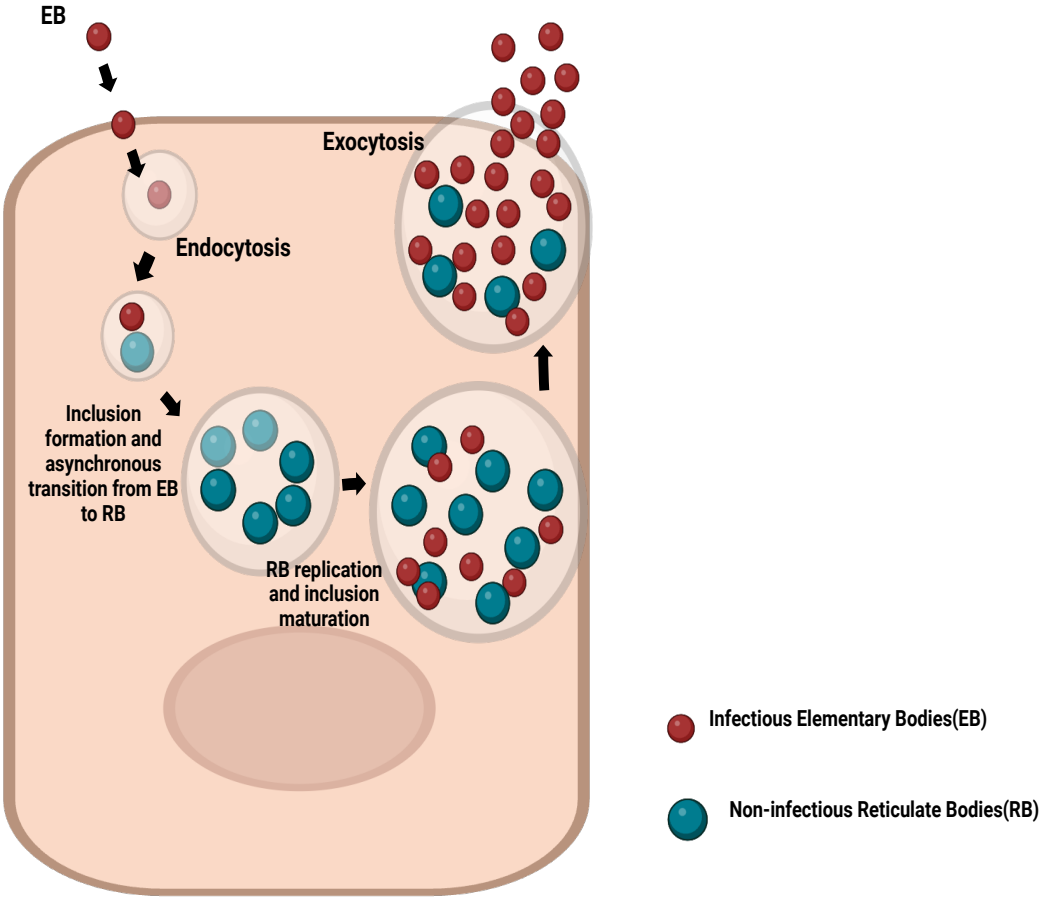

Figure 1. 1 Biphasic life cycle of C. trachomatis in an epithelial cell.

Endocytosis transports the infectious form of *C. trachomatis*, the elementary body (EB, shown by the red circles), into the host cell. The EB undergoes a conversion upon entrance into the on-infectious reticulate body (RB, shown by the blue circles), which is metabolically active. The RB then replicates within a vacuolar compartment known as the inclusion. RBs revert to EBs as the developmental cycle nears completion, thereby inducing host cell lysis and infectious EB discharge into the extracellular environment. EBs subsequently proceed to invade additional host cells[28]. (*Created with BioRender.com by CL Rametse* on Biorender.com)

Treatment

Current antibiotics available and effective in treating *C. trachomatis* infections act intracellularly. In nonpregnant adolescents and adults to treat uncomplicated genital infections the 2021 CDC guidelines currently highly recommends doxycycline 100mg twice daily for a week or azithromycin as an alternative in a single dose or over four days[24]. These drugs target protein biosynthesis by interacting with ribosomal units. Azithromycin is the preferred initial option for treating pregnant women, but amoxicillin can be used as an alternative[24] . It is

important to assess, examine, and provide medical care for sexual partners. Conducting a test before 3-4 weeks after finishing therapy may not yield accurate results due to the presence of lingering nucleic acids from the bacterium. Treatment typically eliminates the infection but does not repair any pre-existing tissue damage caused by inflammation[24]. For over two decades, developed nations have implemented public health strategies that promote the use of screening, treatment, and barrier contraception. However, in South Africa and most low-income countries, syndromic management remains the standard approach, meaning there is no active screening for chlamydia even in those who are asymptomatic.

Neisseria gonorrhoeae

Gonorrhoea is an STI caused by the bacterium *Neisseria gonorrhoeae.* This is the second most common cause of bacterial STIs globally, following chlamydia. In 2020, there were 82.4 million new gonorrhoea infections globally as estimated by the WHO model[25]. Locally (SA), the overall combined prevalence of gonorrhoea in women and men between ages 15-47 years was 5.1% , with 2.3 million new cases in women and 2.2 million in men[17]. The urogenital tract, oropharynx, rectum, or conjunctiva are all affected by *N. gonorrhoeae,* and recurrences of the infection are frequent [52]. Although urogenital infections, particularly in women, frequently manifest without symptoms, *N. gonorrhoeae* is linked to significant morbidity regardless of the presence of symptoms[52.] Additionally, infection during pregnancy is linked to low birth weight and potentially blinding neonatal conjunctivitis[87,88]. *N. gonorrhoeae* has the potential to induce epididymitis in males [52]. Most occurrences of rectal and pharyngeal N. gonorrhoeae are asymptomatic and are common among MSM, but they can also occur in women and, in the case of pharyngeal infection, in men who only have intercourse with women[53]. *N. gonorrhoeae* contributes to the spread of human immunodeficiency virus (HIV) transmission[54]. Globally, gonorrhea is significantly underdiagnosed and underreported[55]. Greater than half of sexually transmitted infections (STIs) remain unidentified or unreported, even in high-income economies where STI surveillance systems are firmly established. Like other STIs, *N. gonorrhoeae* disproportionately impacts young adult populations. Based on its susceptibility to death by complement activation, it is categorized as either serum-sensitive or serum-resistant It is possible for strains that are resistant to serum to spread infection widely within the infected[56].

Pathogenesis

The infection caused by *N. gonorrhoeae* begins when the gonococci adhere to epithelial cells

and then invade the surrounding cells. It possesses several surface proteins that enable attachment. *N. gonorrhoeae* employ pili to start attachment to epithelial cells. These are filamentous projections that cover the surface of bacteria. The bacteria's capacity to extend and withdraw enables them to adhere to surfaces from a distance and approach the epithelial cells, facilitating cellular invasion. Pili also serve the functions of locomotion and defense.[57]. Additional surface proteins that participate in cellular attachment are lipooligosaccharide (LOS) and opacity-associated protein (Opa). It is probable that LOS causes transmission from males to uninfected sexual partners by attaching to sperm cells[57]. In the process of invading cervical epithelium, bacterial cells engage in interaction with the host cell. Bacterial cells invade the cervical epithelium through the interaction of bacterial cells with complement receptor type 3 (CR3)53 on the host cell.[57]. This communication is initiated by the binding of pili to CR3. Actin in the host cell undergoes significant reorganization as a result, giving rise to pronounced protrusion known as ruffles. Gonococci can then infiltrate host cells through ruffling in the form of giant vacuoles, or macropinosomes, and multiply inside of infected cells[57]. To thwart host innate and adaptive immunity, *N. gonorrhoeae* has developed a variety of defense strategies[56,57]. Though widespread infection is possible*, N. gonorrhoeae* causes localized infection at the anatomic site of inoculation, which is usually the eye conjunctiva or the pharynx in neonates and the urethra, cervix, mouth, or anus in adults.

Treatment

Male and female urogenital N. gonorrhoeae infections are typically treated with a solitary intramuscular or intravenous administration of 500 mg ceftriaxone[58]. In cases where chlamydial infection remains unruled, chlamydia treatment is administered in conjunction with doxycycline 100 mg orally twice daily for a duration of seven days (unless the patient is pregnant).[59]. Antimicrobial resistance has developed in *N. gonorrhoeae*, which has been the target of treatment ever since sulfonamides were initially employed in the 1930s. Gonococcal isolates with significantly high mean inhibitory concentrations for ceftriaxone have been detected in certain regions of Asia and Europe, leading to reported instances of treatment failures involving ceftriaxone. When suspicion is present, resistance-specific guidelines should be adhered to.

Mycoplasma genitalium

The association between *Mycoplasma genitalium* (MG) and sexually transmitted disease syndromes, such as endometritis, cervicitis, and urethritis in men and women, respectively, is

becoming more widely recognized. MG has been identified in cases of NGU and has been linked to recurrent and/or persistent urethritis [60,61]. The etiology of this condition includes asymptomatic and symptomatic urethritis in males. It accounts for around 15%–20% of non-chlamydial urethritis, 20%–25% of non-chlamydial urethritis, and 40% of persistent or recurrent urethritis[62–64]. Geographic region, as well as the presence of risk factors including ethnicity, youth, HIV-positivity, smoking, and high-risk sexual behavior, influence the prevalence of MG infection. Furthermore, it has been demonstrated to be commonly correlated with co-infection with C. trachomatis, particularly among females.[65]. In men with gonococcal urethritis, MG can also cause an infection, although C. trachomatis is the more prevalent causative agent[64,66–69]. Following NGU64 treatment, MG is now recognized as the predominant organism associated with persistent NGU[67]. Contrary to heterosexual men, the prevalence rates of C. trachomatis and MG are comparatively reduced among men who have sex with men (MSM) who have non-communicable urethritis (NGU), with a greater proportion of idiopathic NGU cases observed in MSM[70]. Additionally, Soni et al[71] discovered that the prevalence of MG was higher among men infected with HIV. Inadequate evidence exists to link MG infection with chronic complications such as prostatitis, epididymitis, or infertility in males. The potential ramifications of asymptomatic MG infection in males remain uncertain[68].

Cervicitis, PID (an emerging primary cause of PID), preterm delivery, spontaneous abortion, and infertility have been linked to MG infection in women, with the risk for these outcomes being approximately doubled among those infected with MG [72]. Globally, MG is not included in the WHO STI spectrum estimations, and screening is not included in the recommended protocols for STI management. MG infection is detected in approximately 1-3.3% of men and women in the general population[73,74]. Geographic location-dependent prevalence estimates for MG in patients attending STI clinics range from 1.9% to 36.5%[70,74]. On account of the fact that MG71,72 is not presently screened for in the majority of routine STI screening programs, it is probable that the prevalence of these infections is underestimated.[74,75]A few recent studies have characterized the epidemiology of MG in SA young adults; In a cohort of young males and females presenting with genital discharge syndrome, the prevalence of MG in males and females was 8.9% and 10.6%, respectively. HIV infection was a significant determinant of testing positive[75]. Another study found the prevalence of MG in young adults with asymptomatic STIs in South Africa to be 9.6% and 3.3%, among females and males respectively[76]. When compared to other sexually transmitted infections (STIs), data regarding the prevalence of MG in South Africa is scarce.

Pathogenesis

There are two core aspects to the pathogenesis underlying MG infection: (1) primary infection and host immunity interplay and (2) persistence and immune evasion. The interaction between primary infection and host immunity involves MG's attachment to the host's epithelial cells. This attachment triggers a rapid inflammatory response through the activation of innate immune sensors, such as Toll-like receptors 2 and 6, which are highly expressed [77]; The binding of these receptors to MG and its lipoproteins leads to the activation of NF-κB and the rapid induction of genes involved in the host's defense mechanisms[77]. Strong chemokines are among these proinflammatory signals, which ultimately lead to the recruitment of leukocytes to the site of the infection[78–80]. Despite the infiltration of neutrophils, the generation of inflammatory mediators, and the induction of local and systemic antibodies, MG is capable of persistently evading the immune responses of the host, resulting in chronic urogenital infections. To illustrate, MG was present for a minimum of seven months in 21% of Kenyan female sex workers and for a maximum of two years in two of these women[81]. In conjunction with the documented durability of MG in mouse models of infection[82], chimpanzees[83], male reproductive tract tissues (MG), and macaques, these investigations suggest that urogenital persistence is prevalent in both male and female reproductive tract tissues, potentially due to phase and antigenic variations of their surface-exposed proteins.[84,85].

Treatment

Antibiotics that target the biosynthesis of cell walls, such as ß-lactams including penicillin and cephalosporins, are rendered ineffective against this organism due to the absence of a cell wall. One-gram doses of azithromycin should not be administered due to the high rates of treatment failures and efficient selection of additional resistance to macrolides [86]. Treatment is recommended to involve two-stage therapy approaches, resistance-guided therapy being the preferred modality. Resistance-guided therapy has been shown to achieve cure rates exceeding 90% and ought to be employed whenever feasible[87,88]. Nevertheless, access to macrolide-resistance testing is necessary. In this methodology, doxycycline is administered as an initial empiric therapy to facilitate organism clearance and reduce the burden of microorganisms. Subsequently, high-dose azithromycin is utilized to treat macrolide-sensitive MG infections[89,90].

Parasitic STIs

Trichomonas vaginalis

Trichomonas vaginalis (TV) is a protozoan parasite that is primarily transmitted through sexual contact and causes trichomoniasis. It inhabits the prostate and urethra of males and the lower genitourinary tract of females. It is a motile organism[91]. It is the most common parasitic sexually STI worldwide[92] and infection is asymptomatic in 85% of women and in 77% of men[91]. The WHO reports that TV in Africa occurs ten times as often in women than in men and infections are estimated to be 42.8 million[93]. It is an important source of reproductive morbidity and a facilitator of HIV transmission and acquisition[94], and thus an important public health problem. TV exhibits a comparable bidirectional correlation with herpes simplex virus II (HSV-2) as it does with HIV-1[94]. The simultaneous presence of T. vaginalis infection and prior occurrences of genital herpes are linked to the release of HSV-2. The presence of T. vaginalis was observed in 4.2% of women who had HSV-2 in their genital secretions, compared to 1.7% of women who did not have detectable HSV-2 (P=0.001) [95]. Moreover, although controversial, there is increasing evidence linking T. vaginalis to cervical neoplasia. A meta-analysis revealed that T. vaginalis was linked to a 1.9-fold increase in the incidence of cervical neoplasia [96]. It is not an illness that needs to be reported, and monitoring is not typically carried out, despite its significance for HIV transmission and human reproductive health. Most women (85%)95 and men (77%)96 who have TV don't have any symptoms. Within six months, one-third of asymptomatic women develop symptoms[97]. Geographic variations exist in the worldwide prevalence of T. vaginalis in expectant mothers. According to recent studies, T. vaginalis prevalence among pregnant HIV-positive women was reported to be 20% in South Africa[98]. Pregnant women in Zimbabwe and South Africa also had high incident infection rates (9.2/100 person-years).100,000[99,100]. A TV infection increases the incidence of PID [93,101,102] and tubal pathology in women by 4.7-fold. The risk of preterm labor is also increased by 1.3-fold in women who are infected with TV[103]. In men, complications may include epididymitis, prostatitis, and infertility[103].

Pathogenesis

Primarily, the squamous epithelium of the genital tract becomes infected by TV. TV replicates via binary fission in the lower female genital tract and the male urethra and prostate. As its sole known host, humans transmit television predominantly through sexual contact. Cytotoxic proteins secreted by the organism destroy the mucosal epithelial lining. The typical vaginal pH usually rise's during an infection[104,105]. In women, an infection may persist for extended

durations, months or even years; in males, it typically lasts for less than ten days[92,105] Research has established a correlation between T. vaginalis and the following conditions: candidiasis, chlamydia, gonorrhea ,herpes simplex virus type-1 and type-2, urethritis, vaginitis, cervicitis, and syphilis [92].

Treatment:

For TV, metronidazole (MTZ) is the preferred treatment option. MTZ, a member of the 5-nitroimidazole drug class, and its related compounds tinidazole (TNZ) and secnidazole are said to have an approximate 95% efficacy rate in the treatment of TV infections[10,106]. The treatment regimen for TV, as recommended by the World Health Organization (WHO) and the Centers for Disease Control and Prevention (CDC) of the United States, consists of MTZ 400–500 mg BID for seven days. An alternative treatment regimen of 2g single dose of MTZ or TNZ is alos considered[10,92].

1.2 The interaction between STIs and HIV

The transmission of HIV is typically characterized by a very low level of efficiency and is ex pected to necessitate numerous instances of exposure in the context of penile-vaginal intercourse[107,108] and fewer exposures for penile-rectal exposure [109,110]. A single penile-vaginal sexual encounter between a partner with HIV and an HIV-negative partner (serodifferent) has a low probability of HIV transmission[107–110]. Prior to the development of antiretroviral therapy (ART), HIV transmission in stable serodifferent couples was documented at 8.2 to 12.0 cases per 100 person-years[111,112]. Several factors could increase the risk of HIV transmission[112,113]. Among the most important risk factors are the “classical STIs,” loosely defined bacterial, viral and parasitic infections that cause genital mucosal inflammation and genital lesions (i.e. ulcers). Wasserheit[114] initially coined the term "epidemiologic synergy" to describe the early emergence of the association between HIV and classical STIs (which induce mucosal inflammation or ulcers[115]. Following this, extensive research has been devoted to elucidating the biological mechanisms by which STIs facilitate HIV transmission [114,116–119], although mechanisms are still not fully understood. Such research studies suggested that STIs serve two crucial functions: to increase the susceptibility of those without HIV and to heighten the infectiousness of those living with HIV[120].

STIs increase genital viral loads of people with HIV.

Various studies have compared HIV genital tract secretions in people living with HIV with or

without concomitant STIs. In both in both semen and vaginal secretions, with various STIs (gonorrhoea[121] and trichomonas[125], CMV and other herpes virus co-infections[122], bacterial vaginosis, and other STI) have been shown to be associated with increased HIV concentrations in the genital secretions[101,123,124.] Elevated levels of HIV detected in genital secretions associated with sexually transmitted infections (STIs) may indicate heightened viral replication, increased exudation of contaminated blood and fluids from ulcerated mucosal epithelium and an influx of infected cells into the genital mucosa[120]. ART prevents secondary HIV transmission independent of STI coinfections, according to a several studies[125–128], however, it does not completely sterilize shedding of the virus in the genital secretions of all women or men on ARV therap[129,130]. HIV-1 RNA can be detected in some males seminal plasma (positive seminal viral load) or female genital tract, even in patients on efficacious ART for more than six months, according to a number of studie[131–138].Such shedding of HIV is increased by STIs even in the face of ARV use[139–142].

STIs increase susceptibility to HIV acquisition

It is well documented by both empirical data and mathematical models that persons with STIs (both symptomatic and asymptomatic) have an increased risk of acquiring HIV[104-106]. Furthermore, ulcerative, as opposed to non-ulcerative STIs, have been demonstrated to have a higher risk factor[107]. The likelihood of HIV transmission is significantly increased by other sexually transmitted diseases (STIs). The high STI prevalence and incidence rates in sub-Saharan Africa[13] are believed to have played a role in the spread of HIV infection.

The increased risk of susceptibility to HIV in the presence of an STI in both males and females is still not fully explained. Most studies have demonstrated an increase in the inflammatory profile within the mucosal site to render it more vulnerable to HIV infection. STIs can induce of inducing an influx of HIV target cells or an increase in the per-cell expression of CCR5 and CD4 receptors[120]. Others have found that the presence of ulcers lowers the barrier to infections[101,123,143]. Little work has been done to investigate mechanisms underlying the increased HIV risk in concomitant asymptomatic(non-ulcerative) STI infections in men.

1.3 STIs and HIV prevention trials

The impact of sexually transmitted infections (STIs) on the transmission of HIV prompted a series of randomized clinical studies aimed at decreasing the occurrence of HIV infection in communities[144–149], in serodifferent couples[150–152] and in individuals[153,154]. Out of the nine

clinical trials, only one in Mwanza, Tanzania reported successful prevention of HIV through the treatment of STIs [144]. The divergent outcomes of these trials have been the subject of extensive analysis[119,120,151,152]. The inability of more aggressive or mass treatment of sexually transmitted infections (STIs) to prevent HIV acquisition at the population level can be primarily attributed to the challenges associated with delivering effective medications to the appropriate individuals at the appropriate time and ensuring that trial participants can adhere to the selected antimicrobial regimens. Chesson and colleagues have posited that the treatment of gonorrhea, chlamydia, and syphilis could potentially serve as a financially viable strategy to mitigate the transmission of HIV [155,156]. As stated previously, mass treatment for STIs did not yield the expected benefits as predicted by these models. The difficulty in treating bacterial and viral STIs is illustrated by these results. The findings of no impact on HIV incidence despite treatment[144] raises the concern that STIs may be an indication of risky behavior and HIV exposure, rather than (or at least to the same extent as) facilitating HIV transmission. There is still a need for additional research examining the relationship between STIs and the transmission and acquisition of HIV.

1.4 What are the gaps in knowledge?

There is limited STIs surveillance in men particularly in low-income countries, hence a lack of population-level incidence data and prevalence. Men comprised 35% of the total population living with HIV in 2022, whereas of the total AIDS-related deaths , men constituted 48% of all deaths during the same time frame[18]. This suggests that there are more men dying from AIDS than those who tested and starting therapy. Thus, this highlights the gap in the reporting and screening of STIs in men as the deaths are disproportionate to the prevalence records. Multiple studies have demonstrated that these sexually transmitted infections (STIs) greatly enhance the likelihood of HIV transmission and acquisition. However, the specific biological mechanisms responsible for this phenomenon, particularly in the male genital tract, remain poorly characterized and understood. Vaccine development has been identified as essential to controlling infections as infection rates are still increasing despite available effective mass treatments for the curable STIs. Understanding how STIs effectively impair or manipulate the host cell's immune system is therefore crucial in making these developments towards a vaccine. Exploring these mechanisms could also provide insight into biomarkers of infection and/or correlates of protective immunity and will provide a rational foundation for the design of a vaccine against common STIs.

2. Medical Male Circumcision as an HIV prevention strategy

Medical penile circumcision has become a valued component of HIV prevention policy in Sub-Saharan Africa[157–159]. This was following randomized controlled clinical trials that showed that VMMC is associated with a 58-60% reduced risk of HIV acquisition through heterosexual intercourse[160–162]. According to randomized-controlled trials, it is clear and significantly evident that circumcision in males decreases female-to-male HIV-1 infection risk, however, there is still conflicting evidence on circumcised male-to-female HIV-1 transmission[163,164]. A trial conducted in Uganda in 2011 regarding male-to-female HIV transmission revealed that male circumcision does not effectively diminish the risk of HIV infection among female partners. In fact, the study showed intercourse with HIV-infected circumcised men increased the risk of viral acquisition in female partners[163]. This was subsequently reviewed vigorously and the timing of intercourse following circumcision was found to be a significant confounder of these findings and the observed increased risk in females was likely due to early intercourse soon after male circumcision[157]. Although not statistically significant, a few other other researchers conducted studies that found that male VMMC decreased transmission in female partners[165,166].

2.1 The foreskin

The penile glans, foreskin, shaft, and urethra are all potential sites of HIV-1 acquisition in men[167]. However, research on HIV-1 in the human penis, specifically in areas other than the foreskin, has been constrained due to the scarcity of penile tissue. It is well documented that the most common mode of transmission is by heterosexual intercourse and that the highest incidence of HIV of any age or sex cohort is amongst women of reproductive age[107,168–171]. Consequently, most research to date has focused on male-to-female HIV transmission and female acquisition, with HIV acquisition in men through penile exposure being one of the least studied aspects of HIV transmission. STIs are acquired predominantly via the penis in heterosexual males, whereas it is largely acquired via the rectal or penile epithelium in MSM [167]. Therefore, due to the availability of the foreskin tissue following the rollout of MMC, the foreskin tissue is currently used as the main site to further understand STI susceptibility, acquisition, and transmission mechanisms and factors within the MGT. Although the foreskin tissue is not the whole penile organ system, this tissue can be used to understand some of the immunological changes associated with the presence of an STI (irrespective of the site of infection).

2.2 What are the gaps in knowledge?

It is evident that VMMC reduces the rate of heterosexual HIV-1 transmission, but the mechanisms remain poorly understood. It is still not known what explains the other 40% remaining risk of HIV acquisition in circumcised males. The current explanations include the fact that circumcision removes highly susceptible penile tissue (the foreskin) due to its characterized relatively increased abundance in HIV-target cells, thinner keratin layer (stratum corneum) in the inner foreskin, and the reduced surface area of HIV-susceptible tissue exposed to HIV, which when intact during sex, could effect in increased local trauma and thus increased HIV-1 acquisition risk[172]. By further exploring these potential mechanisms, this PhD will generate data that may lay the foundation to alternative non-invasive preventative methods, outside circumcision.

3. Innate defense of the penile tract

The foreskin is an extension of the skin that covers the penile shaft (starting at the coronal ridge)[173]. It is a very active immune region of the male genital tract[173]. When the penis is not erect, the outer foreskin, which comprises the proximal half of the foreskin, is exposed to the air. Conversely, the inner foreskin, which comprises the distal half, is positioned against the glans, which encloses an anaerobic sub-preputial space[174]. *Ex vivo*, both the inner and outer foreskin tissues are susceptible to HIV challenge due to their abundance of immune cells; however, explant studies indicate that the inner foreskin is more susceptible to infection[175–178]. DC-SIGN, a C-type lectin expressed by dendritic cells (DCs), has the capability of binding to gp120 and potentially facilitates the translocation of HIV-1 from DCs to CD4+ T cells [179,180]. HIV-1-infected CD4+ T-cells can be selectively captured by macrophages, facilitating infection and efficient virus transfer between cells [181]. Surfaces characteristic of the meatus (the distal end of the penile urethra), fossa navicularis (the opening), and foreskin contain these cells [181,182]. An initial hypothesis postulated that the thinner keratin layer (stratum corneum) in the inner foreskin rendered it more vulnerable to HIV. Nevertheless, subsequent blinded investigations have yielded inconclusive or negligible results regarding the disparity in keratin thickness between the two anatomical sites [178,183–186]. The potential explanation for the higher susceptibility of the inner foreskin to HIV ex vivo could be attributed to the significant variations in immunology and microbiome between the inner and exterior foreskins[187]. These are still not well understood.

3.1 Innate immune cells – Langerhans cells, dendritic cells

The initial line of defense against mucosal pathogens is the epidermal innate immune system, which consists of various constituents such as antimicrobial peptides, pattern recognition

receptors (e.g., toll-like receptors), and inflammatory immune cells (e.g., natural killer (NK) cells and neutrophils). These cells primarily engage in phagocytosis and apoptosis of infected cells, respectively[188,189]. Antigen-presenting cells, such as dendritic cells (DCs), Langerhans cells (LCs), and macrophages, present antigens to lymphocytes to initiate innate and adaptive immune responses, respectively. Macrophages predominate in the healthy foreskin and are predominantly distributed throughout the lamina propria. Epithelial stratification is commonly accompanied by an abundance of immune cells, including specialized antigen-presenting Langerhans cells (LCs[190–193]. LCs, which have been detected in the upper epidermal layers, are hypothesized to be the initial cells to come into contact with HIV during infection[193]. Langerhans cells are present in varying quantities in the foreskin and the remaining penile epithelium. Concerning the composition of foreskin secretions, little is known. Research has been conducted on the secretions of immunoglobulins, TLR, antimicrobial proteins, and proinflammatory cytokines, albeit to a limited extent, in the foreskin and urethral tissues[189,194–197].

3.2 Barrier Function

The external genitalia of people assigned male at birth arises entirely from the urogenital sinus and consists of stratified squamous epithelia. This lining extends from the shaft proximally, to the proximal parts of the urethra, the remainder of the urethra being lined by columnar or transitional epithelial cells. As illustrated in Figure 1.2, the foreskin tissue comprises three principal layers: the epidermis, dermis, and hypodermis. The stratified squamous epithelia that line the epidermal layer will serve as the primary subject of investigation and discussion in this chapter. This stratified squamous epithelium is further sub-stratified into five separate strata[198]. The outermost layer of the skin, known as the stratum corneum, consists of corneocytes, which are fully developed keratinocytes[199]. The stratum corneum (SC) consists of a series of interconnected fibers made up of cross-linked keratin 1, keratin 10, filaggrin, involucrin, cornified envelope proteins, and lipids. These components provide the SC with strength, elasticity, and protection[200]. SC thickness studies have provided contradicting results, some of which have shown differences[185] and most non[186,201,202], between inner and outer foreskin. The papillary dermis is the superficial dermis containing loose, thin collagen fibers with elastic fibers and branching small, capillary vessels[203]. The stratum basale contains keratinocytes that constantly regenerate these cells. A stratum lucidum composed of defunct keratinocytes is a thin, transparent layer. The stratum lucidum is characterized by its translucent appearance due to the presence of eleidin, a transparent intracellular protein rather than keratin within its keratinocytes. A thin layer is situated between the lucidum and stratum basale, the stratum

granulosum. Keratin filaments are bound together by cysteine and histidine-rich granules found in the stratum granulosum of keratinocytes[204]. The stratum basale is comprised of basal keratinocytes, immune cells including Langerhans and T cells, and pigment-producing melanocytes[199,204].

The skin has various immune functions, including protecting the host from pathogen invasion. Utilized components include biomolecules, a complex network of resident immune and non-immune cells as well as skin structures and physical barriers[205]. Critical immune barrier function is predominantly located in the stratum corneum (SC), the uppermost stratum of the epidermis. The epidermis prevents microbial infection, restricts the absorption of substances from the environment, and limits passive water loss from deeper tissues. Consequently, SC preservation is essential for its extraordinary capacity to protect the body from microbial and chemical assaults as well as dehydration[205]. The physical barrier function of the epithelial barrier in the penis is maintained by a stratified epithelial cellular sheet. Four primary components are discernible: The components include: (a) epithelial cells; (b) structural proteins that facilitate the formation of adherens junctions (AJs) and tight junctions (Filaggrin, Loricrin, and Involucrin); (c) epithelial products that are secreted from the cells, including mucus, antimicrobial peptides, and a lipid-rich matrix consisting of ceramides, cholesterol, and free fatty acids (FFAs); and (d) epithelial microbiota[205].

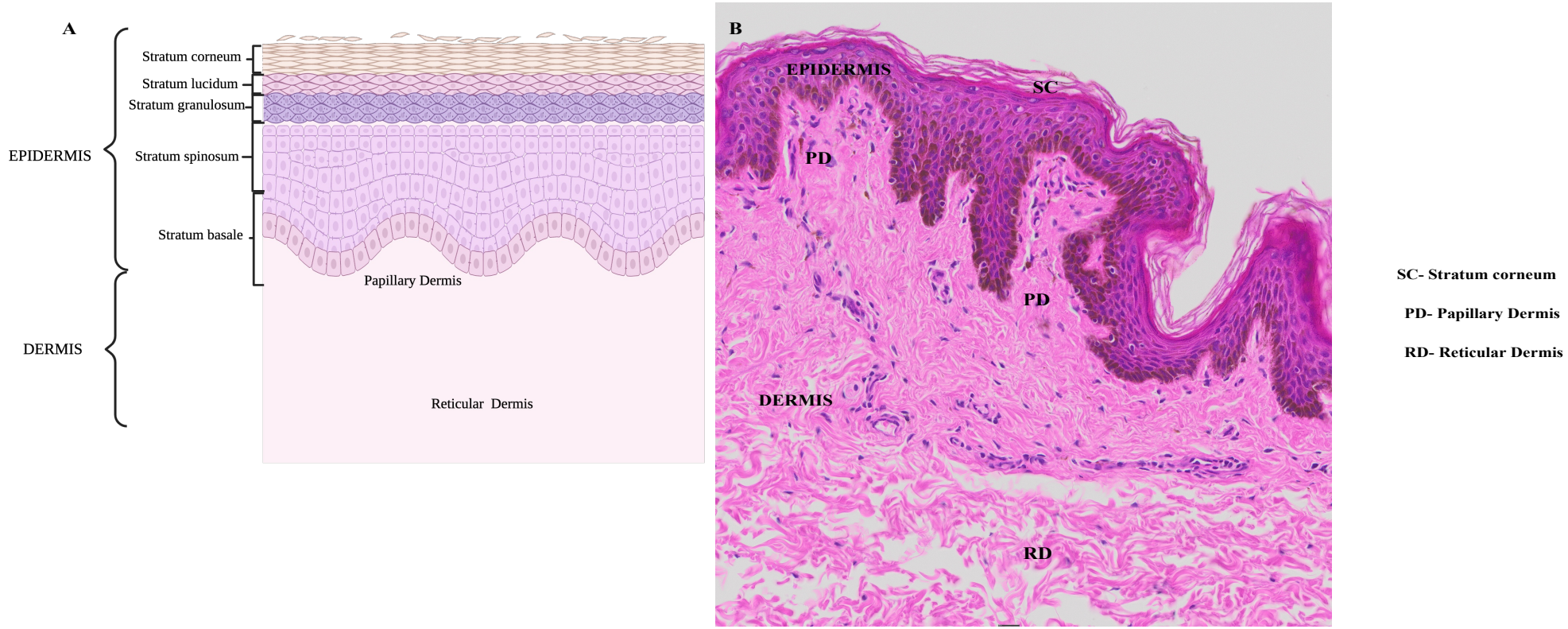

Figure 1. 2 The foreskin histoanatomy.

A visual summary of the various layers of the foreskin by animation showing the strata of the stratified squamous of the top layer, the epidermis (A) which was created *by CL Rametse biorender.com* and (B) a representative image of hematoxylin and eosin-stained outer foreskin from one of the participants in chapter 3 cohort

3.2.1 Barrier Proteins

For the epidermis to function as a stable barrier against the environment, an integrated network of cytoskeletal elements and cellular junctions is required. A limited number of dividing keratinocytes are found in the epithelium, while keratin is expressed in the suprabasal layers of the skin. Keratin is involved in the formation of cornified envelopes, epidermal resistance, and junctional proteins including adherens junctions (AJs), tight junctions (TJs), and desmosomes (DSMs)[206,207]. As these are featured in this PhD, a brief description of filaggrin and involucrin (epidermal envelope proteins), claudins (TJs) and E-cadherin (AJs) follows:

3.2.1.1 Filaggrin (FLG)

Filaggrin exhibits interaction exclusively with intermediate filaments, specifically keratins, while remaining unicompetitive with actin and microtubule intermediate filament. Profilenaggrin, the enormous precursor protein from which filaggrin is derived, is insoluble and highly phosphorylated. Profilaggrin constitutes the primary component of the keratohyalin granules, which are electron-dense structures located in the granular layer of the epidermis. Although the proprotein does not possess keratin-binding activity, it undergoes a multistep process of dephosphorylation and proteolysis into multiple filaggrin monomers during the later phases of epidermal terminal differentiation. [208–211]. Upon binding to keratin intermediate filaments, the free filaggrin induces their aggregation into microfibrils, which consist of densely packed parallel arrays of intermediate filaments. This mechanism facilitates cellular compaction and enables transglutaminases to cross-link keratin intermediate filaments extensively, resulting in the formation of a keratin matrix that is extremely recalcitrant. The matrix serves as a protein scaffold to which the lipids and cornified-envelope proteins that comprise the stratum corneum adhere [210,211].

3.2.1.2 Involucrin (IVL)

IVL, which is primarily found in the granular layers but is also expressed in the upper SC spinous layer, is implicated in the initial step of cornified envelope formation. Cornification begins with desmosomes, where transglutaminase[200,212]. This protein complex also becomes the scaffold for the corneocyte-bound lipid envelope crosslinks IVL with envoplakin, periplakin, and keratin filaments.[200,213]. The initial genes identified within the epidermal differentiation complex (EDC) were IVL and loricrin (LOR). Small proline-rich proteins (SPRR) were subsequently identified. As a consequence, additional gene families were identified, including the S100 family, the late cornified envelope (LCE) family, and the

filaggrin and filaggrin-like family[214–218]. IVL, a member of the SPRR gene family, is a helical rod-shaped protein composed of ten amino acid tandem repeats. It functions as a substrate for the transglutaminase-1 enzyme, which crosslinks numerous SPRR and LCE proteins to IVL to generate the mature cornified envelope (CE). Initiating the CE assembly, IVL expression is a significant marker for early epidermal differentiation [207,214–219]. Barrier function depends on proper CE formation.

3.2.1.3 Junction Proteins (Tight and Adherens junctions)

The most prevalent intracellular junctions in the epithelial compartment of the dermis, which is highly dynamic and exquisitely tuned, are DSMs, AJs, and TJs. These junctions are interspersed across the keratinocyte cell membrane. [220] (Figure 3). In contrast to intestinal epithelium, which consists of a distinct apical and basolateral membrane domain separated by an apical junctional complex, the epidermis is not a traditional polarized epithelium. Conversely, the epidermis exhibits a more extensive degree of polarization due to the fact that distinct epidermal layers manifest a distinct array of junctional and differentiation markers. [221]. As illustrated in Figure 3, hemidesmosomes are exclusive to the basal layer, whereas desmosomes are ubiquitous throughout the layers; however, their quantity and protein composition differ among the various strata[222]. Tight junctions, previously thought nonexistent in the epidermis, have been identified exclusively in the granular layer[223–225].

DSMs and AJs serve as anchoring structures that connect the actin cytoskeleton and intermediate filaments to the plasma membrane, respectively, throughout the epidermal compartment. By means of lectins and cadherin, AJs facilitate cell-cell adhesion, whereas tight junctions establish cell polarity and regulate the passage of ions and small molecules between cells.[226]. DSMs consist of homo/heterodimers of transmembrane proteins that are members of the desmocollin and desmoglein families[227]. The desmoglein subfamily is distinguished by the expression of beta-catenin and E-cadherin[228]. Hemidesmosomes are exclusively found in the basal layer, where they join cells to the basement membrane at the junction of the epidermis and dermis. In contrast, corneo-desmosomes are specifically localized in the most highly differentiated stratum corneum. Conversely, TJs are limited to the uppermost stratum of granules. Nevertheless, additional junctional proteins, including claudin-1 and Zonula occludens (ZO)-1, are also detected in less differentiated layers. This implies that their functions may extend beyond intercellular communication.[229]. In the epidermis, the principal barrier components are TJs and the stratum corneum. The epidermis is the only epithelial

surface that possesses both of these structures, both of which are vulnerable to damage from internal or external perturbations, including inflammation.[230].

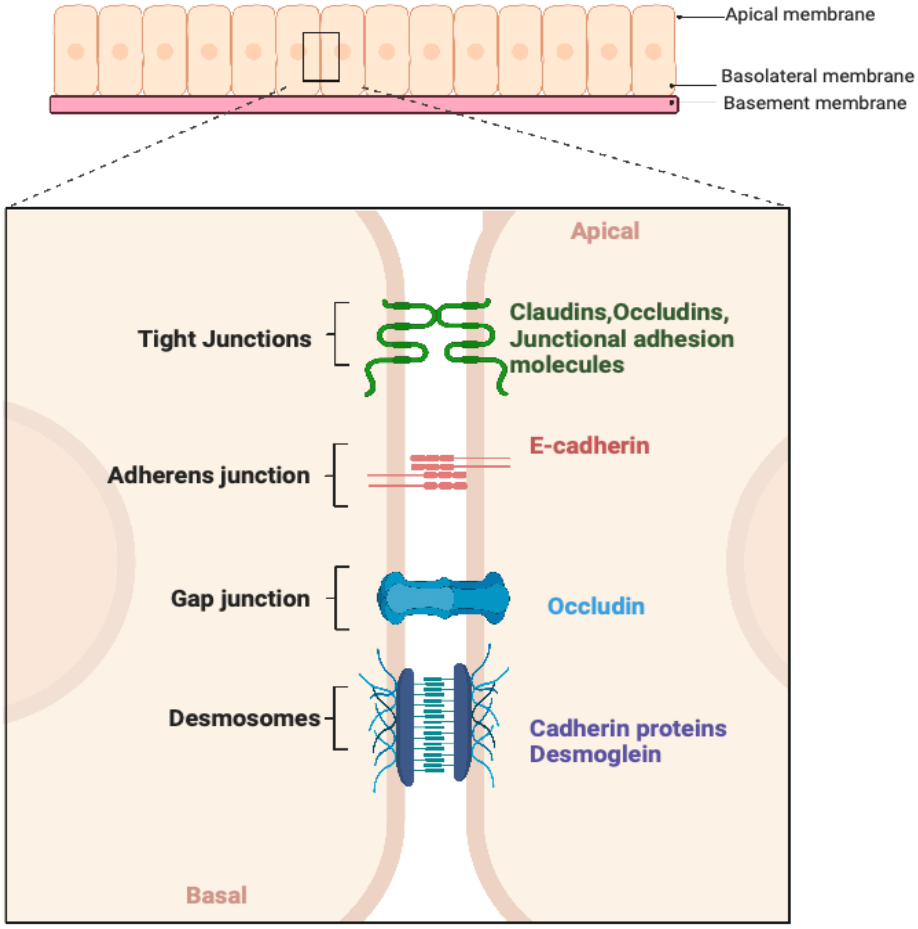

Figure 1. 3 Schematic structures of major tight junction proteins.

At the apex of the cell are situated the adherens junctions, gap junctions, and tight junctions; in contrast, the desmosomes are situated in the basal regions. (created by *CL Rametse* on Biorender.com)

Tight junctions

Epithelial cells are interconnected through a network of intercellular junctions at their lateral membranes[231].The zona occludins, also known as the tight junction, is the most apical intercel lular junction.Anatomically, the tight junction is demonstrated as a sequence of appositions c onnecting the lateral membranes of adjacent cells' exocytoplasmic leaflets.Each cell is enveloped by a belt-like network of these appositions, which connect it to the adjacent cell in the form of an uninterrupted seal. TJs serve as barriers that impede lateral diffusion and regulate solute flux between the outer leaflet of the apical and basolateral plasma membrane domains, thereby impeding the lateral diffusion of lipids and proteins[232,233]. It is now well-established as the primary determinant of paracellular permeability[231]. It has been suggested that the epithelial tight junction serves another purpose besides selectively obstructing permeability between aqueous compartments: mechanically limiting the diffusion of lipids and proteins within the lipid bilayer's plane. [233]. The presence of this barrier facilitates the segregation of lipid and protein constituents of the plasma membrane into unique basolateral and apical domains, a fundamental requirement for directional transepithelial transport.

Claudins

Claudins govern various aspects of permselectivity, such as ionic charge preference, size, and electrical resistance[234]. Tight junction membrane proteins are ubiquitously expressed in all recognized epithelia and endothelia. It appears that multiple distinct claudins are expressed concurrently in various organ systems such as the renal tubules, blood-brain barrier, gut etc. but a varying level based on the organ site. The principal body of evidence regarding pore formation and paracellular barrier function of claudin is derived from an abundance of studies that demonstrate that alterations in paracellular permeability are consistently induced by overexpression, knockdown, or knockout of claudins, as well as by naturally occurring or experimentally introduced mutations of claudins.[234]. Moreover, the impact of mutations that modify cysteines accessible for covalent modification by extracellular probes or that alter charged residues in the extracellular domains of claudins suggests that these domains must line the paracellular pore.[234].

Claudin-1

Claudin-1 is widely expressed in most bodily tissues. [235], it is however, highly expressed in the epidermis and is essential to the skin barrier[225,236]. Claudin-1 abnormalities are the cause of human cutaneous diseases[237–240]. The absence of claudin-1 in mice leads to the breakdown of

the tight barrier which when intact, prevents the passage of water and large molecules at the stratum granulosum of the epidermis. Therefore, these mice die due to extreme lack of hydration throughout the neonatal period[236]. Claudin-1 is also downregulated in other dry skin conditions, such as atopic dermatitis and psoriasis[240,241]. Its predominant function in *in vitro* overexpression experiments is to increase transepithelial resistance as a "barrier claudin"[235,242,243], further suggesting it crucial role in epithelial barrier function.

Claudin-2

Leaky epithelial tissues, such as the proximal tubule of the kidney[244,245] and the intestinal crypts, exhibit a high claudin-2 level of expression.[246]. Upon overexpression in epithelial cell lines, it functions as a cation-permeable paracellular pore with a high conductance. [247–249].

Claudin-3

Numerous epithelia, including those of the respiratory, urinary, gastrointestinal, salivary, and mammary organs, exhibit increased expression of Claudin-3. Additionally, it is a component of the insulin-brain and blood-testis barriers. Multiple investigations have demonstrated that claudin-3 functions as a TJ barrier protein[234].

Claudin-4

Expression of Claudin-4 is highest in the kidney, specifically in the collecting ducts, as well as in the lung. Depending on the cell type under investigation, it functions in vitro as a general barrier[250], or a Na^+ barrier that does not impact Cl^- permeability[251,252] . Additionally, it functions as a Cl^-/anion pore when in interaction with claudin-8. [253].

Claudin-5

The claudin most commonly detected and expressed in endothelial tight junctions is Claudin-5[254]. Endothelial tight junctions, which are impermeable to macromolecules and rigid within the vascular endothelium of the blood-brain barrier [255], unlike other less restrictive endothelium junctions present in other tissues [256]. The permeability of small molecules across the blood-brain barrier is significantly influenced by Claudin-5[234].

Regulation of Claudins

Claudin regulation occurs on various levels, including transcriptional, posttranslational modification, and interaction with cytoplasmic scaffolding proteins[218]. The assembly,

remodeling, and degradation of tight junctions are determined by these processes. IFN- and TNF- are significant regulators of epithelial claudin expression. A considerable body of research has investigated alterations in epithelial paracellular permeability induced by IFN-γ and TNF-α. It has been reported that these cytokines have variable effects on the structure of the TJ, with various mechanistic explanations.[257]. Additional pathways that have been implicated in this regard are PPARγ, SP1, HNF-1α, HNF-4α, CDX1, CDX2, GATA-4, and Grhl2[258–260]In duodenal biopsies obtained from untreated patients infected with HIV, Epple et al..[261] identified barrier impairment, downregulation of claudin-1, and upregulation of claudin-2; this was mediated by HIV-induced cytokines. A few other studies have experimented with and demonstrated in various organ tissues the effect of multiple cytokines on the expression of certain claudin types [262–266].

Adherens Junction: E-cadherin

Cadherin adhesion molecules are crucial factors in tissue architecture and morphogenesis. All cadherins possess calcium-binding extracellular cadherin repeats (EC's). In addition to their role in facilitating cell-to-cell adhesion, cadherins participate in a diverse array of cellular processes such as regulating the cytoskeleton, activating signaling pathways within cells, and controlling polarity[226]. Following the establishment of cell-cell adhesion, adherens junctions, which are specialized cell junctions composed of cadherins, form an association with the actin cytoskeleton.[267]. Classical cadherins, protocadherins, and atypical cadherins are the three distinct forms of cadherins. Cadherins of the classical variety are classified as type I or type II. Strong cell–cell adhesion is mediated by type I classical cadherins, which include neuronal (N-cadherin) and epithelial (E-cadherin) cadherin. Vascular epithelium (VE) cadherin and other type II classical cadherins are devoid of the conserved histidine alanine valine (HA) tripeptide motif found in the most distal extracellular cadherin repeats (EC)[268].

E-cadherin can establish a transcellular network that permits the coordination of the behavior of entire tissues or groups of cells. Studies *in vitro* have demonstrated that E-cadherin is essential for the formation of adherent junctions. For the assembly of additional junctional complexes, including desmosomes, gap junctions, and tight junctions, its adhesive activity is also vital[269–271]. The occurrence of this intricate junctional assembly aligns with the process of cell polarity establishment, and the presence of numerous protein complexes that are crucial for polarity is abundant at the cell junctions. These findings indicate a close association between junction formation and polarity[272]. Loss of E-cadherin can affect the proper formation of tight junctions. E-cadherin deficiency may impede the formation of appropriate tight

junctions. ZO-1 serves as the most direct link between adherens and tight junctions; via α-catenin[273]. This is hypothesized to be a transitional phase in the formation of tight junctions.

3.3. What are the gaps in knowledge?

Many barrier studies in the MGT to date have largely focused on comparing stratum corneum/keratin thickness in the foreskin with very limited studies examining other components contributing to barrier function in the penis. Other key components that have been proven to significant determine epithelial barrier function/permeability are still significantly underexplored, especially in the MGT. These include envelope structural proteins such as filaggrin and involucrin, junctional proteins such as claudins (TJs) and E cadherin (AJs). Additionally, little is known about how the presence of asymptomatic STIs affects their expression and function which is a significant co-factor in further understanding HIV acquisition and transmission in the MGT. Our study employs existing techniques used to measure skin barrier commonly in cosmetics in a novel way within the MGT to examine the barrier function no-invasively in other penile anatomical sites beyond the foreskin tissue. Studies examining other penile sites beyond the foreskin (glans, shaft) in the MGT are significantly limited due to tissue availability.

4. Adaptive immune Defense of the penile tract

4.1 T and B cells

Immune cells such as B and T cells have been shown to be present in the urethra, coronal sulcus, glans and foreskin tissue of human adult penis tissue[195]. $CD3^+$ T cells comprise the predominant subset of immune cells in every penile region. $CD4^+$ T cells continue to predominate as the subpopulation of T cells that mediate an extensive array of interactions with other immune actor cells. Thus, $CD4^+$ T cells constitute 50% of all T cells in the penile region, in contrast to the female vaginal tract[274]. $CD4^+$ T cells serve as susceptible targets for HIV infection, as the virus specifically attaches to the CD4 receptor located on the surface of helper T-cells, leading to viral replication within these cells. [195]. However, other studies have shown that $CD8^+$ predominate over $CD4^+$ T cells in the male genital tract and that $CD8^+$ T cells are more enriched in the foreskin versus the blood circulation[275]. $CD4^+$ and $CD8^+$ T cells are present in the epithelium and lamina propria of the penile areas and predominantly exhibit a quiescent memory pattern. The primary homing receptor identified in these T cells in the penis is CCR10. However, the expression levels of CCR3, CCR6, and CCR9, in addition to CCR10,

vary across different areas of the penis. In the foreskin tissue compared to the blood , $CD4^+$T cells have been shown to express higher frequency of CCR5 and interleukin-17, whilst $CD8^+$T cells produce higher levels of interferon-γ and tumor necrosis factor-α. There are ongoing comparisons between differences in the densities of these cells in the inner and outer foreskin. Some studies have shown that the inner foreskin has a higher density of $CD4^+$ T cells and langerin-expressing Langerhans' cells (LCs) than the outer foreskin[177,276].The glans has been shown to be a superior effector site than the other sites due to higher abundance of these cells with higher number of terminally differentiate effector $CD8^+$ T cells. Penile memory B cells are abundant in all the penile anatomical site, comprising up to 75% of the glans B cell population. In addition, the proportion of active memory B cells in the urethra was 30%, whereas in the glans it was only 15%. Memory B cells that have been activated undergo differentiation into plasma cells, which are responsible for the release of antibodies. As a result, these cells become a significant focus for vaccine-induced immunity.

4.2 The effect of STIs on foreskin immunity

In the foreskin, the inner versus outer foreskin has been shown to be more susceptible to HIV-1 infection[128,277]. Mechanisms explaining these differences are still not well understood. The presence or lack of specific T-cell subsets (active versus resting) at the mucosal site of HIV exposure could significantly influence an individual's vulnerability to HIV. The quantity and composition of T-cell subsets are significantly influenced by the presence or absence of prevalent sexually transmitted infections (STIs) in different penile locations. It is postulated that they do so by activating and attracting HIV target cells and disrupting epithelium at the site of infection. For instance, N. gonorrhoeaee species increase the vulnerability of LCs to HIV infection[278]. STI pathogens can also attract and activate other types of cells that are targeted by HIV, such as CD4+ T cells and macrophages. N. gonorrhoeae increases the susceptibility of resting CD4+ T cells to HIV infection by activating TLR 2[278]. Additionally, cells that have receptors for HIV-1 aggregate near HSV-2 lesions and remain there even after the infection has been resolved. There is a correlation between asymptomatic HSV-2 infection and a higher density of $CCR5/CD4^+$ T cells in the foreskin[279,280], HPV infection and a higher density of Langerhans cells in the foreskin, and *Chlamydia trachomatis* infection and Chlamydia trachomatis infection and a higher density of both of these cell subsets[281]. More recently, Gray et al[183] demonstrated how the presence of an STI (asymptomatic) increased the presence of both CCR5-coreceptor-expressing CD4+ T cells and Langerhans cells in both the inner and outer foreskin.

4.3 What are the gaps in knowledge?

There are still very limited studies on the effect of common asymptomatic STIs on the immune cell abundance in the inner and outer foreskin issue. Several studies have shown the effect of symptomatic STIs on the immune cell densities in the foreskin tissues[279,280,282], with very few examining the effect of asymptomatic STIs. Understanding the immunobiological changes associated with the presence of common asymptomatic STIs could potentially contribute towards identifying vaccine or alternative STI preventative methods in the male genital tract. An improved understanding of the immune cellular composition and localization of this immune profile in the foreskin with respect to the presence versus absence of aSTIs may provide insight into the association between STIs and the protective mechanisms of circumcision.

5. PrEP in males as an HIV prevention strategy

5.1 Pre-exposure prophylaxis

Pre-exposure prophylaxis (PrEP) is an efficacious prevention tool to offer young men and women.[283] Daily emtricitabine and tenofovir disoproxil fumarate (FTC–TDF) shows high efficacy in men who have sex with men (MSM)[14,25] and heterosexual HIV-serodifferent couples, and is recommended by the World Health Organization (WHO) for high-risk individuals[10,11].On-demand pre-exposure prophylaxis (PrEP) has been shown to be highly effective in reducing HIV infection risk in men who have sex with men (MSM) and heterosexual HIV-serodifferent couples[284,285]. On-demand PrEP is when individuals anticipate their risk for HIV infection, and rather than taking PrEP continuously, only start a course of PrEP prior to times of sexual activity. This strategy is highly effective in MSM?[286] but widespread use is hindered by lack of data on efficacy in other populations, dosing and duration of protection, and regime complexity.

Theoretically, alterations in the sexual networks or behaviors of some PrEP users could result in an increase in sexually transmitted infections. As a result, the most recent CDC recommendation (2021) is that providers see all patients taking PrEP on a quarterly basis (ref), to facilitate the prompt detection of sexually transmitted infections and aid in preventing their spread. Nguyen et al,[287] compared the incidence of sexually transmitted infections (STIs) 12 months prior to and 12 months after the initiation of preventive and therapeutic protection (PrEP). The researchers also examined the disparity in STI rates between individuals receiving

PrEP and those receiving post-exposure prophylaxis (PEP). Following the initiation of PrEP, the study revealed a rise in all non-HIV-associated STIs, with the PrEP group having increased STI incidence compared to the PEP group. According to a meta-analysis of data from twenty observational and clinical trials of PrEP in MSM, sexual behavior and/or the incidence of sexually transmitted infections remained stable or declined[285]. Nevertheless, the subset of MSM who utilized PrEP and participated in high-risk behaviors (such as condomless sex with casual partners) exhibited elevated prevalence rates of gonorrhea, syphilis, chlamydia, and hepatitis C[284,285,288]. Furthermore, an additional meta-analysis projected that the incidence rates of gonorrhea, chlamydia, and syphilis among MSM taking TDF/FTC PrEP were 25.3, 11.2, and 44.6 times higher, respectively, than the incidence rates among MSM not taking PrE[285]. To aid in the reduction of STI incidence in this subgroup, more frequent STI testing, and treatment options may be necessary.

When a STI is acquired, the effectiveness of TDF/FTC PrEP is a second crucial concern. Antiretroviral therapy prevents secondary HIV transmission in serodifferent couples, independent of STI coinfections, according to a number of studies.[125–128,289]. An observational report from Kaiser Permanente California[290], found that 187 STIs were acquired by 687 men who initiated TDF/FTC PrEP. Conversely, there were no documented incident cases of HIV acquisition. PrEP prevented 86% and 96% of HIV infections, respectively, in recent prospective clinical trials involving MSM—IPERGAY and Proud—TDF/FTC, despite the high incidence of STI infections during the trials[291,292]. 43% of MSM randomized to the PrEP arm in the IPERGAY trial developed one or more STIs. 57% of PrEP-treated participants in the Proud study[291], while 36% had rectal gonorrhea or chlamydia. These results demonstrate conclusively that incident STIs do not undermine the preventative efficacy of TDF/FTC PrEP in MSM. Nevertheless, in the pursuit of developing novel PrEP medications, it is essential that each agent exhibits autonomous resistance to the inflammatory alterations induced by a STI. Trials of HIV PrEP have, as previously stated, identified a significant incidence of classic STIs[291–293]. Bolan et al.[294] and Molina et al[159] have documented the efficacy of doxycycline prophylaxis in reducing the prevalence of chlamydia and syphilis among MSM at high risk. In recent studies, it has also been demonstrated to reduce gonorrhea usage among MSM by two-thirds[295,296]. As stated, this STI prophylactic measure is effective only in high-risk population[297].

5.2 What are the gaps in knowledge?

There is convincing evidence that both formulations of PrEP can inhibit HIV-1 infection in the

foreskin tissue, thus the reduced risk in HIV-1 infection rates in those taking PreP. However, the mechanisms underlying this efficacy in HIV-1 inhibition is not examined yet in the foreskin tissue. Tenofovir gel has been evaluated for vaginal and rectal PrEP, with the CAPRISA 004 study showing up to 54% lower HIV-incidence in women in the gel arm[298]. However, in a separate study, women receiving 1% tenofovir gel were shown to have an accumulation of activated endocervical $CD4^+$ T cells, which were associated with increased drug metabolite levels in the tissue[299]. Although these studies focused on topically applied PrEP, their findings raise the issue of host immune activation in response to drug which may undermine the potential efficacy of PrEP. In an effort to identify the impact of oral PrEP in young men on immune status, a randomized clinical triall was undertaken to test the immunological safety of PrEP.

6. Problem statement

6.1 Impact of STI on penile tract innate and adaptive immunity.

6.1.1 Aims and hypothesis

This PhD thesis examines barrier function, the density of HIV target cells and various expressed epithelial barrier proteins and genes in different anatomical sites of the intact penis before VMMC and in foreskin tissue after surgical removal. How these measurements are impacted by urethral asymptomatic STIs is also explored. The central hypothesis is that the inner foreskin has a relatively reduced barrier function compared to the other penile sites, which is further reduced by the presence of asymptomatic STIs (aSTIs). The primary goal of the study was to focus on characterizing the penile skin barrier function, microbiome, and urethral environment and how these change in the presence of common aSTIs and or following VMMC. Relating these changes to the presence of an STI is particularly important, as the mechanism of how STIs increase HIV acquisition remains unclear. Some studies have shown increased inflammation in foreskin tissues in the setting of STIs(including urethral infection -eg chlamydia and gonorrhoeae) while others have shown no changes[184,276,300,301]. Furthermore, VMMC has also been shown to decrease STI prevalence and may impact HIV acquisition by removing activated target cells in the inner foreskin. Thus this study only focused on urethral STIs and not others such as HSV and syphilis which has already been widely documented with respect to the foreskin.

6.1.2 Specific Aims

To test this hypothesis, the following aims are explored:

Aim 1. To describe the prevalence of aSTIs, including *Chlamydia trachomatis, Neisseria gonorrhoeae, Trichomonas vaginalis* and *Mycoplasma genitalium* at two medical circumcision clinics in the Western Cape, South Africa.

Aim 2: To characterize *in vivo* and *ex vivo* penile barrier function, as measured by transepithelial water loss (TEWL), surface hydration and water content in the glans, foreskin and shaft and further examine how this is impacted by common aSTI and VMMCAim 3: To evaluate inflammatory-associated changes in the inner and outer foreskin associated with aSTIs.Aim 4: To characterize transcriptome signatures of macrophage (CD68) and epithelial(PanCK) cells in foreskins of asymptomatically Chlamydia-infected males**.**

Aim 5: To examine the impact of *in vivo* Oral Pre-Exposure Prophylaxis (PrEP) on claudin-1 expression and lymphoid/myeloid cells in the foreskin (Published manuscript)

CHAPTER 2

Prevalence of asymptomatic sexually transmitted infections among men attending MMC recruitment site clinics

Table of Contents

2.1 INTRODUCTION 49

2.2 METHODS 49

2.2.1 Cohort description and Study design 49

2.2.2 Recruitment and data collection 50

2.2.3 Specimen collection and testing 50

2.2.4 Data management and analysis 50

2.2.5 Ethical considerations 51

2.3 RESULTS 52

2.3.1 Population characteristics 52

2.3.2 STI Prevalence 54

2.3.3 Factors associated with asymptomatic STIs in young menError! Bookmark not defined.

2.4 DISCUSSION 62

2.1 INTRODUCTION

This chapter describes the prevalence of asymptomatic *Chlamydia trachomatis, Neisseria gonorrhoeae, Trichomonas vaginalis* and *Mycoplasma genitalium* at two MMC clinics in the Western Cape, South Africa, and lays the foundation for the chapters that follow.

Sexually transmitted infections (STIs) pose a significant public health challenge in both affluent and resource-constrained environments[302]. Untreated STIs can lead to many complications such as infertility, infections in the upper genital tract, cervical cancer, persistent pelvic pain, and chronic infections caused by HIV and hepatitis [25,303]. Disease or symptom-specific syndromes, such as pelvic pain, discharge, ulcerative genital disease, discharge and nonulcerative genital disease inform the approach to STI diagnosis and treatment[25,304]. Numerous patients, nevertheless, present with asymptomatic disease, thereby augmenting the likelihood of complications and persistent transmission within the community. Thirteen percent (95% CI 8.9% to 17.8%) was estimated as the overall efficacy of syndromic STI services in treating curable symptomatic episodes in rural KwaZulu-Natal (KZN), the epicenter of the HIV epidemic. Furthermore, the study revealed that the prevalence of gonorrhea and chlamydia has not decreased since the implementation of syndromic management[297]. Therefore, screening is a critical method for identifying and treating individuals who are infected but would otherwise remain undetected. Costs prevent routine screening for all potential STIs in all patients; It is more practical to conduct focused screening of asymptomatic patients belonging to certain risk categories. To date, in upper income countries, rationale for screening recommendations in males differ between males who have sex with only females and MSM. Routine screening of heterosexual males without HIV for STIs is not recommended unless they have a history of STI or are seeking STI evaluation. This PhD examined the prevalence of aSTIs in males who self -identify as heterosexual.

2.2 METHODS

2.2.1 Cohort description and Study design

This study was a cross-sectional analysis of cis-gender persons assigned male at birth recruited as part of a study that sought to examine barrier function, the density of HIV target cells and various expressed epithelial barrier proteins and genes in different anatomical sites of the intact penis before VMMC and in foreskin tissue after surgical removal. How these measurements are impacted by aSTIs was also explored. Male volunteers who were undergoing voluntary medical male circumcision (MMC) were recruited through two clinics in TC-Newman and

Mitchells Plain, Western Cape. These clinics are run by the Provincial Department of Health and approved Non-Profit Organization MMC facilities. This study was conducted from January 2019- March 2022. The South African STI Treatment Guidelines recommend syndromic management of STIs in PHC facilities was applied[305].

2.2.2 Recruitment and data collection

Eligibility criteria for the main study and for participants in this analysis included (1) males seeking VMMC; (2) age 18-45 years; (3) HIV seronegative with documented testing within the past 30 days (4) able to provide informed consent. Prior to enrolment, consent was obtained, and each participant received risk reduction counseling by the study staff. Rapid HIV testing was performed prior to VMMC (standard of care at the local circumcision clinics). Blood was drawn from enrolled participants who tested HIV positive and were to be sent for a confirmatory ELISA at the National Health Laboratory Service and these participants were excluded. Other exclusion criteria were the presence of overt STI symptoms and signs, such genital warts, discharges, penile/scrotal swelling or ulcers. Participants were interviewed by a research nurse assistant in either English, Afrikaans or isiXhosa using a structured questionnaire, which included questions on socio-demographic characteristics, genital hygiene habits and STI symptom screening (see Appendix I). After being interviewed, an external genitalia physical examination was performed to assess for STI-defining signs and symptoms. The exterior of the penis was inspected for any abnormalities or signs of infection including ulcers, lice, sores, scarring or warts, and for discharge (colour, odour, thickness, and purulence).

2.2.3 Specimen collection and testing

First pass urine samples were collected from a total of 320 HIV-negative male participants to screen for the prevalence of common curable aSTIs including: *Chlamydia trachomatis, Neisseria gonorrhoeae, Trichomonas vaginalis* and *Mycoplasm genitalium* using multiplex PCR. STI testing was performed at the National Institute for Communicable Diseases, Centre for STI and AIDS in Johannesburg (which is part of the National Health Laboratory Services). The presence of asymptomatic STIs was reported immediately upon receipt of results to the clinic for participant management. Participants were also encouraged to return with their partners for treatment of the relevant aSTI.

2.2.4 Data management and analysis

All data collected were stored in physical folders which were filed and locked in a cabinet.

Additionally, the same data was entered and stored electronically using REDCap (Research Electronic Data Capture). Regular data quality checks were conducted, and any discrepancies were identified for further verification and rectification. Participant data was directly linked by assigning individual participant IDs to consent forms and specimen collection containers.

Prevalence was operationally defined as the ratio of positively testing individuals to the total number of individuals who underwent testing. To compare categorical variables (proportions), the Chi-square test (X2) or its non-parametric equivalent was utilized. To identify factors associated with infection, odds ratios (OR) and their corresponding 95% confidence intervals (CI) were computed utilizing univariate and multivariate logistic regression. Every data analysis was performed using STATA.

2.2.5 Ethical considerations

Permission to conduct the study was obtained from the management of the clinical sites used. Ethical clearance was obtained from the University of Cape Town, Faculty of Health Sciences, Research Ethics Committee (Sub-study HREC Ref number: HREC REF 601/2020, parent study Ref number: HREC REF 071/2017) and written informed consent was sought from all participants before they were enrolled in the study.

2.3 RESULTS

2.3.1 Population characteristics

Out of 320 HIV-negative participants enrolled, 80.6% and 19.4% were recruited from the TC Newman and Mitchells Plain clinics, respectively (Table 1). There were no participants who tested HIV seropositive during recruitment. The age range of the participants was a median of 25 years; interquartile range (IQR)18-45. Eighty-one percent of participants were of mixed race (Table 2.1). The majority (73.5%) of participants were single with 11.1% cohabiting. Eighty-two percent of participants had not completed high school, with slightly more participants being employed than unemployed. The minority of the participants were students and the majority of participants lived in formal housing and mostly had adequate sanitation and electricity infrastructure.

Table 2. 1 Socio-demographic characteristics of young men tested for Chlamydia trachomatis, Neisseria gonorrhea, Trichomonas vaginalis and Mycoplasm genitalium at two medical circumcision clinics in the Western Cape (WC), South Africa (n=320).

Characteristic	No.	%
Clinical site		
Mitchells Plain	62	19.4
TC Newman	258	80.6
Race		
Black	51	15.9
Mixed	261	81.6
Other	8	2.5
Marital status		
Co-habiting	34	11.1
Married	47	15.4
Single	225	73.5
Total	306	100
Occupation		
Employed	150	47.5
Student	34	10,.8
Unemployed	132	41.8
Education level		
Primary (grade 1-6)	5	1.6
High school (grade 7-12)	261	82.1
Tertiary	52	16.4
Housing type		
Formal	297	93.4
Informal	21	6.6
Running water		
No	1	0.3
Yes	316	99.7
Electricity		
No	7	2.2
Yes	309	97.8
Toilet facilities		
No	1	0.3
Yes	312	99.7

2.3.2 STI Prevalence

The overall asymptomatic STI prevalence rate was 15.9% (51/320 participants). Prevalence was higher in Mitchell's Plain (19.4%) versus TC Newman (15.1%) (Table 2.2). In this study, the majority of the aSTI positive participants were mono-infected (11%). A total of 17 of the 51 aSTI-positive participants were co-infected with multiple STIs (5.3%).

Table 2.3.A shows the prevalence of a specific aSTI irrespective of clinical site. Chlamydia was the most common cause of STIs in this cohort, this is both for mono-infections and multiple infections. A total of 39 participants were chlamydia-positive either as a mono-infection or a co-infection (12.2%%). Of the chlamydia-positive participants, almost two thirds were mono-infections and over one third were co-infected with two or more organisms (Table 2.3.B). *Mycoplasma genitalium* was the second most common organism in aSTI-positive participants, but much lower than chlamydia (Table 2.3.B). Mycoplasma genitalia were predominantly associated with another infection.

Table 2. 2 STI prevalence by Clinical site.STI prevalence (any STI) in young men by their site of recruitment, STI screening for *Chlamydia trachomatis, Neisseria gonorrhoeae, Trichomonas vaginalis and Mycoplasma genitalium* from Mitchells Plain and TC Newman clinical sites for running voluntary medical male circumcision programs in the Western Cape province, SA

	Mitchells plain n=62			**TC Newman (n=258)**			**Total**		
	n	**%**	**95% CI**	**n**	**%**	**95% CI**	**n**	**%**	**95% CI**
STI									
One (N, %)	7	11.3	5.4-22.2	27	10.5	7.3-14.9	34	11	7.7-14.5
2 or More	5	8.1	3.3-18.3	12	4.7	2.7-8.0	17	5.3	3.3-8.3
Total	12	19.4	11.4-30.9	39	15.1	11.2-20	51	15.9	12.3-20.3

Table 2.3 0-a Patterns of STI infections among South African young men. STI prevalence by causative organisms amongst the 320 young men screened for asymptomatic STIs

.

	Chlamydia trachomatis			***Neisseria gonorrhoeaee***			***Trichomonas vaginalis***			***Mycoplasma genitalium***			**Total**		
	n	**%**	**95% CI**	**n**	**%**	**95% CI**	**n**	**%**	**95% CI**	**n**	**%**	**95% CI**	**n**	**%**	**95% CI**
STI															
One	24	7.5	5.1-10.9	2	0.6	0.1-2.5	4	1.25	0.4-3.4	4	1.25	0.4-3.4	34	10.6	7.7 - 14.5
With coinfection	15	4.7	2.8-7.5	9	2.8	1.4-5.5	4	1.25	0.4-3.4	10	3.1	1.7-5.7	17	5.3	3.3 - 8.4
Total	39	12.2	9.0 - 16.3	11	3.4	2.0 - 6.1	8	2.5	1.3-5.0	14	4.3	2.6 - 7.3	51	16	12.3 - 20.4

Table 2.3 0-b Patterns of STI infections among South African young men. STI proportions/patterns by causative organisms amongst the 51 young men who screened positive for asymptomatic STIs.

	Chlamydia trachomatis			***Neisseria gonorrhoeaee***			***Trichomonas vaginalis***			***Mycoplasma genitalium***			**Total**		
	n	**%**	**95% CI**	**n**	**%**	**95% CI**	**n**	**%**	**95% CI**	**n**	**%**	**95% CI**	**n**	**%**	**95% CI**
STI															
One	24	61,5	[45.1,75.7]	2	18.2	[4.4,52.0]	4	50	[19.2,80.8]	4	28.6	[10.8,57.0]	34	66.7	[52.3,78.5]
2 or More	15	38.5	[24.3,54.9]	9	81.8	[48.0,95.6]	4	50	[19.2,80.8]	10	71.4	[43.0,89.2]	17	33.3	[21.5,47.7]
Total	39	100		11	100		8	100		14	100		51	100	

2.3.3 Factors associated with asymptomatic STIs in young men

In a univariate analysis of sociodemographic factors associated with any STI, marital status was significantly associated with lower odds of having an STI relative to cohabiting men (0.26 OR, 95% CI 0.07-0.93, p=0.03, Table 2.4). Educational status also showed a significant association with STI prevalence, where tertiary education was significantly associated with lower odds of having an STI as compared to only having high school as the highest level (5.63 OR, 95% CI 0.1-8.24, p=0.02). It was noticeable that the STI's were predominantly among both the employed and unemployed as compared to the young men who identified as students. Infrastructural factors such as type of housing, toilet, and electricity facilities had no association with STI prevalence. Surprisingly, reported condom use and the number of sexual partners also did not impact STI prevalence, although STI prevalence was highest among those who reported having more than two sexual partners (17.7%).In the CRF attached in appendix I, all the sexual risk taking data and hygiene data were reported and considered in analysis, they did not significantly associate or correlate with data findings.

In a multivariate analysis including factors significantly associated with STI in the univariate analysis (Table 2.5) and other factors previously documented to be significantly associated. Both marital and educational status remained significantly associated with the risk of STI infection. Having a tertiary education (compared with lower levels of education) is associated with significantly lower odds of having an STI (6.29 OR, 95% CI 1.23-28.91, p=0.024). Being married was significantly associated with lower odds of having an STI than cohabiting men (3.30 OR, 95% CI 0.08-1.21, p=0.08). The ORs for "sexual activity status" (OR 3.37, 95% CI 0.41-27.16), p=025) and "number of sexual partners" (OR 1.43, 95% CI 0.54-3.77) suggest that being sexually active and having multiple sexual partners is associated with a higher odd of having an STI although not statistically significant. Age and employment status do not show up as important predictors of acquiring an STI in this cohor

Table 2.1. Factors associated with prevalent STI (either Chlamydia trachomatis, Neisseria gonorrhoeae, Trichomonas vaginalis or Mycoplasm genitalium) (Univariate analysis).

		Any STI	Any STI		
Variables		Yes n (%)	No n (%)	OR (95% CI)	P value
Clinical site					
	Mitchells Plain	12 (19.4)	50 (80.6)	ref	
	TC Newman	39 (15.1)	219 (84.9)	0.74 (0.4-1.5)	0.41
Demographics					
Age					
	<25 but >18 years	23 (15)	130 (85.0)	ref	0.67
	> =25 years	28 (16.8)	139 (83.2)	1.14 (0.6-2.1)	
Race					
	Black	5 (9.8)	46 (90.2)	ref	
	Coloured	44 (16.9)	217 (83.1)	1.87 (0.7-4.9)	0.21
	Other	2 (40)	3 (60.0)	3.06 (0.4-19.4)	0.23
Employed					
	Yes	22 (14.7)	128 (85.3)	1.78(0.5-6.3)	0.38
	No	24 (18.2)	108(81.8)	2.30 (0.6-8.1)	0.20
	Student	3 (8.8)	31(91.2)	ref	
Marital status					
	Co-habiting	9 (26.5)	25 (73.2)	3.87 (1.1-13.9)	**0.03**
	Married	4 (8.5)	43 (91.5)	ref	
	Single	36 (16)	189 (84.0)	2.05 (0.7-6.1)	0.12
Education					
	Primary (grade 1-6)	1 (20.0)	4 (80.0)	6.25 (0.5-84.8)	0.17
	High school (grade 7-12)	48 (18.4)	213 (81.6)	5.63 (1.3-23.9)	**0.02**
	Tertiary education	2 (3.8)	50 (96.2)	ref	
Type of Housing					
	Formal	48 (16.2)	249 (83.8)	ref	
	Informal	2 (9.5)	19 (90.5)	0.55 (0.1-2.4)	0.43
Electricity					
	Yes	48 (15.5)	261 (84.5)	0.46 (0.1-2.4)	0.36
	No	2 (28.6)	5 (71.4)	ref	
Reported current sexual activity					

	Yes	44 (17.3)	211 (82.7)	ref	
	No	7 (11.3)	55 (88.7)	0.61 (0.3-1.4)	0.26
Reported more than one sexual partner					
	Yes	14 (20.9)	53 (79.1)	1.48 (0.7-2.9)	0.27
	No	31 (15.1)	174 (84.9)	ref	
Condom use					
	Yes	30 (16.9)	148 (83.1)	1.13 90.6-2.3)	0.73
	No	14 (15.2)	78 (84.8)	ref	
Number of lifetime sexual partners					
	1 partner	8 (16)	42 (84)	ref	
	2+ partners	37 (17.7)	172 (82.3)	1.13 (0.4-2.6)	0.76

Table 2. 2. Multivariate analysis of factors associated with prevalent STIs.

		Any STI	Any STI		
Variables		Yes n (%)	No n (%)	OR (95% CI)	P value
Age					
	<25 but >18 years	23 (15)	130 (85.0)	ref	
	> =25 years	28 (16.8)	139 (83.2)	1.43 (0.6-3.3)	0.40
Employed					
	Yes	22 (14.7)	128 (85.3)	0.69 (0.1-3.1)	0.63
	No	24 (18.2)	108(81.8)	0.76 (0.2-3.4)	0.73
	Student	3 (8.8)	31(91.2)	ref	
Marital status					
	Co-habiting	9 (26.5)	25 (73.5)	3.30 (0.9-12.5)	**0.08**
	Married	4 (8.5)	43 (91.5)	ref	
	Single	36 (16)	189 (84.0)	2.44 (0.7-8.3)	0.15
Education					
	High school (grade 7-12)	48 (18.4)	213 (81.6)	6.29 (1.3-31.0))	**0.024**
	Tertiary education	2 (3.8)	50 (96.2)	ref	
Reported current sexual activity					
	Yes	44 (17.3)	211 (82.7)	ref	
	No	7 (11.3)	55 (88.7)	0.28 (0.03-2.3)	0.23

Number of lifetime sexual partners					
	1 partner	8 (16)	42 (84)	ref	
	2+ partners	37 (17.7)	172 (82.3)	1.35 (0.5-3.5)	0.54

2.4 DISCUSSION

STIs continue to pose a significant global public health challenge, with millions of individuals worldwide affected by these infections. STIs not only carry a social stigma, but they have also been found to contribute significantly to the transmission of HIV by causing inflammation in the vaginal area and leading to negative reproductive health outcomes in women. This chapter has described the prevalence of common asymptomatic STIs among young adult cis men who all self-identified as heterosexual at local circumcision clinics in the Western Cape. The overall prevalence of asymptomatic STIs in this cohort was 15.9%, the highest contributor to this high prevalence rate is that of chlamydia infections (12.2%), consistent with both local and global studies[13,304]. According to the most recent Spectrum-STIs[306] estimates, the prevalence of chlamydia in South Africa had been reported to be 6%. In this cohort, the prevalence of asymptomatic STIs is double that of the last reported rate[306]. This is of substantial public health concern and emphasizes the need for screening in young adults. In the USA and other developing countries, screening is recommended for young adults who are sexually active and have other associated risk factors[25,307]. In SA and some other developing countries, a syndromic approach is still used for both diagnosis and treatment of STIs, which could explain these high rates of asymptomatic chlamydia infections in young adult men[304].

The other STI observed among these young adult men was MG (4.3%), followed by *N. gonorrhoeae* (3.4%), and the least was TV (2.5%). These findings appear to be in contrast with global estimates, where *N.gonorrhoea* is the second most common cause of bacterial STI [25]. However, the second most common bacterial STI in this cohort was MG. This could be explained by the fact that *N.gonorrhoeae* in men almost always presents symptomatically, with asymptomatic infections being 10% in men versus 50% in women [55,106,308,309]. Hence, the comparatively diminished incidence rates observed in this cohort, in contrast to the global rates encompassing symptomatic *N. gonorrhoeae* infections, can be attributed to the organism's natural history and the exclusive recruitment of asymptomatic males for this PhD study. Another study found the prevalence of MG in young adults with asymptomatic STIs in South Africa to be 9.6% and 3.3%, among females and males respectively[79], thus our current asymptomatic rates , although in a different geographical region, are consistent with these findings. Previous research has documented a correlation between MG infection and the acquisition and transmission of HIV[79] described in chapter 1, section 1.1. Similar to other sexually transmitted infections (STIs), MG induces persistent secretion of inflammatory cytokines that compromise the integrity of the epithelial barrier and heighten vulnerability to

HIV[310–312]. These associated complications and increased HIV risk emphasize the importance of considering proactive screening of MG in young men. It is still concerning that currently local and global STI management guidelines do not recommend screening of this STI. Due to a paucity of data regarding this STI rates, much of its treatment is also neglected. Although MG STI prevalence ranked second in this cohort, we show that most of these infections are co-infections, of those with MG positive aSTIs, the majority were due to co-infections (71.4%) as opposed to single infection (28.6%) (Table 3B). This is consistent with documented data in literature on this STI. It has been demonstrated by various studies to be frequently associated with chlamydia co-infection, especially in women[65].

As expected, sociodemographic factors impacted the risk of having any of the screened STI in this study. We observed in this study that marital status and tertiary education status had a significant impact on lowering risks to acquire any STI. These findings are consistent with some studies that have demonstrated in both local and global studies the effect of socio-economic factors such as marital and education status on STI risk[25,43,55,313].

This study shows that men have a high burden of asymptomatic STIs and thus men should equally receive this attention in STI testing. Of concern, the current approach of managing STIs is that it is still being employed in numerous countries with a high prevalence of HIV, despite the acknowledgment of the significant epidemiological and biological connections between STIs and HIV. Moreover, the extensive economic and service load caused by HIV in many sub-Saharan countries has worsened the already insufficient and inadequate care for sexually transmitted infections (STIs). Point-of-care diagnostics and technology must undergo rigorous and systematic testing in diverse urban and rural environments. Finally, this chapter has laid a foundation for the prevalence of asymptomatic STIs, penile barrier function measurements and foreskin collection was performed on a subset of these participants and details of these analyses are shown in the following chapters.

CHAPTER 3

Measurements of *in vivo* and *ex vivo* Penile Epithelial Barrier Function

Table of Contents

3.1 INTRODUCTION 65

3.2 METHODS 71

3.2.1 Cohort Description 71

***3.2.2 In vivo* barrier measures** 71

3.2.2.1 Meter data measurements 71

3.2.2.2 Application of Meter Devices to penile skin 71

3.2.2.3 Optimization of meter studies 73

***3.2.3 Ex vivo* barrier measures** 73

3.2.3.1 Primer design 73

3.2.3.2 RNA Extraction 74

3.2.3.3 cDNA synthesis 74

3.2.3.4 Primer Annealing Temperature (Ta) 74

3.2.3.5 Determination of optimal primer concentration 75

3.2.3.6 qPCR reaction efficiency 75

3.2.3.7 Reference gene validation 76

3.2.3.8 RT-qPCR Assays 76

3.2.3.9 Data Analysis 76

3.3 RESULTS 78

***3.3.1 In Vivo* Barrier Function** 78

3.3.1.1. Different anatomical sites show different barrier function and hydration/moisture status 78

3.3.1.2 Durable changes in penile barrier integrity months post circumcision 79

3.3.1.3 The impact of asymptomatic STIs on barrier function before MMC 82

***3.3.2 Ex Vivo* Barrier Function** 83

3.3.2.1 Lower expression of epithelial barrier proteins in the inner versus outer foreskin tissue in STI-negative men 83

3.3.2.2 Impact of aSTI status on foreskin epithelial barrier proteins mRNA expression 84

3.4 DISCUSSION 87

3.1 INTRODUCTION

This chapter describes two aspects of penile epithelial barrier function: *in vivo* measurement of skin hydration/water loss and *ex vivo* tight junction gene expression in surgically removed foreskins. The overall aim is to understand possible anatomical sites of the penis that could be portals of entry for HIV and to identify potential mechanisms for the effectiveness of MMC in preventing HIV acquisition. The impact of asymptomatic STIs on measurements made may facilitate our understanding of these mechanisms and in parallel explain why sub-clinical STIs could enhance HIV acquisition in uncircumcised males.

The penis consists of the root, body, and glans of the male genitals. It consists of different regions: (i) the foreskin, a stratified keratinized epithelium, (ii) the glans, a stratified keratinized epithelium; (iii) the urethra, a pseudo-stratified non-keratinized epithelium; (iv) the penile shaft, keratinized stratified epithelium[314,315]. These are all potential sites of HIV-1 acquisition. The vulnerability of the penis to sexually transmitted infections (STIs) is predominantly determined by the inherent attributes of the immune systems in each of these anatomical regions[314]. HIV-1 is predominantly transmitted through sexual contact, and the epithelial surfaces that line the genital area serve as the principal site of transmission[314,315]. While it has been documented that male circumcision can decrease the risk of males contracting HIV-1 by 60%, the precise mechanisms through which HIV-1 enters the male genital tract remain relatively unknown[315,316].

The epithelium serves as the initial barrier for viral penetration into the submucosa. The structural configuration of the epithelium varies across the genital mucosa, which has significant implications for viral transmission[317]. Uncertainty surrounds the pathophysiologic mechanism underlying compromised barrier function and HIV-1 transmission, which encompasses various sites such as the intestinal and genital tracts[261,318–321]. In addition to the impact of antiviral peptides, it is probable that the structure and composition of the exposed epithelium significantly influence its vulnerability to viral entry. The anorectal epithelium demonstrates the greatest likelihood of HIV transmission (0.3–5%), surpassing that of the genital epithelium of the female (0.05–0.5%) and male (0.04–0.14%), followed by the least susceptible epithelium, the buccal mucosa (0.01%)[317]. Implying that the probability of HIV transmission during one sexual act of anal intercourse is approximately 0.3-5%.

Multiple studies have suggested that the inner foreskin is more susceptible to HIV infection

than the outer foreskin[178,182,276,322]. Furthermore, a recent study[277] has shown that the interaction of HIV with penile epithelium resulted in the virus being more readily able to enter the epithelia of the inner foreskin and glans of uncircumcised individuals, which remain within an enclosed environment when the foreskin is intact.

In vivo barrier function

The skin is the sole epithelial surface that possesses both a stratum corneum (SC) and tight junctions (TJs)[323]. TJ keratinocyte dysfunction may account for a significant number of the effects of a compromised skin barrier[324]. For instance, increased skin TEWL can be readily attributed to FLG mutations , a well-established measure of skin barrier integrity that is significantly elevated in both lesional and nonlesional skin of AD patients[325–328]. TEWL is a measure of water passively diffusing from the deeper skin layers to the external environment and when the skin barrier is damaged, TEWL increases[329]. Hydration is a fundamental requirement for the proper operation of the epidermis. Despite being essential for cellular survival, the water content of the stratum corneum (SC) is also significant because it influences the appearance, metabolism, mechanical properties, and barrier function of the skin.[330–332]. The hydration of the outer layer of the skin, known as the stratum corneum (SC), relies on the ability of viable epidermal keratinocytes to transport water and solutes, the availability of water from the body, the capacity of the SC to bind water, and the rate at which water evaporates through the skin (TEWL)[333]. Transport of water and solutes can take place either via the cells (transcellular) using aquaporins (AQPs) or through the extracellular space (paracellularly) using tight junctions (TJ's).

The water-holding capacity of the stratum corneum (SC) is determined by its structure and composition, specifically the presence of hygroscopically active chemicals resulting from the breakdown of filaggrin, as well as other tiny osmolytes or 'humectants'.[334,335]. SC hydration is diminished in aged skin, eczema, atopic dermatitis, hereditary ichthyosis, and psoriasis[336–338]. Two types of pores in the epidermis are hypothesized to be involved in water homeostasis: AQPs and TJ. Therefore , measures such as TEWL and SC hydration can reflect the integrity of TJ and aquaporins and structural proteins such as filaggrin[339].

Two valuable skin parameters are commonly measured in dermatological studies, TEWL and water content. Water content can be measured across different levels of the skin. The water content within the uppermost layer of the epidermis (stratum corneum) is called stratum

corneum hydration (SCH) or surface hydration (Figure 1). TEWL and SCH skin measurements represent distinct facets of skin physiology. Numerous investigations continue to scrutinize the precise potential quantitative correlation between these two variables, whether an increase in TEWL results in an increase in the SCH and vice versa. Skin dryness is commonly assessed using the stratum corneum electrical capacitance or conductance parameter-based SCH [340,341]. In contrast, TEWL is often used to measure skin barrier function, as reflected by the amount of skin water loss[342–344].

In vivo, the diffusion of water across the stratum corneum is a passive process (Figure 3.1). The water content of the innermost cell layer of the stratum corneum is in equilibrium with the nearby moist granular layer, while the outermost cell layer is in equilibrium with the surrounding environment[329]. As a result, the outer layer of the stratum corneum is drier than the core cornified layer. Consequently, a difference in concentration within the outermost layer of the skin leads to a constant movement of water from the body through the skin and into the surroundings, known as transepidermal water loss (TEWL)[329], as indicated by the "vapor" label in Figure 1. When the skin barrier is damaged, TEWL increases. This has commonly been demonstrated in studies that have examined dermatological pathologies such as atopic dermatitis, or the efficiency of specific cream formulations for skin dryness.

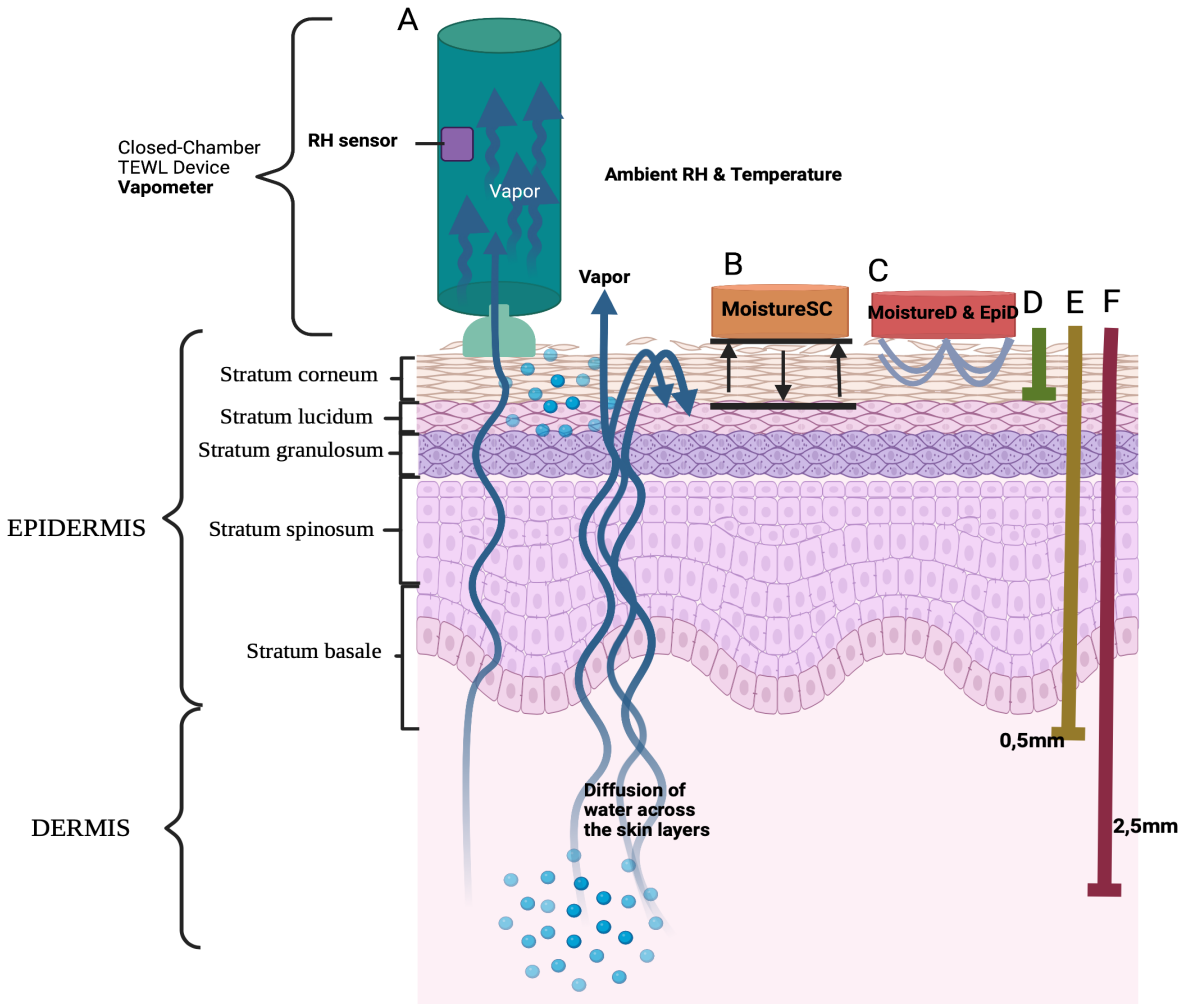

Figure 3. 1 Mechanics of Skin Hydration & Meter machines measurement principles.

1)Water diffusion in the skin; Water diffuses continuously from deeper tissues into the environment via the stratum corneum and into the environment because of a natural water concentration gradient. This gradient fluctuates in response to changes in the ambient temperature and relative humidity. This diagram demonstrates that the water content is highest in the deeper tissues and lowest in the upper skin layer, as indicated by the blue dots in the upper epidermal layers as opposed to the lower layers. While the overall movement occurs in accordance with this gradient, from the deeper tissues to the environment via the different layers of skin (blue arrows), a portion of this water is retained within the skin and not lost. This function of retaining moisture is exclusive to the stratum cornuem (SC). The blue dots in the SC represents the SC hydration (SCH) level. **2)Measurement of water movement and hydration in skin:** Water vapor from the passive diffusion moves across the skin surface and

collects in the chamber formed by the Vapometer device A. This causes humidity to rise with time. Sensors (purple square in the vapometer) measure the rate of increase in relative humidity, this is the indirect measure of TEWL. (B) Shows the body and probe of MoistureSC device. The black lines below the probe on the Stratum corneum represent the electromagnetic field plates formed by the probe and epidermis that determine the dielectricity of the stratum corneum (B). EpiD and MoistureD transmit microwaves which are shown in grey (C), these are reflected and reabsorbed to be used to calculate the dielectric constant which is proportional to the hydration levels (E and F). D, E and F illustrate the depth and tissue layers measured by the MoistureSC, EpiD and MoistureD respectively. (*Created with BioRender.com by CL Rametse* on Biorender.com)

Stratum corneum hydration (SCH)

The stratum corneum can receive water from the body's internal sources and can also absorb water from the outside environment. Water is transported to this tissue by the sweat glands and through diffusion from the overlying tissues, originating from within the body (Figure 1). Sweat glands are inactive over most of the body except when environmental temperatures exceed 29 °C. Due to the established water concentration gradient in the stratum corneum, internal body fluids continuously diffuse into the environment via the skin. As the surface layer becomes moister, the concentration gradient diminishes, resulting in a reduced TEWL[345–348].

Transepidermal water loss (TEWL)

TEWL is the most employed objective metric for evaluating the barrier function of skin[230,324]. It represents the amount of condensed water that diffuses per unit time across a fixed area of stratum corneum to the skin surface. TEWL in humans ranges between 300 and 400 mL per day, depending on the anatomical location. There are a range of instruments available in cosmetics that can measure TEWL, Surface Hydration and Water Content through the various layers. Numerous variables can affect TEWL measurements, including inherent subject factors, as well as environmental and instrumental differences. It is well demonstrated in literature that environmental factors such as temperature and hudimity significantly affect the skin barrier function measures. In high humidity, the amount of water loss will decrease due to the drop in the water vapor pressure gradient[213,349]. TEWL varies in different anatomic sites and is inversely related to the corneocyte size. When air temperatures exceed those of the skin, the only physiological avenue for heat loss is through the recruitment of eccrine sweating, meaning there will be more water loss across the skin barrier. Thus, this suggests that to make vigorous

stipulations from meter data, environmental factors should always be recorded. In this project we also validated measuring humidity and temperature at each reading that was made for each participant. Correlative analysis between the readings and environmental data showed (**Appendix I, Figure 1**) looking at multivariance analysis that both the room humidity and temperature strongly correlated with all the meter machines readings, and this was a strong correlation. This was then accounted for our final analysis of the meter readings to make more pragmatic conclusion's.

As an illustration, water loss will be reduced in environments with high humidity because of the water vapor pressure gradient diminishing. Current TEWL measurements use devices placed in contact with skin and collect water vapour flux into a chamber for a fixed amount of time or until a particular volume has been achieved, using open or closed chamber methods[343,344,350,351]. The resulting measurement yields information on two components of TEWL. Water diffusion through the intact epidermis is influenced by the difference in water vapor pressure between the epidermis and the surrounding air. This TEWL component is most directly related to skin barrier function. The other component is sweat-related activity from eccrine glands, which is variable and. Distinguishing between the contributions of TEWL and those caused by eccrine activation to TEWL is challenging, despite the utilization of certain methods for this objective. [352].

Relationship between Transepidermal Water Loss and Stratum Corneum Hydration

The concentration gradient of water between the stratum granulosum and the stratum corneum is the driving force responsible for TEWL. However, the motion of water molecules is hindered within the stratum corneum by restraining forces; these forces diminish as the tissue attains hydration[333]. There may be a mechanical relationship between SCH and TEWL, given that TEWL is dependent on the water pressure gradient between the epidermis and the air[333,353]. If true, an analogy is that TEWL would increase with increasing SCH[329]. Despite the limited availability of data, in a recent study, Mayrovitz et al. (2023)[329] identified a noteworthy positive nonlinear correlation ($p < 0.001$) between SCH and TEWL in the skin of hands. This correlation was observed exclusively when SCH levels surpassed a predetermined threshold. This implies that conditions with increased SCH may partly account for elevated TEWL values.

Aim, Objectives, and Hypothesis

This study aims to characterize stratified squamous epithelial barrier components of the

foreskin, shaft, and glans. The aim is to characterize the penile epithelial barrier across these anatomical sites and how measurements differ in the presence and absence of the measured aSTIs depicted in Chapter 2. The central hypothesis is that the inner foreskin has a relatively reduced barrier function compared to the other penile sites, which is further reduced by the presence of aSTIs.

To test this hypothesis the following objectives are explored:

(a) To characterize the variability that exists between the foreskin, glans, and shaft barrier function before and after medical penile circumcision using innovative in vivo measurements.

(b) To assess how skin barrier function changes after circumcision and which anatomical sites are most affected.

(c) To assess whether an asymptomatic STI alters skin barrier function.

3.2 METHODS

3.2.1 Cohort Description

Persons assigned male at birth were recruited into this study cohort and ethics described in **Chapter 2, section 2.2.1** In addition to the inclusion criteria described in the chapter, volunteers had to be willing to have follow-up skin measurements using the meter machines.

3.2.2 In vivo barrier measures

3.2.2.1 Meter data measurements

Using the Vapometer, MoistureMeterSC, MoistureMeterD and MoistureMeterEpiD hand-held meters from Delfin Technologies (Kuopio, Finland), TEWL, surface hydration, and water content were measured at different anatomical sites of the penile tissue, as well as the hip as a control site. Measurements were taken in five replicate readings on the penile shaft, glans, inner foreskin, and hip. Measurements at the first pre-circumcision visit and then follow-up at 2, 12 and 24 weeks after circumcision in the glans and shaft. After removing pants and undergarments, each participant was asked to wait for 15 minutes to allow for acclimation to the examination room temperature and humidity before taking readings. Alongside these measures, temperature and humidity were recorded and were included in the final analysis and interpretation of the collected data.

3.2.2.2 Application of Meter Devices to penile skin

Four meters by Delfin Technologies: One measures water loss across the SC (Vapometer,

Figure 1A) and the other three measure water content in the SC (MoistureSC, Figure 1B) and in both the epidermis and dermis (MoistureD and EpiD, Figure 1C). the Vapometer, which measures TEWL in grams of water lost, per hour, per square meter of the skin surface. The MoistureMeterSC meter only measures SFH (au units) of the stratum corneum with a measuring depth of approximately 30 mm, whilst the MoistureMeterD and EpiD, which both measure water content (in %) in the epidermis and dermis. The depth of measurement for each meter depends on the size of the probe. We used probe size 20mm sensor contact diameter (which measures up to a depth of 2,5mm, Figure 3.1F) and 8mm sensor contact diameter (0,5 mm depth measurement, Figure 3.1E), respectively[354]. These are non-invasive instruments for measuring skin moisture and loss. These are hand-held, portable, and wireless.

The VapoMeter[355]operates with the closed-chamber measurement principle, which measures TEWL (Figure 3.1). At the core of the vapometer is a humidity sensor mounted in the measurement chamber. Prior to instrument application, this sensor measures the ambient environmental conditions. Subsequently, it detects the variations in humidity within a small volume that is hermetically sealed on one side. The digital display of the instrument's screen corresponds to the automatically calculated evaporation rate ($g/m^2/h$), which is determined by the change in relative humidity and temperature during the measurement period[333]. As the measurement area remains enclosed throughout the duration of the measurement, ambient airflow has no effect on the evaporation rate. This is one of the features that makes it extremely useful in establishing valid TEWL values.

The MoistureSC[356] meter measures surface hydration within the stratum corneum. It does this by measuring the dielectric constant of the skin, through utilizing a specific electromagnetic field at 1.25 MHz. MoistureMeterSC functionality is predicated on the capacitive layered structure of the skin. While the dry stratum corneum layer functions as an insulator, the probe and the highly conductive epidermal layer constitute the capacitor plates. The depth at which the MoistureMeterSC measures moisture fluctuates according to the thickness of the dry layer of the stratum corneum. By employing this methodology, skin hydration assessments become exceptionally precise and replicable.

MoistureD[357] is utilized to quantify the water content of specific regions of biological tissues. Noninvasive estimation of the tissue dielectric constant (TDC) converts it to a percentage water content (PWC) scale ranging from 0% to 100% on the skin in a matter of seconds. When

exposed to tissue, the MoistureMeterD Compact generates a low-power 300 MHz microwave field. By absorbing and reflecting a portion of the signal, it is possible to determine the dielectric constant, which is proportional to the water content of the tissue being measured. Water content and edema contribute to an increase in value. Finally, EpiD operates on the same principle as the MoistureD meter. MoistureD and EpiD both measure water in both the epidermis and dermis. The main difference between the two is measurement depths. In this study, the EpiD meter measured water content and oedema in the epidermis and the upper dermis (Figure 3.1, E) whereas MoistureD measures into the deeper tissues (Figure 3.1, F).

3.2.2.3 Optimization of Meter Studies

Prior to the main study measurements collection described above, two key optimization studies were conducted to ensure optimal valid readings with the meters. One, which examined various cleaning methods and whether they had a significant impact on meter readings, is discussed and shown in **Figure 2, Appendix I.** The other, assessed the variability of repeat readings for each meter at each penile anatomical site to determine optimal repeat numbers to use to record valid results and an adequate control site (**Figure 3, Appendix I)**.

3.2.3 Ex vivo barrier measures

RT-qPCR

Foreskin (FS) tissue collection and processing; FS tissue samples were collected from a subset of males. Following surgery, foreskins were separated into inner and outer tissues at the circumcision clinics by the surgeon. These were then immediately collected into DMEM collection medium supplemented with 10% heat-inactivated fetal bovine serum, 10 U-ml−1 penicillin, and 10 µg-ml−1streptomycin. The samples were then transported to the BSL2 laboratory, in the Division of Immunology at the University of Cape Town within hours. Further processing is dependent on the study used downstream (Chapter 3-5). FS tissue was examined for epithelial barrier structural protein and tight junction gene- expression using reverse transcription-quantitative polymerase chain reaction (RT-qPCR) from extracted RNA. This was the choice of method due to that fact that in another objective there has been heavy imaging of both target cells and tight junction protein. For quantification that is high specific and high throughput, we use RT-qPCR for this objective.

3.2.3.1 Primer design

Given their involvement in barrier function, we chose the genes E-cadherin, Claudin 1-5,

Filaggrin & involucrin. We used the housekeeping genes glyceraldehyde-3-phosphate dehydrogenase (GAPDH) and TATA-box binding protein (TBP), selected based on literature (refs). The primers used for the study were either selected from literature or designed using the NCBI Primer-Blast software **(Appendix I, Table 1)**. The qPCR primers were synthesized by IDT and were resuspended in TE buffer (10mM Tris, pH 8.0, 1mM EDTA) to a 100µM stock concentration, as per manufacturer instructions.

3.2.3.2 RNA Extraction

Total RNA was extracted from foreskin tissue samples using the RNeasy Plus Universal Mini Kit per the manufacturer's protocol[265]. The concentration and purity of the total RNA were determined using a NanoDrop ND8000 spectrophotometer. Further Quantification of RNA was done on the Qubit 4.0 Fluorometer with the Qubit® RNA HS Assay Kit[266] and the RNA Screentape using the Agilent Tapestation **(Appendix I, Figure 3).**

3.2.3.3 cDNA synthesis

The extracted RNA of different samples was diluted to the same concentration (125 ng/µL), and 1 µg was reverse-transcribed into cDNA with MaximaTM H Minus cDNA Synthesis Master Mix with dsDNase (Thermo scientific) and stored at −80°C. No Reverse Transcription control reactions were performed alongside to assess for genomic DNA contamination of the RNA samples. A non-template control (NTC) reaction was also included to assess for reagent contamination. Sample 1666PCR027 had no tissue (i.e the tube was empty) and was therefore used as a negative extraction control. Samples with concentrations outside the functional range for the TapeStation assay were re-quantitated and re-analyzed. Samples 1666PCR029, 1666PCR032, 1666PCR066 and 1666PCR072 were degraded as can be seen with low RINe values. Therefore, more samples were selected to replace these samples together with their pairs (both inner and outer samples) Overall, there were only 4 samples that were degraded for no with no obvious apparent explanation. Finally, for the qPCR inhibitor assay – 12 samples were selected that had slightly lower A260/A230 ratios than the rest of the samples and 12 samples that had good ratios and a qPCR assay was ran to determine whether any qPCR inhibitors may be present in these samples. None of the samples contain inhibitors, Figure 3, Appendix I shows RNA extraction quality check (QC) using nanodrop, Qubit and Tape Station.

3.2.3.4 Primer Annealing Temperature (Ta)

A range of annealing temperatures (55.3-65.3°C) were tested using multiple qPCR experiments

(**Appendix I, Table 2**). A dissociation step was included at the end of the PCR run. The choice of optimal temperature was based on not having non-specific amplification.

3.2.3.5 Determination of optimal primer concentration

Varying amounts of the forward and reverse primer (**Appendix I , Table 3**) were mixed with pooled cDNA to select optimal concentrations summarised in **Appendix I , Table .4.**

3.2.3.6 qPCR reaction efficiency

PCR efficiency was determined using standard curves (shown in **Appendix I, Figure 4)** generated with -2 and 5-fold dilutions of the pooled cDNA template (from all samples) for each target gene. Each assay was run in triplicate with each sample consisting of 2µl cDNA, both forward and reverse primers at the optimized final concentrations, 5µL 2X PowerUp SYBR Green Mastermix (Thermo Fisher) in a total reaction volume of 10µL. An NTC was included for each assay as a negative control. Reactions were performed on the QuantStudio 12K Flex PCR System (Applied Biosystems) using the optimized cycling parameters[358] (section 5.4). Standard curves were generated by plotting the CT values against the log of each serial dilution.

3.2.3.7 Reference gene validation

Reference genes were validated using using the web-based tool RefFinder[359] which runs four well-established algorithms (GeNorm, BestKeeper, NormFinder and comparative delta-CT) to simultaneously compare and rank all candidate reference genes (from most to least stable).

3.2.3.8 RT-qPCR Assays

qPCR was performed in a total volume of 10ul reactions utilizing 2 µl of each cDNA sample diluted 1:100 as template, 5µl of 2x PowerUp SYBR Green I Mastermix (Thermo Fisher), and both the forward and reverse primers at the optimized final concentrations. Each reaction was run in triplicate. Reactions were performed on the QuantStudio 12K Flex Real-Time PCR System (Applied Biosystems) using the following cycling parameters: UDG activation at 50°C for 2 min; initial denaturation at 95°C for 2 min followed by 40 cycles of 95°C for 15 secs, 15 sec and 61.3°C. A melt curve analysis was performed on all reactions at the end of the PCR run using default parameters.

3.2.3.9 Data Analysis

***In vivo* meter data**

Averaged repeat data points measured at each penile anatomical site (inner, outer foreskin, glans, and shaft). In order to compare the different sites across the penis, repeat readings from each meter were normalized using the matching hip control sites to transform the results to a relative form. The groups of each meter measures were divided by its hip control value. Normalized values were compared(hence the scale) between different penile anatomical sites. All statistical analysis was conducted using R statistical computing environment[360]. Data was adjusted for the effect of humidity and room temperatures which were collected at the time of measurements. *t*-test was used to compare measurements across the different sites in STI negative men, and between STI positive versus negative groups.

***Ex vivo* qPCR data**

Data were entered in an Excel spreadsheet. The data for target gene expression were normalized by a combination of two reference genes (GAPDH and TBP) found to be the most stable. Normalized Relative gene expression values of target genes were calculated using the Pfaffl Method[361]. Mann-Whitney test was used to compare these target genes' mean normalized expression values between inner versus outer foreskin tissue in STI-negative men, and between STI positive versus negative groups.

3.3 RESULTS

3.3.1 In Vivo Barrier Function

3.3.1.1. Different anatomical sites show different barrier function and hydration/moisture status

In order to compare the different sites across the penis, repeat readings from each meter were normalized using the matching hip control sites to transform the results to a relative form. The groups of each meter measures were divided by its hip control value. Normalized values were compared(hence the scale) between different penile anatomical sites. Water content of the epidermal and dermal layers showed similar patterns by both Moisture and EpiD meters. Using both meters, the inner foreskin tissue (median 71.2%) and glans (median 69.7%) both measured significantly higher water content (%) than the shaft (median 62.1%) (Figure3. 2A1and 2). Water content (%) at both inner foreskin and glans were not significantly different. *In vivo* measurements of the barrier function of the penile glans, inner foreskin, and shaft show that the TEWL of the inner foreskin (median 27.6 g/hr/m^2) and glans (median 22.3 g/hr/m^2) of the uncircumcised penis were higher compared to the shaft (median 16.2 g/hr/m^2) ($p<0.0001$, Figure 3.2.A4). This was associated with higher SCH in the inner foreskin (median 92.3 au), which was significantly ($p<0.0001$) higher than both the glans (median 68.4 au) and shaft (median 52.3 au, Figure 3.2.A3). There was no significant difference between the glans and shaft surface hydration as measured by the MoistureSC meter (Figure3. 2.A3).

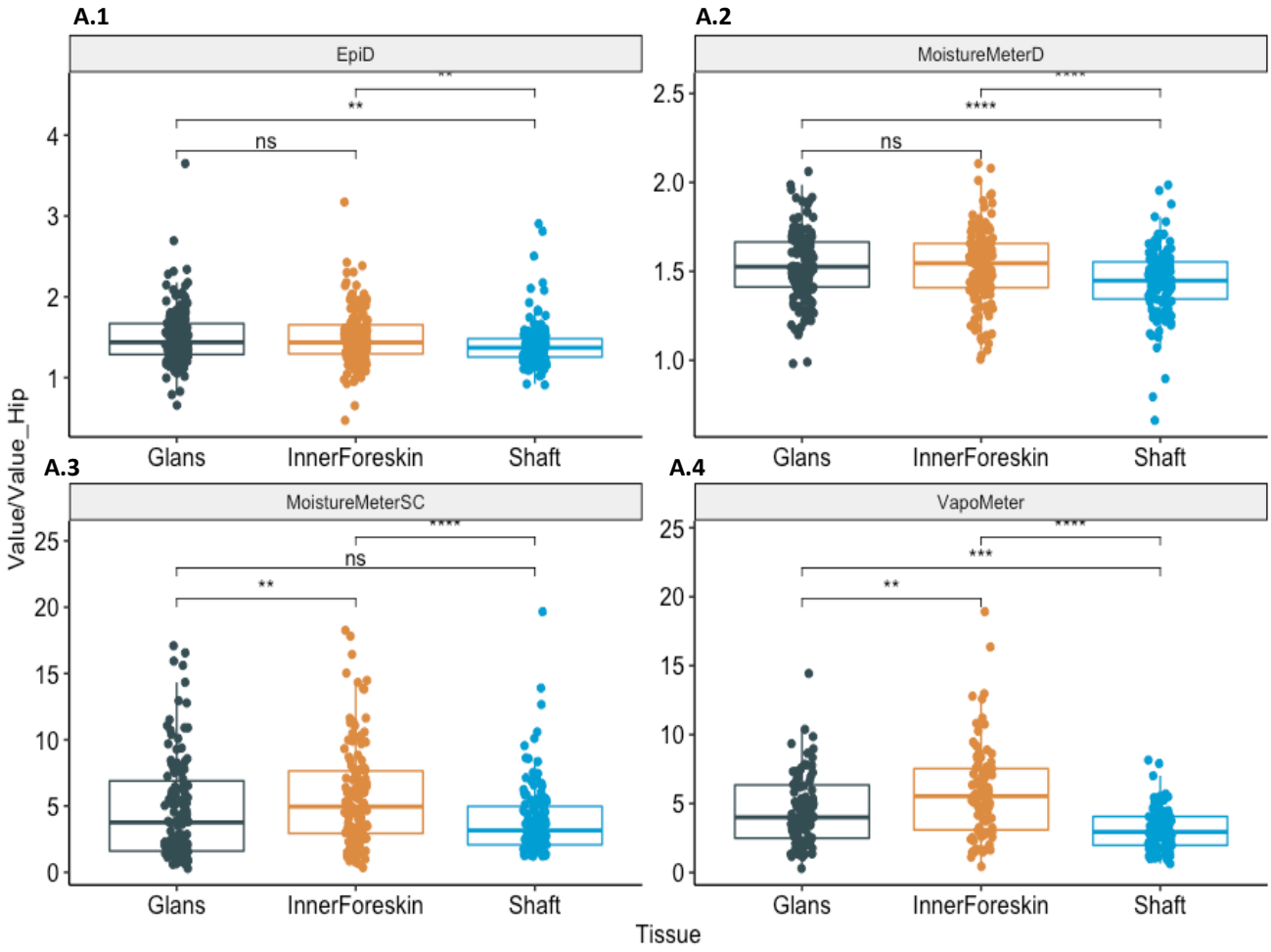

Figure 3. 2Barrier function meter measurements in males in South Africa (n=203) before MMC (normalised by hip) in various penile anatomical sites.

Graphical representation of the various proxy measures for barrier function within various parts of the penile anatomical sites. A1 an A2 (n=203) shows both dermal and epidermal readings of water content expressed in normalized % in the glans, inner foreskin, and shaft respectively. A3 and A4 are readings restricted to the stratum corneum of the various sites, the surface hydration (A3 n=203) and the transepithelial Water Loss (TEWL n=184, A4).

3.3.1.2 Durable changes in penile barrier integrity months post circumcision

We measured penile barrier integrity longitudinally in a subset of participants, where pre- and post-MMC measures were taken (n=16). Measures showed that the hydration of the glans using Moisture SC and D (32.4 vs 67.8 au, p=0.013 and 58.8 vs 67.9%, p=0.001) significantly increased post-circumcision, with TEWL remaining unchanged in the first 3 months When looking at the data across all follow-up time points (Figure 3.3), as pre-MMC (Visit 1), 2 weeks post-MMC (Visit 2), 3 months (Visit 3) and 6 months (Visit 4), there was an upward trend for moistureSC of the glans (Figure 3.3. On the other hand, after 24 weeks post-VMMC, the TEWL

in the glans (median 32.3 vs 16.4 g/hr/m^2, p=0.011) significantly decreased to almost match the shaft readings.

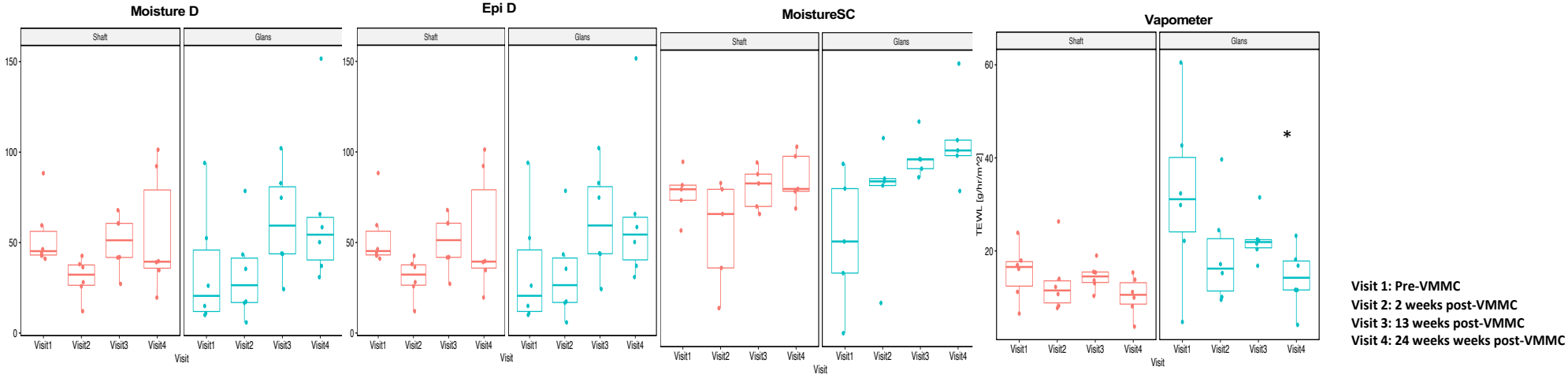

Figure 3. 3 Durable changes in penile barrier integrity months post-circumcision.

Longitudinal measurements in a single cohort of males (n=16, all aSTI negative) from pre-circumcision (Visit 1), 2-weeks (V2) and 3 months post circumcision. Readings from both the stratum corneum and epidermis with dermis are shown, left water content (%), middle surface hydration(au) in the stratum corneum and right TEWL. Follow-up measures are only in the shaft and glans and post circumcision most if not all the foreskin is removed. After 24 weeks post-VMMC, TEWL in the glans significantly decreased to match the lower (pre-circumcision) in shaft reading (p=0.011).

3.3.1.3 The impact of asymptomatic STI status and penile glans, shaft & foreskin sites before MMC

203 males were included in this analysis, of which 49 to had at least one detectable STI in first-pass urine, including *Chlamydia trachomatis, Neisseria gonorrhoeae, Trichomonas vaginalis* and *Mycoplasma genitalium* as described in chapter 2. For this analysis, asymptomatic STI-positive men were grouped together (red) and were compared to the rest of the men who tested negative (blue, Figure 3.4). The MoistureSC showed a significantly higher in SCH (68 vs 101.2 au, p=0.003) in the glans of STI-positive compared to those who are STI-negative. The same higher readings were observed in the inner foreskin, although not significantly. There were no differences between shaft readings in the aSTI negative versus positive groups. Additionally, vapometer readings showed no differences in TEWL in all the anatomical sites between the two groups. The other meter machines, which measure both epidermal and dermal water content readings, did not show any differences in measures in the various penile anatomical sites by STI status.

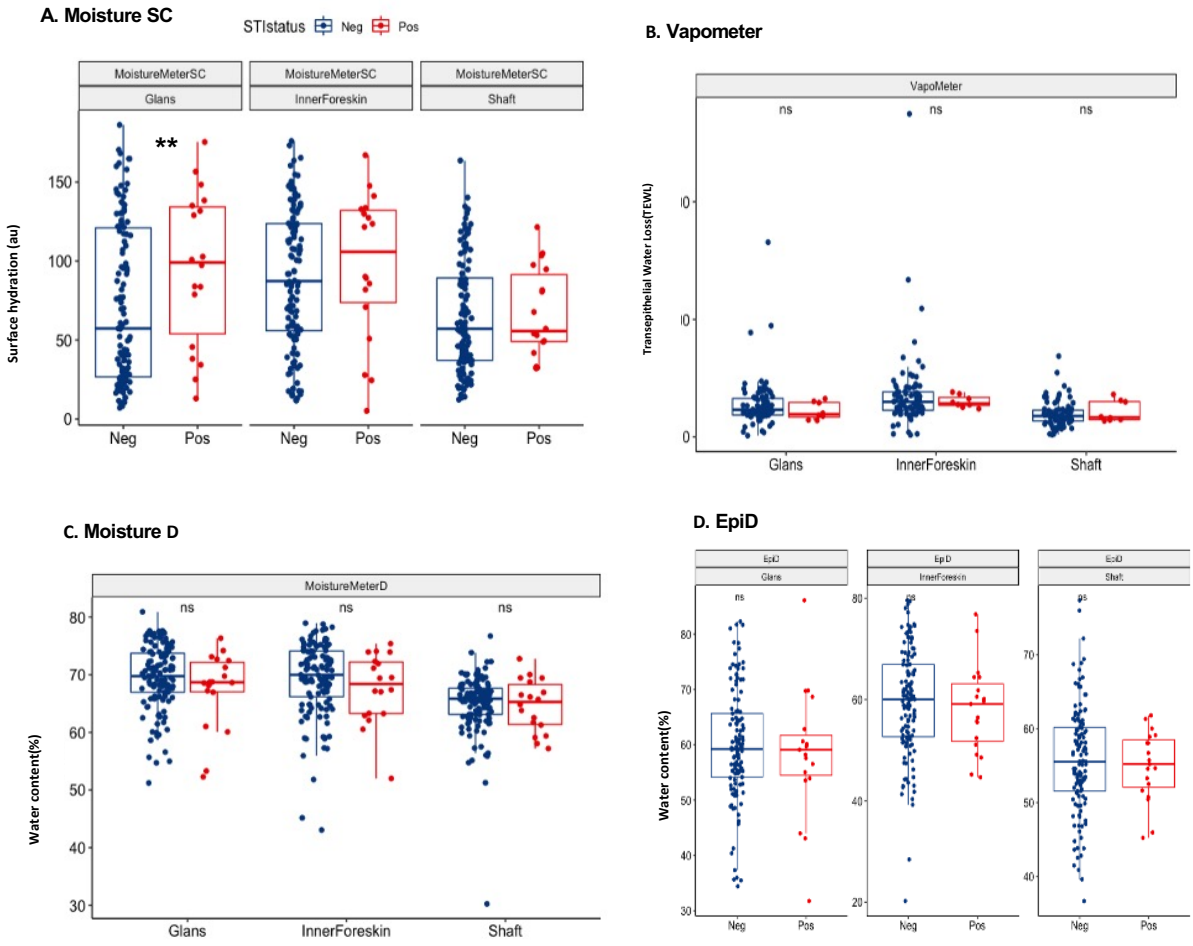

Figure 3. 4 aSTI infected men have increased SC moisture in their penile glans in vivo.

Barrier function by STI status for the four-meter machines. Epidermal and dermal readings of various meter readings in the glans, inner foreskin, and shaft respectively. Top left, surface hydration (SFH) measures in the various anatomical sites, followed by Vapometer showing TEWL readings for the same anatomical sites on the top right. Bottom left to right shows the Moisture D and EpiD which both measure epidermal and dermal water content (%). Panels show aSTI neg (blue) and aSTI (red) readings in the various anatomical sites, all taken at pre-circumcision (n=203, aSTI pos=49).

In summary; i) Prior to medical penile circumcision, the penile glans and inner foreskin have a significantly lower barrier function(higher TEWL) as compared to the penile shaft in aSTI negative males, ii) The glans and inner foreskin have significantly higher moisture as reflected by higher SCH (surface hydration readings), iii) medical penile circumcision results in an improved barrier function in the penile glans long term following the procedure, and finally, iv) The presence of any aSTI results in increased moisture within the SC lining the penile glans, thus rendering it more "moist" compared to those without an aSTI.

3.3.2 Ex Vivo Barrier Function

3.3.2.1 Lower expression of epithelial barrier proteins in the inner versus outer foreskin tissue in STI-negative men

The mRNA expression of Claudin 1,2,4,5, E-cadherin, Filaggrin 1,2, and involucrin was compared between the inner and outer foreskin tissue of STI neg men via RT qPCR (Figure 3.5). mRNA expression of Claudin-2 (median mean normalized expression (MNE)= 1.05 vs 1.91; p=0.001) , Claudin-4 (median MNE 0.91 vs 2.47, p=0.003) , Claudin-5 (median MNE 1.28 vs 2.54, p=0.042) , E-cadherin (median MNE 0.97 vs 1.54, p=0.0009), and Filaggrin 2 (median MNE 1.04 vs 3.83, p=0.0001) were significantly lower in the inner foreskin compared to the outer. Therefore, most of the assessed proteins show significant differential expression between the two tissue sites, except Claudin-1, and involucrin

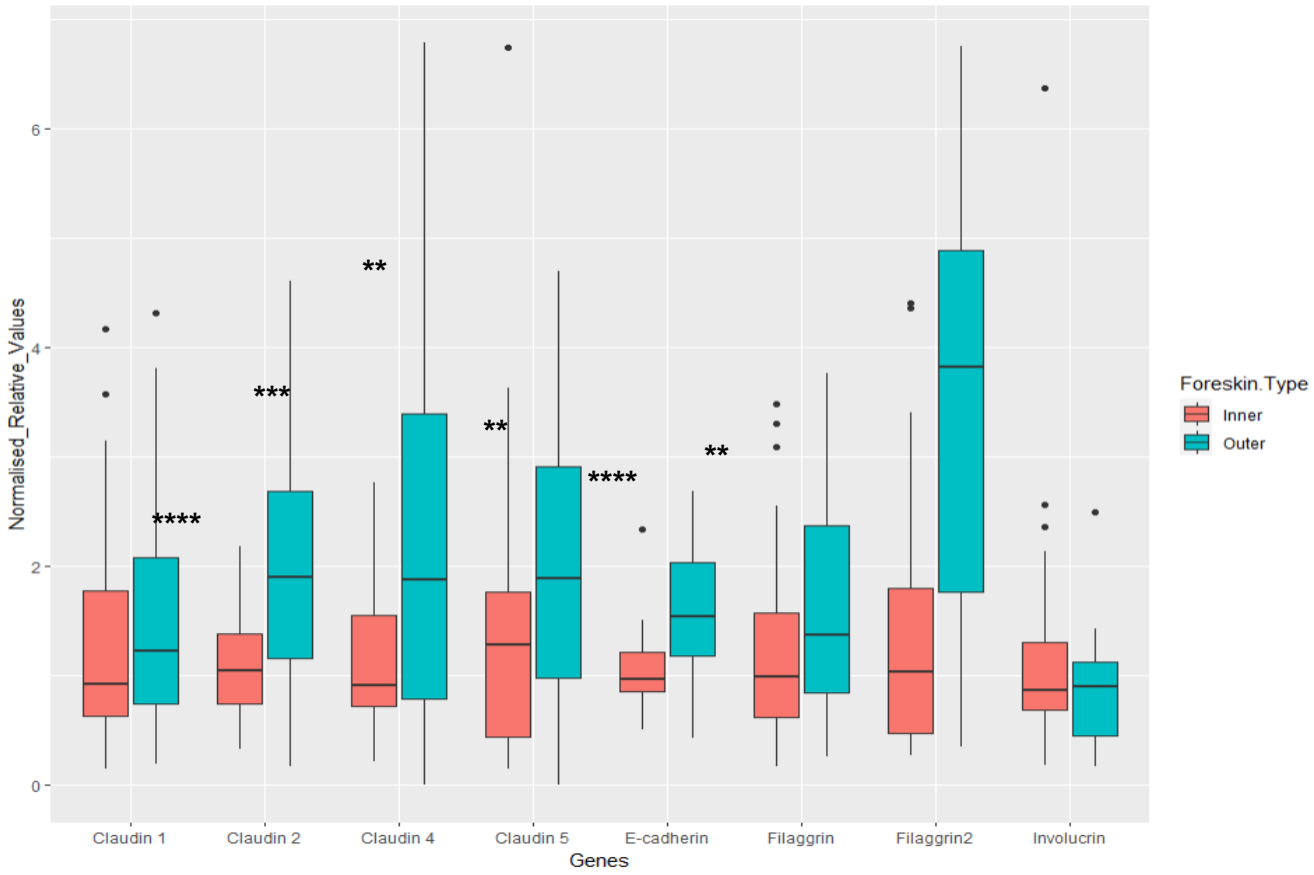

Figure 3. 5 Inner vs outer foreskin epithelial barrier proteins gene expressions in STI negative men.

mRNA expression of Claudin 1,2,4,5, E-cadherin, Filaggrin 1,2, and involucrin was compared between the inner (n=48 tissues) and outer (n=48 tissues) foreskin tissue (total n=96) of aSTI negative men. The inner foreskin had significantly lower expression of all the markers except Claudin-1 and involucrin.

3.3.2.2 Impact of aSTI status on foreskin epithelial barrier proteins mRNA expression

mRNA expression of Claudin 1, 2, 4, 5, E-cadherin, Filaggrin 1,2, and involucrin were compared between aSTI-negative men (n=24) and age-matched aSTI-positive men for any STI (n=24) in both inner and outer foreskin separately (i.e. N=96 total samples). Unsupervised clustering analysis did not show any clustering by aSTI status (Figure 3.6A). Thus, showing that there is no difference in expression of any of the TJ proteins by aSTI status in the combined foreskin tissue(both inner and outer). When this analysis was sub stratified by foreskin tissue site, as shown in figure 3.6B, expressions were compared between aSTI positive versus negative men in the inner foreskin (figure 3.6B plot A) and the same in the outer foreskin tissue

(figure 3.6B plot B).In both sites, the presence of an aSTI did not significantly affect the TJ expressions. Further analysis was done to compare the differential expression between the inner and outer foreskin sites by aSTI status. This was motivated by the various studies examining and reporting on possible explanations for the differences in HIV susceptibility between inner and outer,as this is still a gap in knowledge in the field. However, when comparing the differential mRNA expressions between the inner and outer foreskin tissue in aSTI positive men, claudin-1 and filaggrin 1 showed a significant difference between the two tissue sites, with the inner foreskin showing lower expressions (Figure 3.7). Claudin-1 was significantly less expressed (p=0.009) in the inner (median MNE 0.66 (IQR 0.36-0.91)) versus the outer (median MNE 1.50 (IQR 0.82-1.66)) foreskin tissues in those with any aSTI compared to those without. Additionally, filaggrin-1 was significantly less (p=0.04) expressed in the inner (median MNE 0.59 (IQR 0.28-0.98)) versus the outer (median MNE 1.16 (IQR 0.71-4.10) foreskin tissue in the presence of an STI.

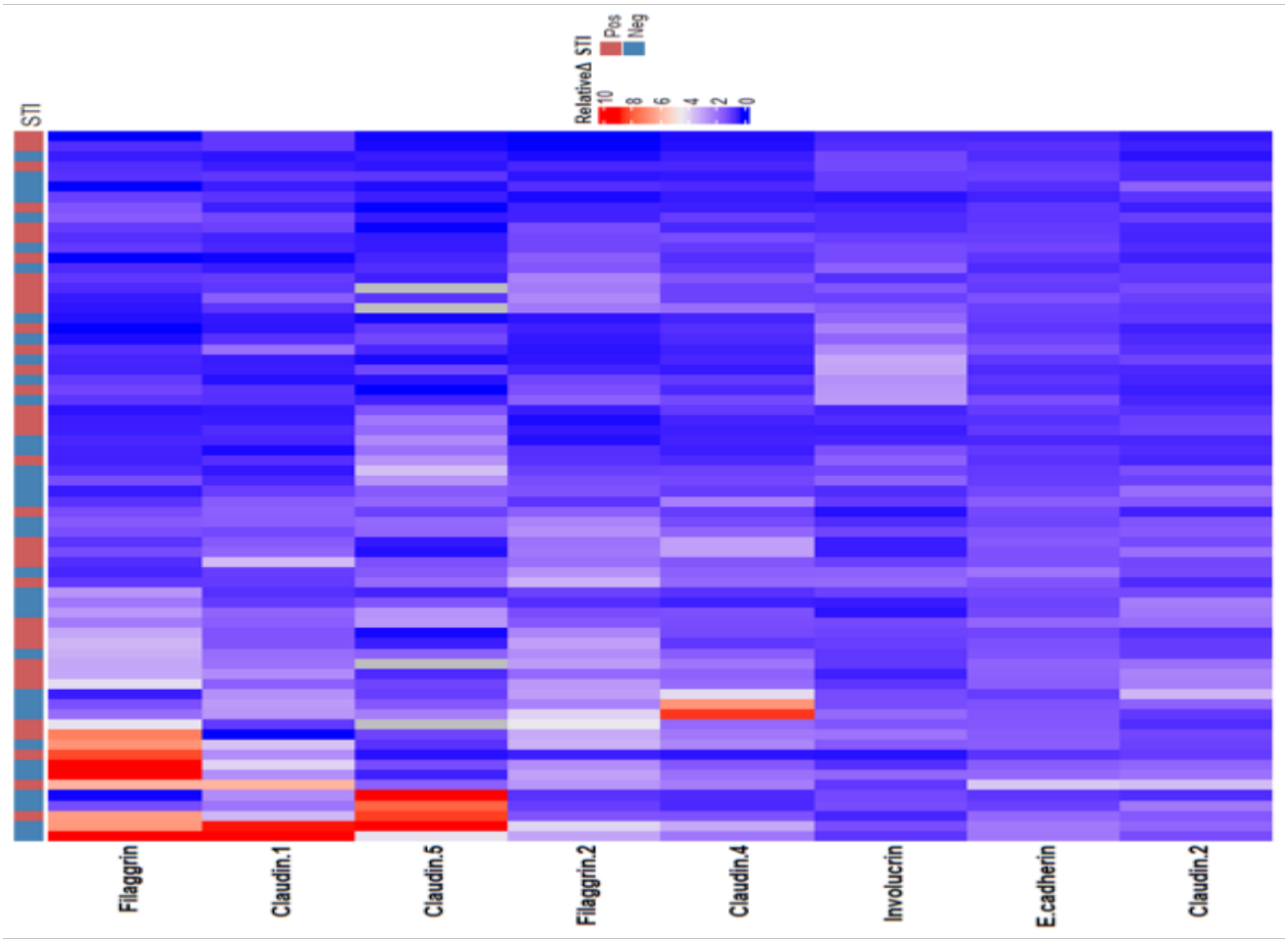

Figure 3.6. A A Heatmap of epithelial barrier protein mRNA expression by aSTI status. Unsupervised hierarchical clustering analysis of mRNA barrier proteins expression between STI positive and negative show that there is no clustering by STI status (using R). mRNA

expression levels are indicated using a color scale, ranging from purple (low) to red (high). The columns are the individual participants and their STI status (red=STI pos, blue-STI neg), and the rows mRNA expression of Claudin 1, 2, 4, 5, E-cadherin, Filaggrin 1,2, and Involucrin in whole tissue foreskins (combined inner and outer)

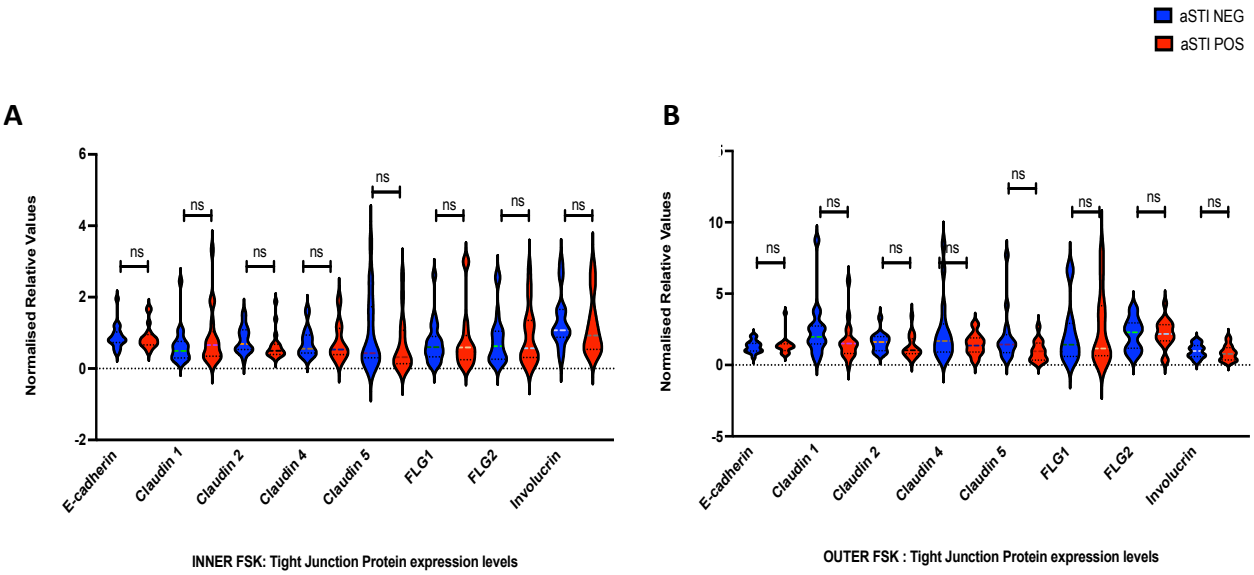

Figure 3.6. B Epithelial barrier protein mRNA expression by aSTI status

(A)The inner foreskin gene expression between men with and without aSTI, (B)the outer foreskin.

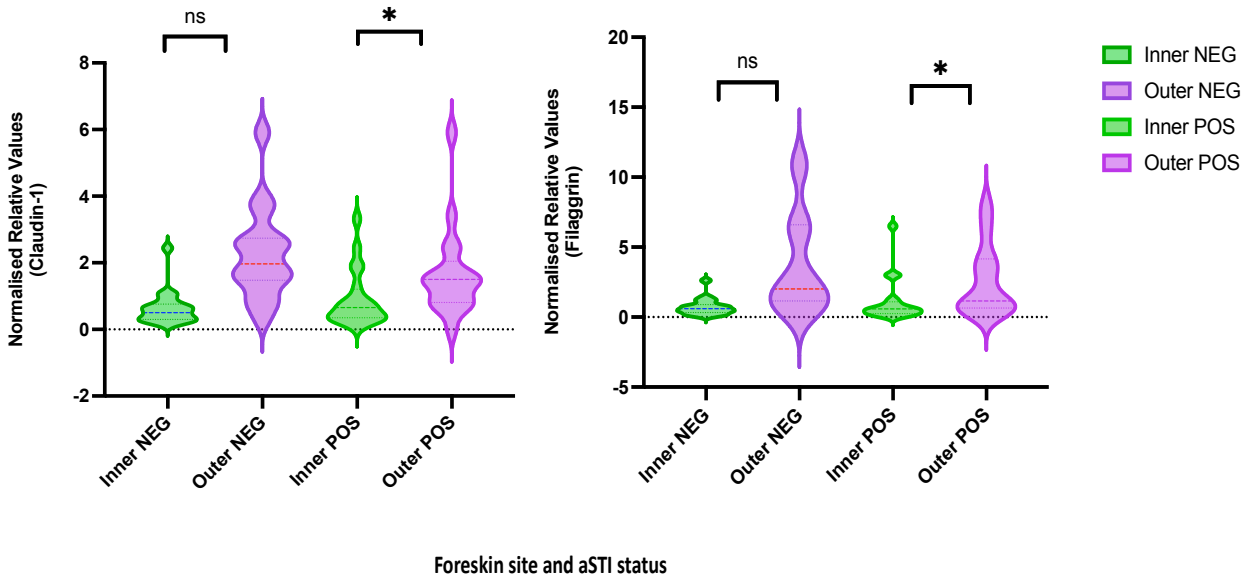

Figure 3.7 1 Impact of aSTI status on differential epithelial barrier proteins.

mRNA expression in the inner vs outer foreskin. mRNA expression of Claudin 1, 2, 4, 5, E-cadherin, Filaggrin 1,2, and Involucrin was compared between the inner (n=24) and outer (n=24) foreskin tissue (n=96) in sTI pos men (B)compared to the STI neg group,

3.4 DISCUSSION

Removal of the penile foreskin has been shown to drastically reduce HIV risk in males who have penetrative sex[277,362]. Following this finding, several studies have examined foreskin tissue to identify what factors render it highly susceptible to HIV. Many of the studies have compared the inner and outer foreskin keratin thickness and HIV target cells[178,182,276,322]. Very few studies have examined factors contributing towards penile epithelial barrier function. The pathophysiologic mechanisms associated with compromised barrier function in the genital tract are still unclear. This study is the first to examine epithelial penile barrier function both in vivo and by barrier protein gene expression at various penile anatomical sites.

The inner foreskin has the least intact barrier function and mRNA expression of key epithelial barrier function structural and junctional proteins.

Here, using the gold standard proxy measure for barrier function, TEWL, we show that relative to both the penile shaft and glans, the inner foreskin has the lowest barrier function. This is true regardless of STI status. Prior studies have suggested the inner foreskin to be more susceptible to HIV infection. These studies demonstrated a higher abundance of immune HIV target cells and more virus penetration in and on the inner aspect of the foreskin than the outer aspect of the foreskin[182,276,277,322] Increased viral penetration was demonstrated in some studies following in vitro HIV challenge studies in cultured foreskin and penile tissue [182,276,277,322]. The data shown in this PhD suggest, that apart from the abundance of target immune cells, a naturally compromised/less intact barrier function could be another mechanism explaining the increased susceptibility to HIV-1 infection at this tissue site. It has been shown that exposure to HIV-1 may lead to impairment in mucosal epithelium's barrier function, which could result in the translocation of HIV-1 and/or luminal bacteria that could serve as the source of immune activation during HIV-1 infection[363]. Therefore, this implies that a compromised barrier function is important in the initial events of mucosal HIV-1 infection. The penile glans also has higher TEWL relative to the shaft, suggesting less intact barrier function. Although studies of the penile glans tissue are limited, those conducted in cadavers have shown that the glans is the most susceptible site of HIV-1 infection in the penis[182], and therefore a compromised barrier function of this mucosal site could be one explanation for this.

Associated with these much higher TEWL readings in the inner foreskin and glans compared to the shaft, were higher SCH measures in the uncircumcised penis. Here, we find that the inner foreskin is the moistest anatomical site of the penis. This could simply be explained by the anatomical configuration of this mucosal site. The inner foreskin is not often exposed to air[182], therefore the described equilibrium existing between the outermost layer (SC) and the environment[333] would be such that the gradient does not favor the movement of water to the outside as compared to the glans and the shaft. Whether a linear relationship between SCH and TEWL exists, since TEWL depends on the epidermal-to-air water pressure gradient, has been explored previously in other tissues, although not in the foreskin[316,329,333,353]. Our data is, however, consistent with a recent study that showed that a significant positive nonlinear correlation ($p < 0.001$) between SCH and TEWL in the hands of males that occurred when SCH exceeded a threshold level[329], implying that conditions resulting in increased SCH may in part account for elevated TEWL values. Whether the inner foreskin and glans having higher TEWL because they have high SCH is unknown and would require further investigation. Additionally, higher moisture readings in the uncircumcised penile glans and inner foreskin could also explain the relatively increased risk of HIV susceptibility reported at these sites. Previous studies have hypothesized one of the reasons underlying this observed increased risk to be due to penile wetness in the uncircumcised penis. This was thought to be due to increased risk of penile trauma during sex and increased length of adherence time by HIV virions to the surface of target cells if the penis is more “wet”[364].

One of the key components defining the epithelial barrier is it’s structural proteins, such as filaggrin, involucrin, and proteins involved in the formation of TJs and AJs, such as claudins and cadherins[323]. To our knowledge, our study is the first to examine the differences in the mRNA expression of claudin 1,2,4,5, E-cadherin, filaggrin 1,2, and involucrin in the inner versus outer foreskin tissue in both the absence and presence of common aSTIs. Our study shows that the inner foreskin has a significantly lower expression of Claudin-2,4,5, E-cadherin and Filaggrin 2 in the inner foreskin tissue compared to the outer foreskin tissue. The precise mechanisms regulating FLG expression are still not fully comprehended; however, its importance in maintaining the integrity of the skin barrier has been established through the correlation between null mutations in the FLG gene and two exceedingly prevalent skin diseases in humans[208]. FLG mutations are acknowledged as a significant risk factor for Alzheimer's disease (AD)[365] ,and the gene is also implicated in Ichthyosis vulgaris

syndrome[366]. FLG2 protein levels are also reduced in the SC and epidermal regions of individuals with AD[367,368], individuals with dandruff (SC) as evidenced by a lipid raft disruption model[277] and in ichthyosis peeling skin[369,370] Indicating that FLG2 has a significant function in maintaining the balance and integrity of the epidermis and barrier formation. In our study, Filaggrin 2 is differentially expressed between the two tissue sites in the absence of an aSTI, with the inner foreskin expressing lower levels as compared to the outer. This further suggests that the inner foreskin naturally has a less intact barrier function than the outer.

We found that mRNA expression of E-cadherin is significantly lower in the inner versus outer foreskin tissue. This is an important finding as it has been recently established that E-cadherin is important for cell-to-cell adhesion and is crucial for assembling other junctional complexes such as desmosomes, gap junctions, and tight junctions. Its contribution to defining the epidermal barrier has been demonstrated by showing increased TEWL leading to perinatal death associated with early loss of E-cadherin[268]. Therefore, the lower expression of E-cadherin in the inner versus outer foreskin could further explain the observed increase in TEWL readings of the same men and explain the increased susceptibility of the inner foreskin to HIV-1 infection.

Claudins are tight junction membrane proteins that are expressed in all known epithelia and endothelia. Furthermore, in all epithelia, there appear to be multiple different claudins expressed simultaneously. However, some Claudins are expressed in some organs more than others. Claudin-2 and 4 are predominantly expressed in the kidney epithelial and Claudin-5 is predominantly in endothelial cells in the brain[234,371]. Our study shows that the inner foreskin tissue has significantly lower mRNA expression of claudins 2,4 and 5, these are all important for determining tight junction permeability. Notable, is that claudin-1 showed no differential expression between the two-issue sites without an aSTIs. Given that Claudin-1 is a major determinant of barrier function[236], one would have expected lower expressions in the inner foreskin in concert with all the other findings described so far. Finally, involucrin is a key scaffolding protein in the formation of the mature cornified envelope that surrounds keratinocytes in the SC[216]. The fact that gene expression of this protein is at the same level between the two tissue sites further validates all the studies that have compared keratin thickness in the inner versus outer foreskin and found no difference. Additionally, single involucrin knockout mice models showed no significant differences in response to physical and biochemical barrier challenges.

This PhD study shows, at both an *in vivo* and molecular level, that the inner foreskin is much more compromised in its barrier function and integrity. These findings could be part of the explanation for the observed increased susceptibility for HIV-1 infection of the inner versus outer foreskin tissue[277] and why the removal of this tissue is associated with a significant reduction in HIV-1 risk (refs).

Medical penile circumcision is associated with changes in the penile barrier function; a new consideration for the observed protection

The impact of foreskin removal on lowering HIV acquisition is well described[158,372,373], but molecular events leading to HIV acquisition are unclear. The glans may be an important portal of entry for HIV during insertive sex[195]. In this study, we show that medical penile circumcision improves the barrier function of the glans. In the first three months following circumcision, there is a significant increase in surface hydration measures in the glans with no obvious trends or significant changes in TEWL readings initially. This increased hydration may be due to acute post-surgical trauma-associated tissue changes. By 6 months post-circumcision, a significant decrease in TEWL and associated drop in the water content of the penile glans occurred, although this was not significant.

These findings suggest the following: 1) the changes associated with medical penile circumcision in the glans and shaft is time dependent. 2) the mechanisms underlying the associated risk reduction in the circumcised penis could be partly explained by the fact that circumcision improves barrier function in the glans. A major limitation of this study, however, is the significant loss of follow-up 6 months post-VMMC which was due to the lockdown during the COVID pandemic, resulting in a small sample size at this time point. Long-term follow-up was only in those who were aSTI negative, coincidently, as no aSTI positive men presented for follow-up at all three visits post VMMC.

Asymptomatic STIs alter the barrier components of the inner foreskin and glans.

This PhD shows two key findings when examining the effect of aSTIs on the penile epithelial barrier; 1) the presence of an aSTI significantly increases penile glans moisture as evidenced by increased SCH readings *in vivo*, 2) the presence of an aSTI is associated with differential mRNA expression of claudin 1 and filaggrin 1 in the inner versus outer foreskin tissue.

Claudin-1 has been shown to be major determinant of epithelial barrier function and mutations in Filaggrin1 have been associated with major dermatological pathologies, both resulting in significantly compromised epithelial barrier when knocked out. When we examine the effect

of an aSTI on the mRNA expression of various structural and junctional barrier proteins was examined, only claudin-1 and filaggrin-1 were significantly impacted. Important to mention is that these changes could also be due to the small sample size and perhaps the expression of these two proteins could be differentially expressed independent of aSTI status if the sample expression is due to the positive STI status, this could be highlighting one of the possible mechanisms explaining how aSTIs cause changes that could increase risk of acquiring HIV-1.

In summary, our study shows the inherent compromised epithelial barrier function of the inner foreskin tissue, both in vivo and at a molecular level. It sheds light on potential mechanisms underlying the reduced HIV acquisition risk following VMMC, which is an increased penile glans barrier function (a site that happens to be the most susceptible across all the susceptible penile sites). It is shown that aSTIs compromise the epithelial barrier function by decreasing the expression of structural and junctional barrier proteins. These could all be used as potential targets for deriving alternative prevention strategies for men, such as gel products that could be designed to target structural and junctional epithelial barrier function or other molecular factors determining TEWL and moisture of the human penis.

CHAPTER 4

Histopathology and immune cell measurements in foreskins from asymptomatic STI positive and negative male participants

Table of Contents

4.1 INTRODUCTION 93

4.2 METHODS 95

4.2.1 Cohort description 95

4.2.2. Sample collection and processing 95

4.2.3 Histopathology 95

4.2.4 Immunophenotyping of lymphocytes in the foreskin by Flow Cytometry 97

4.2.4.1 Cell isolation by liberation of spontaneously migrating cells (crawl assay) ... 97

4.2.4.2 Lymphocyte characterization 97

4.2.5 Data analysis 98

4.3 RESULTS 98

4.3.1. Prevalence of immune cell infiltration in the foreskin by STI Status 98

4.3.2 The effect of aSTIs on immune cell abundance in the foreskin epidermis, papillary and reticular dermis ..... **Error! Bookmark not defined.**

4.3.3 The effect of STI status on stratum corneum size and spongiosis 103

4.3.4 Immunoqualitative characterization of lymphocytic infiltrates in the foreskin tissue ..... **Error! Bookmark not defined.**

4.4. DISCUSSION 109

4.1 INTRODUCTION

There are still very limited studies on the effect of common asymptomatic STIs on immune cell abundance in the inner and outer foreskin. However, the majority of studies to date have been conducted in those with ulcerative STIs. The purpose of this chapter is to evaluate inflammatory cell infiltrates by locating and quantifying various immune cells in the epithelia of both the inner and outer foreskin, the presence or absence of spongiosis, the thickness of the overlying layer of keratin, and how these are impacted by the presence of one or more of common STIs (*Chlamydia trachomatis*, *Neisseria gonorrhoeae*, *Trichomonas vaginalis,* and *Mycoplasm genitalium*). An improved understanding of the immune cellular composition & localisation of this immune profile in the foreskin, particularly in the presence versus absence of aSTIs, may provide insight into the association between STIs and the protective mechanisms of circumcision.

The male genital tract is a point of entrance for a variety of bacterial and viral sexually transmitted pathogens, including such as human papillomavirus (HPV)[374], *Chlamydia trachomatis*[375] or *Neisseria gonorrhoeaee* [309]. Moreover, as mentioned earlier in Chapter 1, human immunodeficiency virus type 1 (HIV-1) has been shown to infect numerous male genital tract components, including the foreskin[177,195,376–379]. Medical penile circumcision protects males against various sexually transmitted infections (STIs), such as herpes simplex virus (HSV)-2 and further reduces the risk of heterosexual males contracting HIV[279,380]. In light of these findings and the additional observation that an increased foreskin surface area is linked to a heightened susceptibility to HIV-1 infection[172], the foreskin appears to play a critical role in uncircumcised men acquiring STIs.

Thus, it is critical to comprehend the biological mechanisms through which the presence of the foreskin may heighten the risk of contracting STIs. Several mechanisms underlying this observation have been proposed, including that the foreskin contains several HIV target cells permissible to infection. Additional research has demonstrated that the cellular density of the foreskin may exhibit variability in response to the presence of sexually transmitted infections (STIs), including chlamydia and gonorrhea[116,381–383]. Furthermore, a number of epidemiological investigations have documented an elevated frequency and prevalence of HIV infection among those who have STIs[114,116–118,382–384]. There is, however, limited data regarding the effect of common asymptomatic STIs (aSTIs) on the cellular immunologic composition of the foreskin. This chapter will begin to address the cellular composition of the foreskin by

applying standard histological analysis along with flow cytometry of isolated cells. For a recap, foreskin anatomy has been previously described in **Chapter 1, Section 1.**

4.2 METHODS

4.2.1 Cohort description

The study cohort is described in **Chapter 2 , Section 2.2.1.**

4.2.2. Sample collection and processing

Foreskin sample collection and processing was described in **Chapter 3, Section 3.2.3.** Foreskin tissue samples were separated into inner and outer, and then dissected into pieces sized 0.5cm x 0.5cm and stored in OCT at -80°C. A portion of the tissue was used for cell isolation for lymphocytes immunophenotyping. *Chlamydia trachomatis, Neisseria gonorrhoeae, Trichomonas vaginalis* and *Mycoplasm genitalium* were diagnosed using multiplex PCR as described in **Chapter 2, Section 2.2.3.**

4.2.3 Histopathology

Upon thawing of samples at room temperature, samples were fixed in 10% formalin on the Leica TP 1020 Processor in cassettes. Tissue pieces were then embedded in paraffin blocks. Three 5µm thick paraffin sections were cut using a microtome (Leica Microtome Sliding 2000R), mounted, and stained with hematoxylin & eosin (H and E) for differentiation of the epithelial and stromal microanatomy and assessment of inflammatory infiltrates. The tissues were examined on an Olympus BX43 microscope by a dermatopathologist who was blinded as to STI status. Immune cells were counted manually in squared millimeters in areas identified as hotspots. Hotspot areas were determined as follows: by identifying the region with the most immune cells on 200x magnification, on further magnification (400x magnification) in this region cells were counted in four (4) sequential 400x fields (i.e. in a square).

An ordinal scoring system was developed to assess four main parameters. Variables were assessed as previously described[60]:

- **Spongiosis:**

0 = Absent

1 = Mild (intercellular bridges present, <25% the thickness of a resting lymphocyte)

2 = Moderate (intercellular bridges present, 26-100% the thickness of a resting lymphocyte)

3 = Severe (intercellular bridges present with bullous formation)

- **Intensity of immune cell infiltrates per square millimeter.** Immune cell infiltrates were defined as accumulations of lymphocytes (identified by their mononuclear morphology), neutrophils (identified by their multilobulated nuclei), or 'other' (plasma cells, eosinophils) by methods described below. 0 = 0-20 inflammatory cells / mm2

1 = 21-50 cells / mm2

2 = 51-100 cells / mm2

3 = >100 cells / mm2

- **Number of absolute individual cell types (per mm^2):**

Plasma cells = Mononuclear inflammatory cells with an amphophilic cytoplasm, eccentric nucleus, and clock-face type chromatin. These are differentiated B-lymphocyte cells capable of producing immunoglobulins[203].

Neutrophils = Inflammatory cells with multilobulated nucleus (3 or more lobes connected by fine nuclear material strands) with cytoplasmic granules. These are granulocytes containing azurophilic granules (lysosomes) and specific granules involved in acute inflammatory response to bacterial infection and removal of the bacteria by phagocytosis[203].

Eosinophils = Inflammatory cells with a bilobed nucleus and the cytoplasm containing eosinophilic granules. These are mucosal tissue-residing leukocytes. Blood and bone marrow eosinophils are recruited to the sites of immune response during Th2-type inflammation[203].

Lymphocytes = Mononuclear inflammatory cell with a round-to-ovoid dense nucleus and minimal pale basophilic cytoplasm. These are responsible for the specificity of adaptive immune responses and include T cells, B cells, and Innate lymphoid cells[203].

Non-pigmented macrophages = Inflammatory cells with an indented/reniform/coffee-bean/kidney bean shaped nucleus, and a pale eosinophilic cytoplasm. Macrophages are derived from blood monocytes that differentiate into various tissues after leaving the circulation. They participate in the phagocytosis, eradication, and detection of bacteria and other pathogens. Furthermore, they are capable of presenting antigens to T cells and stimulating inflammation via the secretion of cytokines that stimulate other cells[203].

Mast cells = inflammatory cells with numerous coarse cytoplasmic granules (eosinophilic to basophilic) without multilobed nuclei. The classic function of mast cells involves the inflammatory cascade mediated via membrane-bound IgE[203].

- **Stratum corneum thickness in mm**

4.2.4 Immunophenotyping of lymphocytes in the foreskin by Flow Cytometry

4.2.4.1 Cell isolation by liberation of spontaneously migrating cells (crawl assay)

Lymphocyte phenotypes in an unrelated subset of participants were examined. Due to the random sampling, this happened to be only in aSTI negative men. Cells were liberated from foreskin tissue using a previously described assay[385–388].1cm^2 block of tissue and incubating in dispase overnight at 4ºC for the separation of the dermis from the epidermis. The hypodermis was mechanically removed from the epidermis prior to allowing cells to spontaneously crawl from the epidermis-stripped tissue. To allow for this, these epidermal sheets were then incubated for 48 hours in complete RPMI with 10% FCS at 37 ºC in sterilized culture Petri dishes for the spontaneous migration of cells. After a 48-hour period, cellular suspensions were obtained by passing them through 70 µm cell strainers [Corning (Sigma Aldrich Cat. No: CLS431751-50EA)]. The supernatant was discarded after the cells were rinsed with PBS and centrifuged at 400g for 5 minutes. Utilizing a TC20 cell counter, cells were resuspended in PBS and enumerated (BIO-RAD, Model no. TC20TM Automated Cell counter) and to determine and record viability.

4.2.4.2 Lymphocyte characterization

Foreskin cells were transferred to a 96-well plate at a concentration of 2×10^6cells per well. To measure viability, live/dead dye solution (Vivid, Life technologies, Cat. No. L34955) was prepared at a dilution of 40:1 in PBS, and 1µl was added to 49µl of PBS in each well before cell resuspension. The plate was incubated at room temperature (RT) for 20 min in the dark. To ensure all free amine groups were removed, cells were washed twice with 100 FACS buffer and the plate was centrifuged at 2100rpm for 3 min. A 4- color staining panel was used; this was after optimizations for our initially planned 14-color panel (inclusive of permeabilization and intracellular markers) were halted due to time constrains following 12 months hiatus from the lab during covid. A master mix including anti-CD3 V450, anti-CD4 PerCP-Cy5.5, anti-CD8 BV570 and anti-CD45 APC (**Appendix II,Table 1**) was prepared and added to the cell pellets. All markers were titrated before establishing optimal concentrations (**Appendix II, Figure 1.1-1.4**). The plate was then incubated at RT for 20 min. The cells were washed twice with FACS buffer as before and the plate was centrifuged at 2100rpm for 3 min. The supernatant was removed, and cells were resuspended in labelled 5ml Falcon tubes (BD Biosciences) in 200 µl of FACS buffer (1:10) and stored at 4°C. Samples were acquired within 24 hours of staining using the BD LSRII flow cytometer and data was analyzed using FlowJo version v.10.7.1 (FlowJo, LLC)

4.2.5 Data analysis

The prevalence and extent of inflammatory changes between STI positive and negative samples were assessed by $\chi 2$ tests. Differences in immune cell abundance were compared by the Mann-Whitney test.

4.3 RESULTS

4.3.1. Prevalence of immune cell infiltration in the foreskin by STI Status

Inflammatory or immune cell infiltrates as defined as immune cells which leave the blood circulation to enter(infiltrate) the inflamed connective tissue [203] were assessed in both inner and outer foreskin tissue samples from young men with (n=36) and without STIs (n=57). Immune infiltrates were detected in all three different sites in the layers of the foreskin, the epidermis, papillary and reticular dermis. Overall, 21% of the foreskin tissues (20/93) had any immune cell infiltration in the epidermis. Of these 12 were in men with aSTIs Of those with any STI, 33.3% (12/36) had epidermal infiltrates versus 14% (8/57) without STIs (Table 4.1) . (p=0.027). There was a significant relationship between the intensity of cell infiltrates (mild, moderate, or severe) and aSTI status (p=0.001). Notably, not all $aSTI^+$ men epidermal infiltrates.

Overall, cell infiltrates were predominantly localized in the papillary dermis (Figure 4.1 A, B and C), regardless of STI status (80.6, STI^+ v s 64.9, STI^-, p=0.105, Table 1). Although infiltrates were present in participants without any aSTI (Figure 4.1 D, E and F), The presence of reticular dermis cell infiltration was significantly associated with aSTI status (p=0.028). Additionally, the severity of cell infiltration in the reticular dermis tended to increase with STI status (p=0.082) although not significantly associated.

Table 4. 1 The prevalence and intensity of immune cell infiltration in the foreskins of STI$^+$ and STI$^-$ men.

	Epidermal Infiltration					Papillary Dermal Infiltration					Reticular Dermal Infiltration				
	STI$^-$ pos	N=36	**STI neg**	N=57		**STI$^-$ pos**	N=36	**STI neg**	N=57		**STI$^-$ pos**	N=36	**STI neg**	N=57	
	n	%	n	%	***P*[b]**	**n**	%	n	%	***P***	**n**	%	n	%	***P***
Any Cell Infiltrate[a]	12	33.3	8	14.0	0.027	29	80.6	37	64.9	0.105	6	16.7	2	3.5	0.028
Mild	3	8.3	8	14.0		8	22.2	16	28.1		4	11.1	1	1.8	
Moderate	7	19.4	0	0	0.001	7	19.4	12	21.1	0.074	2	5.6	1	1.8	0.082
Severe	2	5.6	0	0		14	38.9	9	15.8		0	0	0	0	

[a]Distribution of immune cell infiltrates throughout the tissue.

[b] As determined by the Chi square test [1]

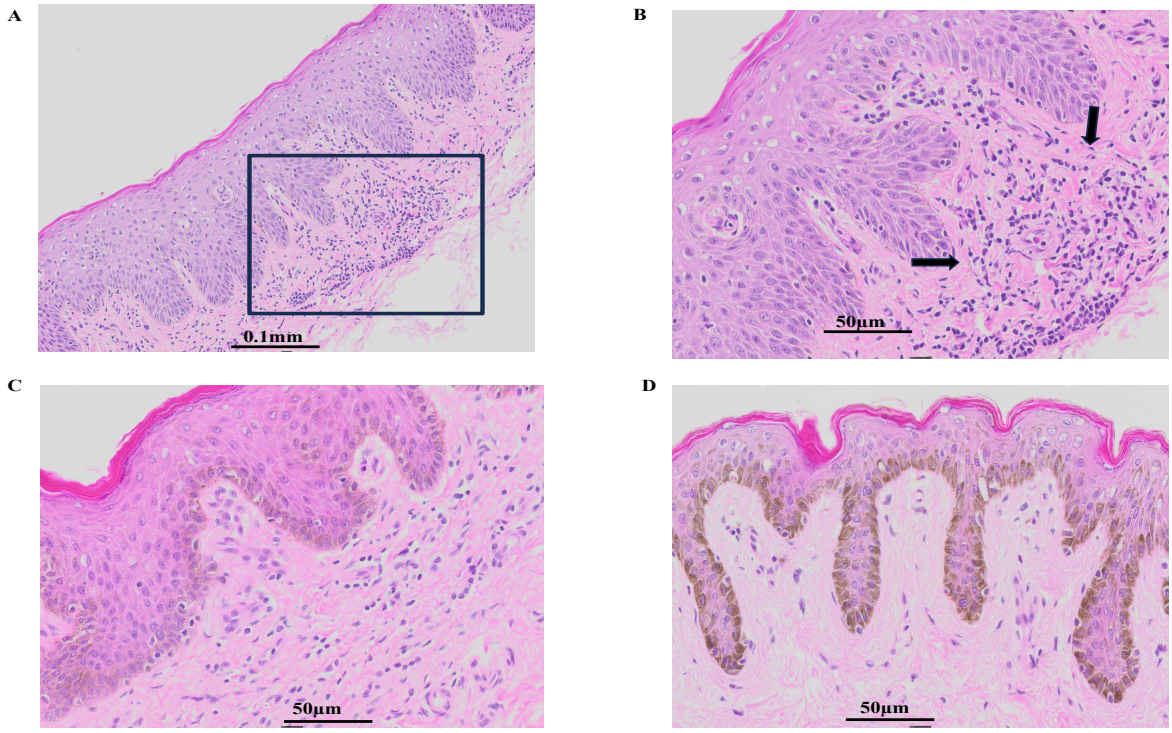

Figure 4. 1Photomicrograph of hematoxylin and eosin-stained foreskin tissues with and without aSTIs.

(A) inner foreskin from an asymptomatic sexually transmitted infection (aSTI) infected participant demonstrating focal immune cell infiltrates which are predominantly lymphocytic and in the papillary dermis with mild epidermal infiltrates (selected area), 5x magnification **(B)** high power view of the selected area, showing lymphocytic infiltration, 20x magnification **(C)** inner foreskin from an aSTI participant, 20x magnification versus **(D)** inner foreskin from another participant without an aSTI, also at 20x magnification, both showing the difference in the density of immune cell infiltrates (lymphocytic).

4.3.2 The effect of aSTIs on immune cell abundance in the foreskin epidermis, papillary and reticular dermis

Quantitative analysis of absolute immune cell counts revealed that the presence of an aSTI resulted in a significant increase across all three anatomical sites. The epidermis (10.4 vs 24.8 cells per mm^2, p=0.025), papillary dermis (61.4 vs 119.9 cells per mm^2, p=0.004), and reticular (6.5 vs 13.6 cells per mm^2, p=0.012) (Table 4.2). The predominant cell type in all the regions was lymphocytes, with most of the cells being in the papillary dermis (Table 4.2 and Figure 4.1 A, B & C). The papillary dermis also had macrophages which were completely absent in the epidermis. Macrophage abundance in the papillary dermis was significantly higher in those

with any aSTI(p=<0=0.0001). Other cell types were almost all not present across all the different tissue sites regardless of aSTI status.

Table 4. 2 Immune cell density in the different locations in the foreskin tissues of STI^+ and STI^- men

[a] As determined by the Mann-Whitney test

	Absolute counts average								
Cell type:	**Epidermal**			**Papillary dermis**			**Reticular dermis**		
	STI neg	**STI pos**	**P[a]**	**STI neg**	**STI pos**	**P**	**STI neg**	**STI pos**	**P**
Inflammatory cells per square mm	10.4	24.8	**0.0255**	61.4	119.9	**0.0039**	6.5	13.6	**0.0120**
Lymphocytes	10.4	24.6	**0.0288**	53.0	105	**0.0050**	5.2	10.6	**0.0199**
Macrophages	0	0	- - - -	7	12.9	**<0.0001** - - -	0.8	1.1	N/A
Mast cells	0	0		0.4	0.4		0.3	0.5	N/A
Eosinophils	0	0		0	0.25		0	0.1	N/A
Plasma	0	0		0	2.1		0.1	1	N/A
Neutrophils	0	0		0	0.03		0	0	N/A

4.3.3 The effect of STI status on stratum corneum size and spongiosis

Stratum corneum (SC) size was measured and compared between inner and outer foreskin tissue in men without any aSTI and further compared by aSTI status. There was no significant difference in SC thickness between the inner and outer foreskin tissues regardless of STI status (Figure 3 A and B). Therefore, the presence of an aSTI does not change foreskin SC thickness. Finally, the prevalence of spongiosis was independent of aSTI status (Table 4.3, Figure 4.2 B and C). Furthermore, the severity of spongiosis was not significantly associated with aSTI status ($p=0.37$). Notably, there was more spongiosis in the foreskin samples of those without STIs than those with STIs (56.8 vs 34.7%) although not statistically significant.

Table 4. 3 The prevalence of spongiosis in the foreskin tissues of aSTI^{+} and aSTI^{-} men.
(A) Shows the differences in the extent of spongiosis between men with and without aSTIs. **(B)** Reports the overall prevalence of spongiosis by aSTI status.

A

	Spongiosis			
	STI pos		**STI neg**	
	n	%	n	%
Overall	19,0	43.2	**25**	56.8
Mild	14	73.7	21	84
Moderate	5	26.3	4	16
Severe	1	5.3	0	0

B

	Prevalence (%)	
	With spongiosis	**No spongiosis**
STI neg	56.8(n=25)	34.7 (n=17)
STI pos	43.2(n=19)	65.3 (32)
total	47.3(n=44)	52.7(n=49)

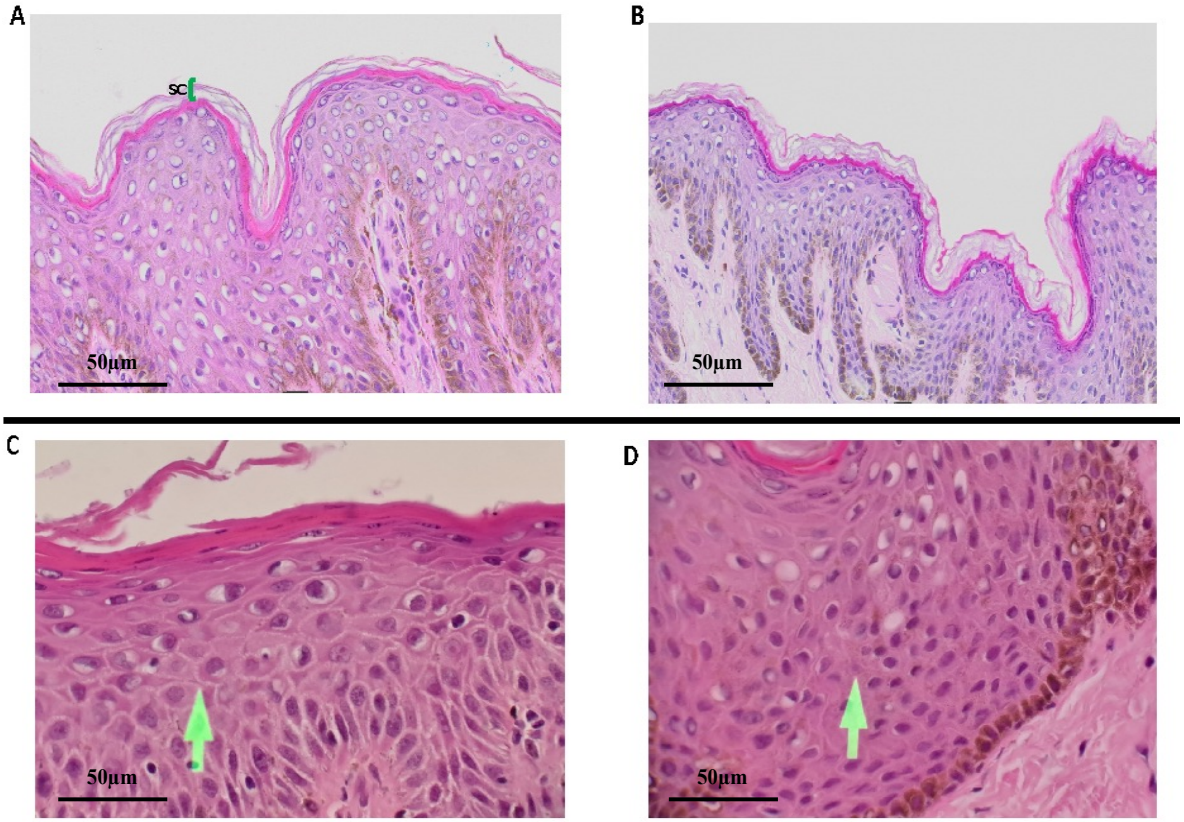

Figure 4. 2 Photomicrograph of hematoxylin and eosin-stained foreskin.

(**A**) a participant without an asymptomatic sexually transmitted infection (aSTI) demonstrating stratum corneum (SC) thickness (**B**) asymptomatic sexually transmitted infection (aSTI) participant demonstrating stratum corneum (SC) thickness which shows no significant difference between **(A)** foreskin with **(C)** and without **(D)** spongiosis shown in the green arrows.

4.3.4 Phenotypic characterization of lymphocytic infiltrates in the foreskin tissue

Foreskin cells were acquired on a BD LSRII flow cytometer after staining with the 5-color panel described above. T cells were identified based on the expression of $CD45^+$ and comprised between 3-4% of total recorded events from digested, filtered foreskin tissue (Figure 4.3 A, B, and C, **Appendix II, Figure 2 for Gating Strategy**). Forward and side scatter gating allowed for easier identification of lymphocytes. We report proportions of $CD3^+$, $CD3^+4^+$ or $CD3^+8^+$ (Figure 4). The majority of foreskin $CD3^+$ cells were found to express either $CD4^+$ (median, 34.5% of $CD3^+$ cells) or $CD8^+$ (median, 61.5% of CD3 cells) in the inner foreskin and $CD4^+$ (median, 46.9% of $CD3^+$ cells) or CD8 (median, 50.8% of CD3 cells) in the outer foreskin (Figure 4.3 D). Therefore, we identified no significant difference in proportions of $CD8^+CD3^+$T

cells in the inner versus outer foreskin (61.5 vs 50.8%, p=0.084, Figure 4.3 D) tissue and $CD4^+CD3^+$ T cells in the inner versus outer foreskin (34.5 vs 46.9%, p=0.250, Figure 4.3 D) tissue. However, when comparing the proportion of $CD4^+$ vs $CD8^+$ T cells by tissue site (Figure 3E), there was a significant difference in the proportions of $CD4^+$T-cells versus $CD8^+$ T-cells in the inner foreskin (34.5 vs 61.5% p= 0.007, Figure 4.3 E), but not the outer tissue.

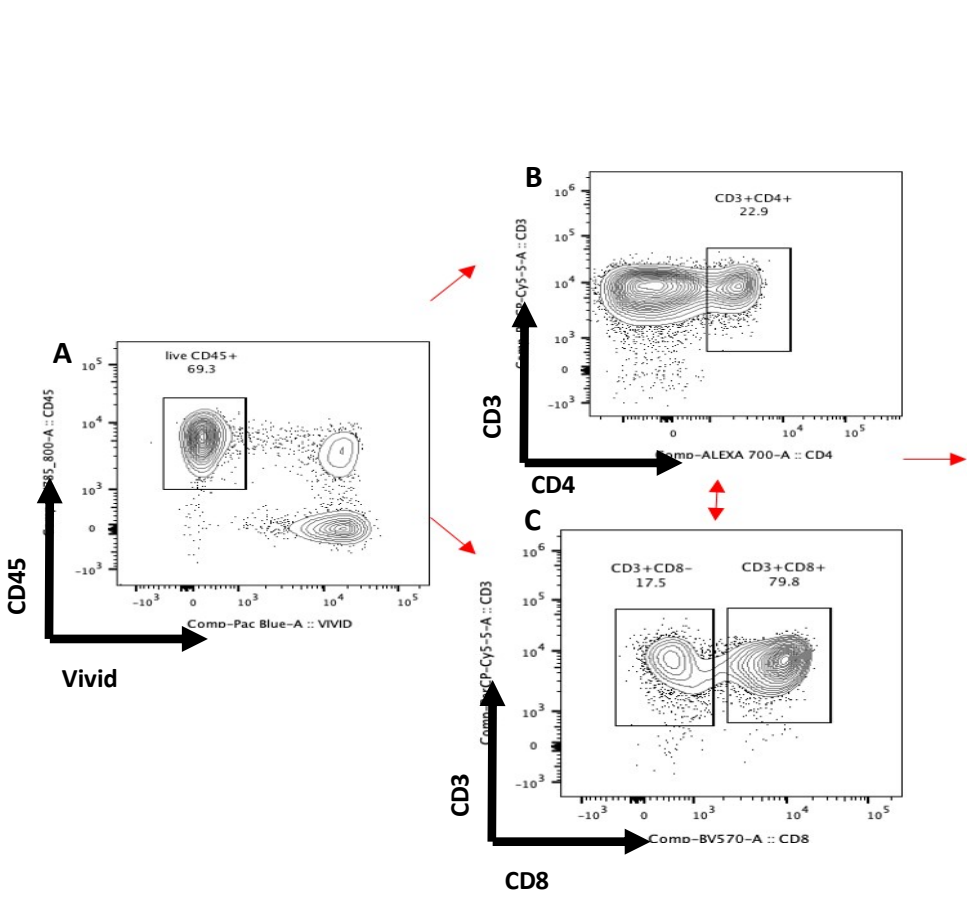
A
live CD45+
69.3
CD45
Vivid
Comp-Pac Blue-A :: VIVID
B
CD3+CD4+
22.9
CD3
CD4
Comp-ALEXA 700-A :: CD4
C
CD3+CD8-
17.5
CD3+CD8+
79.8
CD3
CD8
Comp-BV570-A :: CD8

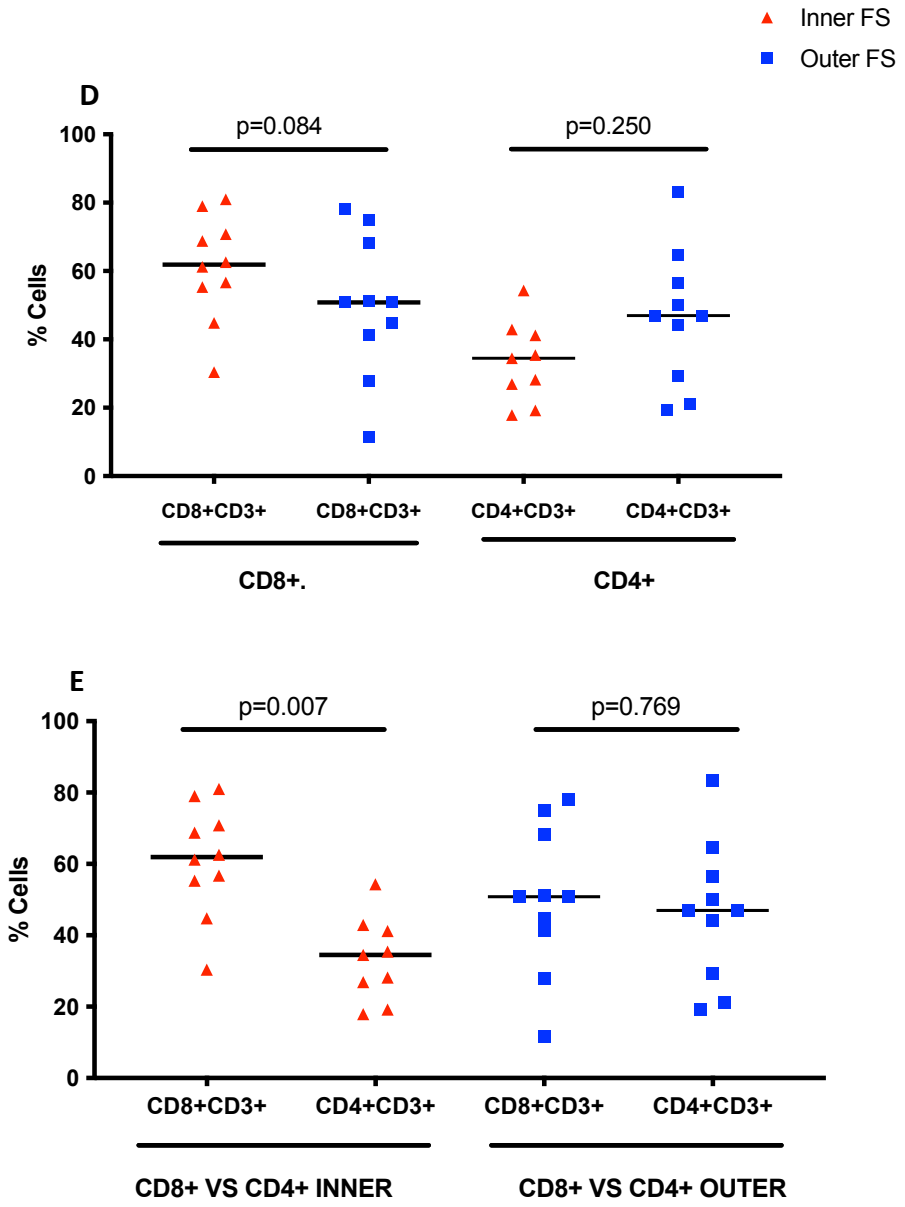
Inner FS
Outer FS
D
p=0.084
p=0.250
% Cells
CD8+CD3+
CD8+CD3+
CD4+CD3+
CD4+CD3+
CD8+.
CD4+
E
p=0.007
p=0.769
% Cells
CD8+CD3+
CD4+CD3+
CD8+CD3+
CD4+CD3+
CD8+ VS CD4+ INNER
CD8+ VS CD4+ OUTER

Figure 4. 3 Foreskin lymphocyte infiltrate cells are predominantly CD4 and CD8 cells in aSTI negative men.

Foreskin cells from 10 men -20 samples of inner and outer foreskins- were isolated and acquired on a BD LSRII flow cytometer. Representative plots are shown (A, B, C). (A) CD3+ T cells were defined as the proportion of CD45+ cells expressing CD3 (B) $CD4^+$ T cells were gated on $CD3^+CD4^+$ cells gated from $CD45^+$ live cells. The gate defining $CD8^+$ T cells was created based on $CD3^+CD8^+$ events gated from $CD45^+$ live cells gate. Both $CD4^+$ and $CD8^+$ T Cells were defined using $CD4^+$ and $CD8^+$ FMO (fluorescence minus one). (D) Proportions of $CD4^+$ and $CD8^+$ cells in the inner versus outer foreskin tissue sites. (E) Proportions of $CD4^+$ versus $CD8^+$ cells in the inner and outer foreskin tissue.

4.4. DISCUSSION

Understanding the immunobiological changes associated with the presence of common asymptomatic STIs is crucial in potentially identifying alternative STI preventative methods in the male genital tract. This is important because classic STIs remain a significant public health burden. Additionally, their bidirectional effect on the incidence and prevalence of HIV-1 further compounds the urgency. Previous studies in the female genital tract have shown that increased genital concentrations of immune cell–recruiting chemokines and that genital inflammatory status contributes to increased risk of HIV acquisition in these women[118]. This chapter examined both quantitatively and qualitatively, the effect of common asymptomatic STIs on the presence of immune cell infiltrates in the foreskin of men living without HIV-1.

This PhD shows that immune cell infiltrates in the papillary dermis, compatible with inflammation[203], are present in both the foreskin tissue in men with and without any aSTI . This finding implies that other factors other than STIs may cause inflammation in this area. These include factors such as urethral and prepupal microbiome and viral STIs. This project did not test for viral STIs as there is a lot documented on these on the male genital tract. Microbiome studies have been conducted by our co-investigators and correlative studies will be published upon completion. This is consistent with studies that describe the foreskin tissue as an "inflammatory tissue", that the foreskin contains a higher concentration of dendritic cells, activated $CD4^+$ T cells that express the HIV co-receptor CCR5, and $CD4^+$ T cells of the Th17 subset, when compared to the blood[389–391]. Furthermore, in the uncircumcised penis, this increased density in immune cells in the inner foreskin tissue has been linked to higher levels of inflammatory cytokines and chemoattractant chemokines that are present in the adjacent sub-preputial space[174,183].

Histological measurements show that total immune cell density was higher in the epidermis, papillary dermis and reticular dermis in men with versus without aSTIs. These were predominantly lymphocytic infiltrates in the papillary dermis. These findings were consistent with previous findings in our lab that showed an increase in the density of $CD4^+CCR5^+$ cells foreskin epithelia of men with aSTIs[167]. Additionally, Johnson et al[493]., also showed that foreskin inflammation was increased with the presence of HSV-2 infections[493]. Thus this observed finding in this PhD study of increased lymphocytic immune cell density in the various layers of the foreskin tissue could be highlighting adaptive immune response to aSTIs in the foreskin. Alternatively, this could also be due to inflammation initiated by innate mechanisms

such as TLR. This can't be linked to a specific aSTIs as this analysis included all four aSTIs that were screened for in these men. $CD4^+$ T cells, macrophages, and dendritic cells (DCs), such as Langerhans cells (LCs), are among the first cells to be infected by and transmit HIV-1 in the genital mucosa.

We then immunophenotyped these "lymphocytic infiltrates" using flow cytometry in men without an aSTI Our lab previously developed techniques utilizing expedited tissue processing and use of the spontaneous migration of cells (crawl assay) that enabled us to isolate viable T cells from foreskin tissue with retention of the expression of T cell markers[183]. This has allowed for the characterization of foreskin T cell subsets. Here we found that in the foreskin of men without an aSTI, lymphocytic infiltrates predominantly constitute $CD4^+$ and $CD8^+$ T cells. Furthermore, this abundance of T-cells was similar across the two foreskin tissue sites, inner versus outer. However, we show that the inner foreskin tissue had a higher proportion of CD8 T cells as compared to $CD4^+$ T cells, thus a low CD4:CD8 ratio. Recent research has revealed that tissue compartments include a significant number of resident $CD4^+$ and $CD8^+$ T cells. These cells differ in their gene expression, physical characteristics, and functions compared to T cells found in the circulation. Furthermore, these differences can be observed across different tissues[392–394]. Previous studies have shown that $CD8^+$ T cells are more enriched in the foreskin versus the blood [275]. However, we did not include markers in the immunophenotyping panel to characterize whether these cells are tissue-resident effector/memory T cells. Tissue-resident memory and effector $CD4^+$ and $CD8^+$ TRMs are still largely understudied in the human genital tract. Tissue-resident memory (TRM) T cells that are resident in tissues are crucial targets of vaccination strategies due to the fact that they either facilitate local immune responses or interact directly with other immune cells[395]. The capacity of $CD4^+$ helper T cells (Th) to direct and assist $CD8^+$ T cells, B cells, and innate immune cells underscores their significance in the immune response to pathogens[396]. Future studies could ascertain whether these $CD4^+$ and $CD8^+$ T cell populations in the foreskin tissue are tissue-resident or not, memory or effector, and if the differences in ratios impact tissue infectivity by various STIs.

In this study, these "lymphocytic infiltrates" were then immunophenotyped using flow cytometry in men without an aSTI. Our lab previously developed techniques utilizing expedited tissue processing and use of the spontaneous migration of cells (crawl assay) that enabled us to isolate viable T cells from foreskin tissue with retention of the expression of T cell markers[169]. This has allowed for the characterization of foreskin T cell subsets. The data in this study found

that in the foreskin of men without an aSTI, lymphocytic infiltrates predominantly constitute $CD4^+$ and $CD8^+$ T cells. Furthermore, this abundance of T-cells was similar across the two foreskin tissue sites, inner versus outer. However, it is known that the inner foreskin tissue has a higher proportion of CD8 T cells as compared to $CD4^+$ T cells, thus a low CD4:CD8 ratio[258]. Recent research has revealed that compared to T cells found in the circulation, tissue compartments include a significant number of resident $CD4^+$ and $CD8^+$ T cells[370-372]. These cells differ in their gene expression, physical characteristics, and functions compared to T cells found in the circulation. Furthermore, these differences can be observed across different tissues[370–372]. Previous studies have shown that $CD8^+$ T cells are more enriched in the foreskin versus the blood [258]. However, we did not include markers in the immunophenotyping panel to characterize whether these cells are tissue-resident effector/memory T cells. Tissue-resident memory and effector $CD4^+$ and $CD8^+$ TRMs are still largely understudied in the human genital tract. Tissue-resident memory (TRM) T cells that are resident in tissues are crucial targets of vaccination strategies since they either facilitate local immune responses or interact directly with other immune cells[373]. The capacity of $CD4^+$ helper T cells (Th) to direct and assist $CD8^+$ T cells, B cells, and innate immune cells underscores their significance in the immune response to pathogens[374]. Future studies could ascertain whether these $CD4^+$ and $CD8^+$ T cell populations in the foreskin tissue are tissue-resident or not, memory or effector, and if the differences in ratios impact tissue infectivity by various STIs.

This study examined the prevalence and severity of spongiosis in all the foreskin tissue samples from men with and without aSTIs. We showed that the prevalence of spongiosis was independent of the measured aSTI status. Thus, spongiosis occurs in the foreskin of men with and without aSTIs. Spongiosis refers to the accumulation of fluid between the cells of the epidermis, specifically the keratinocytes. The accumulation of fluid (oedema) can lead to the elongation and stretching of keratinocytes, resulting in the formation of vesicles within the upper layer of the skin (intraepidermal vesicles) with a spongy appearance (spongiotic) [366]. The presence of spongiosis is typically followed by the migration of lymphocytes, and occasionally neutrophils or eosinophils, to the epidermis[366,367]. It is a characteristic histopathologic appearance in eczematous dermatitis[366,367]. Spongiosis has not been evaluated in the penile foreskin before. The presence of spongiosis in the foreskin tissue could have an effect on the microbiome diversity within the preputial space, and thus be one of the various explanations for the documented penile 60-fold reduction in anaerobic taxa overall post VMMC[173].

Finally, we show that there is no significant difference in SC thickness between the inner and outer foreskin tissue in healthy young men without aSTIs. This finding of no difference in SC thickness is consistent with the current consensus that this is not what mainly explains the differences in HIV-1 acquisition risk between circumcised and uncircumcised men[164,169,171]. Additionally, our lab has previously shown that filaggrin size (one of the structural components of the stratum corneum) is not affected by the presence of an aSTI. This chapter additionally shows the SC in totality is also not affected by the presence of any aSTI.

Asymptomatic STIs may not be clinically visible but cause ongoing active immunobiological changes locally. These result in increased inflammation in various regions of the foreskin tissue and an increased abundance of immune cells. The foreskin, however, also has an "activated immune state" despite the absence of aSTIs, suggesting the complexity of all the factors that render the foreskin tissue a primary site for HIV-1 infections.

CHAPTER 5

Spatial Transcriptomic Profiling of foreskin Epithelial and Macrophage cells in STI positive and negative participants

Table of Contents

5.1 INTRODUCTION 114

5.2 METHODS 118

5.2.1 Cohort description 118

5.2.2 Tissue sections ..... **Error! Bookmark not defined.**

5.2.3 Spatial transcriptomics using GeoMx 118

5.2.3.1 Slide preparation and Regions of Interest (ROI) selection 119

5.2.3.2 NGS Readout 120

5.2.3.3 Optimizations 120

5.2.4 Data analysis 121

5.3 RESULTS 121

5.3.1 Spatially resolved gene expression data of macrophage cells in the presence versus absence of asymptomatic chlamydia infection of the inner and outer foreskin tissue 121

5.3.2 Differentially expressed genes of macrophage in the presence versus absence of asymptomatic chlamydia infection of the inner and outer foreskin tissue 128

5.3.3 Spatially resolved gene expression data of PanCK+ cells in the presence versus absence of asymptomatic chlamydia infection of the inner and outer foreskin tissue 133

5.3.4 Differentially expressed genes in PanCK+ cells in the presence versus absence of asymptomatic chlamydia infection of the inner and outer foreskin tissue 135

5.3.5 HIV-1-associated macrophage and epithelial cell gene expression changes in the presence versus absence of asymptomatic chlamydia infection of the inner and outer foreskin tissue 140

5.4 DISCUSSION 143

5.1 INTRODUCTION

Currently, our understanding of the changes in the levels of both protein-coding and non-coding genes in host cells infected with *C. trachomatis* is limited. The diverse genetic compositions, as well as the various methodologies and types of organisms employed, continue to present certain constraints. In recent times, dual RNA-Seq[397,398]has enabled the simultaneous profiling of the transcriptomes of infected epithelial cells and *C. trachomatis.* This has revealed early chlamydial gene expression and intricate host cell responses that were previously unknown[397]. However, to date, the derived transcriptional profiles in these studies have only represented the average gene expression across the entire population of cells that were sampled[399]. The analysis may become distorted when subsets of cells with dominant gene expression profiles are considered[400], potentially masking the transcriptional profiles of other potentially significant cell subsets[6,401]. To date, there very limited transcriptomics studies in the foreskin and not in the context of chlamydial infection. Most of the transcriptomics work to date has been from *in vitro* infections and from isolated cells from tissues. With the recent availability of digital spatial profiling[402], gene expression within the two-dimensional context of tissue architecture can be measured. In this chapter, gene expression of epithelial cells (as marked by $PanCK^+$) and macrophage cells (as marked by $CD68^+$) within foreskin architecture was measured from STI^+ and STI^- males from both the inner and outer compartment. Although these are urethral STIs , it is apparent from our previous chapters that these STIs also have an immune effect on the local foreskin tissue in the uncircumcised. We use this advanced technique to explore these associated changes within the two-dimensional context of the foreskin tissue architecture.

After infection with C. trachomatis and subsequent manipulation of the immune and metabolic response of the host cell, the host cell genome adapts by modifying the expression of critical genes and cytokines. These cytokines are vital for cellular survival and proper functioning, and they also play significant roles in the pathogen's clearance [403–405]. Inhibition of protein synthesis during *C. trachomatis* infection leads to the reprogramming of the host cells [405,406]. Significant alterations in the expression of genes within the host cell could potentially lead to divergent outcomes in the context of antibiotic treatment for *C. trachomatis* and the persistence of the bacteria's forms. Moreover, during host cell invasion, certain chlamydial and host genes may operate in concert[405]. Prior research has concentrated primarily on chlamydial transcriptomes throughout the developmental cycle of various chlamydial species[407–409]. A microarray characterized the epithelial cell transcriptome in response to plasmid-bearing or

plasmid-less *C. trachomatis*. Furthermore, it has been reported that host cells infected with *C. trachomatis* demonstrate alterations in protein synthesis as well as other signaling pathways of the host cell[410]. It has been reported that host cells infected with *C. trachomatis* demonstrate alterations in protein synthesis as well as other signaling pathways of the host cell[9,411]. Therefore, further understanding of transcriptome changes in both the infected and uninfected host cells within the infected host are fundamental to understanding how *C. trachomatis* can evade the immune response and chronically infect with long-term local complications within the genital tracts of both males and females. This is for both directly and undirectedly affected tissues, as in this case.

Immunobiology of epithelial cells during *C. trachomatis* infection

The pathogenesis of chlamydia infection has been described in chapter 1, section 1.1. Epithelial cells, which are the primary cellular components that facilitate bacterial replication, play a pivotal role in the initial infection of chlamydia. They serve as innate defenders and sentries, and later collaborate in the elimination of the bacteria through adaptive immunity[9]. Although urethral epithelial cells, which are the initial targets for *C. trachomatis* infection, were initially viewed as passive components in host defense generally and in C. *trachomatis* defenses specifically, subsequent studies argued against a passive epithelial model. It has been demonstrated that epithelial cells infected with Chlamydia generate chemokines and inflammatory mediators, which are possibly accountable for the recruitment of innate and adaptive effector cells and may directly contribute to immunopathology[412–415]. Chlamydial infection induces a prevailing cellular immune response distinguished by $CD4^+$ and $CD8^+$ T cells that secrete antigen-specific IFN-γ[416,417]. In vitro, chlamydial growth is inhibited by IFN-mediated tryptophan depletion; persistent exposure leads to infection eradication.

It is well known that *C. trachomatis* infection of epithelial cells can induce pro-inflammatory cytokine production, such as interleukin 1 (IL-1), interleukin-6 (IL-6)[418], tumor necrosis factor alpha (TNF-α)[412,419], CXC-chemokine ligand 1 (CXCL1), CXCL8 (also known as interleukin-8, IL-8), CXCL16, granulocyte/ monocyte colony-stimulating factor (GM-CSF) [412,419], chemokines CC-chemokine ligand 5 (CCL5) and CXCL10, and they secrete cytokines that promote the production of IFN-γ, including IFN-α, IFN-β and IL-12[419,420]. Classical innate immune cells, such as natural killer (NK) cells and DCs, which are abundant in the genital mucosa, can also be recruited by infected cells[421]. T helper 1 (Th1)-cell cytokines, which comprise many cytokines secreted by infected cells, play a crucial role in directing the immune

response against *C. trachomatis* in the direction of a protective Th1-type response. While certain cytokines do contribute to the pathology associated with *C. trachomatis* infection, these cytokines collectively stimulate inflammation and facilitate immune cell recruitment, thus playing an active role in the formation of both innate and adaptive immune responses.

This chapter provides unique knowledge on epithelial and macrophage cell changes in response to C. *trachomatis* from the male genital tract.

Immunobiology of macrophages during *C. trachomatis* infection

Several chemokines and proinflammatory cytokines are secreted by epithelial cells in the early stages of chlamydia infection; these substances induce local inflammation and leukocyte recruitment[422,423]. The initial interaction between *C. trachomatis* and mononuclear phagocytes occurs in the mucosa of the genital tract. C. trachomatis is engaged by tissue-resident macrophages and monocytes present in the genital mucosa. EBs are released from lysed epithelial cells once the developmental cycle has concluded[424]. Macrophages exhibit direct recognition of the bacteria at the site of infection via innate immune receptors. *C. trachomatis* recognition activates signaling pathways dependent on P38/ERK and MyD88, according to an abundance of evidence, suggesting that pattern recognition receptors (PRRs) play a role in chlamydial sensing[48,49,425]. As a result of the detection and response of chlamydial infection by both intracellular and surface receptors, distinct signaling pathways are initiated. In particular, *C. trachomatis* recognition has been attributed to members of the nucleotide-binding oligomerization domain (NOD)-like receptor family and the toll-like receptor (TLR) family[51,426]. Monocytes and macrophages are endowed with an extensive array of pattern recognition receptors (PRRs) that distinguish pathogen-associated molecular patterns (PAMPs), which are conserved structural motifs. Several cytokines, chemokines, and growth factors, including IL-1β, IFN-γ, TGF-β1, TGF-β2, TNF-α, -6, IL-8, TNF-α, IL-10, IL-1α, IL-3, IL-4, IL-5, IL-6,-12, IL-9, IL-10, IL-11, IL-15, IL-16, IL-17, IL-18, MIP-2 are all highly activated cells upon macrophage engagement with *C. trachomatis*[423,424,427–429]. Various mechanisms are employed by macrophages to impede the growth of C. trachomatis. These include lysosome trafficking[430,431], autophagy,perforin-2[432] interaction, induction of reactive oxygen and nitrogen species[433], and restriction of host cell nutrient access[434,435].

This study will be exploring how macrophages within the foreskin respond to asymptomatic urethral aSTIs. As described above, with chlamydia, the infection primarily infects epithelial

cells in the mucosa, with macrophages and an influx of neutrophils to the tissue to form immune inductive sites in the mucosa. These inductive sites, which contain B cells, T cells, dendritic cells, and macrophages, coordinate the initiation of an acquired immune response, including the deployment of a secretory IgA (sIgA) response. Although we examined the effect of urethral chlamydia infection on the foreskin tissue, the immune response in these cells was the interest. Due to the fact that this study has demonstrated that aSTIs, although primarily urethral in their nature, influence the local foreskin tissue immune response.

The intracellular fate of *C. trachomatis* macrophages differs significantly from the normal developmental cycle seen in epithelial cells:

The intracellular trafficking and fate of *C. trachomatis* in macrophages are not yet fully understood. However, the intracellular adjustment of *C. trachomatis* in phagocytic and epithelial cells exhibits significant disparities[436–438]. A previous comprehensive review has examined the infection of immune cells with *C. trachomatis*[439]. The disparities in intracellular transportation and the signaling triggered by *C. trachomatis* in epithelial cells and macrophages may elucidate the reason why phagocytes are unable to produce typical inclusions[440]. In addition, IFN- γ, which is recognized for its ability to stimulate macrophages in response to viral, bacterial, or protozoan infections, directly induces autophagy and disrupts the normal development of *C. trachomatis* by activating IFN-inducible guanylate binding proteins[441,442]. Autophagy is a significant factor in the processing of *C. trachomatis*, as the bacterium typically fails to evade the intracellular endocytic pathways within macrophages. This accounts for the challenge associated with the formation of macrophage inclusions[439].

The transcriptome of genital tract epithelial cells and macrophages in *C. trachomatis* - infected mucosa

Transcriptomic investigations have examined gene expression in both infected host cells and chlamydial-specific expression, either independently or concurrently[443–447]in other tissues outside the male genital tract. Transcriptomic investigations have examined gene expression in both infected host cells and chlamydial-specific expression, either independently or concurrently[414,448–456]. Typically, there is an increase in the activity of genes in epithelial host cells that are responsible for producing cytokines, promoting inflammation, transmitting signals, and enhancing innate immunity. Conversely, there is a decrease in the activity of genes involved in metabolism and regulating the cell cycle.

Recently, single-cell RNA sequencing (scRNA) has been utilized to analyze the expression patterns of individual cells. The scRNA analysis revealed significant changes in over 100 genes and pathways, with some showing downregulation and others showing upregulation. The primary genes impacted were those involved in regulating RNA and protein metabolism, specifically RPS15, RPL18,RPL3, PABPC1,EIF2S3 and MAGOH[9], with most showing increased expression. HLA-A (Major Histocompatibility Complex, Class I), IFTI3 (Interferon Induced Protein With Tetratricopeptide Repeats 3), ISG15 (ISG15 Ubiquitin Like Modifier), OASL (2′-5′-Oligoadenylate Synthetase Like), IL6, and genes associated with cholesterol and fatty acid synthesis are genes that are possibly involved in the ongoing immune response to infection[9] . It is well established that C. trachomatis can manipulate intracellular signaling, survival, and growth by exploiting a variety of host lipids.[457–459]. Metabolism-related metallothionein (MT) genes (MT1E, MT2A, and MT1X) were upregulated in response to increased expression of vimentin (VIM), a type III intermediate filament (IF) found in the cytoskeleton that is essential for preserving cell shape and integrity[460]. Increases in intracellular zinc concentration, reactive oxygen species (ROS), and proinflammatory cytokines induce MT upregulation[461].

Study aim: To characterize transcriptome signatures of macrophage (CD68) and epithelial (PanCK) cells in foreskins of asymptomatically Chlamydia-infected males**.**

We hypothesize that in males with *C. trachomatis* infection, the macrophages and epithelial cells are enriched towards a pro-inflammatory signature.

5.2 METHODS

5.2.1 Cohort description

Study cohort and ethics described in **Chapter 2, section 2.2.1** For the purpose of this sub-study, only participants who tested positive for *Chlamydia trachomatis* with no other coinfection were included as cases. Cases in this study were defined by participants who tested exclusively for asymptomatic *C. trachomatis* and the controls those without any aSTI, controls and cases were age matched.

5.2.2 Tissue sections

Formalin-fixed, paraffin-embedded (FFPE) tissue blocks prepared in **Chapter 4, Section 4.2.3** were selected for this sub-study. A total of sixteen samples of inner and outer foreskin tissue, from four cases and four controls were included.

5.2.3 Spatial transcriptomics using GeoMx

5.2.3.1 Slide preparation and Regions of Interest (ROI) selection

For GeoMx digital spatial profiling (DSP) slide preparation, we followed the GeoMx DSP slide preparation user manual (MAN-10150). In brief, FFPE blocks containing foreskin tissue were sectioned at 5 μm thin, and placed on apex adhesive slides (Leica 102822-1, Figure 5.1). The slides were placed overnight in the incubator at 37C prior to baking at 60°C for 4 four hours to remove excess paraffin wax. The FFPE slides were then deparaffinized and rehydrated using serial washes of CitriSolv, 100% ethanol, 95% ethanol and 1X PBS. Target retrieval was performed on the slides by heating up a staining jar containing 1X Tris EDTA to 99°C in a steamer, adding the slides to the staining jar, and letting them incubate for 5 minutes. RNA targets were exposed by treating the tissues with a 1μg/mL concentration of Proteinase K followed by fixation with 10% neutral buffered formalin (NBF). After all tissue pretreatments were done, tissue slides were incubated overnight with RNA probe mix (GeoMx Human Whole Transcriptome Atlas; a pool of in situ hybridization probes with UV photocleavable oligonucleotide barcodes). The next day, stringent washes were performed using a solution of 100% formamide and 4X SSC followed by blocking for non-specific signal. Tissues were then stained with tissue visualization markers: CD68-AF647 at 1:100 (Santa Cruz, sc-20060), panCK-532 at 1:100 (NanoString Technologies) and nuclear dye SYTO13 at 1:10 (NanoString Technologies).2ul, 2ul, 20ul. Choice of final markers was also influenced by optimization of markers with limited time. An attempt was made to optimize CD4 and CD45 alongside the other markers and they seemed to require more time beyond the limited time I had on my research visit trip at the `MayoClinic.

For GeoMx DSP sample collections, we followed the GeoMx DSP instrument user manual (MAN-10133-04). Slides were loaded onto the NanoString™ Digital Spatial Profiler instrument and then scanned to visualize whole tissue images. For each slide, a maximum total of 96 Regions of Interest (ROI) were selected from the inner and outer foreskins; epidermis, and dermis. Flexible ROI strategy-regions of interest (ROIs) were manually defined , in that for the foreskin tissue, ROIs were selected across the three regions – epidermis, papillary and reticular dermis. Areas with obvious color signal of cells of interest (magenta-CD68 and green-PanCK in our case) were demarcated. selected in different areas of the tissue defined by certain spatial locations and/or morphological markers. Furthermore, a minimum of 100 to 300 cells per ROI for reliable quantification of transcriptsThe probe barcodes from the various cell types

were sequentially collected using serial UV illumination of each compartment after fluorescent cell-specific markers were used to subdivide each ROI into compartments.

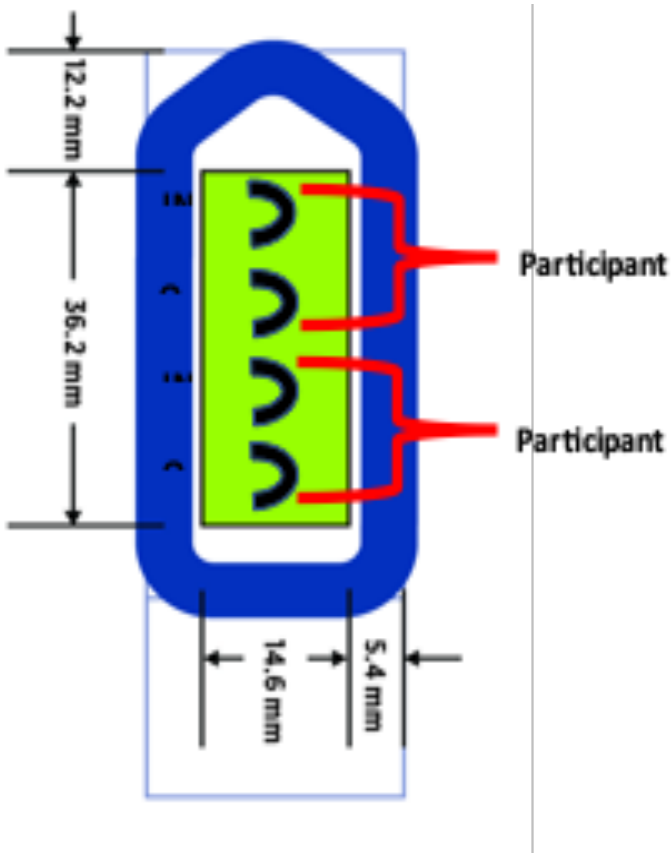

Figure 5. 1 Slide preparation for DSP analysis. Showing tissue placement and orientation per slide. (*Created by CL Rametse*)

5.2.3.2 NGS Readout

Each GeoMx DSP sample plus non-template controls (NTCs) were uniquely indexed using the i5 × i7 dual-indexing system of Illumina. Four µl of a GeoMx DSP sample was used in a PCR reaction with 1 µM of i5 primer, 1 µM i7 primer and 1× NSTG PCR Master Mix. Thermocycler conditions were 37 °C for 30 min, 50 °C for 10 min, 95 °C for 3 min, 18 cycles of 95 °C for 15 s, 65 °C for 60 s, 68 °C for 30 s, and final extension of 68 °C for 5 min. PCR reactions were purified with two rounds of AMPure XP beads (Beckman Coulter) at 1.2× bead-to-sample ratio. The libraries were then sent to the Mayo Clinic Sequencing Core to be sequenced using the Illumina Nextseq 1000/2000 platform and for quality checks. Libraries were paired end sequenced (27 × 27).

5.2.3.3 Optimizations

The protocol GeoMx used in this study was optimized for the key steps for using foreskin tissue samples shown in **Appendix III, Table 1** as this was the first studying this tissue type.

5.2.4 Data analysis

Following each phase of analysis, data quality is evaluated in an iterative process. The assessment of the overall assay performance commences with the utilization of Quality Control (QC) metrics documented in the nCounter data files (RCC files). Background correction and data normalization are then performed, followed by an additional round of data quality assurance. In conclusion, the resulting ratios, fold changes, and differential expression are evaluated as per previously described principles. Analysis was performed similar to previously described[462]. Differential gene expression analysis was performed to compare different STI statuses; *C. trachomatis* infected versus uninfected in macrophage (CD68) and epithelial (PanCK) cells of the inner and outer foreskin tissue sites using generalized estimating equations (GEEs) to account for multiple ROIs per subject and adjusted for both age and for multiple comparisons using the R computing environment[360]. We compared expression level of each gene (>8,000 genes in total) in paired (case and control samples) from many regions of interest (ROI) using t-test. For pathway enrichment analysis, we used gene set enrichment analysis (gsea).: A false discovery rate (FDR) of <0.05 was used as the significance threshold. Only pathways with pathway sizes >50 were included in the analysis.

5.3 RESULTS

Differentially expressed genes (DEGs)

5.3.1 Spatially resolved gene expression data of macrophage cells in the inner and outer foreskin tissue in the presence versus absence of asymptomatic chlamydia infection.

Differentially expressed genes (DEGs) were first examined by comparing the foreskin tissue(n=8 foreskins with 16 tissue samples in total) of chlamydia infected and non-infected men. This analysis was done in both the inner and outer foreskins separately. Foreskin tissue sections were stained with pan-cytokeratin (PanCK, which is the epithelial cells marker in this study), CD68 (macrophage marker), and SYTO13 (DNA marker) as shown in Figure 1A and B. The expression level of each gene was compared between cases (CT positive) and control (CT negative) from regions of interest (ROI).

DEGs were stratified by inner vs outer foreskin, as these two sites have been shown to vary significantly inherently in their immunological phenotype and immune response to various

infections[169]. Figure 5.2 A and B shows images of inner (A) and outer (B) foreskin in chlamydia infected men from different representative participants. The pan-macrophage marker CD68 appeared to be distributed in both the epidermal and dermal layer. However, in the foreskin tissues of chlamydia-negative men (Figure 5.2 C and D), macrophages were strictly confined to the dermis, with little or no macrophages in the epidermal layer. Notably, in the men with chlamydia, macrophages in the epidermis appeared to be within vessels compared to tissue macrophages in the dermis. Qualitatively, both cases and controls had macrophages.

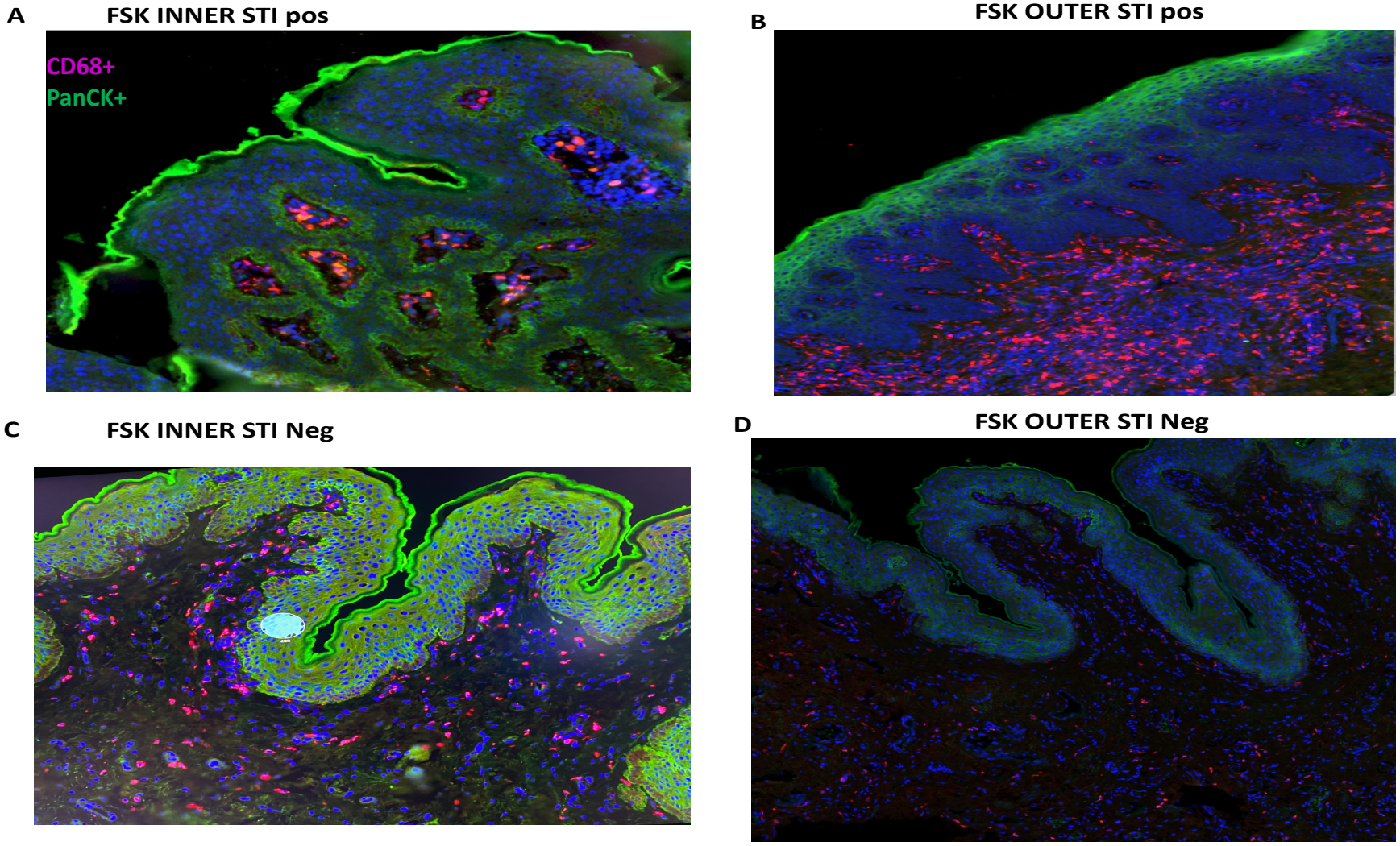

Figure 5. 2 Spatially Resolved Transcriptomics with NanoString GeoMX Profiler.

Representative image of an inner foreskin tissue section from a chlamydia-infected (case) man stained with pan-cytokeratin (green) to identify epithelial cells, CD68 (magenta) to identify macrophages and SYTO13 (blue) to identify nuclei. (**A**-**B**) Foreskin tissue from a chlamydia infected man, (**A**) inner foreskin and (**B**) outer foreskin tissue (cases). (**C**-**D**) Foreskin tissue from a uninfected man, (**C**) inner foreskin and (**D**) outer foreskin tissue (controls).

In CD68+ cells within the inner foreskin tissue, there were 21 genes significantly upregulated (a fold-increase >2 , adj. $p<0.05$). and 3 down regulated genes (fold-decrease <0.5, adj. $p<0.05$) in chlamydia infected vs uninfected men, as shown in Figure 5.3 A. For the outer foreskin tissue, there were 111 significantly downregulated and three upregulated genes in chlamydia infected vs uninfected men (Figure 5.3 B). There was minimal to no overlap in the affected genes between the two tissue sites (Figure 5.3 C). Cystatin A was the only common gene but was upregulated in the inner foreskin and downregulated in the outer foreskin in the presence of chlamydia infection. It codes for a precursor protein of cornified cell envelope in keratinocytes and plays a role in epidermal development and maintenance[463].

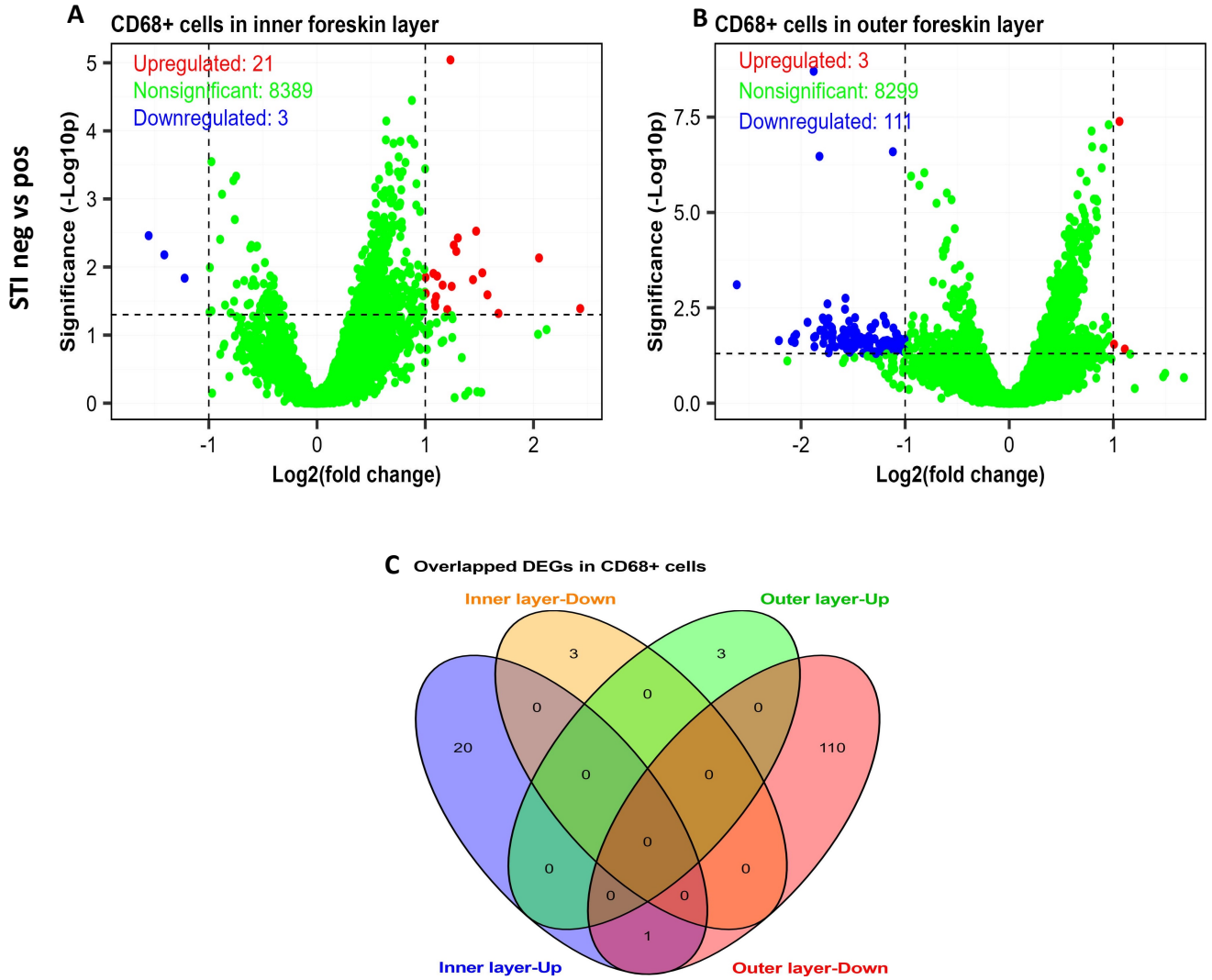
A
CD68+ cells in inner foreskin layer
Upregulated: 21
Nonsignificant: 8389
Downregulated: 3
STI neg vs pos
Significance (-Log10p)
Log2(fold change)
B
CD68+ cells in outer foreskin layer
Upregulated: 3
Nonsignificant: 8299
Downregulated: 111
Significance (-Log10p)
Log2(fold change)
C
Overlapped DEGs in CD68+ cells
Inner layer-Down
Outer layer-Up
Inner layer-Up
Outer layer-Down
20
3
3
110
1

Figure 5. 3 Differentially expressed genes (DEGs) in Foreskin CD68 cells (Macrophages) using NanoString GeoMX spatial transcriptomic profiling.

Volcano plots showing the genes expressed in the inner (A) and (B) outer foreskin tissue of men with an asymptomatic chlamydial infection versus uninfected men. Age adjustments were made to the data prior to their evaluation using generalized estimating equations (GEEs) that accounted for multiple ROIs per case. The red dots indicate upregulated genes and the blue dots downregulated genes in asymptomatic chlamydial infection versus chlamydia uninfected males. The horizontal dotted line indicates the significance threshold of FDR < 0.05, and the vertical dashed line indicates the effect size of 0. The grey dots indicate genes that were not significant at FDR < 0.05. The top genes ranked by a combination of both adj *p*-value <0.05 and fold-increase of >2 or decrease of <0.5 are numbered for each tissue site. (C) Venn diagram comparing the transcriptomic signatures in the inner versus outer foreskin in asymptomatic chlamydial infection and uninfected male macrophage cells.

5.3.2 Differentially expressed genes of macrophages of the inner and outer foreskin tissue, in men with and without asymptomatic chlamydia infection.

Figure 5.4 A and B shows the genes that are up- and down-regulated in the inner and outer foreskin in men with chlamydia infection. Using an FDR cutoff of ≤0.05 and log fold change (LFC) cutoff of ≥2.0, we identified 21 upregulated genes (**Appendix III, Table 2**) and three genes downregulated (fold-decrease <0.5, adj. p<0.05) in CD68+ cells within the inner foreskin tissue. Figure 3B shows only the top 10 ranked DEGs in the inner and outer foreskin tissue. These included genes associated with keratinization and tight junction formation in the skin, KRT14 and MICALL2,which were amongst the most upregulated genes in CD68+ cells of the inner foreskin tissue.KRT14 encode the cytoskeleton of epithelial cells[214]. MICALL2 encodes a protein that enables filamin binding activity, such as in bicellular tight junction. Genes associated with the antigen presentation in macrophages, HLA-DQA1, HLA-DQB1, and HLA-DRB1 were also among the most upregulated in the inner foreskin, suggesting that these cells were in an activated state. These belong to MHC II and play a central role in the immune system by presenting peptides/antigens derived from foreign agents (i.e. infections)[443]. Of note, IL7R, is a shared receptor for IL-2, 4, 7, 9, and 15[464]. Only two genes in the top 10 DEGs in CD68+ cells of the inner foreskin were downregulated, one of which is complement factor D (CFD), involved in the innate complement pathway activation. and insulin like growth factor binding protein 5 (IGFBF5).

Analysis of the outer foreskin tissue, using a false discovery rate (FDR) cutoff of ≤0.05 and log fold change (LFC) cutoff of ≥2.0 and (fold-decrease <0.5, adj p<0.05, identified top 10 affected genes (Figure 3B). Most genes differentially expressed in this list includes ribosome proteins, RPLP1, RPL22, RPL26 and RPL7. The most significantly downregulated genes were the adaptor related protein complex 3 subunit beta 1 (AP3B1) and aquaporin 3 (AQP3). AP3B1 plays a role in cell organelle biogenesis[463]. Notable, of the 113 downregulated genes in the outer foreskin tissue, 61 of them were RPL/ribosomal proteins (**Appendix III, Table 2**).

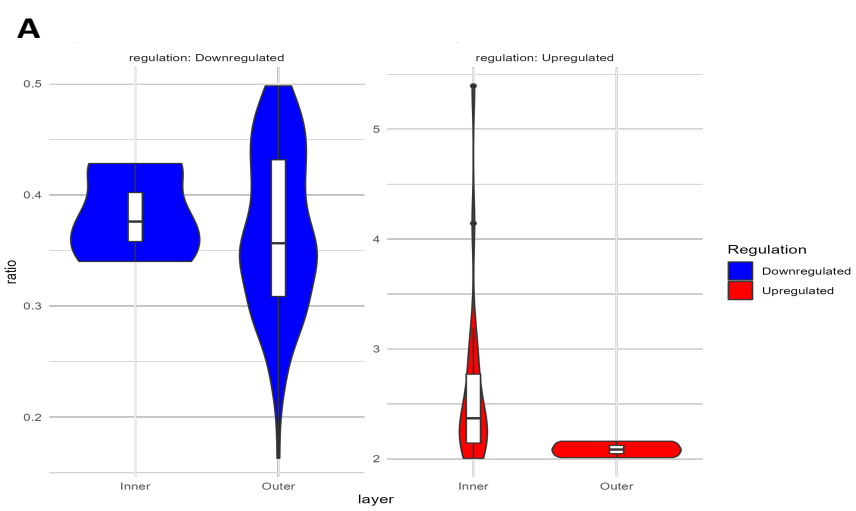
A
regulation: Downregulated
regulation: Upregulated
ratio
0.5
0.4
0.3
0.2
5
4
3
2
Inner
Outer
Inner
Outer
layer
Regulation
Downregulated
Upregulated

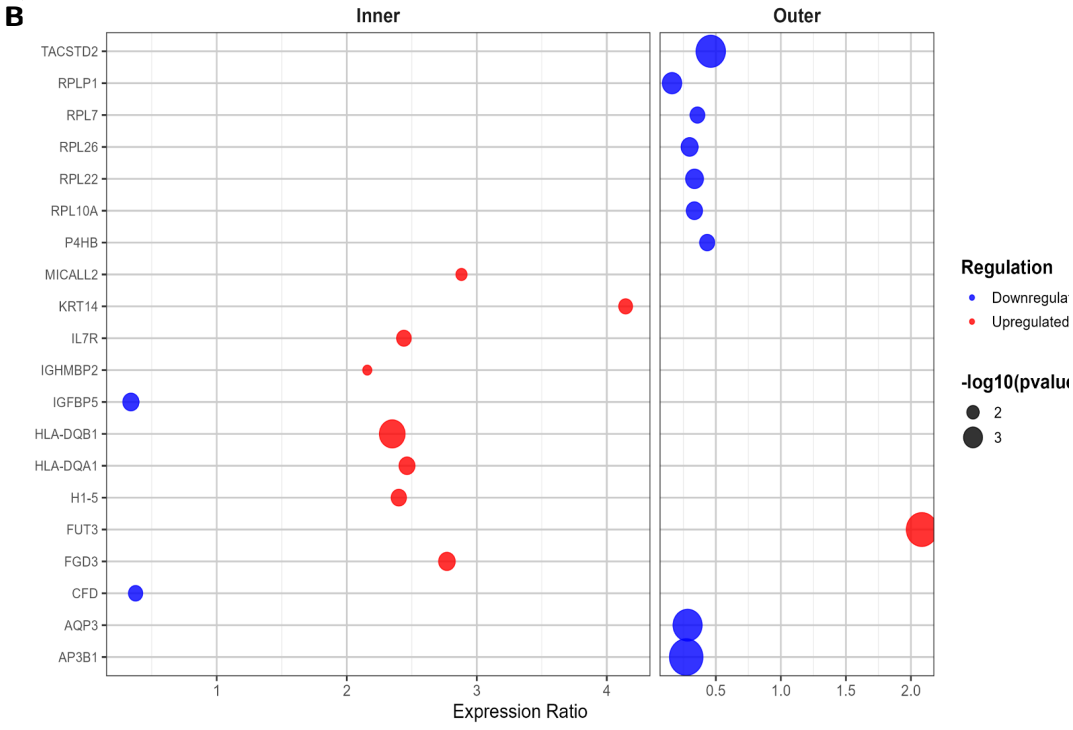
B
Inner
Outer
TACSTD2
RPLP1
RPL7
RPL26
RPL22
RPL10A
P4HB
MICALL2
KRT14
IL7R
IGHMBP2
IGFBP5
HLA-DQB1
HLA-DQA1
H1-5
FUT3
FGD3
CFD
AQP3
AP3B1
1
2
3
4
0.5
1.0
1.5
2.0
Expression Ratio
Regulation
Downregula
Upregulated
-log10(pvalu
2
3

Figure 5. 4 Identification of differentially expressed genes and associated biological processes in macrophages of the inner and outer foreskin tissues of men infected versus uninfected with asymptomatic chlamydia infection.

(A) Box plots showing the overall distribution of differential expression of all genes both adj p-value <0.05 and fold-increase of >2 or decrease of <0.5 between in the inner and outer foreskin of infected versus uninfected tissues. Downregulated genes shown in the blue and upregulated genes in the red. (B) Shows the top 10 ranking genes which have either been upregulated or downregulated for both the inner and outer foreskin tissue. Blue, showing downregulated genes and red upregulated. The size of circle shows the level of significance, the bigger the size the lower the p-value, all genes in (B) were significantly differentially expressed adj p<0.01.

Gene set enrichment analysis (gsea) was used for the pathway enrichment analysis and only pathways with sizes >50 were included. In macrophages from the inner foreskin tissue, a total of 291 pathways were significantly (adj $p<0.05$) enriched, with 26 pathways being upregulated and 265 downregulated in chlamydia infected versus uninfected men (**Appendix III, Table 3**). In the outer foreskin tissue, 149 pathways were significantly enriched, 141 of which were downregulated and 8 were upregulated (**Appendix III, Table 4**). Figure 5.5 A and B shows the top 20 ranked pathways that were most significantly ($p <0.01$) either upregulated or downregulated in both the inner and outer tissue. For the inner foreskin, the most significant pathways in CD68+ cells include downregulation of the RNA Polymerase I Promoter Opening, DNA methylation, and RUNX1 which regulates the transcription of genes involved in the differentiation of hematopoietic stem cells (HSCs). Pathways involved in extracellular matrix organization and IGF transport and uptake by the insulin-like Growth Factor Binding Proteins (IGFBPs) were amongst the most upregulated in the same compartment.

In the outer foreskin tissue, some of the most significantly downregulated pathways in CD68+ cells included Eukaryotic Translation Elongation, L13a-mediated translational silencing of Ceruloplasmin expression and peptide chain elongation. Of note, the downregulation was exaggerated in the outer versus inner foreskin as evidenced by a very low normalized enrichment score (nes) (<-8 vs -4).Top upregulated pathways in CD68+ cells interestingly was predominated by mitochondrial function related pathways, these include mitochondrial translation, termination, translation initiation and elongation. Of note, TNF signaling pathways were upregulated in the outer foreskin CD68_cells and a downregulation in adaptive immune system pathway. The inner and outer tissue sites had unique pathway enrichment patterns, with almost no overlap in the top20 ranked affected pathways.

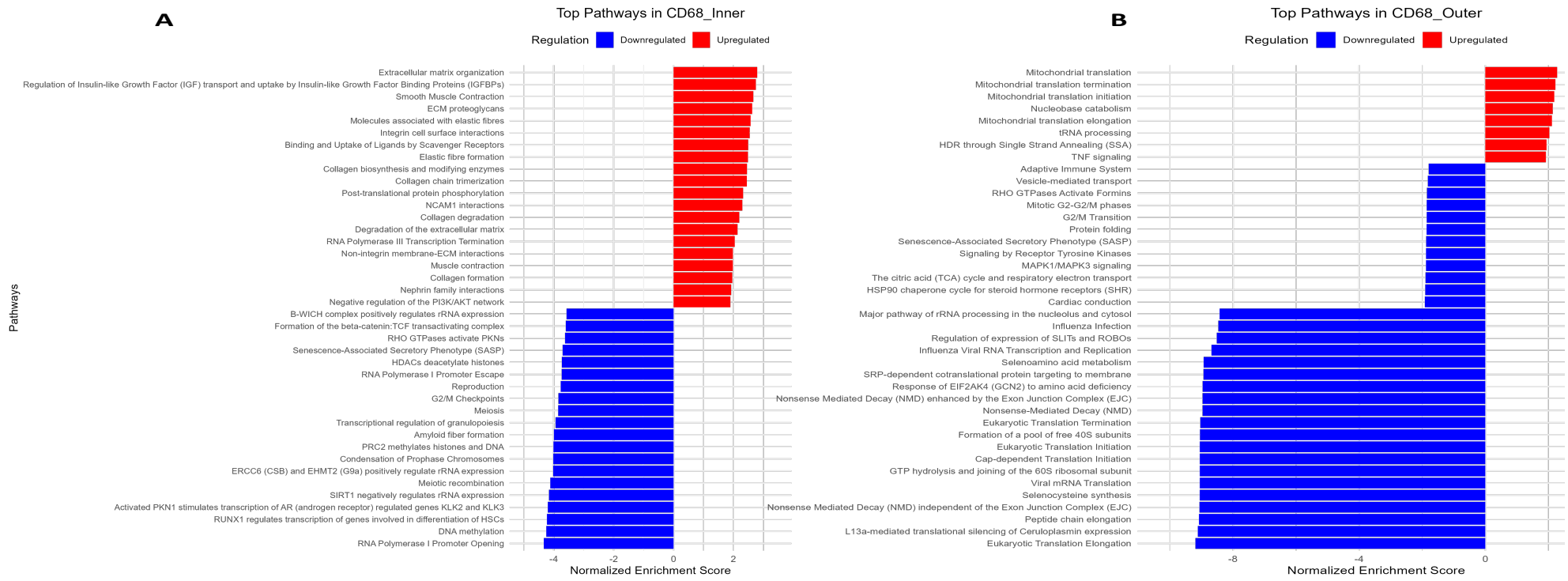

Figure 5. 5 Identification of differentially expressed genes and associated biological processes in macrophages of the inner and outer foreskin tissues of men infected versus uninfected with asymptomatic chlamydia infection.

(A and B) shows associated top 20 enriched pathways (adj p <0.01) in each tissue site, (A) in the inner foreskin and (B) in the outer foreskin. As gene expression increases, we see increased expression of associated functional pathways.

5.3.3 Spatially resolved gene expression data of PanCK+ cells in the inner and outer foreskin tissue, in the presence versus absence of asymptomatic chlamydia infection.

In PanCK+ cells within the inner foreskin tissue, there were eight genes significantly upregulated (a fold-increase >2, adj. $p<0.05$). and seven down regulated genes (fold-decrease <0.5, adj. $p<0.05$) in chlamydia infected versus uninfected men, as shown in Figure 5.6 A. For the outer foreskin tissue, there were 63 significantly upregulated and 43 upregulated genes in chlamydia infected vs uninfected men (Figure 5.6 B). Examination of the overlap of up- and downregulated genes between the inner and outer foreskin tissue showed a similar finding as with macrophages, there was minimal to no overlap in the affected genes between the two tissue sites (Figure 5.6 C). Three genes were upregulated in the inner foreskin and downregulated in the outer foreskin in the presence of chlamydia infection. The three genes were MICALL2, ACP7, and FGD3.

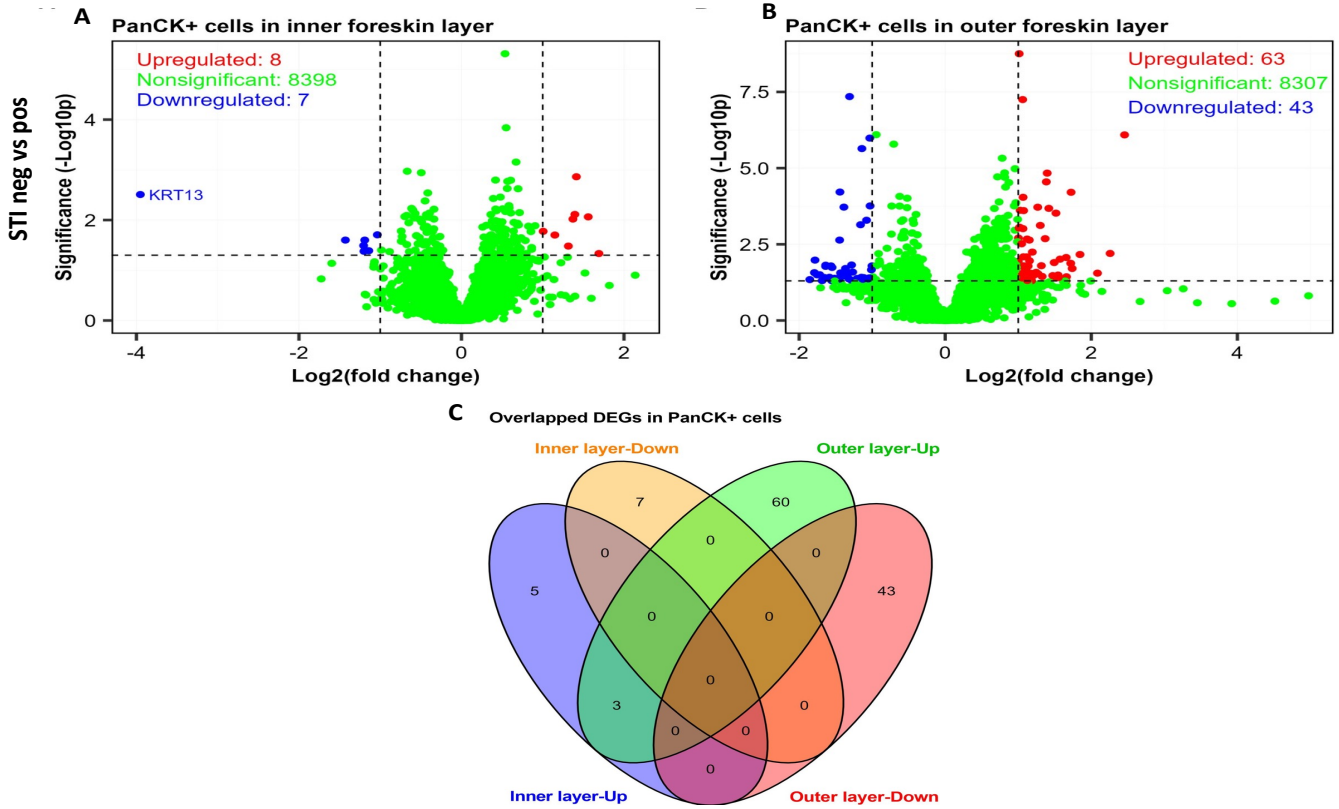

Figure 5. 6 Differentially expressed genes (DEGs) in Foreskin PanCK cells (Epithelial) using NanoString GeoMX spatial transcriptomic profiling.

Volcano plots showing the genes expressed in the inner (A) and (B) outer foreskin tissue of men with an asymptomatic chlamydial infection versus chlamydia uninfected men. Age adjustments were made to the data prior to their evaluation using generalized estimating equations (GEEs) that accounted for multiple ROIs per case. (C) Venn diagram comparing the transcriptomic signatures in the inner versus outer foreskin in asymptomatic chlamydial infected and uninfected males' epithelial cells.

5.3.4 Differentially expressed genes in PanCK+ cells in the inner and outer foreskin tissue, in the presence versus absence of asymptomatic chlamydia infection.

Figure 5.7 A and B shows the genes that are up- and down-regulated in the inner and outer foreskin in the presence of chlamydia infection. Using a false discovery rate (FDR) cutoff of ≤0.05 and log fold change (LFC) cutoff of ≥2.0 & fold-decrease <0.5, p<0.05. Figure 5.7 B shows only the top 10 ranked DEGs in PanCK + cells in both the inner and outer foreskin tissue sites (**Appendix III, Table 5**). In the inner foreskin tissue, PanCK+ cells showed significant upregulation in genes such as FYVE, RhoGEF and PH domain containing 3 (FDG3), which is also upregulated in CD68+cells of the inner foreskin tissue, IL36G, which belongs to the interleukin-1 family, S100A12 and MICALL2 which both contribute to the epidermal barrier, CHI3L1 and KYNU.

Analysis of the outer foreskin tissue, using a false discovery rate (FDR) cutoff of ≤0.05 and log fold change (LFC) cutoff of ≥2.0 and (fold-decrease <0.5, p<0.05, identified the top 10 affected genes shown in Figure 6B. These included the upregulation of genes, AL bHLH transcription factor 1 (TAL1), late cornified envelope 3A (LCE3A) involved in defense response to gram-negative and positive bacterium;, catenin delta 2 (CTNND2) an adhesive junction associated protein, CUGBP Elav-like family member 4 (CELF4) which regulates mRNA processing, CEA cell adhesion molecule 9 (CEACAM9) and acid phosphatase 7 (ACP7) and the downregulation of genes: ribosomal protein L22 (RPL22), parathymosin (PTMS), nascent polypeptide associated complex subunit alpha (NACA) and H2A clustered histone 20 (H2AC20)

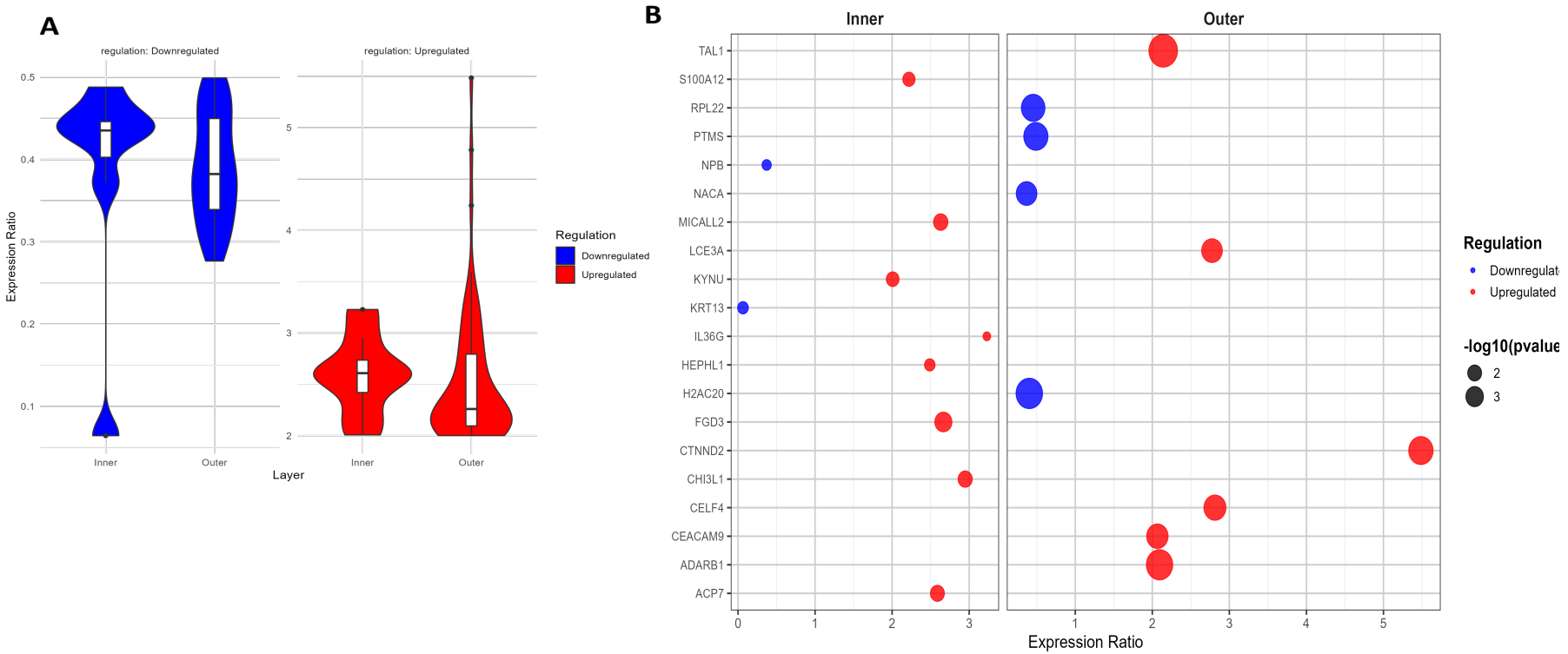

Figure 5. 7 Identification of differentially expressed genes and associated biological processes in Epithelial cells of the inner and outer foreskin tissues of men infected versus uninfected with asymptomatic chlamydia infection.

(A) Box plots showing the overall distribution of differential expression of all genes both adj *p*-value <0.05 and fold-increase of >2 or decrease of <0.5 between in the inner and outer foreskin of infected versus uninfected men. Downregulated genes shown in the blue and upregulated genes in the red. (B) Shows the top 10 ranking genes which have either been upregulated or downregulated for both the inner and outer foreskin tissue.

Blue, showing downregulated genes and red upregulated.The size of circle shows the level of significance, the bigger the size the lower the p-value, all genes in (B) were significantly differentially expressed $p<0.01$.

Gene enrichment analysis of PanCK+ cells of the inner foreskin tissue showed a total of 147 pathways significantly enriched, with only 40 of the pathways being upregulated and 107 downregulated in chlamydia infected versus uninfected men (**Appendix III, Table 6**). In the outer foreskin tissue, a total of 119 pathways were significantly enriched, 115 of which were downregulated and only 4 of these were upregulated (**Appendix III, Table 7**). Figure 5.8 A and B shows the top 20 ranked pathways that were most significantly either upregulated or downregulated in both the inner and outer tissue. In the inner foreskin, the most significantly top enriched pathways in PanCK+ cells include the upregulation in eukaryotic translation elongation. Formation of a pool of free 40S subunits, Nonsense Mediated Decay (NMD) independent of the Exon Junction Complex (EJC) pathway and pathways associated with eukaryotic translation termination and initiation. Down regulated pathways of RNA Polymerase I Promoter Opening, DNA methylation and condensation of Prophase Chromosomes.

For the outer foreskin tissue, pathways in PanCK+ cells that were the most significantly enriched included upregulation pathways involved in formation of the cornified envelope, keratinization, RHO GTPase activate NADPH Oxidases, Toll like receptor Cascade and neutrophil degranulation. Downregulated pathways included eukaryotic translation elongation and termination, peptide chain elongation, viral mRNA translation and Nonsense Mediated Decay (NMD) independent of the Exon Junction Complex (EJC) pathway.

Notably, the top two most downregulated pathways in the panCK+ cells and CD68+ cells in the inner foreskin of chlamydia infected versus uninfected men were the same: RNA Polymerase I Promoter Opening and DNA methylation. Furthermore, in the same cells of the outer foreskin, eukaryotic translation elongation was the most downregulated pathway. Finally, in both the inner and outer foreskin PanCK+ cells of chlamydia infected versus uninfected men, keratinization, and formation of the cornified envelope pathways were upregulated. The outer foreskin pathways were predominantly downregulated compared to the inner and like CD68+ cells, the pathways enriched were unique to each site with very minimal overlap. Downregulated pathways in chlamydia infected versus uninfected men included the HIV infection pathway, in both tissue sites and interferon signalling in the inner foreskin tissue. Overall, the most significantly and largely enriched pathways were those related to RNA and DNA synthesis and, metabolism.

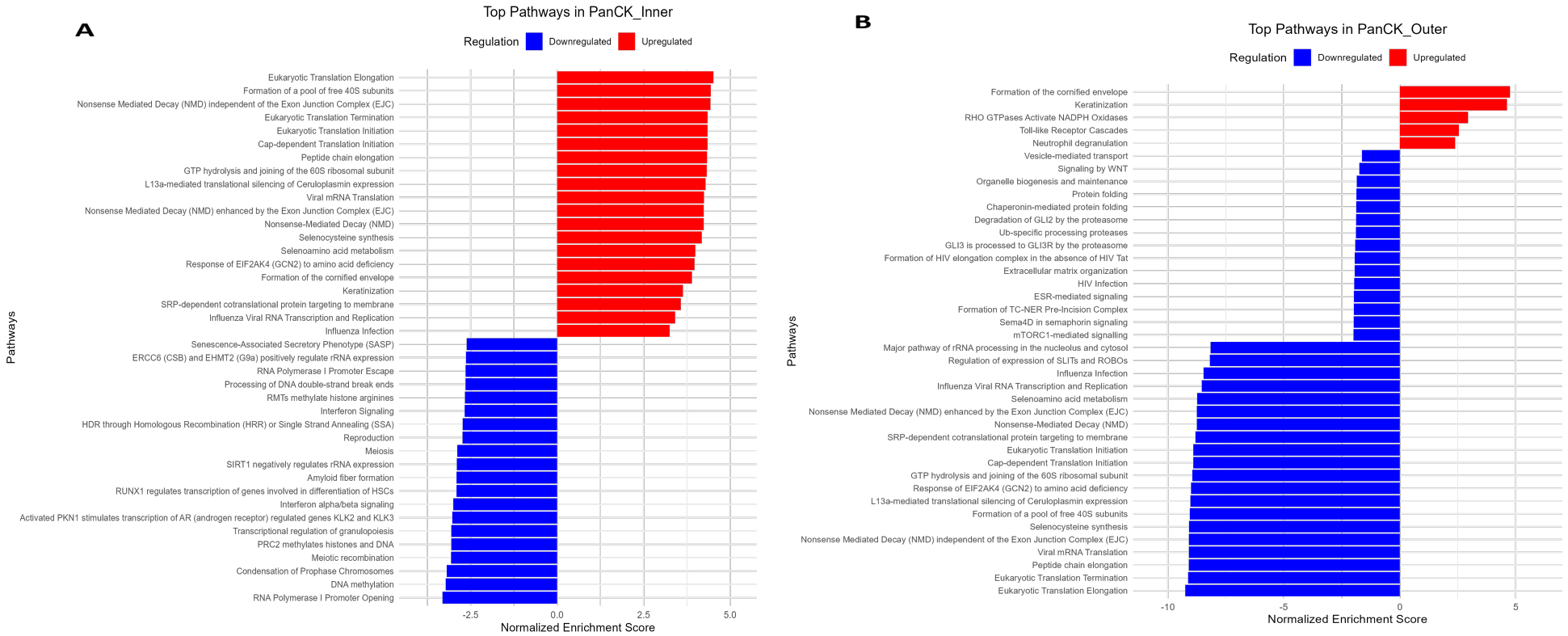

Figure 5. 8 Identification of differentially expressed genes and associated biological processes in epithelial cells of the inner and outer foreskin tissues of men infected versus uninfected with asymptomatic chlamydia infection. (A and B).

Shows associated top 20 enriched pathways (<0.01) in each tissue site, (A) in the inner foreskin and (B) in the outer foreskin. As gene expression increases, we see increased expression of associated functional pathways.

5.3.5 HIV-1-associated macrophage and epithelial cell gene expression changes in the inner and outer foreskin tissue, in the presence versus absence of asymptomatic chlamydia infection.

Finally, in this study, analysis revealed a significant number of genes known and proven previously to directly interact with HIV-1 that were significantly upregulated in the inner and outer foreskin tissue in chlamydia infected versus uninfected men. Overall, there were 61 HIV-related genes that were significantly downregulated in the outer foreskin and 1 in the inner foreskin tissue. In epithelial (panCK+) cells, 3 and 5 genes were upregulated in the inner and outer foreskin tissue respectively. Three and 21 genes were downregulated in the inner versus outer foreskin tissue respectively. Figure 5.9 A and B**, CD68 inner:** IL7R, IGHMBP2, HLA-DQB1, HLA-DRB1, HLA-DQA1, H3C10, H1-5, FSCN1 ,CFD. **CD68 outer**; AP3B1, PTMA, RPL10A, RPL26, RPL27, RPL34, RPL7, RPS19, YWHAZ. Figure 5.9 C**, PanCK inner:** HES1, CHI3L, KYNU, IL36G (up), Down; ZFP36, JUN and CHI3L. **PanCK outer**: SMPD3, PCSK6, ATG9B, ABHD16A, ATG9B, down; VVIM, MT1X, H2AC20, CXCL14, CD81 and CD63.

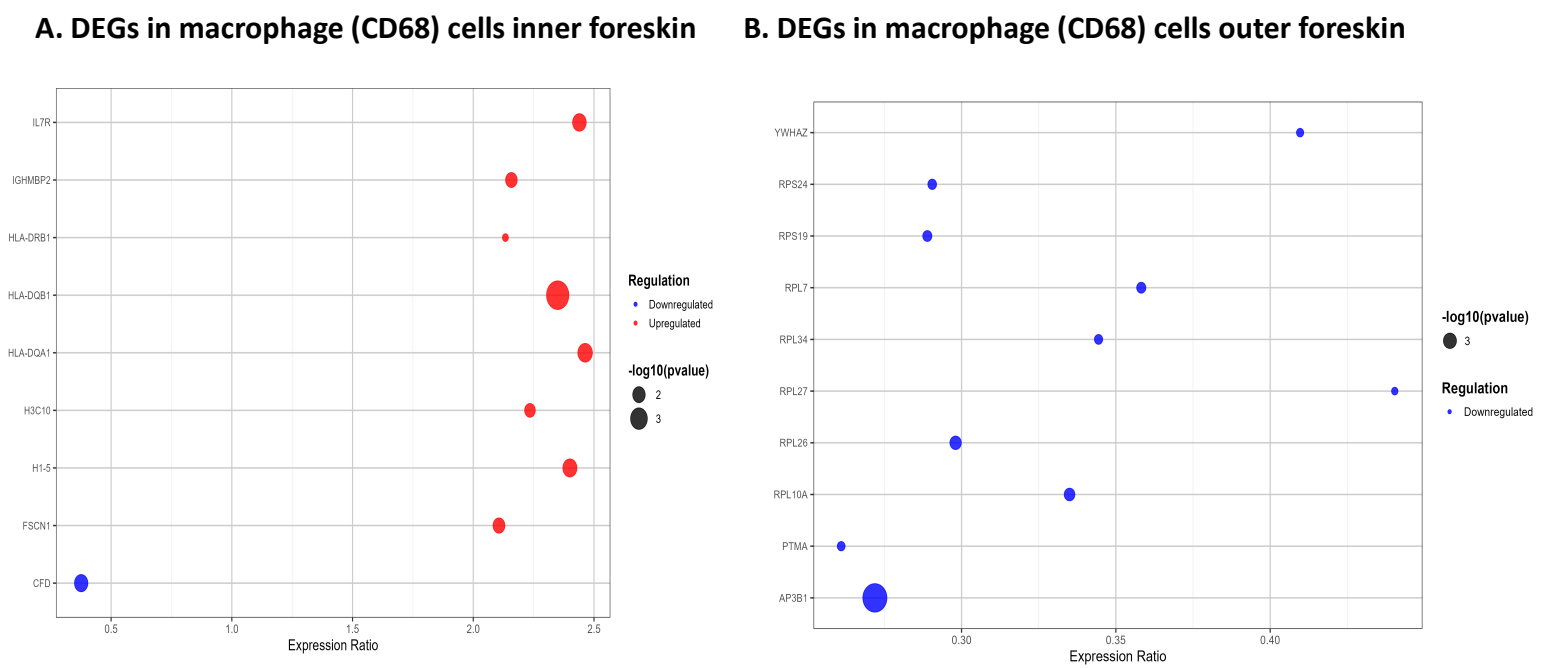

Figure 5.9. A HIV-1 infection associated genes differential expression in macrophages of the inner and outer foreskin tissues of men infected versus uninfected with asymptomatic chlamydia infection.

Differential expression of top ten (10) genes proven to have HIV-1 interactions, ranked by the lowest p-value (all <0.01) (A)Upregulated genes in the inner foreskin tissue, fold-increase of >2. (B) Downregulated genes in the outer foreskin, decrease of <0.5

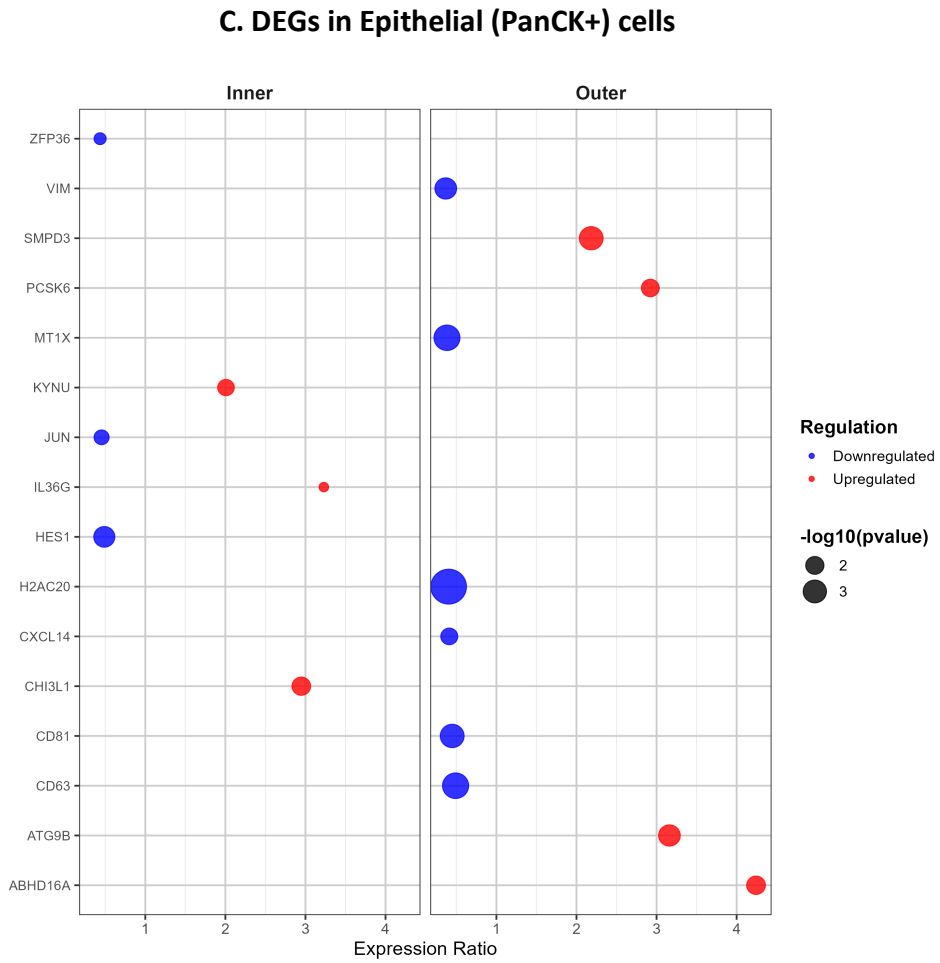

Figure 5.9. B HIV-1 infection-associated genes differential expression in macrophages of the inner and outer foreskin tissues of men infected versus uninfected with asymptomatic chlamydia infection.

Differential expression of top ten (10) genes proven to have HIV-1 interactions, ranked by the lowest p-value (all adj $p<0.01$) (A)Upregulated genes in the inner foreskin tissue, fold-increase of >2. (B) Downregulated genes in the outer foreskin, decrease of adj $p<0.05$.

5.4 DISCUSSION

In the previous chapters of this PhD, the focus has been on examining the impact of aSTIs on barrier integrity, penile epithelial tissue architecture and immune cell infiltrates. This chapter extended this analysis by measuring spatial gene expression of foreskin macrophages and epithelial cells in response to asymptomatic urethral chlamydial infection. This is the first study, to our knowledge, to examine the spatial transcriptomics of macrophages and epithelial cells of the foreskin within the context of chlamydia infection.

Transcriptome signatures of macrophage cells in the inner and outer foreskin tissue, in the presence versus absence of asymptomatic chlamydia infection.

In examining the transcriptome signatures in macrophages within the foreskin tissue of chlamydia infected versus uninfected participants there is a clear distinction in the host response induced in the inner versus outer foreskin tissue. In the inner foreskin tissue, the most significantly genes affected were those associated with immune pathway-associated genes (HLA-DQA1, HLA-DQB1 and HLA-DRB1, IL7R) and skin keratinization genes (KRT14, and MICALL2.) with majority showing increased expression. The HLA-genes in question are all components of MHC II molecules (alpha and beta analogs) that are found on antigen-presenting cells (macrophages in this instance). These cells serve a critical function in the immune system by providing $CD4^+$ T lymphocytes with peptides or antigens originating from foreign agents[403].Class II MHC molecules are therefore indispensable for antigen-specific immune response initiation. Gene knockout studies in mice have demonstrated that $CD4^+$ T-helper type 1 responses are both essential and adequate for the eradication of chlamydia infection from the genital tract in the context of *C. trachomatis* infection. [404,465,466]. Therefore, the upregulation of these in macrophages of the foreskin tissue in men infected with chlamydia is evidence of an elicited immune response, likely due in response to the local immune activation following urethral infection.

Another significantly upregulated gene was Kerartin-14 (K14). This is typically expressed in the epidermal basal layer. It is crucial for the integrity of the epidermal barrier[467]. KRT14 was significantly upregulated in the inner foreskin, which could be shedding light on other innate mechanisms by which host cells respond to chlamydia infection. Mutations in this gene, alongside keratin 5 (K5) together have been shown to be the most commonly occurring amongst patients with a common genetic bullous skin diseases fragility of the skin and separation of tissue through basal keratinocytes that resulted in intraepidermal blistering upon mild mechanical trauma, Epidermolysis bullosa simplex (EBS). This suggests their essential

role in the maintenance of epidermis integrity and resilience against physical traumas[468,469]. Keratinization pathway was also significantly upregulated in both the inner and outer foreskin epithelial cells. Various viral proteases have been shown to cleave host cell keratins[470,471], which may cause cytoskeleton collapse and facilitate viral release[467]. Therefore, highlighting the important role of intact keratin filament in facilitating or inhibiting infections. which may cause cytoskeleton collapse and facilitate viral release[467]. Additionally, cleavage of host Keratin 8 by a Chlamydia-Secreted Protease has also been previously shown[472], demonstrating the significance of keratinization in *C. trachomatis* infection. Therefore, highlighting the important role of keratinization in *C. trachomatis* infection and of intact keratin filaments in facilitating or inhibiting infections.

In the outer foreskin tissue, transcriptome signatures in macrophages of the chlamydia infected versus uninfected tissues revealed that the predominant genes affected were those with processes governing RNA and ribosomal proteins essential for protein sythensis, RPLP1, RPL22, RPL26 and RPL7, and these were mainly downregulated. Ohmer et al. demonstrated that *C. trachomatis* infection of HeLa cells significantly inhibits the infected host cell's protein synthesis. The ribosomal profile of the infected cell exhibited alterations concurrent with this inhibition, suggesting that translation initiation was obstructed. This occurred presumably as a component of a stress response[473]. There are, however, other studies have found an upregulation with these genes in epithelial cells of other tissues in the presence of *C. trachomatis* infection[9].

Significantly enriched pathways were mostly associated with cell metabolism, cell cycle regulation, and immunological pathways such as TNF signaling and adaptive immune system upregulation in the outer tissue, consistent with previous findings in other studies[410,451,474]. It has been demonstrated that TNFα monoclonally inhibits chlamydial proliferation when applied to host cells prior to infection[475] . TNFα, a cytokine known for its cytotoxic and antibacterial properties[476] is significantly secreted *in vitro* and *in vivo* during chlamydial infections[477,478]. It is involved in the regulation of the immune system and inflammation but via different mechanisms. It has been demonstrated that decreased expression of tumor necrosis factor receptor I on the surface of the host cell facilitates infection with *C.trachomatis*[479]. Thus significant upregulation of this pathway o the outer foreskin is a reflection of some of the known host immune responses associated with *C.trachomatis* infection.

Transcriptome signatures of epithelial in the inner and outer foreskin tissue, in the presence versus absence of asymptomatic chlamydia infection.

In examining the transcriptome signatures of epithelial (marked with PanCK) cells in the foreskin tissue of those infected and uninfected with *C.trachomatis*, upregulation and downregulation effects affected the inner and outer foreskin sites in a proportional manner as compared to in macrophage cells. Furthermore, the inner foreskin overall showed significant changes in very few genes in epithelial cells versus macrophages. This could suggest that host cell immune responses to chlamydia infection are more prominently within immune (macrophages) cells as opposed to other surrounding tissue (epithelial) cells.

In the inner foreskin tissue, genes affected included an upregulation in IL36G , which belongs to the interleukin-1 (IL1) family[480]. Interleukins (ILs), which are expressed and secreted by various cells including mast cells, eosinophils, and macrophages, serve as the primary mediators of inflammation and innate immunity[481]. A number of local or systemic responses to viral and bacterial infections are induced by these multifunctional cytokines, which also play a role in the development of chronic inflammatory diseases[480,481]and has been observed in chlamydial infections[482,483]. This response further highlights the immune role epithelial cells also play within the genital tract in that, they are not passive by-standers, but play an active role in recruiting an immune response in the presence of infections. FDG3 is also a gene that was upregulated in both CD68+ and PanCK + cells in the inner foreskin, where this gene is involved in the regulation of small GTPase activity. Small GTPase proteins , alongside other highly conserved and soluble cellular factors are responsible for tightly controlling intracellular membrane trafficking and organelle biogenesis[484]. These are often exploited by *C.trachomatis* to facilitate its intracellular trafficking and inclusion formation[485]. The observation of increased expression of this gene indicates that its function was significantly heightened in the infected tissues; therefore, this indicates that this is a crucial mechanism in the pathogenesis of chlamydia infection in both cell types.

In epithelial cells of the outer foreskin tissue of those infected versus uninfected by chlamydia, most upregulated genes are associated with transcriptional, RNA synthesis, metabolic processes and epidermal layer structural proteins. One of which includes LCE3A, late cornified envelope 3A, has been shown to possess broad-spectrum antimicrobial activity and to be upregulated by Th1 cytokines [486]. Primary mediators of protective immunity against Chlamydia are Th1 cells[404], this could highlight a consequence of response to chlamydia infection. The outer foreskin pathways were predominantly downregulated compared to the inner. Downregulated pathways included the HIV infection pathway, in both tissue sites and interferon signaling in the inner foreskin tissue. These could be shedding light on some of the factors that could further be explored in explaining the bidirectional relationship between HIV-

1 susceptibility and *C. trachomatis*.[3,6]

Chlamydia infection alters results in pronounced protein synthesis in both epithelial and macrophage cells of men infected with chlamydia.

The two most top downregulated pathways in the PanCK+ cells and CD68+ cells in the inner foreskin were the same, RNA Polymerase I Promoter Opening, DNA methylation. RNA Polymerase I synthesizes ribosomal (r)RNA, a vital constituent of the cellular protein synthesis apparatus that facilitates cell proliferation and underlies numerous key biological mechanisms. As previously noted in the results, in the outer foreskin of CD68+ cells, almost 60% of the significantly downregulated DEGs were ribosomal proteins. This pronounced reduction in protein translation has been described in other studies (infected HeLa cells) before[487], and it has been hypothesized that this could be due to a stress response by the host cell to the infection, affecting structure and signaling of the host cell. DNA methylation controls gene expression by enlisting proteins that suppress gene activity or by impeding the interaction between transcription factors and DNA. Extensive evidence suggests that bacterial infections can induce epigenetic-mediated transcriptional regulatory alterations in the host cell, including DNA methylation via bacterial effectors and proteins[488–490]. Thus, this result could suggest that *C. trachomatis* has the same effect on the foreskin tissue of infected men, both in macrophage and epithelial cells.

Furthermore, in the same cells of the outer foreskin, eukaryotic translation elongation was the most downregulated pathway for both cell types. A crucial phase in protein synthesis, translation elongation involves the ribosome continuing to translate each codon by adding the corresponding amino acid to the growing chain. These essential ribosomal related protein translation processes are the most significantly downregulated in the outer foreskin tissue, in both cell types. This highlights how in the presence of urethral *C. trachomatis,* primarily disrupts host cell protein synthesis in order to survive or elicit these changes as a side effect of its own replication within the foreskin tissue.

In both the inner and outer foreskin PanCK+ cells, keratinization, and formation of the cornified envelope pathways were upregulated in the presence of chlamydial infection. *C. trachomatis* primarily infects non-keratinized epithelial cells , hence in the male genital tract, the first port of infection entry is via the penial urethra[491,492]. An upregulation in keratinization pathways in the foreskin epithelial cells of both the inner and outer foreskin tissue highlights that this layer plays a protective effect against the infection.

Finally, in this study, genes known and proven previously to interact with HIV-1 that were significantly upregulated in the inner and outer foreskin tissue in chlamydia infected versus uninfected men. One of which is IL7R has been shown to interact with HIV-1 proteins Tat and Vif. The upregulation of IL-7R expression in human macrophages by HIV-1 Tat results in an increase in HIV-1 replication[464,493]. In this study, foreskin tissues with *C. trachomatis* infection showed significant up regulation in this receptor and thus could contribute to the underlying mechanisms explaining the increased risk of HIV-1 infection in *C .trachomatis* infected people. Adaptor related protein complex 3 subunit beta 1(AP3B1), which is the most downregulated gene in the outer foreskin macrophages upon chlamydia infection, interacts with the scaffolding protein clathrin[494]. This protein has been shown to be a cellular cofactor for viral budding[197]. This could be shedding light on some of the factors that could further be explored in explaining the bidirectional relationship between HIV-1 susceptibility and *C. trachomatis*. These genes have been demonstrated to be factors essential for intracellular bacterial (chlamydia) growth and inclusion biogenesis[495]. Additionally, this could shed light on some of the protective immune response within the host cell.

A confounding factor to consider in this study design was that cells within surgical removed tissue samples. This procedure itself could have effects on the activity of cells. Various studies have demonstrated that surgery and sample processing performed of tissues could have an effect on gene expression profiles[496–498]. Additionally, in samples that were from the STI positive men, single cell analysis did not differentiate which cells were directly infected and which were affected due to their adjacency to the infected cells, i.e., the infection is urethral yet all these changes are observed in the foreskin. It would be interesting in further studies to be able to examine foreskin tissue samples from infected men for the presence of direct infection or the presence of EBs etc

In conclusion, to our knowledge, this is the first study to examine the transcriptome signatures of both epithelial and macrophages in situ of the male foreskin tissue in men infected asymptomatic *C. trachomatis infection*. We show that the effect and type of host cell response not only differs by cell type but also by tissue site. The foreskin's inner tissue shows predominantly immune associated enrichment in response , whilst the outer foreskin showed more metabolic, RNA and DNA processing and transcription changes. However, both tissue sites and cell types show significant changes in HIV-1 associated genes. This study enabled the spatial analysis of this gene expression profiling, which revealed that based on where in the

tissue a cell is (inner versus outer foreskin), the response to the presence of chlamydial infection in the genital tract is unique. Although the major processes affected in both cell types and tissue sites were related to RNA synthesis. Our data have yielded a novel perspective of the complex host epithelia and macrophage cell response to infection and will inform further studies of transcriptional regulation and epigenomic regulatory elements in *Chlamydia*-infected people.

CHAPTER 6

The impact of Pre-exposure Prophylaxis on immune cells in foreskins from HIV uninfected participants

Table of Contents

6.1 Abstract **150**

6.2 INTRODUCTION **151**

6.3 METHODS **152**

6.3.1 Cohort description 152

6.3.2 Randomization and masking 152

6.3.3 Tissue sampling 152

6.3.4 Immunohistochemistry imaging and analysis 153

6.3.5 Ex-vivo challenge of foreskin tissue 153

6.3.6 Tissue drug metabolites 154

6.3.7 RNA sequencing of foreskin tissue 154

6.3.8 Data analysis 154

6.3.9 Ethics approvals 154

6.4 RESULTS 155

6.4.1 Impact of emtricitabine–tenofovir disoproxil fumarate or emtricitabine–tenofovir alafenamide on the density of CD4RCCR5R and CCR5 expression on CD4R cells in the foreskin. 155

6.4.2 Impact of emtricitabine– tenofovir disoproxil fumarate or emtricitabine–tenofovir alafenamide on the density of CD1a^{+} cells and claudin-1 expression in the foreskin. 159

6.4.3 Impact of emtricitabine–tenofovir disoproxil fumarate or emtricitabine–tenofovir 164

alafenamide on the anatomical location of CD1a^{+} cells in the foreskin. 164

6.5 DISCUSSION **166**

[Article published in *AIDS,* 2023, DOI: doi: 10.1097/QAD.0000000000003619]

In previous chapters, this PhD has focused on the observed differences in barrier integrity and in immune cells in the FS after VMMC. These observational studies give some insight into the potential mechanisms of how MMC may prevent HIV infection, especially with a concomitant STI. This chapter extends the observational work of this PhD into an intervention study. Provision of Pre-Exposure Prophylaxis (PrEP) is a highly effective technique for preventing the acquisition and transmission of HIV. This chapter integrates elements from the previous chapters, but within the framework of antiretroviral medications. It examines the impact of PrEP on foreskin immunity after VMMC and complements the previous chapters by describing immune cells and tight junctions in the foreskins and how these are potentially modulated *in vivo* by antiretroviral medications (ARVs) used for pre-exposure prophylaxis.

6.1 Abstract

Objectives: As topical Pre-Exposure Prophylaxis (PrEP) has been shown to cause immune modulation in rectal or cervical tissue, our aim was to examine the impact of oral PrEP on lymphoid and myeloid changes in the foreskin in response to dosing and timing of drug administration. **Design:** HIV-negative males (n=144) were recruited in South Africa and Uganda into an open-label randomised controlled trial in a 1:1:1:1:1:1:1:1:1 ratio to control arm (with no PrEP) or one of eight arms receiving emtricitabine-tenofovir disoproxil fumarate (F/TDF) or emtricitabine-tenofovir alafenamide (F/TAF) at one of two different doses, 5h or 21h before undergoing voluntary medical male circumcision (VMMC). **Methods:** After dorsal-slit circumcision, foreskin tissue-sections were embedded into Optimal Cutting Temperature (OCT) media and analysed, blinded to trial allocation, to determine numbers of CD4+CCR5+, CD1a+ cells and claudin-1 expression using xxx. Cell densities were correlated with tissue-bound drug metabolites and p24 production after *ex vivo* foreskin challenge with HIV-1bal. **Results:** There was no significant difference in CD4+CCR5+ or CD1a+ cell numbers in foreskins between treatment arms compared with the control arm. Claudin-1 expression was 34% higher (p=0.003) relative to controls but was no longer statistically significant after adjusting for multiple comparisons. There were no correlations between CD4+CCR5+, CD1a+ cell numbers, or claudin-1 expression and tissue-bound drug metabolites, nor with p24 production after *ex vivo* viral challenge. **Conclusion**: Short course (on-demand) dosing and timing of on-demand PrEP and *in situ* drug metabolite levels in tissue have no effect on numbers or anatomical location of lymphoid or myeloid HIV target cells in foreskin tissue.

6.2 INTRODUCTION

Due to a combination of antiretroviral availability, increased HIV testing, and the introduction of a range of HIV prevention tools, HIV incidence and mortality in Africa has declined [499]. However, HIV remains a global burden, with approximately 320,000 people newly infected in Africa in 2022[499]. The most common mode of HIV transmission is by heterosexual intercourse with HIV incidence highest among women of reproductive age[500]. Most HIV prevention strategies have focused on preventing male-to-female HIV transmission, whereas preventing HIV acquisition in men is relatively understudied. Voluntary medical male circumcision (VMMC) has been shown to reduce HIV infection in men by 50–60%[161,162,501], demonstrating that the foreskin plays an important role in HIV susceptibility in male individuals. As a result, VMMC has been rolled out as a standard of preventive care in Africa, with more than 26 million circumcisions having been performed between 2008 and 2019. Although effective, VMMC uptake is unevenly distributed across countries in Africa[502], and additional prevention strategies are required, including pre-exposure prophylaxis (PrEP). On-demand oral doses of tenofovir/ emtricitabine (TDF/FTC) PrEP has been shown to be highly effective in MSM couples, with efficacy in serodiscordant heterosexual documented only in the daily PrEP regimen[503–505]. Furthermore, on demand emtricitabine–tenofovir disoproxil fumarate (F/TDF) and daily emtricitabine–tenofovir alafenamide (F/TAF) are also highly effective in MSM[506]. Tenofovir gel has been evaluated for vaginal and rectal PrEP[298,507], with the CAPRISA 004 study[298] showing up to 54% lower HIV incidence in women in the gel arm. However, in another study, women receiving 1% tenofovir gel had an accumulation of activated endocervical $CD4^+$ T cells, which were associated with increased drug metabolite levels in the tissue[299]. Although these studies focused on topically applied PrEP, their findings raise the issue of host immune activation, which may undermine the potential efficacy of PrEP. In an effort to identify the impact of oral PrEP in young men on immune status, we undertook a randomized clinical trial[508] to test the secondary outcome of immunological safety by measuring numbers of $CD4^+$ $CCR5^+$ and $CD1a^+$ cells in relation to claudin-1 barrier integrity in the foreskin.

6.3 METHODS

6.3.1 Cohort description

Between 19 October 2019 and 5 March 2021, 144 HIV- negative males aged 13–24 years were enrolled from South Africa and Uganda (72 per country) into an open- label controlled trial (NCT03986970) and randomized in a 1 : 1 : 1 : 1 : 1 : 1 : 1 : 1 : 1 ratio to control arm (no PrEP) or one of eight arms receiving F/TDF or F/TAF at one of two different doses (double dose on day 1 only, or double dose on day 1 plus single dose on day 2) before undergoing a standard of care programme of VMMC at 5 or 21 hours after receiving drug [14]. Participants from communities in South Africa and Uganda expressing an in interest in VMMC were approached to participate in the clinical trial. Participants took tablets at each clinic site under directly observed therapy (DOT). In Uganda, participants stayed overnight in the hospital for the 21-h dose but in SA they went home and returned the next day. Eligibility criteria included being clinically eligible for circumcision, weighing >35 kg, and being able to give written informed consent. Appendix IV, Supplementary Figure 1, shows the number of participants screened and the numbers enrolled into each arm that went onto be circumcised.

6.3.2 Randomization and masking

Random allocation sequence was generated by an independent statistician using Stata, stratified by country and using a block size of 9. Participants not able to continue in the study following randomization were excluded according to protocol, and an additional set of randomization codes generated using the same approach, to ensure a target sample size of 16 evaluable participants per trial arm was attained. Sequentially numbered opaque envelopes labelled with unique randomization identifier and containing the allocated intervention arm were prepared by two administrators not otherwise involved in the study. At time of randomization, clinical staff opened the sequential envelope and scheduled the participant to receive PrEP (if applicable) and VMMC, as per randomization arm. Participants and care providers were not blinded to trial arm. Laboratory outcome assessors were blinded until all measurements were completed. An independent statistician scrambled sample identifiers for laboratory investigation using Stata.

6.3.3 Tissue sampling

VMMC was performed using the dorsal slit method. Foreskin tissue was placed immediately in cold DMEM and transported to the laboratory on ice within 30 min. All tissues were immediately dissected into 8 x 2.5 mm pieces (four for inner and four for outer) and snap-frozen in Optimal Cutting Temperature (OCT) compound and stored in 80□C freezers and were all later shipped to the University of Cape Town and processed for immunohistochemistry,

imaging and analysis as previously described[508].

6.3.4 Immunohistochemistry imaging and analysis

The density of $CD4^+CCR5^+$ cells was assessed from 72 participants from South Africa and 40 from Uganda. A more limited number of samples were assessed for CD1a and claudin-1 expression including all control arm participants (n=16) and four randomly selected from each of the eight treatment trial arms (n=40 from South Africa and 40 from Uganda 80 in total). Appendix IV, Supplementary Figure 1 shows the breakdown of participants analyzed per arm along with the number of images collected and quantified. OCT snap-frozen tissues were sectioned (5–10 mm thick) using a Leica CM1850 Cryostat (Illinois, USA) and processed as described[508]. Tissues was stained with primary antihuman $CD4^+$ antibody (1 : 50 dilution; Sigma, St. Louis, Missouri, USA); secondary Cy5 antibody (1 : 500; AEC Amersham, Johannesburg, South Africa); antihuman primary MC-5 CCR5 antibody (1 : 10; courtesy of Prof. Mathias Mack) and secondary Cy3 antibody (1 : 1000; AEC Amersham);primary antihuman claudin-1 antibody (1 : 200; Thermofisher, Waltham, Massachusetts, USA) and secondary DarB antibody (1 : 1000, AEC Amersham); primary antihuman CD1a antibody (Ltc Tech SA, Randburg, South Africa) and secondary Cy5 antibody (1 : 500; AEC Amersham). Cell nuclei were stained with DAPI (Hoechst). Negative controls were stained with isotype mouse or rabbit and kidney tubular tissue and positive controls for CCR5 on tonsillar tissue (Appendix IV, Supplementary Figure 2). Ten images for each section were collected using DeltaVision RT systems and softWoRx software (Applied Precision Instruments) and quantified using Image J and Pipsqueak (Appendix IV, Supplementary Figure 3). Percentage of claudin-1 expression was calculated by dividing the number of pixels taken up by claudin-1 staining (Fig. 2d and e) by the total epidermal area for each foreskin section. We also delineated between CD1aþ cells inside the claudin-1 staining (intrinsic, iCD1a) and $CD1a^+$ cells outside of the claudin-1 stain (extrinsic, eCD1a) and expressed this as a ratio: eCD1a/iCD1a.

6.3.5 Ex-vivo challenge of foreskin tissue

Foreskin tissue was cut into 2 mm2 explants [509] and cultured by adding an outer and an inner explant per well, in DMEM supplemented with 10% FBS, 2 mmol/l L-glutamine, 2.5 mg of amphotericin B/ml, and antibiotics (100U of penicillin/ml, 100 mg of streptomycin/ml) (Sigma). Explants were immediately challenged with HIV-1BaL at either a high titre [104 TCID50/ml (median tissue culture infective dose/mL)] or low titre (2 10 TCID50/ml), being more physiologically relevant. Control explant tissues received no virus. Foreskin explants were cultured for 15 days with approximately two-thirds of culture supernatant harvested at days 3, 7, 11 and 15, and cultures replenished with fresh medium. p24 was measured in the

supernates by ELISA (Innotest HIV antigen mAb ELISA, Fujirebio Europe, Belgium). The lower limit of quantification (LLQ) for the assay was 0.02998 and p24 concentrations that were below the LLQ of each assay were expressed as half-LLQ values.

6.3.6 Tissue drug metabolites

Concentrations of the active phosphorylated intracellular metabolites – tenofovir-diphosphate (TFV-DP) and emtricitabine-triphosphate (FTC-TP) were determined in foreskin tissue as previously described[510].

6.3.7 RNA sequencing of foreskin tissue

The details of the procedure used for RNA sequencing of foreskin tissue have been previously described[511]. Transcriptomes were derived from combined inner and outer foreskin from each participant.

6.3.8 Data analysis

The following outcomes were summarized both overall and by trial arm: $CD4^+$cell density, CCR5 density, $CD4^+CCR5^+$, proportion of CCR5 expression on $CD4^+$ cells, distance from the epidermis, eCD1a/iCD1a ratio, $CD1a/cm^2$, % claudin expression. Except for the proportion of CCR5 expression on $CD4^+$ cells, outcomes were positively skewed and were, therefore, log-transformed for analysis. The relative effect of trial interventions was assessed through the following comparisons: any PrEP versus control arm, F/TAF versus F/TDF, 2 1 tablets versus 2 tablets, 21h between PrEP and VMMC versus 5 h. Further comparisons also assessed the effect of dosage separately for each drug, and the effect of the interval, separately for each drug and dosage. Mixed effects linear regression models, allowing for clustering within participants since several sections of tissue were imaged for each participant, were used to determine the mean difference and 95% confidence interval (CI) for each comparison, with P values determined by likelihood ratio tests. For all outcomes other than the proportion of CCR5 expression on $CD4^+$cells, parameters were back transformed and reported as geometric mean ratios (GMR). Correlations between each study outcome and pharmacokinetic–pharmacodynamic (PK–PD) parameters were assessed by Pearson's correlation coefficient, using the mean of the imaging outcome from the different sections for each participant.

6.3.9 Ethics approvals

Written informed consent was obtained from all participants aged at least 18 years and emancipated minors (in Uganda); for those less than 18 years and not emancipated minors, their assent with parental consent was obtained. The trial was conducted in accordance with

the principles of the Declaration of Helsinki and Good Clinical Practice and approved in the South African Health Products Regulatory Authority (20181004). Ethical approval was granted from University of Cape Town (290/2018), University of the Witwatersrand (180906B, M1811148 and 180108), Uganda Virus Research Institute research ethics committee (GC/127/18/12/680), Uganda.

6.4 RESULTS

6.4.1 Impact of emtricitabine–tenofovir disoproxil fumarate or emtricitabine–tenofovir alafenamide on the density of CD4RCCR5R and CCR5 expression on CD4R cells in the foreskin.

As CCR5 is the main HIV co-receptor for most transmitted isolates[512,513], we assessed the density of double-expressing $CD4^+CCR5^+$ cells along with the proportion of CCR5 staining on $CD4^+$ cells. Figure 1ac show representative images of single- expressing (a and b) and double-expressing $CD4^+CCR5^+$cells (c) in foreskin tissue in relation to the outer epidermis. Figure 6.1d shows the distribution of double-expressing $CD4^+CCR5^+$ cell density by treatment arm, where no significant differences were identified. Table 6.1 shows results from a mixed effects model where no difference was identified for any comparison between reference and comparator group. Additionally, timing and dose of F/TDF and F/TAF had no significant impact on CCR5 expression on $CD4^+$cells (**Fig. 1e, Appendix IV, Supplementary Table 1**). This finding was consistent at the tissue gene expression level, where there was no significant difference in the expression of CD4 or CCR5 genes between treatment and control arms (**Appendix IV, Supplementary Figures 4A and B**). Collectively, these data show that the density of HIV target cells and CCR5 expression was not modulated by drug dose or timing of PrEP prior to VMMC.

On a subset of samples (South Africa participants), we compared the impact of the drug dose and timing on the density of $CD4^+CCR5^+$cells separately for inner and outer foreskin samples. Supplementary Figures 5A and B (**Appendix IV**) show that PrEP doses from the different arms had no impact on the density of $CD4^+CCCR5^+$cells in either the inner or outer foreskin. There was also no significant difference (p=0.14) in the densities of $CD4^+CCR5^+$ cells between the inner and outer foreskin. However, there was 5.8 times greater expression of CCR5 on $CD4^+$cells in the outer foreskin (p=0.01), inferring that the outer foreskin would be more susceptible to HIV-1 infection.

We then tested the hypothesis that drug may influence the anatomical location of $CD4^+CCR5^+$ cells and possibly drive them either deeper into the tissue or further to the apical layer of the

epidermis. Figure 6.1f and **Appendix IV, Supplementary Table 1**, shows that the distance of potential HIV-1 target cells from the epidermis was not significantly different between treatment arms or relative to the control arm.

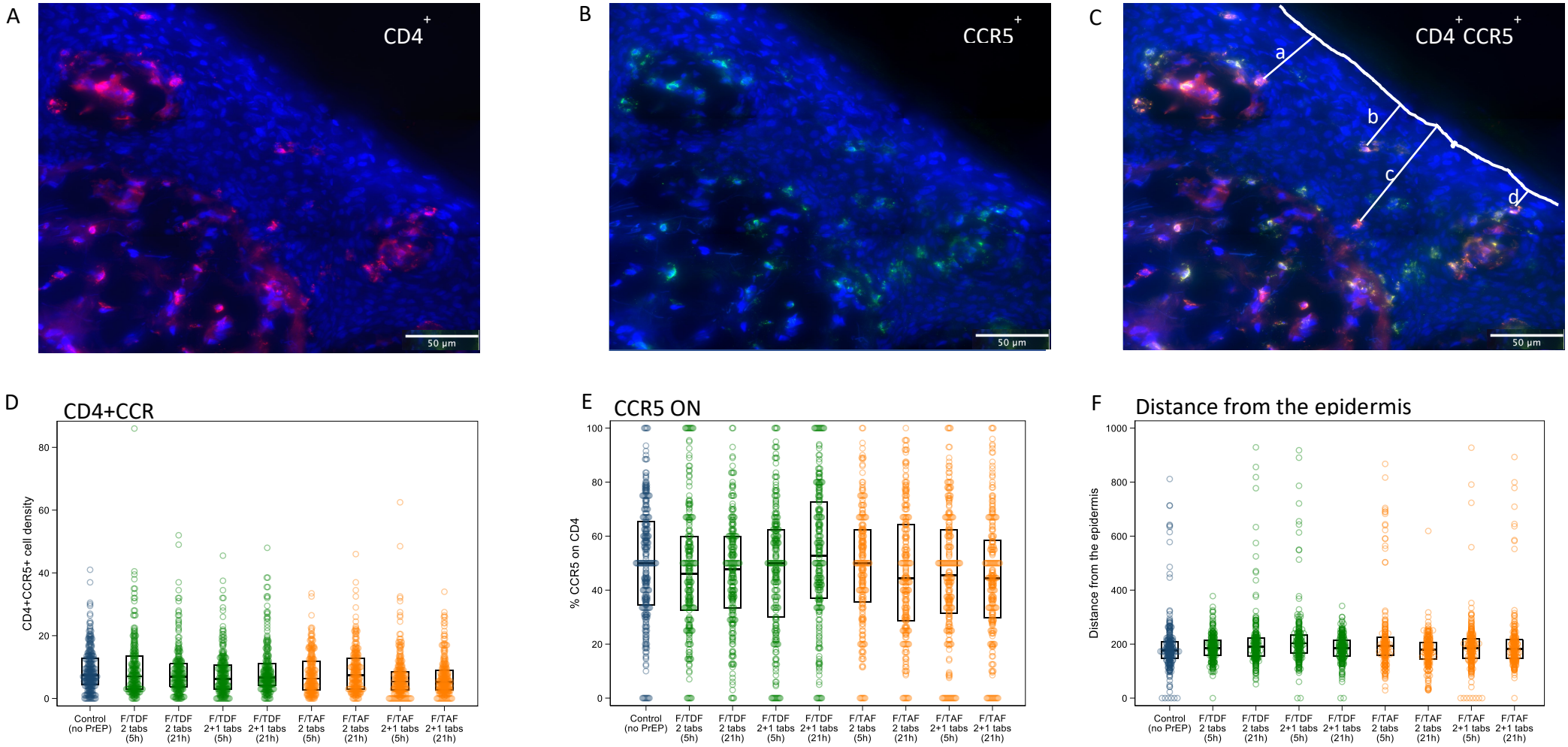

Figure 6. 1 Density of CD4$^+$CCR5$^+$ and CCR5 on CD4$^+$ cells in foreskins from the participants of the CHAPS trial.

(a) Representative image of CD4$^+$ cells in the foreskin; (b) representative image of CCR5$^+$ cells in the foreskin; (c) representative image of dual stained CD4$^+$CCR5$^+$ cells in the foreskin showing the outline of the epidermis layer and representative distances (a, b, c and d) of cells from the surface; (d) numbers of CD4$^+$CCR5$^+$cells in the foreskin across the nine trial arms. Box plots show median lines and interquartile ranges overlayed with each measurement. (e)

Proportion of CCR5 expression on $CD4^+$cells in the foreskin across the nine trial arms. Box plots show median lines and interquartile ranges overlayed with each measurement. (f) Distance of $CD4^+CCR5^+$cells within the foreskin from the outer epidermis from participants across the nine trial arms. Box plots show median lines and interquartile ranges overlayed with each measurement.

6.4.2 Impact of emtricitabine– tenofovir disoproxil fumarate or emtricitabine– tenofovir alafenamide on the density of CD1a$^+$ cells and claudin-1 expression in the foreskin.

CD1a is one of the unique proteins that is expressed on either dendritic cells[514] or epidermal Langerhans cells[515,516] . Furthermore, this marker represents an important cell type as either an HIV target[517] or for delivery of HIV away from sites of infection[517]. We sought to identify whether either of the PrEP regimens, doses, or time of administration prior to VMMC impacted upon the density and location of CD1a$^+$cells from the outer epithelial layer, as measured by claudin-1, one of the tight junction proteins found in the foreskin epidermis[518,519]. Figure 6.2a shows a representative image of CD1a$^+$ cell staining, illustrating the presence of these cells in both epidermis and dermis. Figure 6.2b and Table 6.1 shows that no significant differences existed when comparing between treatment arm permutations for combined samples from both South Africa and Uganda. This was also the case when we analyzed separately by clinical site (**South Africa versus Uganda, Appendix IV, Supplementary Figure 6A and B**), although there was a significantly lower density of CD1a$^+$ cells in samples from Uganda (P 0.03) compared with South Africa.

In addition to using claudin-1 to delineate the outer epithelial surface, we quantified expression as a measure of barrier integrity[520]. Table 6.1 shows the geometric mean of percentage claudin-1 expression was 34% higher (P 0.003) in combined inner and outer foreskin tissue from all participants receiving PrEP, compared with the control arm. After allowing for multiple comparisons, this was no longer significant (P 0.288). Comparing F/TAF double dose given 5 h before VMMC versus F/TAF double dose given 21 h prior to circumcision, resulted in 28% lower expression of claudin-1 (P ¼ 0.007, Table 1 and Fig. 6.2c), which was no longer significant after allowing for multiple comparisons.

A

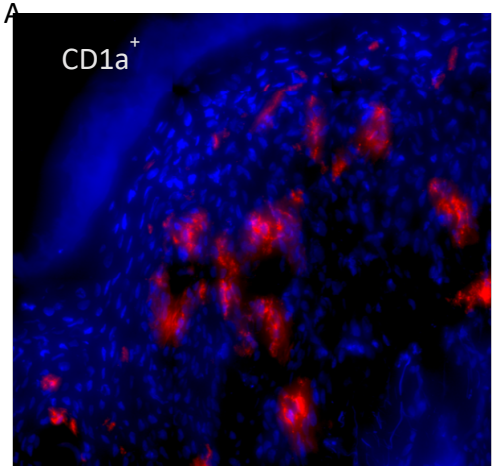
CD1a+

B

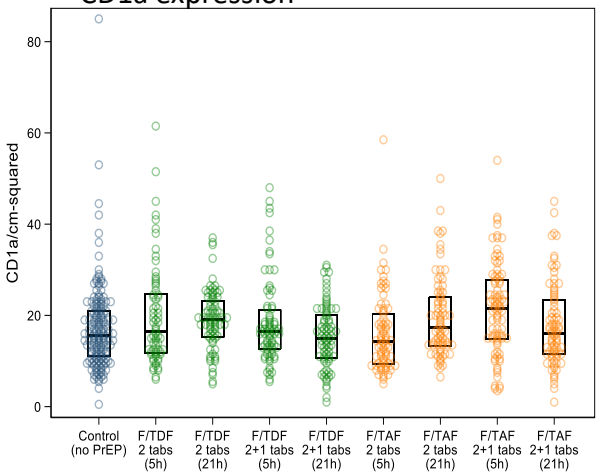
CD1a expression
CD1a/cm-squared
0
20
40
60
80
Control (no PrEP)
F/TDF 2 tabs (5h)
F/TDF 2 tabs (21h)
F/TDF 2+1 tabs (5h)
F/TDF 2+1 tabs (21h)
F/TAF 2 tabs (5h)
F/TAF 2 tabs (21h)
F/TAF 2+1 tabs (5h)
F/TAF 2+1 tabs (21h)

C

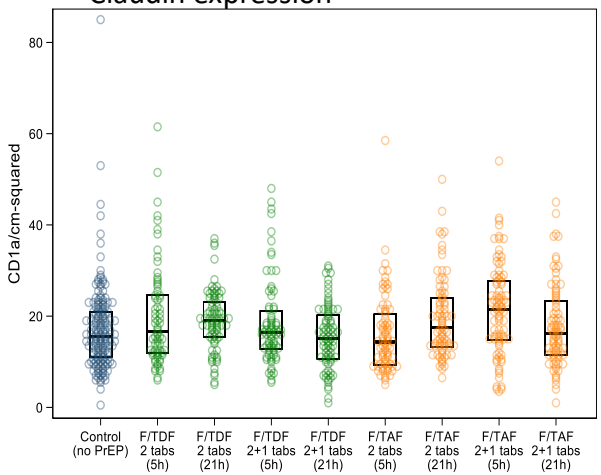
Claudin expression
CD1a/cm-squared
0
20
40
60
80
Control (no PrEP)
F/TDF 2 tabs (5h)
F/TDF 2 tabs (21h)
F/TDF 2+1 tabs (5h)
F/TDF 2+1 tabs (21h)
F/TAF 2 tabs (5h)
F/TAF 2 tabs (21h)
F/TAF 2+1 tabs (5h)
F/TAF 2+1 tabs (21h)

D

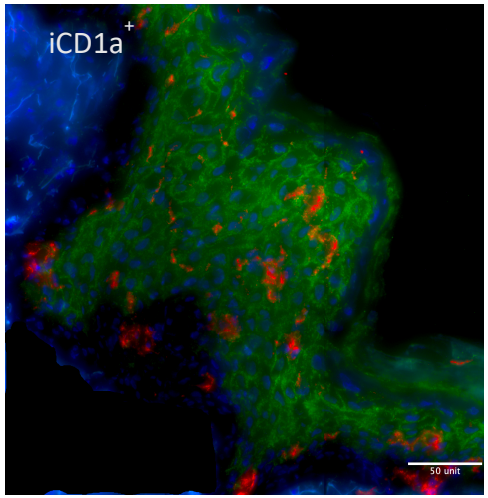
iCD1a+
50 unit

E

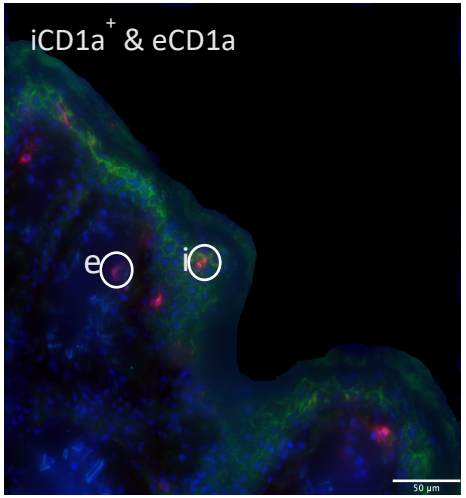
iCD1a+ & eCD1a
e
i
50 µm

F

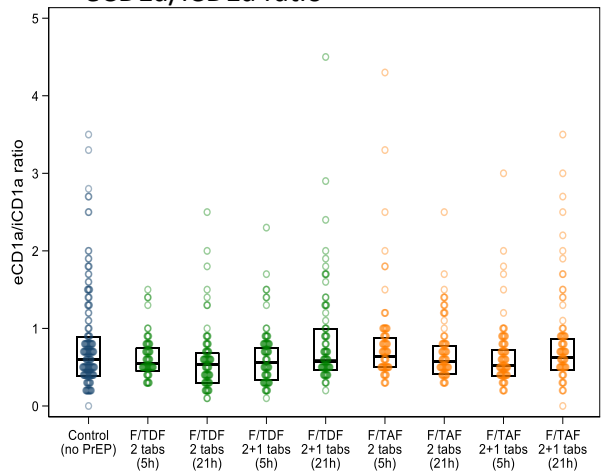
eCD1a/iCD1a ratio
eCD1a/iCD1a ratio
0
1
2
3
4
5
Control (no PrEP)
F/TDF 2 tabs (5h)
F/TDF 2 tabs (21h)
F/TDF 2+1 tabs (5h)
F/TDF 2+1 tabs (21h)
F/TAF 2 tabs (5h)
F/TAF 2 tabs (21h)
F/TAF 2+1 tabs (5h)
F/TAF 2+1 tabs (21h)

Figure 6. 2 Density of CD1a$^+$ and claudin-1 expression in the foreskins of men in different trial arms.

(a) Representative image of CD1a$^+$ cells located in the foreskin; (b) combined density of CD1a$^+$ cells in foreskins (cells/cm2) across the different trial arms; (c) combined expression of claudin-1 across the different trial arms; (d) representative image showing the presence of CD1a cells within (intrinsic, i) claudin-1 expression; (e) representative image of CD1a$^+$ cells within (intrinsic, i) claudin-1 expression and outside (extrinsic, e). The white circled cells delineate iCD1a from eCD1a; (f) combined ratio of eCD1a/iCD1a across the trial arms.

Table 6. 1 Comparisons between trial arms for $CD4^+CCR5^+$, $CD1a^+$ cells, claudin-1 expression and ratio of eCD1a/iCD1a.

Results from mixed effects models (each image measurement is included in the model and clustering of measurements within each participant is accounted for by including a random effect).

		$CD4^+CCR5^+/cm^2$		**$CD1a^+/cm^2$**		**% claudin-1 expression**		**ratio eCD1a/iCD1a**	
Reference Group	Comparator Group	Geometric mean Ratio (95% CI)	*P*	Geometric mean Ratio (95% CI)	*P*	Geometric mean Ratio (95% CI)	*P*	Geometric mean Ratio (95% CI)	*P*
Effect of any PrEP versus no PrEP									
Control arm	Any PrEP	0.84 (0.50, 1.41)	.51	1.10 (0.89, 1.35)	.39	**1.34 (1.11, 1.62)**	**.003**	0.92 (0.75, 1.13)	.43
Overall effects of drug, dosage and interval									
F/TDF (all)	F/TAF (all)	0.82 (0.55, 1.22)	.33	1.04 (0.86, 1.26)	.71	0.93 (0.79, 1.10)	.42	1.15 (0.95, 1.39)	.15
2 tabs (both drugs)	2+1 tabs (both drugs)	0.80 (0.54, 1.19)	.28	0.97 (0.80, 1.18)	.75	0.99 (0.83, 1.17)	.87	1.04 (0.85, 1.26)	.72
5 hours (all regimens)	21 hours (all regimens)	1.09 (0.74, 1.63)	.66	0.95 (0.78, 1.15)	.61	0.88 (0.75, 1.04)	.14	1.03 (0.85, 1.25)	.77
Effects of dosage, separately for each drug									
F/TDF, 2 tabs	F/TDF, 2+1 tabs	0.92 (0.55, 1.53)	.75	0.85 (0.65, 1.11)	.23	0.93 (0.73, 1.19)	.58	1.17 (0.88, 1.56)	.28
F/TAF, 2 tabs	F/TAF, 2+1 tabs	0.71 (0.38, 1.30)	.26	1.10 (0.83, 1.45)	.51	1.04 (0.81, 1.32)	.77	0.93 (0.72, 1.19)	.55
Effects of interval, separately for each drug and dosage									
F/TDF, 2 tabs (5h)	F/TDF, 2 tabs (21h)	0.82 (0.40, 1.68)	.60	1.01 (0.69, 1.47)	.96	1.04 (0.76, 1.42)	.82	0.77 (0.50, 1.17)	.22
F/TDF, 2+1	F/TDF, 2+1 tabs	1.35 (0.64, 2.86)	.43	0.81 (0.55, 1.19)	.28	0.83 (0.58, 1.20)	.33	1.39 (0.98, 1.98)	.07

tabs (5h)	(5h)								
F/TAF, 2 tabs (5h)	F/TAF, 2 tabs (21h)	1.20 (0.52, 2.75)	.67	1.27 (0.91, 1.76)	.15	1.15 (0.91, 1.47)	.24	0.84 (0.58, 1.22)	.35
F/TAF, 2+1 tabs (5h)	F/TAF, 2+1 tabs(21h)	1.07 (0.43, 2.69)	.88	0.80 (0.52, 1.23)	.31	**0.62 (0.43, 0.88)**	**.007**	1.24 (0.88, 1.75)	.21

6.4.3 Impact of emtricitabine–tenofovir disoproxil fumarate or emtricitabine–tenofovir alafenamide on the anatomical location of CD1a$^+$ cells in the foreskin.

To better gauge the location of CD1a$^+$cells in relation to the epidermis, we measured the ratio of CD1a$^+$cells between those located within the area of claudin-1 staining (intrinsic, i), being exclusively expressed in the epidermis, or located outside claudin-1 expression (extrinsic, e). Figure 6.2d and e show representative images of iCD1a (d) and a mix of iCD1a and eCD1a staining (e), respectively. Figure 6.2f and Table 1 show that there were no differences in the anatomical location of CD1a$^+$ cells between the eight treatment arms compared with the control arm, suggesting that drug exposure was not eliciting any migration of CD1a$^+$ cells within the foreskin. No association between the density of CD4$^+$CCR5$^+$ and CD1a$^+$ cells and claudin-1 expression with foreskin tissue drug metabolite levels or p24 production after *ex-vivo* viral challenge. One of the secondary objectives of the clinical trial was to identify the immune safety profile of the different PrEP dosing and timing[521]. Additional evidence to show this was made by correlating the density of HIV target cells with drug metabolite levels in the tissue. Figure 3 shows a lack of correlation between drug metabolites (TFV-DP and FTC-TP) in whole foreskin tissue with densities of CD4$^+$CCR5$^+$, CD1a$^+$ cells, % CCR5 expression on CD4þ cells and claudin-1 expression. This would suggest that the protective effect of PrEP is independent of the density of HIV target cells in the tissue. This was underscored by a lack of association between CD4$^+$CCR5$^+$, % CCR5 expression and CD1a$^+$cell numbers with p24 production after ex-vivo challenge with low or high viral titer (Fig. 3). Likewise, there was no relationship between p24 production and the location of CD1a$^+$ cells in relation to claudin-1 (Table 1). There was a weak negative association between claudin-1 expression and p24 production after high titre viral challenge (r= 0.28, P 0.01, Fig. 3). This would suggest a trend of higher claudin-1 expression and an association with lower viral replication upon ex-vivo high-dose challenge.

Figure 6. 3 Forest plots of correlations of TVF-DP, FTC-TP and p24 (high and low dose) with log10 cell densities, distance from the epidermis, % claudin and eCD1a/iCD1a ratio. Pearson correlation coefficients with 95% confidence intervals are shown for each comparison. The vertical line indicates a correlation coefficient of zero.

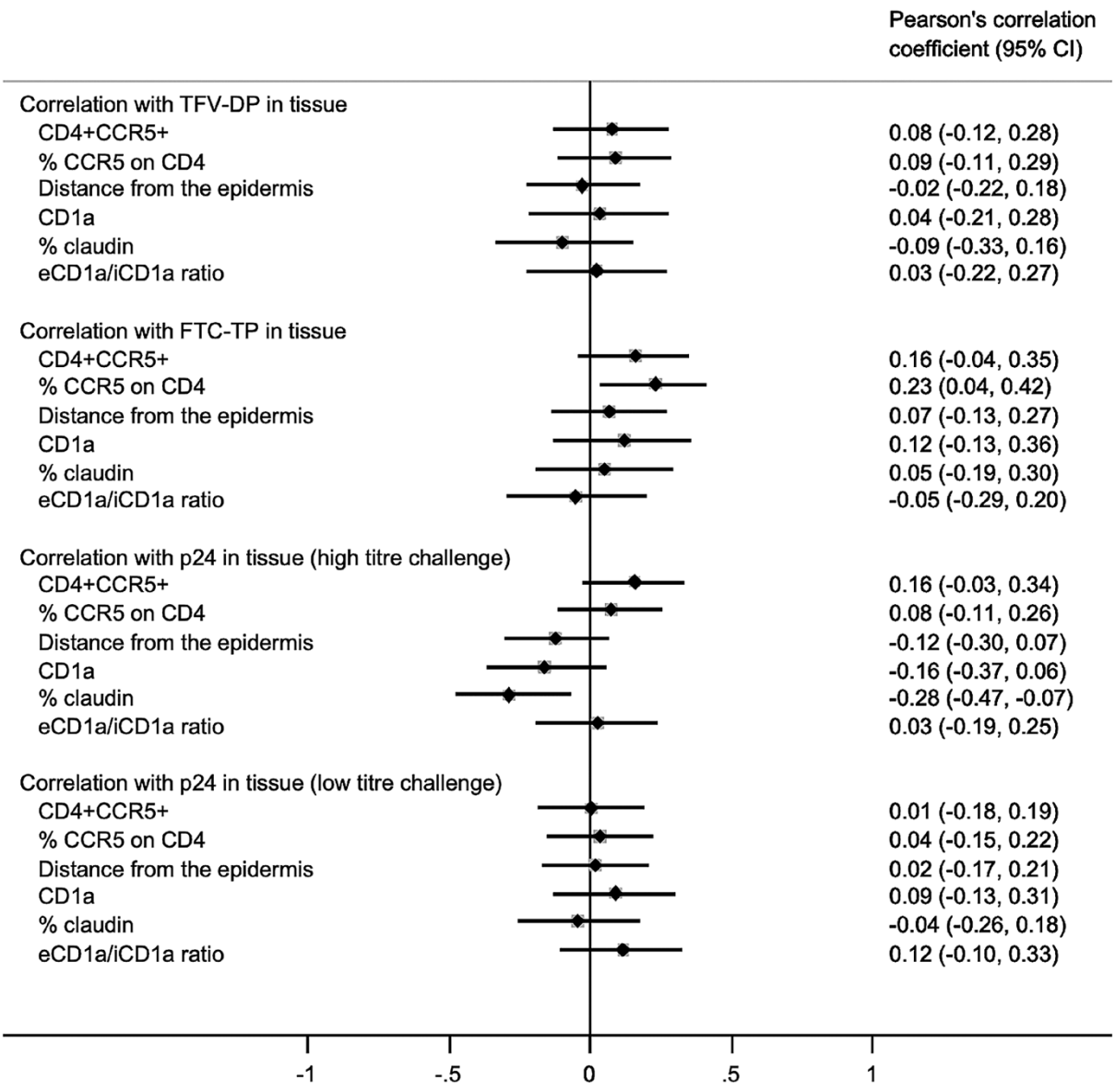

6.5 DISCUSSION

We show, in a randomized clinical trial[521], that short- course oral dosing and scheduling of on-demand F/TAF or F/TDF PrEP had no impact on the density of HIV target cells in foreskin tissue when men were circumcised at 5 or 21 h after taking drug. This was a novel trial where we aimed to show, as a secondary objective, that different types of PrEP and dosing schedules were not associated with immune activation in situ. We showed that $CD4^+CCR5^+$ cells, as measured quantitively and by gene expression levels in the tissue, were similar across different dosing and timing of drug administration. Importantly, we show that the expression of the HIV co- receptor CCR[511,522], well established to be increased upon cell activation[522,523], was not impacted by drug dose. This was similarly the finding with $CD1a^+$ cells in the foreskin showing that epithelial dendritic cells[514,524] and/or epidermal Langerhans cells[516] were consistently present across the different trial arms but unchanged in numbers. In contrast to studies using topical PrEP whereby 1% tenofovir gel increased T-cell densities in rectal tissue[507] and $CD4^+$ T-cell activation in endocervical tissue[525], we show in our study that oral PrEP dosing has no effect on local foreskin T-cell immunity. Previously, we showed that the CHAPS study resulted in modulation of gene expression in the foreskin resulting in a potentially unfavorable environment for HIV replication[511]. Collectively, these findings show that short-term oral PrEP does not induce immunologic activity in the foreskin.

The foreskin protects the host from invasion of a myriad of pathogens and does so by employing physical barriers and an intricate network of resident immune cells[526] and can be regarded as a persistently 'inflamed' tissue[193]. There is a fine distinction between Langerhans cells and dermal dendritic cells. Langerhans cells have been shown to reside in the epidermis and can act as immune sentinels by actively sampling environmental antigens[381], whereas dermal dendritic cells have been found in the papillary dermis[527]. CD1a has been shown to mark both dendritic cells[514] and epidermal Langerhans cells[515,516], and the epidermal location of $CD1a^+$ cells in our study would be consistent with staining for Langerhans cells. Although we could not differentiate between these two myeloid populations, their numbers were not modulated by PrEP dosage or timing and nor associated with drug metabolites in the tissue or p24 production after low-dose or high-dose ex-vivo HIV challenge. Although the HIV challenge model is a proxy for in-vivo HIV transmission and acquisition in tissue, our finding suggests that the presence of in-situ HIV targets cells in the tissue is independent of downstream viral replication.

Physical barrier function in the skin resides within the stratum corneum, which relies on the arrangement of epithelial cells and tight junction proteins. The importance of tight junction proteins, claudin-1 particularly, was demonstrated to be crucial for survival in mice[520], where deletion of claudin-1 resulted in death shortly after birth because of defects in epidermal barrier function. There was tantalizing evidence, albeit not significant after multiple comparisons, that claudin-1 expression may be enhanced with PrEP. Interestingly, the shorter exposure to drug (5 h) resulted in lower claudin-1 expression compared with the longer duration (21 h) and infers that longer PrEP exposure may be more beneficial. This would suggest that barrier function may be enhanced with longer drug exposure and may represent a novel finding but needs to be explored in larger studies. It is known that respiratory epithelial barriers can be altered by type 2 cytokines (such as IL-4 and IL-13) and impacting on claudin and filaggrin to compromise epithelial barriers[528,529]. However, our observation that oral PrEP may enhance claudin-1 expression requires further validation experiments and offers a potentially unique insight into how PrEP may function beyond its direct anti-viral effects.

To our knowledge, this is the first time that the effects of oral PrEP has been assessed on immune cells in foreskin tissue. One of the limitations of this study was not being able to assess the impact of PrEP on separated inner and outer foreskin for all samples (Uganda, for example) because of inadequate sample collection. Additionally, this study does not address the possible role of fibroblasts and epithelial cells in the foreskin accumulating F/TAF and F/TDF[530] and the consequent long-term impact on numbers of $CD4^+CCR5^+$ and $CD1a^+$ cells within the tissue, it does show that short-term 'on-demand' oral PrEP is immunologically well tolerated and does not induce higher numbers of activated $CD4^+$ T cells in a vulnerable anatomical site for HIV acquisition in male individuals.

CHAPTER 7

Thesis Summary and Discussion

This PhD described the prevalence of common asymptomatic STIs among young adult men who all self-identified as heterosexual men at local circumcision clinics in the Western Cape, South Africa (Chapter 2). There was a 15.9% prevalence of asymptomatic STIs, including common STIs such as *Chlamydia trachomatis, Neisseria gonorrhoeae, Trichomonas vaginalis,* and *Mycoplasm genitalium,* with the highest contributor to this high prevalence rate being 12.2% caused by C. *trachomatis*. These are two-fold higher than C. *trachomatis* prevalence estimates for South Africa. Notably, the second commonest aSTIs in this cohort is *Mycoplasma genitalia (MG),* at a prevalence rate of 4.3%, with the majority of infections being co-infections (71.4%) as opposed to mono-infections (928.6%). These are higher (1.1-3.3%) than the global estimated prevalence rates of MG in the general population[70,74] and higher than recent estimated rates in SA[76]. Of concern is that globally, MG is not included in the WHO STI spectrum estimations, and screening is not included in the recommended protocols for STI management.

Following identifying sites of high burden of aSTI, participants were enrolled into a study to examine how aSTIs affect various aspects of genital tract barrier integrity and immunity. The rationale for this is two-fold: a) to understand potential mechanisms of how MMC prevents HIV infections and b) to understand how an STI, especially sub-clinical, may exacerbate susceptibility to HIV-1 infection. Chapter 3 examines the barrier function in various key anatomical penile sites, the glans, inner foreskin, and shaft of the uncircumcised penis. Not only is the inner foreskin inherently of the lower barrier function (compared to the glans and shaft) as demonstrated by both *in vivo* lower TEWL readings and *ex vivo* lower expression of Claudin-2,4,5, E-cadherin and Filaggrin 2 in ASTI negative men, but this is further compromised by the presence of an aSTI. This is evidenced by the differential mRNA expression of claudin 1 and filaggrin 1 in the inner versus outer foreskin tissue in the presence of an aSTI. This was additionally associated with in vivo findings of significantly increased significantly increases penile glans moisture as evidenced by increased SCH readings. Over time, the penile glans barrier function improves. Most studies aimed to examine the differences in barrier function among foreskin anatomical sites have largely focused on assessing the keratin layer, of which contradicting results[177,178,184,531] exist to date in comparing especially the inner versus outer foreskin sites. This study is the first to employ existing methods commonly used in cosmetic dermatology in a novel way to examine barrier function *in vivo* in

these sites, and additionally, at a molecular level, examine junctional and SC structural proteins in the presence and absence of aSTI. These results confirm both on the *in vivo* and *ex vivo* level that indeed the inner foreskin is more compromised in its barrier shield against pathogens and thus making this site truly the most probable mechanistic explanation for the significant reduction in HIV-1 susceptibility risk in its removal in the circumcised men.

In Chapter 4, this study further examined quantitatively and qualitatively the effect of these common asymptomatic STIs on the presence of immune cell infiltrates in the foreskin of men living without HIV-1. We firstly document that the foreskin tissue is inherently infiltrated by immune cells, predominantly within the papillary dermis as compared to the epidermis and reticular dermis irrespective of aSTI status. Further immune profiling in another cohort using flow cytometry revealed that in men without any aSTI, lymphocytic infiltrates predominantly constitute CD4+ and CD8+ T cells, with the inner foreskin tissue site having higher proportion of CD8 T cells as compared to CD4+ T cells, thus a low CD4:CD8 ratio. In the presence of aSTIs, we show that the total immune cell density was significantly higher in all layers of the total foreskin tissue, with a predominant infiltration by lymphocytes that were largely in the papillary dermis. one study showed higher rates of inflammation in the foreskin dermis versus the epidermis in HIV/Herpes Simplex Virus-2 (HSV-2) uninfected men, which also increased significantly in the presence of HSV infection[301]. Another also showed increased $CD4^+$ T cell foreskin cell abundance in men with asymptomatic herpes[532]. This is also consistent with this PhD, summarized in this study with respect to other STIs besides herpes. We hypothesize that this influx of lymphocytic cells within both the epidermis and dermis during an aSTI infection is part of the explanation for the documented associated increased risk of HIV-1 with STIs.

Chapter 5 explores the effects of *C.trachomatis* on the transcriptomic signatures of two important cell types in the foreskin tissue: epithelial cells and macrophages.. The study reports that in both macrophage and epithelial cells, the most significant genes affected were those associated with immune pathway-associated genes. These include, HLA-DQA1, HLA-DQB1 and HLA-DRB1, IL7R), IL36G., TNF pathways. On the other hand, in the outer foreskin, the predominant genes and pathways affected were associated with RNA synthesis and DNA metabolism. Notably, we show that *C.trachomatis* results in pronounced changes in protein synthesis in both epithelial and macrophage cells of infected foreskin tissue. In addition, chlamydia-infected men exhibited patterns of substantial upregulation in the inner foreskin relative to uninfected men, whereas changes in gene expression were predominantly

downregulated in the outer foreskin tissue. This study is the first to examine the spatial transcriptomics in the foreskin tissue of asymptomatically chlamydia-infected men, and thus provide a fundamental basis and identification of the genes and pathways enriched in response to this infection, giving more understanding of the pathogenesis, one of the major one being that protein translation is a key component impacted by *C.trachomatis* infection in the foreskin tissue and its downregulation upregulation varies based on whether it's in the inner or outer foreskin tissue.

One of the limitations of this PhD was an inability to match all *in vivo* measures of barrier function with TJ gene expression, histopathology and spatial transcriptomics. Although the numbers analyzed were adequate to achieve statistical significance, making matching associations was confounded by logistical issues, such as the need for meter calibrations on periodic occasions. The high cost of digital spatial profiling also limited the numbers of tissues that could be analyzed. The other limitation was the fact that foreskin tissue was analyzed post-surgical removal, where response to stress during surgery and sample handling itself may impact gene expression of the tissues[496–498].

Finally, given the new era in increased PrEP roll-out, especially in developing countries now, the study examined the effect of PreP on the foreskin local tissue immunity. Overall, despite the dosing and formulation, there was no change in the density of $CD4^{+}$T cells, their expression of CCR5 receptors, $CD1a^{+}$ cells and epidermal claudin-1 expression. These findings are only the effect of that short-term 'on-demand' oral PrEP on the foreskin immunology and barrier components (claudin-1). Thus, although short-term protection was proven in this trail using *ex vivo* infection models[508], it would be important in future studies to the run the same analysis long-term. Other future studies would be to run similar study as in chapter 3 with the meter readings and match the samples across, all participants ie, collect meter readings, foreskin samples, urethral swaps and urinary samples to allow for correlative analysis which makes it more multidimensional and informative. Using the nanostring technology, it would be important to repeat the experiment, but on ex vivo tissue explants with HIV-1 infection to study the spatial immune changes in the various sites of the foreskin (dermis versus epidermis) by STI status and by active viral infection.

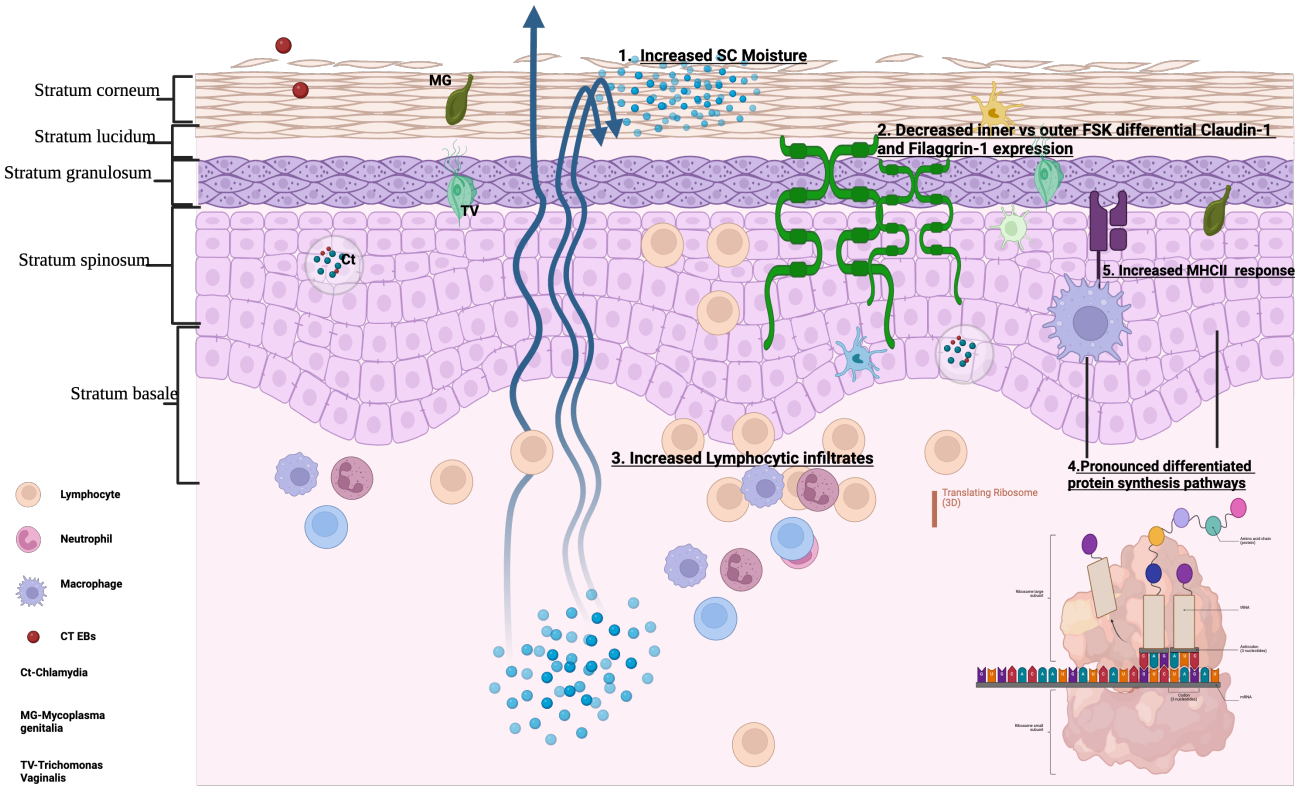

Figure 7. 1 Thesis results summary: *in vivo* and *ex vivo* molecular penile tract responses to asymptomatic STIs.

Depicted are several in vivo and ex vivo molecular changes evoked by the presence of common asymptomatic STIs such as *Chlamydia trachomatis, Neisseria gonorrhoeae, Trichomonas vaginalis,* and *Mycoplasm genitalium* in the various anatomical penile sites. In the presence of an STI, there is increased moisture in the stratum corneum (SC) as measured by significantly increased surface hydration. . This is also associated with a significant differential expression the claudin-1 and filaggrin-1 in the inner foreskin as compared to the outer. These two changes both render the epidermal barrier "weakened' or have less intact barrier function as compared to that hose in the STI-infected men. With this weakened barrier, aSTIs also cause a significant influx of lymphocytic infiltrates, which are predominantly in the papillary dermis, these consist of mainly HIV-target $CD4^+$ T-helper and $CD8^+$ Cytotoxic T-cells. Infection with *C. trachomatis* results in significant activation of macrophages (also HIV target cells) with increased expression of MHC class II receptors and being more dispersed in both the epidermal and dermal layer compared to uninfected men. Associated with these changes, both epithelial and

macrophages have pronounced changes in protein and DNA synthesis which highlights how *C. trachomatis* hijacks host metabolism to survive. (*Created with BioRender.com by CL Rametse* on Biorender.com)

REFERENCE LIST

1. Kofoed, K., Gerstoft, J., Mathiesen, L. R. & Benfield, T. Syphilis and Human Immunodeficiency Virus (HIV)-1 Coinfection: Influence on CD4 T-Cell Count, HIV-1 Viral Load, and Treatment Response. *Sex. Transm. Dis.* **33**, 143–148 (2006).
2. Masese, L. *et al.* Changes in the contribution of genital tract infections to HIV acquisition among Kenyan high-risk women from 1993 to 2012. *AIDS* **29**, 1077–1085 (2015).
3. Dzakah, E. E. *et al.* Chlamydia trachomatis Stimulation Enhances HIV-1 Susceptibility through the Modulation of a Member of the Macrophage Inflammatory Proteins. *J. Invest. Dermatol.* **142**, 1338-1348.e6 (2022).
4. Lewis, D. A. *et al.* Urethritis/Cervicitis Pathogen Prevalence and Associated Risk Factors Among Asymptomatic HIV-Infected Patients in South Africa. *Sex. Transm. Dis.* **39**, 531–536 (2012).
5. Smith, K. S. *et al.* Biological and Behavioral Factors Associated With Positive Chlamydia Retests. *Sex. Transm. Dis.* **44**, 417–422 (2017).
6. Silva, G. A. R. da *et al.* Chlamydia trachomatis asymptomatic urethritis recurrence among males living with HIV-1. *Rev. Inst. Med. Trop. São Paulo* **60**, (2018).
7. Hafner, L. M., Wilson, D. P. & Timms, P. Development status and future prospects for a vaccine against Chlamydia trachomatis infection. *Vaccine* **32**, 1563–1571 (2014).
8. Ali, H. *et al.* A new approach to estimating trends in chlamydia incidence. *Sex. Transm. Infect.* **91**, 513–519 (2015).
9. Hayward, R. J., Marsh, J. W., Humphrys, M. S., Huston, W. M. & Myers, G. S. A. Early Transcriptional Landscapes of Chlamydia trachomatis-Infected Epithelial Cells at Single Cell Resolution . *Frontiers in Cellular and Infection Microbiology* vol. 9 Preprint at (2019).
10. WHO. *Guidelines for the Management of Symptomatic Sexually Transmitted Infections*. *Guidelines for the management of symptomatic sexually transmitted infections* (2021).
11. Kularatne, R. S. *et al.* Adult gonorrhea, chlamydia and syphilis prevalence, incidence, treatment and syndromic case reporting in South Africa: Estimates using the Spectrum-STI model, 1990-2017. *PLOS ONE* **13**, e0205863 (2018).
12. Pagaoa, M. *et al.* Trends in Nationally Notifiable Sexually Transmitted Disease Case Reports During the US COVID-19 Pandemic, January to December 2020. *Sex. Transm. Dis.* **48**, 798–804 (2021).
13. WHO. WHO STI Worksheet (2022).
14. Jones, J. *et al.* Sexually transmitted infection screening, prevalence and incidence among South African men and transgender women who have sex with men enrolled in a combination HIV prevention cohort study: the Sibanye Methods for Prevention Packages Programme (MP3) proje. *J. Int. AIDS Soc.* **23**, (2020).
15. Mullick, S. Sexually transmitted infections in pregnancy: prevalence, impact on pregnancy outcomes, and approach to treatment in developing countries. *Sex. Transm. Infect.* **81**, 294–302 (2005).
16. Ganor, Y. *et al.* The adult penile urethra is a novel entry site for HIV-1 that preferentially targets resident urethral macrophages. *Mucosal Immunol.* **6**, 776–786 (2013).

17. Rowley, J. & Korenromp, E. User guide to the Spectrum-STI Module Estimating national STI burdens and trends. (2020).
18. Joint United Nations Programme on HIV/AIDS (UNAIDS), 2022. IN DANGER: UNAIDS Global AIDS Update 2022. *DANGER UNAIDS Glob. AIDS Update 2022* **2022**, 1–22 (2022).
19. Cornell, M., Majola, M., Johnson, L. F. & Dubula-Majola, V. HIV services in sub-Saharan Africa: the greatest gap is men. *The Lancet* **397**, 2130–2132 (2021).
20. Laurent, C. *et al.* HIV pre-exposure prophylaxis for men who have sex with men in west Africa: a multicountry demonstration study. *Lancet HIV* **8**, e420–e428 (2021).
21. Phiri, M. M. *et al.* Closing the gap: did delivery approaches complementary to home-based testing reach men with HIV testing services during and after the HPTN 071 (PopART) trial in Zambia? *J. Int. AIDS Soc.* **25**, (2022).
22. Zhang, J. *et al.* Discontinuation, suboptimal adherence, and reinitiation of oral HIV pre-exposure prophylaxis: a global systematic review and meta-analysis. *Lancet HIV* **9**, e254–e268 (2022).
23. Johnson, L. & Dorrington, R. Modelling the impact of HIV in South Africa's provinces: 2021 update. *South. Afr. J. HIV Med.* **18**, 94 (2017).
24. Workowski, K. A. *et al.* Sexually Transmitted Infections Treatment Guidelines, 2021. *MMWR Recomm. Rep.* **70**, 1–187 (2021).
25. WHO. *Global Health Sector Strategies on, Respectively, HIV, Viral Hepatitis and Sexually Transmitted Infections for the Period 2022-2030*. *Braz Dent J.* vol. 33 (2022).
26. Bachmann, N. L., Polkinghorne, A. & Timms, P. Chlamydia genomics: providing novel insights into chlamydial biology. *Trends Microbiol.* **22**, 464–472 (2014).
27. Malhotra, M., Sood, S., Mukherjee, A., Muralidhar, S. & Bala, M. Genital Chlamydia trachomatis: an update. *Indian J. Med. Res.* **138**, 303–16 (2013).
28. Elwell, C., Mirrashidi, K. & Engel, J. Chlamydia cell biology and pathogenesis. *Nat. Rev. Microbiol.* **14**, 385–400 (2016).
29. Johnson, L. F., Alkema, L. & Dorrington, R. E. A Bayesian approach to uncertainty analysis of sexually transmitted infection models. *Sex. Transm. Infect.* **86**, 169–174 (2010).
30. Korenromp, E. L. *et al.* What proportion of episodes of gonorrhoea and chlamydia becomes symptomatic? *Int. J. STD AIDS* **13**, 91–101 (2002).
31. Detels, R. *et al.* The incidence and correlates of symptomatic and asymptomatic Chlamydia trachomatis and Neisseria gonorrhoeae infections in selected populations in five countries. *Sex. Transm. Dis.* **38**, 503–9 (2011).
32. Stamm, W. E. *et al.* Causes of the Acute Urethral Syndrome in Women. *N. Engl. J. Med.* **303**, 409–415 (1980).
33. Molano, M. *et al.* The Natural Course of Chlamydia trachomatis Infection in Asymptomatic Colombian Women: A 5-Year Follow-Up Study. *J. Infect. Dis.* **191**, 907–916 (2005).
34. Marrazzo, J. Predicting chlamydial and gonococcal cervical infection: implications for management of cervicitis. *Obstet. Gynecol.* **100**, 579–584 (2002).
35. Crum, C. P. *et al.* The distal fallopian tube: a new model for pelvic serous carcinogenesis. *Curr. Opin. Obstet. Gynecol.* **19**, 3–9 (2007).

36. Folkins, A. K. *et al.* A candidate precursor to pelvic serous cancer (p53 signature) and its prevalence in ovaries and fallopian tubes from women with BRCA mutations. *Gynecol. Oncol.* **109**, 168–173 (2008).
37. Zardawi, I. M. Primary Fallopian Tube Carcinoma Arising in the Setting of Chronic Pelvic Inflammatory Disease. *Case Rep. Med.* **2014**, 1–7 (2014).
38. Hedger, M. P. Immunophysiology and Pathology of Inflammation in the Testis and Epididymis. *J. Androl.* **32**, 625–640 (2011).
39. Redgrove, K. A. & McLaughlin, E. A. The Role of the Immune Response in Chlamydia trachomatis Infection of the Male Genital Tract: A Double-Edged Sword. *Front. Immunol.* **5**, (2014).
40. Crichton, J., Hickman, M., Campbell, R., Batista-Ferrer, H. & Macleod, J. Socioeconomic factors and other sources of variation in the prevalence of genital chlamydia infections: A systematic review and meta-analysis. *BMC Public Health* **15**, 729 (2015).
41. Aghaizu, A. *et al.* Frequency and risk factors for incident and redetected Chlamydia trachomatis infection in sexually active, young, multi-ethnic women: a community based cohort study. *Sex. Transm. Infect.* **90**, 524–528 (2014).
42. Batteiger, B. E. *et al.* Repeated Chlamydia trachomatis Genital Infections in Adolescent Women. *J. Infect. Dis.* **201**, 42–51 (2010).
43. Hwang, L. Y., Ma, Y. & Moscicki, A.-B. Biological and Behavioral Risks for Incident Chlamydia trachomatis Infection in a Prospective Cohort. *Obstet. Gynecol.* **124**, 954–960 (2014).
44. Jørgensen, M. J. *et al.* Chlamydia trachomatis infection in young adults — association with concurrent partnerships and short gap length between partners. *Infect. Dis.* **47**, 838–845 (2015).
45. O'Connell, C. M. & Ferone, M. E. Chlamydia trachomatis Genital Infections. *Microb. Cell* **3**, 390–403 (2016).
46. Numazaki, K., Asanuma, H. & Niida, Y. Chlamydia trachomatisinfection in early neonatal period. *BMC Infect. Dis.* **3**, 2 (2003).
47. Moulder, J. W. Interaction of chlamydiae and host cells in vitro. *Microbiol. Rev.* **55**, 143–190 (1991).
48. Wang, Y. *et al.* Chlamydial Lipoproteins Stimulate Toll-Like Receptors 1/2 Mediated Inflammatory Responses through MyD88-Dependent Pathway. *Front. Microbiol.* **8**, (2017).
49. Zhou, H. *et al.* pORF5 plasmid protein of Chlamydia trachomatis induces MAPK-mediated pro-inflammatory cytokines via TLR2 activation in THP-1 cells. *Sci. China Life Sci.* **56**, 460–466 (2013).
50. Datta, B., Njau, F., Thalmann, J., Haller, H. & Wagner, A. D. Differential infection outcome of Chlamydia trachomatis in human blood monocytes and monocyte-derived dendritic cells. *BMC Microbiol.* **14**, 209 (2014).
51. Yilma, A. N., Singh, S. R., Fairley, S. J., Taha, M. A. & Dennis, V. A. The Anti-Inflammatory Cytokine, Interleukin-10, Inhibits Inflammatory Mediators in Human Epithelial Cells and Mouse Macrophages Exposed to Live and UV-Inactivated Chlamydia trachomatis. *Mediators Inflamm.* **2012**, 1–10 (2012).
52. Unemo, M. *et al.* Gonorrhoea. *Nat. Rev. Dis. Primer* **5**, 79 (2019).

53. Chan, P. A. *et al.* Extragenital Infections Caused by Chlamydia trachomatis and Neisseria gonorrhoeae : A Review of the Literature. *Infect. Dis. Obstet. Gynecol.* **2016**, 1–17 (2016).
54. Beck, E. J. *et al.* Case-control study of sexually transmitted diseases as cofactors for HIV-1 transmission. *Int. J. STD AIDS* **7**, 34–38 (1996).
55. WHO. *Infection Surveillance*. *Southern Medical Journal* vol. 70 (2018).
56. Whelan, J., Abbing-Karahagopian, V., Serino, L. & Unemo, M. Gonorrhoea: a systematic review of prevalence reporting globally. *BMC Infect. Dis.* **21**, 1152 (2021).
57. Quillin, S. J. & Seifert, H. S. Neisseria gonorrhoeae host adaptation and pathogenesis. *Nat. Rev. Microbiol.* **16**, 226–240 (2018).
58. Moran, J. S. & Levine, W. C. Drugs of choice for the treatment of uncomplicated gonococcal infections. *Clin. Infect. Dis. Off. Publ. Infect. Dis. Soc. Am.* **20 Suppl 1**, S47-65 (1995).
59. Blondeau, J. M., Hansen, G., Metzler, K. & Hedlin, P. The role of PK/PD parameters to avoid selection and increase of resistance: mutant prevention concentration. *J. Chemother. Florence Italy* **16 Suppl 3**, 1–19 (2004).
60. Jensen, J. S. *et al.* Mycoplasma genitalium: a cause of male urethritis? *Sex. Transm. Infect.* **69**, 265–269 (1993).
61. Horner, P. J. *et al.* Association of Mycoplasma genitalium with acute non-gonococcal urethritis. *The Lancet* **342**, 582–585 (1993).
62. du Plessis, T., Walls, G., Jordan, A. & Holland, D. J. Implementation of a pharmacist-led penicillin allergy de-labelling service in a public hospital. *J. Antimicrob. Chemother.* **74**, 1438–1446 (2019).
63. Taylor-Robinson, D. & Jensen, J. S. Mycoplasma genitalium: from Chrysalis to Multicolored Butterfly. *Clin. Microbiol. Rev.* **24**, 498–514 (2011).
64. Seña, A. C. *et al.* Chlamydia trachomatis, Mycoplasma genitalium, and Trichomonas vaginalis infections in men with nongonococcal urethritis: predictors and persistence after therapy. *J. Infect. Dis.* **206**, 357–65 (2012).
65. Huppert, J. S. *et al.* Mycoplasma genitalium detected by transcription-mediated amplification is associated with Chlamydia trachomatis in adolescent women. *Sex. Transm. Dis.* **35**, 250–4 (2008).
66. Black, V. *et al.* The detection of urethritis pathogens among patients with the male urethritis syndrome, genital ulcer syndrome and HIV voluntary counselling and testing clients: should South Africa's syndromic management approach be revised? *Sex. Transm. Infect.* **84**, 254–258 (2008).
67. Horner, P. J., Blee, K., Falk, L., van der Meijden, W. & Moi, H. 2016 European guideline on the management of non-gonococcal urethritis. *Int. J. STD AIDS* **27**, 928–937 (2016).
68. Wetmore, C. M. *et al.* Demographic, Behavioral, and Clinical Characteristics of Men With Nongonococcal Urethritis Differ by Etiology: A Case-Comparison Study. *Sex. Transm. Dis.* **38**, 180–186 (2011).
69. Gottesman, T., Yossepowitch, O., Samra, Z., Rosenberg, S. & Dan, M. Prevalence of Mycoplasma genitalium in men with urethritis and in high risk asymptomatic males in Tel Aviv: a prospective study. *Int. J. STD AIDS* **28**, 127–132 (2017).
70. Leung, A. *et al.* Mycoplasma genitalium is associated with symptomatic urethritis. *Int. J. STD AIDS* **17**, 285–288 (2006).

71. Soni, S. *et al.* The prevalence of urethral and rectal Mycoplasma genitalium and its associations in men who have sex with men attending a genitourinary medicine clinic. *Sex. Transm. Infect.* **86**, 21–24 (2010).
72. Cohen, C. R. *et al.* Mycoplasma genitalium Infection and Persistence in a Cohort of Female Sex Workers in Nairobi, Kenya. *Sex. Transm. Dis.* **34**, 274–279 (2007).
73. Sonnenberg, P. *et al.* Epidemiology of Mycoplasma genitalium in British men and women aged 16–44 years: evidence from the third National Survey of Sexual Attitudes and Lifestyles (Natsal-3). *Int. J. Epidemiol.* **44**, 1982–1994 (2015).
74. Jensen, J. S., Cusini, M., Gomberg, M. & Moi, H. 2016 European guideline on Mycoplasma genitalium infections. *J. Eur. Acad. Dermatol. Venereol.* **30**, 1650–1656 (2016).
75. Mahlangu, M. P., Müller, E. E., Venter, J. M. E., Maseko, D. V. & Kularatne, R. S. The Prevalence of Mycoplasma genitalium and Association With Human Immunodeficiency Virus Infection in Symptomatic Patients, Johannesburg, South Africa, 2007–2014. *Sex. Transm. Dis.* **46**, 395–399 (2019).
76. Kaida, A. *et al.* A high burden of asymptomatic genital tract infections undermines the syndromic management approach among adolescents and young adults in South Africa: implications for HIV prevention efforts. *BMC Infect. Dis.* **18**, 499 (2018).
77. McGowin, C. L., Ma, L., Martin, D. H. & Pyles, R. B. Mycoplasma genitalium -Encoded MG309 Activates NF-κB via Toll-Like Receptors 2 and 6 To Elicit Proinflammatory Cytokine Secretion from Human Genital Epithelial Cells. *Infect. Immun.* **77**, 1175–1181 (2009).
78. McGowin, C. L., Radtke, A. L., Abraham, K., Martin, D. H. & Herbst-Kralovetz, M. Mycoplasma genitalium Infection Activates Cellular Host Defense and Inflammation Pathways in a 3-Dimensional Human Endocervical Epithelial Cell Model. *J. Infect. Dis.* **207**, 1857–1868 (2013).
79. Dehon, P. M. *et al.* Histological Evidence of Chronic Mycoplasma genitalium –Induced Cervicitis in HIV-Infected Women: A Retrospective Cohort Study. *J. Infect. Dis.* **213**, 1828–1835 (2016).
80. Ma, L. & Martin, D. H. Single-Nucleotide Polymorphisms in the rRNA Operon and Variable Numbers of Tandem Repeats in the Lipoprotein Gene among Mycoplasma genitalium Strains from Clinical Specimens. *J. Clin. Microbiol.* **42**, 4876–4878 (2004).
81. Cohen, C. R. *et al.* Mycoplasma genitalium Infection and Persistence in a Cohort of Female Sex Workers in Nairobi, Kenya. *Sex. Transm. Dis.* **34**, 274–279 (2007).
82. Wood, G. E., Patton, D. L., Cummings, P. K., Iverson-Cabral, S. L. & Totten, P. A. Experimental Infection of Pig-Tailed Macaques (Macaca nemestrina) with Mycoplasma genitalium. *Infect. Immun.* **85**, (2017).
83. Ma, L. *et al.* Extensive Variation and Rapid Shift of the MG192 Sequence in Mycoplasma genitalium Strains from Patients with Chronic Infection. *Infect. Immun.* **82**, 1326–1334 (2014).
84. Fraser, C. M. *et al.* The Minimal Gene Complement of Mycoplasma genitalium. *Science* **270**, 397–404 (1995).
85. McGowin, C. L. & Totten, P. A. The Unique Microbiology and Molecular Pathogenesis of Mycoplasma genitalium. *J. Infect. Dis.* **216**, S382–S388 (2017).

86. Horner, P. *et al.* Should we be testing for urogenital Mycoplasma hominis , Ureaplasma parvum and Ureaplasma urealyticum in men and women? – a position statement from the European STI Guidelines Editorial Board. *J. Eur. Acad. Dermatol. Venereol.* **32**, 1845–1851 (2018).
87. Read, T. R. H. *et al.* Outcomes of Resistance-guided Sequential Treatment of Mycoplasma genitalium Infections: A Prospective Evaluation. *Clin. Infect. Dis.* **68**, 554–560 (2019).
88. Durukan, D. *et al.* Resistance-Guided Antimicrobial Therapy Using Doxycycline–Moxifloxacin and Doxycycline–2.5 g Azithromycin for the Treatment of Mycoplasma genitalium Infection: Efficacy and Tolerability. *Clin. Infect. Dis.* **71**, 1461–1468 (2020).
89. Li, Y., Le, W.-J., Li, S., Cao, Y.-P. & Su, X.-H. Meta-analysis of the efficacy of moxifloxacin in treating Mycoplasma genitalium infection. *Int. J. STD AIDS* **28**, 1106–1114 (2017).
90. Mondeja, B. A. *et al.* Macrolide-resistant Mycoplasma genitalium infections in Cuban patients: an underestimated health problem. *BMC Infect. Dis.* **18**, 601 (2018).
91. Kissinger, P. Epidemiology and Treatment of Trichomoniasis. *Curr. Infect. Dis. Rep.* **17**, 31 (2015).
92. Kissinger, P. Trichomonas vaginalis: a review of epidemiologic, clinical and treatment issues. *BMC Infect. Dis.* **15**, 307 (2015).
93. Moodley, P., Wilkinson, D., Connolly, C., Moodley, J. & Sturm, A. W. Trichomonas vaginalis Is Associated with Pelvic Inflammatory Disease in Women Infected with Human Immunodeficiency Virus. *Clin. Infect. Dis.* **34**, 519–522 (2002).
94. Masha, S. C., Cools, P., Sanders, E. J., Vaneechoutte, M. & Crucitti, T. Trichomonas vaginalis and HIV infection acquisition: a systematic review and meta-analysis. *Sex. Transm. Infect.* **95**, 36–42 (2019).
95. Boselli, F., Chiossi, G., Bortolamasi, M. & Gallinelli, A. Prevalence and determinants of genital shedding of herpes simplex virus among women attending Italian colposcopy clinics. *Eur. J. Obstet. Gynecol. Reprod. Biol.* **118**, 86–90 (2005).
96. ZHANG, Z.-F. & BEGG, C. B. Is Trichomonas vaginalis a Cause of Cervical Neoplasia? Results from a Combined Analysis of 24 Studies. *Int. J. Epidemiol.* **23**, 682–690 (1994).
97. Petrin, D., Delgaty, K., Bhatt, R. & Garber, G. Clinical and Microbiological Aspects of Trichomonas vaginalis. *Clin. Microbiol. Rev.* **11**, 300–317 (1998).
98. Price, C. M. *et al.* Prevalence and Detection of Trichomonas vaginalis in HIV-Infected Pregnant Women. *Sex. Transm. Dis.* **45**, 332–336 (2018).
99. Teasdale, C. A. *et al.* Incidence of sexually transmitted infections during pregnancy. *PLOS ONE* **13**, e0197696 (2018).
100. Van Gerwen, O. T. & Muzny, C. A. Recent advances in the epidemiology, diagnosis, and management of Trichomonas vaginalis infection. *F1000Research* **8**, 1666 (2019).
101. Kissinger, P. & Adamski, A. Trichomoniasis and HIV interactions: a review. *Sex. Transm. Infect.* **89**, 426–433 (2013).
102. COTCH, M. F. *et al.* Trichomonas vaginalis Associated With Low Birth Weight and Preterm Delivery. *Sex. Transm. Dis.* **24**, 353–360 (1997).
103. COTCH, M. F. *et al.* Trichomonas vaginalis Associated With Low Birth Weight and Preterm Delivery. *Sex. Transm. Dis.* **24**, 353–360 (1997).
104. Harp, D. F. & Chowdhury, I. Trichomoniasis: evaluation to execution. *Eur. J. Obstet.*

Gynecol. Reprod. Biol. **157**, 3–9 (2011).
105. Krieger, J. N. Trichomoniasis in men: old issues and new data. *Sex. Transm. Dis.* **22**, 83–96 (1995).
106. Hazra, A., Collison, M. W. & Davis, A. M. *CDC Sexually Transmitted Infections Treatment Guidelines, 2021*. *Jama* vol. 327 (2022).
107. Boily, M.-C. *et al.* Heterosexual risk of HIV-1 infection per sexual act: systematic review and meta-analysis of observational studies. *Lancet Infect. Dis.* **9**, 118–129 (2009).
108. Powers, K. A., Poole, C., Pettifor, A. E. & Cohen, M. S. Rethinking the heterosexual infectivity of HIV-1: a systematic review and meta-analysis. *Lancet Infect. Dis.* **8**, 553–563 (2008).
109. Baggaley, R. F., White, R. G. & Boily, M.-C. HIV transmission risk through anal intercourse: systematic review, meta-analysis and implications for HIV prevention. *Int. J. Epidemiol.* **39**, 1048–1063 (2010).
110. Baggaley, R. F. *et al.* Does per-act <scp>HIV</scp> -1 transmission risk through anal sex vary by gender? An updated systematic review and meta-analysis. *Am. J. Reprod. Immunol.* **80**, (2018).
111. Fideli, Ü. S. *et al.* Virologic and Immunologic Determinants of Heterosexual Transmission of Human Immunodeficiency Virus Type 1 in Africa. *AIDS Res. Hum. Retroviruses* **17**, 901–910 (2001).
112. Quinn, T. C. *et al.* Viral Load and Heterosexual Transmission of Human Immunodeficiency Virus Type 1. *N. Engl. J. Med.* **342**, 921–929 (2000).
113. Cohen, M. S. Amplified transmission of HIV-1: missing link in the HIV pandemic. *Trans. Am. Clin. Climatol. Assoc.* **117**, 213–24; discussion 225 (2006).
114. Wasserheit, J. N. Epidemiological synergy. Interrelationships between human immunodeficiency virus infection and other sexually transmitted diseases. *Sex. Transm. Dis.* **19**, 61–77 (1992).
115. Piot, P. & Laga, M. Genital ulcers, other sexually transmitted diseases, and the sexual transmission of HIV. *BMJ* **298**, 623–624 (1989).
116. Piot, P. & Laga, M. Genital ulcers, other sexually transmitted diseases, and the sexual transmission of HIV. *BMJ* **298**, 623–624 (1989).
117. Ghys, P. D. *et al.* The associations between cervicovaginal HIV shedding, sexually transmitted diseases and immunosuppression in female sex workers in Abidjan, Côte d'Ivoire. *AIDS* **11**, F85–F93 (1997).
118. Passmore, J.-A. S., Jaspan, H. B. & Masson, L. Genital inflammation, immune activation and risk of sexual HIV acquisition. *Curr. Opin. HIV AIDS* **11**, 156–162 (2016).
119. Mayer, K. H. & Venkatesh, K. K. Interactions of HIV, Other Sexually Transmitted Diseases, and Genital Tract Inflammation Facilitating Local Pathogen Transmission and Acquisition. *Am. J. Reprod. Immunol.* **65**, 308–316 (2011).
120. Galvin, S. R. & Cohen, M. S. The role of sexually transmitted diseases in HIV transmission. *Nat. Rev. Microbiol.* **2**, 33–42 (2004).
121. Cohen, M. S. *et al.* Reduction of concentration of HIV-1 in semen after treatment of urethritis: implications for prevention of sexual transmission of HIV-1. *The Lancet* **349**, 1868–1873 (1997).
122. Gianella, S. *et al.* Shedding of HIV and Human Herpesviruses in the Semen of Effectively

Treated HIV-1–Infected Men Who Have Sex With Men. *Clin. Infect. Dis.* **57**, 441–447 (2013).
123. Passmore, J.-A. S., Jaspan, H. B. & Masson, L. Genital inflammation, immune activation and risk of sexual HIV acquisition. *Curr. Opin. HIV AIDS* **11**, 156–162 (2016).
124. Wang, C. C. *et al.* The Effect of Treatment of Vaginal Infections on Shedding of Human Immunodeficiency Virus Type 1. *J. Infect. Dis.* **183**, 1017–1022 (2001).
125. Rodger, A. J. *et al.* Sexual Activity Without Condoms and Risk of HIV Transmission in Serodifferent Couples When the HIV-Positive Partner Is Using Suppressive Antiretroviral Therapy. *JAMA* **316**, 171 (2016).
126. Bavinton, B. R. *et al.* Viral suppression and HIV transmission in serodiscordant male couples: an international, prospective, observational, cohort study. *Lancet HIV* **5**, e438–e447 (2018).
127. Cohen, M. S. *et al.* Antiretroviral Therapy for the Prevention of HIV-1 Transmission. *N. Engl. J. Med.* **375**, 830–839 (2016).
128. Rodger, A. J. *et al.* Risk of HIV transmission through condomless sex in serodifferent gay couples with the HIV-positive partner taking suppressive antiretroviral therapy (PARTNER): final results of a multicentre, prospective, observational study. *The Lancet* **393**, 2428–2438 (2019).
129. Pasquier, C. *et al.* Patterns of residual HIV-1 RNA shedding in the seminal plasma of patients on effective antiretroviral therapy. *Basic Clin. Androl.* **27**, 17 (2017).
130. Cu-Uvin, S. *et al.* Genital tract HIV-1 RNA shedding among women with below detectable plasma viral load. *AIDS* **24**, 2489–2497 (2010).
131. Dulioust, E. *et al.* No detection of HIV 1-RNA in semen of men on efficient HAART in the past 4 years of a 2002–2009 survey. *AIDS* **24**, 1595–1598 (2010).
132. Sheth, P. M. *et al.* Persistent HIV RNA shedding in semen despite effective antiretroviral therapy. *AIDS* **23**, 2050–2054 (2009).
133. Ferraretto, X. *et al.* Timing of Intermittent Seminal HIV-1 RNA Shedding in Patients with Undetectable Plasma Viral Load under Combination Antiretroviral Therapy. *PLoS ONE* **9**, e88922–e88922 (2014).
134. Halfon, P. *et al.* Semen May Harbor HIV Despite Effective HAART: Another Piece in the Puzzle. *PLoS ONE* **5**, e10569 (2010).
135. Lambert-Niclot, S. *et al.* Low Frequency of Intermittent HIV-1 Semen Excretion in Patients Treated with Darunavir-Ritonavir at 600/100 Milligrams Twice a Day plus Two Nucleoside Reverse Transcriptase Inhibitors or Monotherapy. *Antimicrob. Agents Chemother.* **54**, 4910–4913 (2010).
136. Marcelin, A.-G. *et al.* Detection of HIV-1 RNA in seminal plasma samples from treated patients with undetectable HIV-1 RNA in blood plasma. *AIDS* **22**, 1677–1679 (2008).
137. Marcelin, A.-G. *et al.* Detection of HIV-1 RNA in seminal plasma samples from treated patients with undetectable HIV-1 RNA in blood plasma. *AIDS* **22**, 1677–1679 (2008).
138. Politch, J. A. *et al.* Highly active antiretroviral therapy does not completely suppress HIV in semen of sexually active HIV-infected men who have sex with men. *AIDS* **26**, 1535–1543 (2012).
139. Graham, S. M. *et al.* Genital ulceration does not increase HIV-1 shedding in cervical or vaginal secretions of women taking antiretroviral therapy. *Sex. Transm. Infect.* **87**, 114–

117 (2011).
140. King, C. C. *et al.* Prevalence, Magnitude, and Correlates of HIV-1 Genital Shedding in Women on Antiretroviral Therapy. *J. Infect. Dis.* **216**, 1534–1540 (2017).
141. Sadiq, S. T. *et al.* The effects of antiretroviral therapy on HIV-1 RNA loads in seminal plasma in HIV-positive patients with and without urethritis. *AIDS* **16**, 219–225 (2002).
142. Chen, J. S. *et al.* Effects of Urethritis on Human Immunodeficiency Virus (HIV) in Semen: Implications for HIV Prevention and Cure. *Clin. Infect. Dis.* **73**, e2000–e2004 (2021).
143. Carlson, J. M. *et al.* Selection bias at the heterosexual HIV-1 transmission bottleneck. *Science* **345**, (2014).
144. Grosskurth, H. *et al.* Impact of improved treatment of sexually transmitted diseases on HIV infection in rural Tanzania: randomised controlled trial. *The Lancet* **346**, 530–536 (1995).
145. Wawer, M. J. *et al.* Control of sexually transmitted diseases for AIDS prevention in Uganda: a randomised community trial. *The Lancet* **353**, 525–535 (1999).
146. Ghys, P. D. *et al.* Effect of interventions to control sexually transmitted disease on the incidence of HIV infection in female sex workers. *AIDS* **15**, 1421–1431 (2001).
147. Gregson, S. *et al.* Impact and Process Evaluation of Integrated Community and Clinic-Based HIV-1 Control: A Cluster-Randomised Trial in Eastern Zimbabwe. *PLoS Med.* **4**, e102 (2007).
148. Kamali, A. *et al.* Syndromic management of sexually-transmitted infections and behaviour change interventions on transmission of HIV-1 in rural Uganda: a community randomised trial. *The Lancet* **361**, 645–652 (2003).
149. Kaul, R. *et al.* Monthly Antibiotic Chemoprophylaxis and Incidence of Sexually Transmitted Infections and HIV-1 Infection in Kenyan Sex Workers. *JAMA* **291**, 2555 (2004).
150. Celum, C. *et al.* Acyclovir and Transmission of HIV-1 from Persons Infected with HIV-1 and HSV-2. *N. Engl. J. Med.* **362**, 427–439 (2010).
151. Hayes, R., Watson-Jones, D., Celum, C., van de Wijgert, J. & Wasserheit, J. Treatment of sexually transmitted infections for HIV prevention: end of the road or new beginning? *AIDS* **24**, S15–S26 (2010).
152. Wetmore, C. M., Manhart, L. E. & Wasserheit, J. N. Randomized Controlled Trials of Interventions to Prevent Sexually Transmitted Infections: Learning From the Past to Plan for the Future. *Epidemiol. Rev.* **32**, 121–136 (2010).
153. Watson-Jones, D. *et al.* Effect of Herpes Simplex Suppression on Incidence of HIV among Women in Tanzania. *N. Engl. J. Med.* **358**, 1560–1571 (2008).
154. Celum, C. *et al.* Effect of aciclovir on HIV-1 acquisition in herpes simplex virus 2 seropositive women and men who have sex with men: a randomised, double-blind, placebo-controlled trial. *The Lancet* **371**, 2109–2119 (2008).
155. Chesson, H. W., Kidd, S., Bernstein, K. T., Fanfair, R. N. & Gift, T. L. The Cost-Effectiveness of Syphilis Screening Among Men Who Have Sex With Men: An Exploratory Modeling Analysis. *Sex. Transm. Dis.* **43**, 429–432 (2016).
156. Jenness, S. M. *et al.* Incidence of Gonorrhea and Chlamydia Following Human Immunodeficiency Virus Preexposure Prophylaxis Among Men Who Have Sex With

Men: A Modeling Study. *Clin. Infect. Dis.* **65**, 712–718 (2017).
157. Grund, J. M. *et al.* Association between male circumcision and women's biomedical health outcomes: a systematic review. *Lancet Glob. Health* **5**, e1113–e1122 (2017).
158. (WHO, W. H. O. 'Voluntary medical male circumcision for HIV prevention'. (2019).
159. Rasheed, Z. Male circumcision and human immunodeficiency virus infection: An update on randomized controlled trials and molecular evidences. *Int. J. Health Sci.* **12**, 1–3 (2018).
160. Gray, R. H. *et al.* Male circumcision for HIV prevention in men in Rakai, Uganda: a randomised trial. *The Lancet* **369**, 657–666 (2007).
161. Bailey, R. C. *et al.* Male circumcision for HIV prevention in young men in Kisumu, Kenya: a randomised controlled trial. *The Lancet* **369**, 643–656 (2007).
162. Auvert, B. *et al.* Randomized, Controlled Intervention Trial of Male Circumcision for Reduction of HIV Infection Risk: The ANRS 1265 Trial. *PLoS Med.* **2**, e298 (2005).
163. Wawer, M. J. *et al.* Effect of circumcision of HIV-negative men on transmission of human papillomavirus to HIV-negative women: a randomised trial in Rakai, Uganda. *The Lancet* **377**, 209–218 (2011).
164. Garenne, M. Age-incidence and prevalence of HIV among intact and circumcised men: an analysis of PHIA surveys in Southern Africa. *J. Biosoc. Sci.* 1–13 (2022) doi:10.1017/S0021932022000414.
165. Baeten, J. M. *et al.* Male circumcision and risk of male-to-female HIV-1 transmission: a multinational prospective study in African HIV-1-serodiscordant couples. *AIDS* **24**, 737–744 (2010).
166. Quinn, T. C. *et al.* Viral Load and Heterosexual Transmission of Human Immunodeficiency Virus Type 1. *N. Engl. J. Med.* **342**, 921–929 (2000).
167. Anderson, D., Politch, J. A. & Pudney, J. HIV Infection and Immune Defense of the Penis. *Am. J. Reprod. Immunol.* **65**, 220–229 (2011).
168. Higgins, J. A., Hoffman, S. & Dworkin, S. L. Rethinking Gender, Heterosexual Men, and Women's Vulnerability to HIV/AIDS. *Am. J. Public Health* **100**, 435–445 (2010).
169. Harris, C. *et al.* Immunodeficiency in Female Sexual Partners of Men with the Acquired Immunodeficiency Syndrome. *N. Engl. J. Med.* **308**, 1181–1184 (1983).
170. Redfield, R. R. *et al.* Heterosexually acquired HTLV-III/LAV disease (AIDS-related complex and AIDS). Epidemiologic evidence for female-to-male transmission. *JAMA* **254**, 2094–6 (1985).
171. Exner, T. M., Dworkin, S. L., Hoffman, S. & Ehrhardt, A. A. Beyond the male condom: the evolution of gender-specific HIV interventions for women. *Annu. Rev. Sex Res.* **14**, 114–36 (2003).
172. Kigozi, G. *et al.* Foreskin surface area and HIV acquisition in Rakai, Uganda (size matters). *AIDS* **23**, 2209–2213 (2009).
173. Hernandez, B. Y. *et al.* Circumcision and Human Papillomavirus Infection in Men: A Site-Specific Comparison. *J. Infect. Dis.* **197**, 787–794 (2008).
174. Prodger, J. L. & Kaul, R. The biology of how circumcision reduces HIV susceptibility: broader implications for the prevention field. *AIDS Res. Ther.* **14**, 49 (2017).
175. Fahrbach, K. M., Barry, S. M., Anderson, M. R. & Hope, T. J. Enhanced cellular responses and environmental sampling within inner foreskin explants: implications for the

foreskin's role in HIV transmission. *Mucosal Immunol.* **3**, 410–418 (2010).
176. Dinh, M. H., Fahrbach, K. M. & Hope, T. J. The Role of the Foreskin in Male Circumcision: An Evidence-Based Review. *Am. J. Reprod. Immunol.* **65**, 279–283 (2011).
177. Ganor, Y. *et al.* Within 1 h, HIV-1 uses viral synapses to enter efficiently the inner, but not outer, foreskin mucosa and engages Langerhans–T cell conjugates. *Mucosal Immunol.* **3**, 506–522 (2010).
178. McCoombe SG, S. RV. Potential HIV-1 target cells in the human penis. *AIDS* **20**, 1491–5 (2006).
179. Wu, L. & KewalRamani, V. N. Dendritic-cell interactions with HIV: infection and viral dissemination. *Nat. Rev. Immunol.* **6**, 859–868 (2006).
180. Geijtenbeek, T. B. H. *et al.* DC-SIGN, a Dendritic Cell–Specific HIV-1-Binding Protein that Enhances trans-Infection of T Cells. *Cell* **100**, 587–597 (2000).
181. Baxter, A. E. *et al.* Macrophage Infection via Selective Capture of HIV-1-Infected CD4+ T Cells. *Cell Host Microbe* **16**, 711–721 (2014).
182. Sennepin A, Real F, Duvivier M, Ganor Y, Henry S, Damotte D, Revol M, Cristofari S, B. M. The Human Penis Is a Genuine Immunological Effector Site. *Front Immunol* **14**, 1732 (2017).
183. Gray, C. M. *et al.* Impact of chemokine C–C ligand 27, foreskin anatomy and sexually transmitted infections on HIV-1 target cell availability in adolescent South African males. *Mucosal Immunol.* **13**, 118–127 (2020).
184. Dinh, M. H. *et al.* No Difference in Keratin Thickness between Inner and Outer Foreskins from Elective Male Circumcisions in Rakai, Uganda. *PLoS ONE* **7**, e41271 (2012).
185. Lemos, M. P. *et al.* The Inner Foreskin of Healthy Males at Risk of HIV Infection Harbors Epithelial CD4+ CCR5+ Cells and Has Features of an Inflamed Epidermal Barrier. *PLoS ONE* **9**, e108954 (2014).
186. Dinh, M. H. & Hope, T. J. Keratinization of the adult male foreskin and implications for male circumcision. *AIDS* **24**, 1381–1382 (2010).
187. Galiwango, R. M. *et al.* Characterization of CD4 + T cell subsets and HIV susceptibility in the inner and outer foreskin of Ugandan men. *Am. J. Reprod. Immunol.* **82**, (2019).
188. Cole, A. M. & Cole, A. L. REVIEW ARTICLE: Antimicrobial Polypeptides are Key Anti-HIV-1 Effector Molecules of Cervicovaginal Host Defense. *Am. J. Reprod. Immunol.* **59**, 27–34 (2007).
189. Pudney, J. & Anderson, D. J. Expression of Toll-like Receptors in Genital Tract Tissues from Normal and HIV-infected Men. *Am. J. Reprod. Immunol.* **65**, 28–43 (2011).
190. Deckers, J., Hammad, H. & Hoste, E. Langerhans Cells: Sensing the Environment in Health and Disease. *Front. Immunol.* **9**, (2018).
191. Mayumi, N. *et al.* <scp>E</scp> -cadherin interactions are required for <scp>L</scp> angerhans cell differentiation. *Eur. J. Immunol.* **43**, 270–280 (2013).
192. de Witte, L. *et al.* Langerin is a natural barrier to HIV-1 transmission by Langerhans cells. *Nat. Med.* **13**, 367–371 (2007).
193. Nguyen, A. V. & Soulika, A. M. The Dynamics of the Skin's Immune System. *Int. J. Mol. Sci.* **20**, 1811 (2019).
194. Russo, C. L. *et al.* Mucin gene expression in human male urogenital tract epithelia. *Hum. Reprod.* **21**, 2783–2793 (2006).

195. Anderson D, Politch JA, P. J. HIV infection and immune defense of the penis. *Am J Reprod Immunol* **65**, 220–9. (2011).
196. Rasmussen, S. J. *et al.* Secretion of proinflammatory cytokines by epithelial cells in response to Chlamydia infection suggests a central role for epithelial cells in chlamydial pathogenesis. *J. Clin. Invest.* **99**, 77–87 (1997).
197. Liu, L. *et al.* Defective HIV-1 Particle Assembly in AP-3-Deficient Cells Derived from Patients with Hermansky-Pudlak Syndrome Type 2. *J. Virol.* **86**, 11242–11253 (2012).
198. Baskin L, Shen J, Sinclair A, Cao M, Liu X, Liu G, Isaacson D, Overland M, Li Y, C. G. Development of the human penis and clitoris. *Differentiation* **103**, 74–85 (2018).
199. Hsu, Y.C.; Li, L.; Fuchs, E. Emerging interactions between skin stem cells and their niche. *Nat Med* **20**, 847–856 (2014).
200. Proksch E., Brandner J.M., J. J. M. The skin: An indispensable barrier. *Exp Dermatol* **17**, 1063–1072 (2008).
201. Dinh, M. H. *et al.* No Difference in Keratin Thickness between Inner and Outer Foreskins from Elective Male Circumcisions in Rakai, Uganda. *PLoS ONE* **7**, e41271 (2012).
202. Qin, Q. *et al.* Langerhans' cell density and degree of keratinization in foreskins of Chinese preschool boys and adults. *Int. Urol. Nephrol.* **41**, 747–753 (2009).
203. Barbara Young, Geraldine O'Dowd, P. W. *Wheater's Functional Histology*. (Churchill Livingston, 2013).
204. Ovaere, P.; Lippens, S.; Vandenabeele, P.; Declercq, W. The emerging roles of serine protease cascades in the epidermis. *Trends Biochem Sci* **34**, 453–463.
205. KC., M. Barrier function of the skin: '"la raison d9^etre"' of the epidermis. *J Invest Dermatol* **121**, 231–41 (2003).
206. Simpson, C. L., Patel, D. M. & Green, K. J. Deconstructing the skin: cytoarchitectural determinants of epidermal morphogenesis. *Nat. Rev. Mol. Cell Biol.* **12**, 565–580 (2011).
207. Rice RH, G. H. Presence in human epidermal cells of a soluble protein precursor of the cross-linked envelope: activation of the cross-linking by calcium ions. *Cell* **18**, 681–694 (1979).
208. Sandilands A, Sutherland C, Irvine AD, M. W. Filaggrin in the frontline: role in skin barrier function and disease. *J Cell Sci* **122**, 1285–94 (2009).
209. Steinert, P. M., Cantieri, J. S., Teller, D. C., Lonsdale-Eccles, J. D. and Dale, B. A. Characterization of a class of cationic proteins that specifically interact with intermediate filaments. *Proc Natl Acad Sci* **78**, 4097–4101 (1981).
210. Resing, K. A., Walsh, K. A., Haugen-Scofield, J. and Dale, B. A. Identification of proteolytic cleavage sites in the conversion of profilaggrin to filaggrin in mammalian epidermis. *J Biol Chem* **264**, 1837–1845 (1989).
211. Resing, K. A., Johnson, R. S. and Walsh, K. A. Characterization of protease processing sites during conversion of rat profilaggrin to filaggrin. *Biochemistry* **32**, 10036–10045 (1993).
212. Kypriotou M., Huber M., H. D. The human epidermal differentiation complex: Cornified envelope precursors, S100 proteins and the 'fused genes' family. *Exp Dermatol* **21**, 643–649 (2012).
213. Chiba T., Nakahara T., Kohda F., Ichiki T., M. M. Measurement of trihydroxy-linoleic acids in stratum corneum by tape-stripping: Possible biomarker of barrier function in

atopic dermatitis. *PLoS ONE* **14**, e0210013 (2019).
214. Fuchs E, G. H. . Changes in keratin gene expression during terminal differentiation of the keratinocyte. *Cell* **19**, 1033–1042 (1980).
215. Steinert PM, M. LN. The proteins elafin, filaggrin, keratin intermediate filaments, loricrin, and small proline-rich proteins 1 and 2 are isodipeptide cross-linked components of the human epidermal cornified cell envelope. *J Biol Chem* **270**, 17702–17711 (1995).
216. Robinson NA, LaCelle PT, E. R. Involucrin is a covalently crosslinked constituent of highly purified epidermal corneocytes: evidence for a common pattern of involucrin crosslinking in vivo and in vitro. *J Invest Dermatol* **107**, 101-107. (1996).
217. Nemes Z, Marekov LN, S. PM. Involucrin cross-linking by transglutaminase 1. Binding to membranes directs residue specificity. *J Biol Chem* **274**, 11013–11021 (1999).
218. AV., K. alpha-Helical solenoid model for the human involucrin. *FEBS Lett* **473**, 127–31 (2000).
219. Henry J, Toulza E, H. C. Update on the epidermal differentiation complex. *Front Biosci* **274**, 1517–1532 (2012).
220. Fu, R.; Jiang, X.; Li, G.; Zhu, Y.; Zhang, H. Junctional Complexes in Epithelial Cells: Sentinels for Extracellular Insults and Intracellular Homeostasis. *FEBS J* (2021).
221. FM, W. Stem cell fate and patterning in mammalian epidermis. *Curr Opin Genet Dev* **11**, : 410-417 (2001).
222. Getsios S, Huen AC, G. K. Working out the strength and flexibility of desmosomes. *Nat Rev Mol Cell Biol* **5**, 271–281 (2004).
223. Morita K, Itoh M, Saitou M, Ando-Akatsuka Y, Furuse M, Yoneda K, Imamura S, Fujimoto K, T. S. Subcellular distribution of tight junction-associated proteins (occludin, ZO-1, ZO-2) in rodent skin. *J Invest Dermatol* **110**, 862–866 (1998).
224. Pummi K, Malminen M, Karvonene SL, Peltonen J, P. S. Epidermal tight junctions: ZO-1 and occludin are expressed in mature, developing, and affected skin and in vitro differentiating keratinocytes. *J Invest Dermatol* **117**, 1050–1057 (2001).
225. Brandner JM, Kief S, Grund C, Rendl M, Houdek P, Kuhn C, Tschachler E, Franke WW, M. I. Organization and formation of the tight junction system in human epidermis and cultured keratinocytes. *Eur J Cell Biol* **81**, 253-263 [(2002).
226. Larue L, Ohsugi M, Hirchenhain J, K. R. (. E-cadherin null mutant embryos fail to form a trophectoderm epithelium. *Proc Natl Acad Sci USA* **91**, 8263–8267 (1994).
227. Green, K.J.; Jaiganesh, A.; Broussard, J. A. Desmosomes: Essential Contributors to an Integrated Intercellular Junction Network. *Network.F1000Research* **8**, 2150 (2019).
228. Meng, W.; Takeichi, M. Adherens Junction: Molecular Architecture and Regulation. *Cold Spring Harb Perspect Biol* **1**, (2009).
229. Kirschner, N.; Brandner, J. M. Barriers and More: Functions of Tight Junction Proteins. *Ann N Acad Sci* **1257**, 158-166. (2012).
230. Beck, L.A.; Cork, M.J.; Amagai, M.; de Benedetto, A.; Kabashima, K.; Hamilton, J.D.; Rossi, A. B. Type 2 Inflammation Contributes to Skin Barrier Dysfunction in Atopic Dermatitis. *JID Innov* **2**, 100131 (2022).
231. Farquhar MG, P. GE. .Junctional complexes in various epithelia. *J Cell Biol* **17**, 375–412 (1963).
232. Van Meer G, S. K. The function of tight junctions in maintaining differences in lipid

composition between the apical and the basolateral cell surface domains of MDCK cells. *EMBO J* **5**, 1455–1464 (1986).
233. JM., D. Twenty-first Bowditch lecture. The epithelial junction: bridge, gate, and fence. *Physiologist* **20**, 10–18 (1977).
234. Anderson JM, V. I. C. Physiology and function of the tight junction. *Cold Spring Harb Perspect Biol* (2009).
235. Grosse B, Cassio D, Yousef N, Bernardo C, Jacquemin E, G. E. Claudin-1 involved in neonatal ichthyosis-sclerosing cholangitis syndrome, regulates hepatic paracellular permeability. *Hepatology* (2011).
236. Furuse M, Hata M, Furuse K, Yoshida Y, Haratake A, Sugitani Y, Noda T, Kubo A, T. S. Claudin-based tight junctions are crucial for the mammalian epidermal barrier: a lesson from claudin-1-deficient mice. *J Cell Biol* **156**, 1099–1111 (2002).
237. Hadj-Rabia S, Baala L, Vabres P, Hamel-Teillac D, Jacquemin E, Fabre M, Lyonnet S, De Prost Y, Munnich A, Hadchouel M, S. A. Claudin-1 gene mutations in neonatal sclerosing cholangitis associated with ichthyosis: a tight junction disease. . *Gastroenterology* **127**, 1386–1390 (2004).
238. Kirschner N, Poetzl C, von den Driesch P, Wladykowski E, Moll I, Behne MJ, B. JM. Alteration of tight junction proteins is an early event in psoriasis: putative involvement of proinflammatory cytokines. *Am J Pathol* **175**, 1095–106 (2009).
239. Kirchmeier P, Sayar E, Hotz A, Hausser I, Islek A, Yilmaz A, Artan R, F. J. Novel mutation in the CLDN1 gene in a Turkish family with Neonatal Ichthyosis Sclerosing Cholangitis (NISCH) syndrome. *Br J Dermatol* **170**, 976–8 (2014).
240. De Benedetto A, Rafaels NM, McGirt LY, Ivanov AI, Georas SN, Cheadle C, Berger AE, Zhang K, Vidyasagar S, Yoshida T, Boguniewicz M, Hata T, Schneider LC, Hanifin JM, Gallo RL, Novak N, Weidinger S, Beaty TH, Leung DY, Barnes KC, B. LA. Tight junction defects in patients with atopic dermatitis. *J Allergy Clin Immunol* **127**, 773–786 (2011).
241. Watson RE, Poddar R, Walker JM, McGuill I, Hoare LM, Griffiths CE, O. CA. Altered claudin expression is a feature of chronic plaque psoriasis. *J Pathol* **212**, 450–458 (2007).
242. Inai T, Kobayashi J, S. Y. Claudin-1 contributes to the epithelial barrier function in MDCK cells. *Eur J Cell Biol* **78**, 849–855 (1999).
243. McCarthy KM, Francis SA, McCormack JM, Lai J, Rogers RA, Skare IB, Lynch RD, S. EE. Inducible expression of claudin-1-myc but not occludin-VSV-G results in aberrant tight junction strand formation in MDCK cells. *J Cell Sci* **113**, 3387–3398 (2000).
244. Enck AH, Berger UV, Y. AS. Claudin-2 is selectively expressed in proximal nephron in mouse kidney. *Am J Physiol Ren. Physiol* **281**, : F966-F974 (2001).
245. Kiuchi-Saishin Y, Gotoh S, Furuse M, Takasuga A, Tano Y, T. S. Differential expression patterns of claudins, tight junction membrane proteins, in mouse nephron segments. *J Am Soc Nephrol* **13**, 875–886 (2002).
246. Rahner C, Mitic LL, A. J. Heterogeneity in expression and subcellular localization of claudins 2, 3, 4, and 5 in the rat liver, pancreas, and gut. Gastroenterology. *Gastroenterology* **120**, 411–422 (2001).
247. Amasheh S, Meiri N, Gitter A.H, Schoneberg T, Mankertz J, Schulzke J.D, F. M. . Claudin-2 expression induces cation-selective channels in tight junctions of epithelial cells. *J Cell Sci* **115**, 4969–4976 (2002).

248. Furuse M, Furuse K, Sasaki H, T. S. Conversion of zonulae occludentes from tight to leaky strand type by introducing claudin-2 into madin-darby canine kidney I cells. *J Cell Biol* **153**, 263-272, (2001).
249. Van Itallie C, Fanning AS, A. J. Reversal of charge selectivity in cation or anion selective epithelial lines by expression of different claudins. *Am J Physiol Ren. Physiol* **286**, F1078-F1084, (2003).
250. Michikawa H, Fujita-Yoshigaki J, S. H. Enhancement of barrier function by overexpression of claudin-4 in tight junctions of submandibular gland cells. *Cell Tissue Res* **334**, 255–264 (2008).
251. Van Itallie C, Fanning AS, A. JM. Reversal of charge selectivity in cation or anion selective epithelial lines by expression of different claudins. *Am J Physiol Ren. Physiol* **286**, F1078–F1084 (2003).
252. Van Itallie C, Rahner C, A. JM. Regulated expression of claudin-4 decreases paracellular conductance through a selective decrease in sodium permeability. *J Clin Invest* **107**, 1319–1327 (2001).
253. Hou J, Renigunta A, Yang J, W. S. Claudin-4 forms paracellular chloride channel in the kidney and requires claudin-8 for tight junction localization. *Proc Natl Acad Sci USA* **107**, 18010–18015 (2010).
254. Morita K, Sasaki H, Furuse M, T. S. Endothelial claudin: claudin-5/TMVCF constitutes tight junction strands in endothelial cells. *J Cell Biol* **147**, 185–194 (1999).
255. Reese TS, K. MJ. Fine structural localization of a blood-brain barrier to exogenous peroxidase. *J Cell Biol* **34**, 207–217 (1967).
256. Karnovsky MJ. The ultrastructural basis of capillary permeability studied with peroxidase as a tracer. *J Cell Biol* **35**, 213–236 (1967).
257. Matthias Bruewer, Andreas Luegering, Torsten Kucharzik, Charles A. Parkos, James L. Madara, Ann M. Hopkins, A. N. Proinflammatory Cytokines Disrupt Epithelial Barrier Function by Apoptosis-Independent Mechanisms. *J Immunol* **171**, 6164–6172 (2003).
258. Günzel D, F. M. Claudins and other tight junction proteins. *Comp Physiol* **2**, 1819–1852 (2012).
259. Epple HJ, Schneider T, Troeger H, Kunkel D, Allers K, Moos V, Amasheh M, Loddenkemper C, Fromm M, Zeitz M, S. JD. mpairment of the intestinal barrier is evident in untreated but absent in suppressively treated HIV-infected patients. *Gut* **58**, 220–7 (2009).
260. Amasheh M, Fromm A, Krug SM, Amasheh S, Andres S, Zeitz M, Fromm M, S. JD. TNFalpha-induced and berberine-antagonized tight junction barrier impairment via tyrosine kinase, Akt and NFkappaB signaling. *J Cell Sci* **123**, 4145–4155 (2010).
261. Epple HJ, Schneider T, Troeger H, Kunkel D, Allers K, Moos V, Amasheh M, Loddenkemper C, Fromm M, Zeitz M, S. J. D. Impairment of the intestinal barrier is evident in untreated but absent in suppressively treated HIV-infected patients. *Gut* **58**, 220–227 (2009).
262. Aslam M, Ahmad N, Srivastava R, H. B. TNF-alpha induced NFkappaB signaling and p65 (RelA) overexpression repress Cldn5 promoter in mouse brain endothelial cells. *Cytokine* **57**, 269–275 (2012).
263. Brown RC, Mark KS, Egleton RD, Huber JD, Burroughs AR, D. TP. Protection against

hypoxia-induced increase in blood-brain barrier permeability: role of tight junction proteins and NFkappaB. *J Cell Sci* **116**, 693–700 (2003).
264. Burek M, F. CY. Cloning and characterization of the murine claudin-5 promoter. *Mol Cell Endocrinol* **298**, 19–24 (2009).
265. Stone KP, Kastin AJ, P. W. NFkB is an unexpected major mediator of interleukin-15 signaling in cerebral endothelia. *Cell Physiol Biochem* **28**, 115–124 (2011).
266. Wang L, Zhang X, Liu L, Cui L, Yang R, Li M, D. W. Tanshinone II A down-regulates HMGB1, RAGE, TLR4, and NF-kappaB expression, ameliorates BBB permeability and endothelial cell function, protects rat brains against focal ischemia. *Brain Res* **1321**, 143–151 (2010).
267. Gottardi CJ, Niessen CM, G. B. The adherens junction. In Cell Adhesion. *The Frontiers in Molecular Biology Series, Hames BD, Glover DM, Beckerle M (eds). chap 8, Oxford University Press*.
268. Tunggal JA, Helfrich I, Schmitz A, Schwarz H, Günzel D, Fromm M, Kemler R, Krieg T, N. CM. E-cadherin is essential for in vivo epidermal barrier function by regulating tight junctions. *EMBO J* **24**, 1146–56 (2005).
269. Gumbiner B, Stevenson B, G. A. The role of the cell adhesion molecule uvomorulin in the formation and maintenance of the epithelial junctional complex. *J Cell Biol* **107**, 1575–1587 (1999).
270. Musil LS, Cunningham BA, Edelman GM, G. DA. Differential phosphorylation of the gap junction protein connexin43 in junctional communication-competent and -deficient cell lines. *J Cell Biol* **111**, 2077–2088 (1990).
271. Watabe M, Nagafuchi A, Tsukita S, T. M. Induction of polarized cell–cell association and retardation of growth by activation of the E-cadherin–catenin adhesion system in a dispersed carcinoma line. *J Cell Biol* **127**, 247–256 (1994).
272. Nelson WJ. Adaptation of core mechanisms to generate cell polarity. *Nature* **422**, 766–774 (2003).
273. Itoh M, Nagafuchi A, Moroi S, T. S. Involvement of ZO-1 in cadherin-based cell adhesion through its direct binding to alpha catenin and actin filaments. *J Cell Biol* **138**, 181–192 (1997).
274. Nguyen, P. V, Kafka, J. K., Ferreira, V. H., Roth, K. & Kaushic, C. Innate and adaptive immune responses in male and female reproductive tracts in homeostasis and following HIV infection. *Cell. Mol. Immunol.* **11**, 410–427 (2014).
275. Prodger, J. L. *et al.* Foreskin T-cell subsets differ substantially from blood with respect to HIV co-receptor expression, inflammatory profile, and memory status. *Mucosal Immunol.* **5**, 121–128 (2012).
276. Hirbod T, Bailey RC, Agot K, Moses S, Ndinya-Achola J, Murugu R, Andersson J, Nilsson J, B. K. Abundant expression of HIV target cells and C-type lectin receptors in the foreskin tissue of young Kenyan men. *Am J Pathol* **176**, 2798–805 (2010).
277. Dinh MH, Anderson MR, McRaven MD, Cianci GC, McCoombe SG, Kelley ZL, Gioia CJ, Fought AJ, Rademaker AW, Veazey RS, H. TJ. Visualization of HIV-1 interactions with penile and foreskin epithelia: clues for female-to-male HIV transmission. *PLoS Pathog* **6**, 11 (2015).
278. Ding, J. *et al.* Neisseria gonorrhoeae Enhances HIV-1 Infection of Primary Resting CD4+

T Cells through TLR2 Activation. *J. Immunol.* **184**, 2814–2824 (2010).
279. Prodger, J. L. *et al.* Impact of asymptomatic Herpes simplex virus-2 infection on T cell phenotype and function in the foreskin. *AIDS* **26**, 1319–1322 (2012).
280. Johnson, K. E. *et al.* Effects of HIV-1 and Herpes Simplex Virus Type 2 Infection on Lymphocyte and Dendritic Cell Density in Adult Foreskins from Rakai, Uganda. *J. Infect. Dis.* **203**, 602–609 (2011).
281. Su, H. & Caldwell, H. D. CD4+ T cells play a significant role in adoptive immunity to Chlamydia trachomatis infection of the mouse genital tract. *Infect. Immun.* **63**, 3302–3308 (1995).
282. Tobian, A. A. R. *et al.* Human Papillomavirus Clearance Among Males Is Associated With HIV Acquisition and Increased Dendritic Cell Density in the Foreskin. *J. Infect. Dis.* **207**, 1713–1722 (2013).
283. Fonner, V. A. *et al.* Effectiveness and safety of oral HIV preexposure prophylaxis for all populations. *AIDS* **30**, 1973–1983 (2016).
284. Traeger, M. W. *et al.* Effects of Pre-exposure Prophylaxis for the Prevention of Human Immunodeficiency Virus Infection on Sexual Risk Behavior in Men Who Have Sex With Men: A Systematic Review and Meta-analysis. *Clin. Infect. Dis.* **67**, 676–686 (2018).
285. Kojima, N., Davey, D. J. & Klausner, J. D. Pre-exposure prophylaxis for HIV infection and new sexually transmitted infections among men who have sex with men. *AIDS* **30**, 2251–2252 (2016).
286. Guy Mahiane, S., Pretorius, C. & Korenromp, E. Second Order Segmented Polynomials for Syphilis and Gonorrhea Prevalence and Incidence Trends Estimation: Application to Spectrum's Guinea-Bissau and South Africa Data. *Int. J. Biostat.* **15**, (2019).
287. Nguyen, V.-K. *et al.* Incidence of sexually transmitted infections before and after preexposure prophylaxis for HIV. *AIDS* **32**, 523–530 (2018).
288. Harawa, N. T. *et al.* Serious concerns regarding a meta-analysis of preexposure prophylaxis use and STI acquisition. *AIDS* **31**, 739–740 (2017).
289. Cohen, M. S. *et al.* Prevention of HIV-1 Infection with Early Antiretroviral Therapy. *N. Engl. J. Med.* **365**, 493–505 (2011).
290. Volk, J. E. *et al.* No New HIV Infections With Increasing Use of HIV Preexposure Prophylaxis in a Clinical Practice Setting: Figure 1. *Clin. Infect. Dis.* **61**, 1601–1603 (2015).
291. McCormack, S. *et al.* Pre-exposure prophylaxis to prevent the acquisition of HIV-1 infection (PROUD): effectiveness results from the pilot phase of a pragmatic open-label randomised trial. *The Lancet* **387**, 53–60 (2016).
292. Molina, J.-M. *et al.* Efficacy, safety, and effect on sexual behaviour of on-demand pre-exposure prophylaxis for HIV in men who have sex with men: an observational cohort study. *Lancet HIV* **4**, e402–e410 (2017).
293. Traeger, M. W. *et al.* Association of HIV Preexposure Prophylaxis With Incidence of Sexually Transmitted Infections Among Individuals at High Risk of HIV Infection. *JAMA* **321**, 1380 (2019).
294. Bolan, R. K. *et al.* Doxycycline Prophylaxis to Reduce Incident Syphilis among HIV-Infected Men Who Have Sex With Men Who Continue to Engage in High-Risk Sex. *Sex. Transm. Dis.* **42**, 98–103 (2015).

295. Luetkemeyer, A. F. *et al.* Postexposure Doxycycline to Prevent Bacterial Sexually Transmitted Infections. *N. Engl. J. Med.* **388**, 1296–1306 (2023).
296. Celum, C. & Luetkemeyer, A. F. Doxycycline for Sexually Transmitted Infection Prevention: Evolving Evidence and Implementation Perspectives. *Sex. Transm. Dis.* **48**, 620–621 (2021).
297. White, R. G. *et al.* Low effectiveness of syndromic treatment services for curable sexually transmitted infections in rural South Africa. *Sex. Transm. Infect.* **84**, 528–534 (2008).
298. Abdool Karim, Q. *et al.* Effectiveness and Safety of Tenofovir Gel, an Antiretroviral Microbicide, for the Prevention of HIV Infection in Women. *Science* **329**, 1168–1174 (2010).
299. Liebenberg, L. J. P. *et al.* Genital Immune Cell Activation and Tenofovir Gel Efficacy: A Case-Control Study. *Clin. Infect. Dis.* **75**, 1088–1091 (2022).
300. Patterson, B. K. *et al.* Susceptibility to Human Immunodeficiency Virus-1 Infection of Human Foreskin and Cervical Tissue Grown in Explant Culture. *Am. J. Pathol.* **161**, 867–873 (2002).
301. Johnson, K. E. *et al.* Foreskin inflammation is associated with HIV and herpes simplex virus type-2 infections in Rakai, Uganda. *AIDS* **23**, 1807–1815 (2009).
302. Low, N. *et al.* Global control of sexually transmitted infections. *The Lancet* **368**, 2001–2016 (2006).
303. Trollope-Kumar, K. & Guyatt, G. Syndromic approach for treatment of STIs: time for a change. *The Lancet* **367**, 1380–1381 (2006).
304. 2023-2028 National Strategic Plan for HIV | TB | STIs. (2023).
305. South Africa, D. of Health. Sexually Transmitted Infections management guidelines. *Natl. Dep. Health South Afr.* 1–25 (2018).
306. South African National AIDS Council. National Strategic Plan (NSP) for HIV, TB and STIs 2023-2028 South Afriica. **5th**, 1–192 (2023).
307. LAUMANN, E. O. & YOUM, Y. Racial/Ethnic Group Differences in the Prevalence of Sexually Transmitted Diseases in the United States: A Network Explanation. *Sex. Transm. Dis.* **26**, 250–261 (1999).
308. Unemo, M., Golparian, D. & Eyre, D. W. Antimicrobial Resistance in Neisseria gonorrhoeae and Treatment of Gonorrhea. in 37–58 (2019). doi:10.1007/978-1-4939-9496-0_3.
309. Edwards, J. L. & Apicella, M. A. The Molecular Mechanisms Used by Neisseria gonorrhoeae To Initiate Infection Differ between Men and Women. *Clin. Microbiol. Rev.* **17**, 965–981 (2004).
310. Das, K., De la Garza, G., Siwak, E. B., Scofield, V. L. & Dhandayuthapani, S. Mycoplasma genitalium promotes epithelial crossing and peripheral blood mononuclear cell infection by HIV-1. *Int. J. Infect. Dis.* **23**, 31–38 (2014).
311. McGowin, C. L. *et al.* Persistent Mycoplasma genitalium Infection of Human Endocervical Epithelial Cells Elicits Chronic Inflammatory Cytokine Secretion. *Infect. Immun.* **80**, 3842–3849 (2012).
312. Napierala Mavedzenge, S. & Weiss, H. A. Association of Mycoplasma genitalium and HIV infection: a systematic review and meta-analysis. *AIDS* **23**, 611–620 (2009).
313. Kamali, A. *et al.* Syndromic management of sexually-transmitted infections and

behaviour change interventions on transmission of HIV-1 in rural Uganda: a community randomised trial. *The Lancet* **361**, 645–652 (2003).
314. Szabo, R.; Short, R. V. How does male circumcision protect against HIV infection? *BMJ* **320**, 1592–1594 (2000).
315. Sharma, A.L.; Hokello, J.; Tyagi, M. Circumcision as an Intervening Strategy against HIV Acquisition in the Male Genital Tract. *Pathogens* **10**, 806. (2021).
316. Esra, R. T. *et al.* Does HIV Exploit the Inflammatory Milieu of the Male Genital Tract for Successful Infection? . *Frontiers in Immunology* vol. 7 245 Preprint at (2016).
317. Patel P, Borkowf CB, Brooks JT, Lasry A, Lansky A, M. J. Estimating per-act HIV transmission risk: a systematic review. *AIDS* **28**, 1509–19 (2014).
318. Lim SG, Menzies IS, Lee CA, Johnson MA, P. R. Intestinal permeability and function in patients infected with human immunodeficiency virus. A comparison with coeliac disease. *Scand J Gastroenterol* **28**, 573-580. (1993).
319. Keating J, Bjarnason I, Somasundaram S, Macpherson A, Francis N, Price AB, Sharpstone D, Smithson J, Menzies IS, G. BG. Intestinal absorptive capacity, intestinal permeability and jejunal histology in HIV and their relation to diarrhoea. *Gut* **37**, 623–9 (1995).
320. Sharpstone D, Neild P, Crane R, Taylor C, Hodgson C, Sherwood R, Gazzard B, B. I. Small intestinal transit, absorption, and permeability in patients with AIDS with and without diarrhoea. *Gut* **45**, 70–6 (1999).
321. Stockmann M, Schmitz H, Fromm M, Schmidt W, Pauli G, Scholz P, Riecken EO, S. JD. Mechanisms of epithelial barrier impairment in HIV infection. *Ann N Acad Sci* **915**, 93-303. (2000).
322. Liu A, Yang Y, Liu L, Meng Z, Li L, Qiu C, Xu J, Z. X. Differential compartmentalization of HIV-targeting immune cells in inner and outer foreskin tissue. *PLoS One* **15**, (2014).
323. KC, M. Barrier function of the skin: '"la raison d'etre"' of the epidermis. *J Invest Dermatol* **121**, 231–41 (2003).
324. De Benedetto A, Rafaels NM, McGirt LY, Ivanov AI, Georas SN, Cheadle C, Berger AE, Zhang K, Vidyasagar S, Yoshida T, Boguniewicz M, Hata T, Schneider LC, Hanifin JM, Gallo RL, Novak N, Weidinger S, Beaty TH, Leung DY, Barnes KC, B. LA. Tight junction defects in patients with atopic dermatitis. *Allergy Clin Immunol* **127**, 773–86 (2011).
325. Werner Y, L. M. Transepidermal water loss in dry and clinically normal skin in patients with atopic dermatitis. *Acta Derm Venereol* **65**, 102–5 (1985).
326. Hon KL, Wong KY, Leung TF, Chow CM, N. PC. Comparison of skin hydration evaluation sites and correlations among skin hydration, transepidermal water loss, SCORAD index, Nottingham Eczema Severity Score, and quality of life in patients with atopic dermatitis. *Am J Clin Dermatol* **9**, 45-50. (2008).
327. Nemoto-Hasebe I, Akiyama M, Nomura T, Sandilands A, McLean WH, S. H. Clinical severity correlates with impaired barrier in filaggrin-related eczema. *J Invest Dermatol* **129**, 682–9. (2009).
328. Fallon PG, Sasaki T, Sandilands A, Campbell LE, Saunders SP, M. N. A homozygous frameshift mutation in the mouse Flg gene facilitates enhanced percutaneous allergen priming. *Nat Genet* **41**, 602–8. (2009).
329. Mayrovitz, H. Transepidermal water loss and stratum corneum hydration in forearm

versus hand palm. *Skin Res Technol* **29**, (2023).
330. Blank, I. H. Cutaneous barriers. *J Invest Dermatol* **45**, 249–256 (1965).
331. Scheuplein, R.J. and Blank, I. H. Permeability of the skin. *Physiol Rev* **51**, 702–747 (1971).
332. Tagami, H., Kobayashi, H., Zhen, X.S. and Kikuchi, K. Environmental effects on the functions of the stratum corneum. *J Investig Dermatol Symp Proc* **6**, 87–94 (2001).
333. Gioia F, C. L. The dynamics of transepidermal water loss (TEWL) from hydrated skin. *Skin Res Technol* **8**, 178–186 (2002).
334. Rawlings, A.V. and Harding, C. R. Moisturization and skin barrier function. *Dermatol Ther* **17**, 43–48 (2004).
335. Marty, J. P. NMF and cosmetology of cutaneous hydration. *Ann Dermatol Venereol* **129**, 131–136 (2002).
336. Takenouchi, M., Suzuki, H. and Tagami, H. Hydration characteristics of pathologic stratum corneum–evaluation of bound water. *J Invest Dermatol* **87**, 574–576 (1986).
337. Horii, I., Nakayama, Y., Obata, M. and Tagami, H. Stratum corneum hydration and amino acid content in xerotic skin. *Br J Dermatol* **121**, 587–592 (1989).
338. Thune, P. Evaluation of the hydration and the water-holding capacity in atopic skin and so-called dry skin. *Acta Derm Venereol Suppl Stockh* **144**, 133–135 (1989).
339. Brandner, J. M. Pores in the epidermis: aquaporins and tight junctions. *Int. J. Cosmet. Sci.* **29**, 413–422 (2007).
340. Alanen E, Nuutinen J, Nicklen K, Lahtinen T, M. J. Measurement of hydration in the stratum corneum with the MoistureMeter and comparison with the Corneometer. *Skin Res Technol* **10**, 32–37 (2004).
341. Fluhr J, Gloor E, Lazzerini S, Kleesz P, Grieshaber R, B. E. Comparative study of five instruments measuring stratum corneum hydration (Corneometer CM 820, and CM 825, Skicon 200, Nova DPM 9003, DermaLab). Part I. In vitro. *Skin Res Technol* **5**, 161–170 (1999).
342. Endo K, Suzuki N, Yoshida O, Sato H, F. Y. The barrier component and the driving force component of transepidermal water loss and their application to skin irritant tests. *Skin Res Technol* **13**, 425–435 (2007).
343. Farahmand S, Tien L, Hui X, M. HI. Measuring transepidermal water loss: a comparative in vivo study of condenser-chamber, unventilated-chamber and open-chamber systems. *Skin Res Technol* **15**, 392–398 (2009).
344. Nuutinen J, Alanen E, Autio P, Lahtinen MR, Harvima I, L. T. . A closed unventilated chamber for the measurement of transepidermal water loss. *Skin Res Technol* **9**, 85–89 (2003).
345. Goodman AB, W. A. Insensible water loss fr om humans as a function of vapor concent rations. *J Appl Physiol* **138**, 203–207 (1969).
346. Sprui t D, M. ten K. Humidity of the air a nd water vapor loss of the skin. *Dermatologica* **138**, 418–426 (1969).
347. Lamke LO, W. din. Water evaporation from normal skin under different environmental conditions. *Acta Derm VenereolStock H* **51**, 111–119 (1971).
348. Grice KA , Satta r H, B. H. The effect of ambient humidity on transepidermal water loss. *J Invest Dermatol* **58**, 343–346 (1972).

349. Gioia F, C. L. The dynamics of transepidermal water loss (TEWL) from hydrated skin. *Skin Res Technol* **8**, 178–186 (2002).
350. Barel AO, C. P. Study of the stratum corneum barrier function by transepidermal water loss measurements: comparison between two commercial instruments: Evaporimeter and Tewameter. *Skin Pharmacol* **8**, 186–195 (1995).
351. De Paepe K, Houben E, Adam R, Wiesemann F, R. V. Validation of the VapoMeter, a closed unventilated chamber system to assess transepidermal water loss vs. the open chamber Tewameter. *Skin Res Technol* **11**, 61-69. (2005).
352. Bettley FR, G. KA. . A method for measuring the transepidermal water loss and a means of inactivating sweat glands. *Br J Dermatol* **77**, 627-638. (1965).
353. Blank IH, Moloney J 3rd, Emslie AG, Simon I, A. C. The diffusion of water across the stratum corneum as a function of its water content. *J Invest Dermatol* **92**, 188–194 (1984).
354. Delfin. Meters. *www.Delfin.com*.
355. Vapometer. *http://www.delfintech.com/en/vapome-ter/*.
356. Delfin. MoistureSC. *http://www.delfintech.com/en/ moistureSC*.
357. Delfin. Moisture. *http://www.delfintech.com/en/ moisture*.
358. Real, F. QuantStudio ™ 12K Flex Real -Time PCR System. 1–16 (2015).
359. https://blooge.cn/RefFinder/. No Title.
360. R Core DevelopmentTeam R: A language and environment for statistical computing.[http://www.R-project.org]. Title.
361. Pfaffl, M. W. A new mathematical model for relative quantification in real-time RT-PCR. *Nucleic Acids Res.* **29**, 45e–445 (2001).
362. 139. Shen R, Richter HE, S. PD. Interactions between HIV-1 and mucosal cells in the female reproductive tract. *Am J Reprod Immunol* **71**, 608–17 (2014).
363. Nazli, A. *et al.* Exposure to HIV-1 Directly Impairs Mucosal Epithelial Barrier Integrity Allowing Microbial Translocation. *PLoS Pathog.* **6**, e1000852 (2010).
364. O'Farrell, N. *et al.* Association Between HIV and Subpreputial Penile Wetness in Uncircumcised Men in South Africa. *JAIDS J. Acquir. Immune Defic. Syndr.* **43**, 69–77 (2006).
365. Colin N A Palmer, Alan D Irvine, Ana Terron-Kwiatkowski, Yiwei Zhao, Haihui Liao, Simon P Lee, David R Goudie, Aileen Sandilands, Linda E Campbell, Frances J D Smith, Gráinne M O'Regan, Rosemarie M Watson, Jo E Cecil, Sherri J Bale, John G Compton, John J, S. M. & W. H. I. M. Common loss-of-function variants of the epidermal barrier protein filaggrin are a major predisposing factor for atopic dermatitis. *Nat Genet* **38**, 441–6 (2006).
366. Smith FJ, Irvine AD, Terron-Kwiatkowski A, Sandilands A, Campbell LE, Zhao Y, Liao H, Evans AT, Goudie DR, Lewis-Jones S, Arseculeratne G, Munro CS, Sergeant A, O'Regan G, Bale SJ, Compton JG, DiGiovanna JJ, Presland RB, Fleckman P, M. WH. Loss-of-function mutations in the gene encoding filaggrin cause ichthyosis vulgaris. *Nat Genet* **38**, 337–42 (2006).
367. Broccardo CJ, Mahaffey S, Schwarz J, Wruck L, David G, Schlievert PM, Reisdorph NA, L. DY. Comparative proteomic profiling of patients with atopic dermatitis based on history of eczema herpeticum infection and Staphylococcus aureus colonization. *J Allergy Clin Immunol* **127**, 186–93 (2011).

368. Laurence Pellerin, Julie Henry, Chiung-Yueh Hsu, Stéfana Balica, Catherine Jean-Decoster, Marie-Claire Méchin, Britta Hansmann, Elke Rodriguez, Stefan Weindinger, Anne-Marie Schmitt, Guy Serre, Carle Paul, M. S. Defects of filaggrin-like proteins in both lesional and nonlesional atopic skin. *J. Allergy Clin. Immunol.* **131**, 1094–1102 (2013).
369. Mohamad J, Sarig O, Godsel LM, Peled A, Malchin N, Bochner R, Vodo D, Rabinowitz T, Pavlovsky M, Taiber S, Fried M, Eskin-Schwartz M, Assi S, Shomron N, Uitto J, Koetsier JL, Bergman R, Green KJ, S. E. Filaggrin 2 Deficiency Results in Abnormal Cell-Cell Adhesion in the Cornified Cell Layers and Causes Peeling Skin Syndrome Type A. *Nvest Dermatol* **138**, 1736–1743 (2018).
370. Bolling MC, Jan SZ, Pasmooij AMG, Lemmink HH, Franke LH, Yenamandra VK, Sinke RJ, van den Akker PC, J. MF. Generalized Ichthyotic Peeling Skin Syndrome due to FLG2 Mutations. *J Invest Dermatol* **138**, 1881–1884 (2018).
371. Furuse M, Fujita K, Hiiragi T, Fujimoto K, T. S. Claudin-1 and -2: novel integral membrane proteins localizing at tight junctions with no sequence similarity to occludin. *J Cell Biol* **141**, 1539–1550 (1998).
372. Morris BJ, C. X. The role of circumcision in preventing STIs. In: Gross GE, Tyring SK, editors. Sexually Transmitted Infections and Sexually Transmitted Diseases. Berlin and Heidelberg: *Springer;* 715–739 (2011).
373. WHO/UNAIDS. A framework for voluntary medical male circumcision: effective HIV prevention and a gateway to improved adolescent boys' & men's health in Eastern and Southern Africa by 2021'. 7 (2016).
374. Shigehara, K. *et al.* Prevalence of human papillomavirus infection in the urinary tract of men with urethritis. *Int. J. Urol.* **17**, 563–568 (2010).
375. Al-Mously, N. & Eley, A. Interaction of Chlamydia trachomatis serovar E with male genital tract epithelium results in secretion of proinflammatory cytokines. *J. Med. Microbiol.* **56**, 1025–1032 (2007).
376. Pudney, J. & Anderson, D. J. Immunobiology of the human penile urethra. *Am. J. Pathol.* **147**, 155–65 (1995).
377. Ganor, Y. & Bomsel, M. HIV-1 Transmission in the Male Genital Tract. *Am. J. Reprod. Immunol.* **65**, 284–291 (2011).
378. Zhou, Z. *et al.* HIV-1 Efficient Entry in Inner Foreskin Is Mediated by Elevated CCL5/RANTES that Recruits T Cells and Fuels Conjugate Formation with Langerhans Cells. *PLoS Pathog.* **7**, e1002100 (2011).
379. Ganor, Y. *et al.* The adult penile urethra is a novel entry site for HIV-1 that preferentially targets resident urethral macrophages. *Mucosal Immunol.* **6**, 776–786 (2013).
380. Sennepin, A. *et al.* The Human Penis Is a Genuine Immunological Effector Site. *Front. Immunol.* **8**, (2017).
381. Esra RT, Olivier AJ, Passmore JA, Jaspan HB, Harryparsad R, G. CM. Does HIV Exploit the Inflammatory Milieu of the Male Genital Tract for Successful Infection? *Front Immunol* **7**, 245 (2016).
382. Reynolds, S. J. *et al.* Recent Herpes Simplex Virus Type 2 Infection and the Risk of Human Immunodeficiency Virus Type 1 Acquisition in India. *J. Infect. Dis.* **187**, 1513–1521 (2003).

383. Todd, J. *et al.* Risk Factors Influencing HIV Infection Incidence in a Rural African Population: A Nested Case-Control Study. *J. Infect. Dis.* **193**, 458–466 (2006).
384. Mayer, K. H. & Venkatesh, K. K. Interactions of HIV, Other Sexually Transmitted Diseases, and Genital Tract Inflammation Facilitating Local Pathogen Transmission and Acquisition. *Am. J. Reprod. Immunol.* **65**, 308–316 (2011).
385. Polak, M. E. *et al.* CD70–CD27 Interaction Augments CD8+ T-Cell Activation by Human Epidermal Langerhans Cells. *J. Invest. Dermatol.* **132**, 1636–1644 (2012).
386. Berthier-Vergnes, O. *et al.* TNF-α enhances phenotypic and functional maturation of human epidermal Langerhans cells and induces IL-12 p40 and IP-10/CXCL-10 production. *FEBS Lett.* **579**, 3660–3668 (2005).
387. Salgado, C. G. *et al.* Differential Effects of Cytokines and Immunosuppressive Drugs on CD40, B7–1, and B7–2 Expression on Purified Epidermal Langerhans Cells. *J. Invest. Dermatol.* **113**, 1021–1027 (1999).
388. Koyama, Y. *et al.* Isolation and Culture of Panning Method-enriched Langerhans Cells from Dispase-dissociated Epidermal Cells of the Mouse. *J. Dermatol.* **17**, 211–217 (1990).
389. Prodger, J. L. & Kaul, R. The biology of how circumcision reduces HIV susceptibility: broader implications for the prevention field. *AIDS Res. Ther.* **14**, 49–49 (2017).
390. Galiwango, R. M. *et al.* Characterization of CD4 + T cell subsets and HIV susceptibility in the inner and outer foreskin of Ugandan men. *Am. J. Reprod. Immunol.* **82**, (2019).
391. Anderson, D., Politch, J. A. & Pudney, J. HIV Infection and Immune Defense of the Penis. *Am. J. Reprod. Immunol.* **65**, 220–229 (2011).
392. Wong, M. T. *et al.* A High-Dimensional Atlas of Human T Cell Diversity Reveals Tissue-Specific Trafficking and Cytokine Signatures. *Immunity* **45**, 442–456 (2016).
393. Sathaliyawala, T. *et al.* Distribution and Compartmentalization of Human Circulating and Tissue-Resident Memory T Cell Subsets. *Immunity* **38**, 187–197 (2013).
394. Kumar, B. V. *et al.* Human Tissue-Resident Memory T Cells Are Defined by Core Transcriptional and Functional Signatures in Lymphoid and Mucosal Sites. *Cell Rep.* **20**, 2921–2934 (2017).
395. Yang, Q. *et al.* Cutting Edge: Characterization of Human Tissue-Resident Memory T Cells at Different Infection Sites in Patients with Tuberculosis. *J. Immunol.* **204**, 2331–2336 (2020).
396. O'Neil, T. R. *et al.* The Role of Tissue Resident Memory CD4 T Cells in Herpes Simplex Viral and HIV Infection. *Viruses* **13**, 359 (2021).
397. Humphrys, M. S. *et al.* Simultaneous Transcriptional Profiling of Bacteria and Their Host Cells. *PLoS ONE* **8**, e80597 (2013).
398. Marsh, J. W. *et al.* Bioinformatic analysis of bacteria and host cell dual RNA-sequencing experiments. *Brief. Bioinform.* (2017) doi:10.1093/bib/bbx043.
399. Hebenstreit, D. Methods, Challenges and Potentials of Single Cell RNA-seq. *Biology* **1**, 658–667 (2012).
400. Łabaj, P. P. *et al.* Characterization and improvement of RNA-Seq precision in quantitative transcript expression profiling. *Bioinformatics* **27**, i383–i391 (2011).
401. Saliba, A.-E., Westermann, A. J., Gorski, S. A. & Vogel, J. Single-cell RNA-seq: advances and future challenges. *Nucleic Acids Res.* **42**, 8845–8860 (2014).

402. Nanostring. Digital Spatial Transcriptomics. https://nanostring.com/research-focus/spatial-transcriptomics/.
403. Gondek, D. C., Olive, A. J., Stary, G. & Starnbach, M. N. CD4+ T Cells Are Necessary and Sufficient To Confer Protection against Chlamydia trachomatis Infection in the Murine Upper Genital Tract. *J. Immunol.* **189**, 2441–2449 (2012).
404. Gondek, D. C., Roan, N. R. & Starnbach, M. N. T Cell Responses in the Absence of IFN-γ Exacerbate Uterine Infection with Chlamydia trachomatis. *J. Immunol.* **183**, 1313–1319 (2009).
405. Bastidas, R. J., Elwell, C. A., Engel, J. N. & Valdivia, R. H. Chlamydial Intracellular Survival Strategies. *Cold Spring Harb. Perspect. Med.* **3**, a010256–a010256 (2013).
406. Saka, H. A. *et al.* Quantitative proteomics reveals metabolic and pathogenic properties of Chlamydia trachomatis developmental forms. *Mol. Microbiol.* **82**, 1185–1203 (2011).
407. Belland, R. J. *et al.* Transcriptome analysis of chlamydial growth during IFN-γ-mediated persistence and reactivation. *Proc. Natl. Acad. Sci.* **100**, 15971–15976 (2003).
408. Albrecht, M., Sharma, C. M., Reinhardt, R., Vogel, J. & Rudel, T. Deep sequencing-based discovery of the Chlamydia trachomatis transcriptome. *Nucleic Acids Res.* **38**, 868–877 (2010).
409. AbdelRahman, Y. M., Rose, L. A. & Belland, R. J. Developmental expression of non-coding RNAs in Chlamydia trachomatis during normal and persistent growth. *Nucleic Acids Res.* **39**, 1843–1854 (2011).
410. Porcella, S. F. *et al.* Transcriptional Profiling of Human Epithelial Cells Infected with Plasmid-Bearing and Plasmid-Deficient Chlamydia trachomatis. *Infect. Immun.* **83**, 534–543 (2015).
411. Carabeo, R. A., Dooley, C. A., Grieshaber, S. S. & Hackstadt, T. Rac interacts with Abi-1 and WAVE2 to promote an Arp2/3-dependent actin recruitment during chlamydial invasion. *Cell. Microbiol.* **9**, 2278–2288 (2007).
412. Rasmussen, S. J. *et al.* Secretion of proinflammatory cytokines by epithelial cells in response to Chlamydia infection suggests a central role for epithelial cells in chlamydial pathogenesis. *J. Clin. Invest.* **99**, 77–87 (1997).
413. Wyrick, P. B., Knight, S. T., Paul, T. R., Rank, R. G. & Barbier, C. S. Persistent Chlamydial Envelope Antigens in Antibiotic-Exposed Infected Cells Trigger Neutrophil Chemotaxis. *J. Infect. Dis.* **179**, 954–966 (1999).
414. Hess, S. *et al.* The reprogrammed host:Chlamydia trachomatis-induced up-regulation of glycoprotein 130 cytokines, transcription factors, and antiapoptotic genes. *Arthritis Rheum.* **44**, 2392–2401 (2001).
415. Johnson, R. M. Murine Oviduct Epithelial Cell Cytokine Responses to Chlamydia muridarum Infection Include Interleukin-12-p70 Secretion. *Infect. Immun.* **72**, 3951–3960 (2004).
416. Perry, L. L., Feilzer, K. & Caldwell, H. D. Immunity to Chlamydia trachomatis is mediated by T helper 1 cells through IFN-gamma-dependent and -independent pathways. *J. Immunol.* **158**, 3344–3352 (1997).
417. Morrison, R. P. & Caldwell, H. D. Immunity to Murine Chlamydial Genital Infection. *Infect. Immun.* **70**, 2741–2751 (2002).
418. Darville, T. *et al.* Toll-Like Receptor-2, but Not Toll-Like Receptor-4, Is Essential for

Development of Oviduct Pathology in Chlamydial Genital Tract Infection. *J. Immunol.* **171**, 6187–6197 (2003).
419. Johnson, R. M. Murine Oviduct Epithelial Cell Cytokine Responses to Chlamydia muridarum Infection Include Interleukin-12-p70 Secretion. *Infect. Immun.* **72**, 3951–3960 (2004).
420. Maxion, H. K. & Kelly, K. A. Chemokine Expression Patterns Differ within Anatomically Distinct Regions of the Genital Tract during Chlamydia trachomatis Infection. *Infect. Immun.* **70**, 1538–1546 (2002).
421. Buchholz, K. R. & Stephens, R. S. Activation of the host cell proinflammatory interleukin-8 response by Chlamydia trachomatis. *Cell. Microbiol.* **8**, 1768–1779 (2006).
422. Hvid, M. *et al.* Interleukin-1 is the initiator of Fallopian tube destruction during Chlamydia trachomatis infection. *Cell. Microbiol.* **9**, 2795–2803 (2007).
423. Rank, R. G. *et al.* Host Chemokine and Cytokine Response in the Endocervix within the First Developmental Cycle of Chlamydia muridarum. *Infect. Immun.* **78**, 536–544 (2010).
424. Agrawal, T., Bhengraj, A. R., Vats, V., Salhan, S. & Mittal, A. Expression of TLR 2, TLR 4 and iNOS in Cervical Monocytes of Chlamydia trachomatis-infected Women and Their Role in Host Immune Response. *Am. J. Reprod. Immunol.* **66**, 534–543 (2011).
425. Datta, B., Njau, F., Thalmann, J., Haller, H. & Wagner, A. D. Differential infection outcome of Chlamydia trachomatis in human blood monocytes and monocyte-derived dendritic cells. *BMC Microbiol.* **14**, 209 (2014).
426. Webster, S. J. *et al.* Detection of a microbial metabolite by STING regulates inflammasome activation in response to Chlamydia trachomatis infection. *PLOS Pathog.* **13**, e1006383 (2017).
427. Clifton, D. R. *et al.* A chlamydial type III translocated protein is tyrosine-phosphorylated at the site of entry and associated with recruitment of actin. *Proc. Natl. Acad. Sci.* **101**, 10166–10171 (2004).
428. Nguyen, P. H., Lutter, E. I. & Hackstadt, T. Chlamydia trachomatis inclusion membrane protein MrcA interacts with the inositol 1,4,5-trisphosphate receptor type 3 (ITPR3) to regulate extrusion formation. *PLOS Pathog.* **14**, e1006911 (2018).
429. Packiam, M., Weinrick, B., Jacobs, W. R. & Maurelli, A. T. Structural characterization of muropeptides from Chlamydia trachomatis peptidoglycan by mass spectrometry resolves "chlamydial anomaly". *Proc. Natl. Acad. Sci.* **112**, 11660–11665 (2015).
430. Kang, P. B. *et al.* The human macrophage mannose receptor directs Mycobacterium tuberculosis lipoarabinomannan-mediated phagosome biogenesis. *J. Exp. Med.* **202**, 987–999 (2005).
431. Hmama, Z., Peña-Díaz, S., Joseph, S. & Av-Gay, Y. Immunoevasion and immunosuppression of the macrophage by Mycobacterium tuberculosis. *Immunol. Rev.* **264**, 220–232 (2015).
432. McCormack, R. M. *et al.* Perforin-2 is essential for intracellular defense of parenchymal cells and phagocytes against pathogenic bacteria. *eLife* **4**, (2015).
433. Fang, F. C. Antimicrobial Actions of Reactive Oxygen Species. *mBio* **2**, (2011).
434. Soliman, H., Mediavilla-Varela, M. & Antonia, S. Indoleamine 2,3-Dioxygenase. *Cancer J.* **16**, 354–359 (2010).
435. Krausse-Opatz, B. *et al.* Peptidomic analysis of human peripheral monocytes persistently

infected by Chlamydia trachomatis. *Med. Microbiol. Immunol. (Berl.)* **196**, 103–114 (2007).
436. Gaydos, C. A., Summersgill, J. T., Sahney, N. N., Ramirez, J. A. & Quinn, T. C. Replication of Chlamydia pneumoniae in vitro in human macrophages, endothelial cells, and aortic artery smooth muscle cells. *Infect. Immun.* **64**, 1614–1620 (1996).
437. Sun, H. S. *et al.* Chlamydia trachomatis vacuole maturation in infected macrophages. *J. Leukoc. Biol.* **92**, 815–827 (2012).
438. Hackstadt, T., Scidmore, M. A. & Rockey, D. D. Lipid metabolism in Chlamydia trachomatis-infected cells: directed trafficking of Golgi-derived sphingolipids to the chlamydial inclusion. *Proc. Natl. Acad. Sci.* **92**, 4877–4881 (1995).
439. Herweg, J.-A. & Rudel, T. Interaction of Chlamydiae with human macrophages. *FEBS J.* **283**, 608–618 (2016).
440. Beagley, K., Huston, W. M., Hansbro, P. M. & Timms, P. Chlamydial Infection of Immune Cells: Altered Function and Implications for Disease. *Crit. Rev. Immunol.* **29**, 275–305 (2009).
441. Al-Zeer, M. A., Al-Younes, H. M., Lauster, D., Abu Lubad, M. & Meyer, T. F. Autophagy restricts Chlamydia trachomatis growth in human macrophages via IFNG-inducible guanylate binding proteins. *Autophagy* **9**, 50–62 (2013).
442. MacMicking, J. D. Interferon-inducible effector mechanisms in cell-autonomous immunity. *Nat. Rev. Immunol.* **12**, 367–382 (2012).
443. Johnson, R. M. *et al.* B Cell Presentation of Chlamydia Antigen Selects Out Protective CD4γ13 T Cells: Implications for Genital Tract Tissue-Resident Memory Lymphocyte Clusters. *Infect. Immun.* **86**, (2018).
444. O'Connell, C. M. *et al.* Toll-Like Receptor 2 Activation by Chlamydia trachomatis Is Plasmid Dependent, and Plasmid-Responsive Chromosomal Loci Are Coordinately Regulated in Response to Glucose Limitation by C. trachomatis but Not by C. muridarum. *Infect. Immun.* **79**, 1044–1056 (2011).
445. Beaulieu, L. M. *et al.* Specific Inflammatory Stimuli Lead to Distinct Platelet Responses in Mice and Humans. *PLOS ONE* **10**, e0131688 (2015).
446. Belland, R. J. *et al.* Genomic transcriptional profiling of the developmental cycle of Chlamydia trachomatis. *Proc. Natl. Acad. Sci.* **100**, 8478–8483 (2003).
447. Humphrys, M. S. *et al.* Simultaneous Transcriptional Profiling of Bacteria and Their Host Cells. *PLoS ONE* **8**, e80597 (2013).
448. Coombes, B. K. & Mahony, J. B. cDNA Array Analysis of Altered Gene Expression in Human Endothelial Cells in Response to Chlamydia pneumoniae Infection. *Infect. Immun.* **69**, 1420–1427 (2001).
449. Burton, M. J. *et al.* Conjunctival Transcriptome in Scarring Trachoma. *Infect. Immun.* **79**, 499–511 (2011).
450. Wang, A. *et al.* Transcription factor complex AP-1 mediates inflammation initiated by Chlamydia pneumoniae infection. *Cell. Microbiol.* **15**, 779–794 (2013).
451. Wang, A., Johnston, S. C., Chou, J. & Dean, D. A Systemic Network for Chlamydia pneumoniae Entry into Human Cells. *J. Bacteriol.* **192**, 2809–2815 (2010).
452. Hess, S. *et al.* More than just innate immunity: comparative analysis of Chlamydophila pneumoniae and Chlamydia trachomatis effects on host-cell gene regulation. *Cell.*

Microbiol. **5**, 785–795 (2003).
453. REN, Q., ROBERTSON, S. J., HOWE, D., BARROWS, L. F. & HEINZEN, R. A. Comparative DNA Microarray Analysis of Host Cell Transcriptional Responses to Infection by Coxiella burnetii or Chlamydia trachomatis. *Ann. N. Y. Acad. Sci.* **990**, 701–713 (2003).
454. Schrader, S. *et al.* Expression of inflammatory host genes in Chlamydia trachomatis-infected human monocytes. *Arthritis Res. Ther.* **9**, R54 (2007).
455. Virok, D. *et al.* Infection of U937 Monocytic Cells with Chlamydia pneumoniae Induces Extensive Changes in Host Cell Gene Expression. *J. Infect. Dis.* **188**, 1310–1321 (2003).
456. Xia, M., Bumgarner, R. E., Lampe, M. F. & Stamm, W. E. Chlamydia trachomatis Infection Alters Host Cell Transcription in Diverse Cellular Pathways. *J. Infect. Dis.* **187**, 424–434 (2003).
457. Kumar, Y., Cocchiaro, J. & Valdivia, R. H. The Obligate Intracellular Pathogen Chlamydia trachomatis Targets Host Lipid Droplets. *Curr. Biol.* **16**, 1646–1651 (2006).
458. Cocchiaro, J. L. & Valdivia, R. H. New insights into Chlamydia intracellular survival mechanisms. *Cell. Microbiol.* **11**, 1571–1578 (2009).
459. Elwell, C. A. & Engel, J. N. Lipid acquisition by intracellular Chlamydiae. *Cell. Microbiol.* **14**, 1010–1018 (2012).
460. Mak, T. & Brüggemann, H. Vimentin in Bacterial Infections. *Cells* **5**, 18 (2016).
461. Rice, J. M., Zweifach, A. & Lynes, M. A. Metallothionein regulates intracellular zinc signaling during CD4+ T cell activation. *BMC Immunol.* **17**, 13 (2016).
462. Subramanian, A. *et al.* Gene set enrichment analysis: A knowledge-based approach for interpreting genome-wide expression profiles. *Proc. Natl. Acad. Sci.* **102**, 15545–15550 (2005).
463. NIH. Gene.
464. Zhang, M. *et al.* HIV regulation of the IL-7R: a viral mechanism for enhancing HIV-1 replication in human macrophages in vitro. *J. Leukoc. Biol.* **79**, 1328–1338 (2006).
465. Gondek, D. C., Olive, A. J., Stary, G. & Starnbach, M. N. CD4+ T Cells Are Necessary and Sufficient To Confer Protection against Chlamydia trachomatis Infection in the Murine Upper Genital Tract. *J. Immunol.* **189**, 2441–2449 (2012).
466. Redgrove, K. A. & McLaughlin, E. A. The Role of the Immune Response in Chlamydia trachomatis Infection of the Male Genital Tract: A Double-Edged Sword. *Front. Immunol.* **5**, (2014).
467. Khani, P., Farokh Forghani, S., Ataei Kachoei, Z., Zekri, A. & Ghazi, F. Analysis of KRT5 and KRT14 gene mutations and mode of inheritance in Iranian patients with clinical suspicion of Epidermolysis bullosa simplex. *Med. J. Islam. Repub. Iran* **34**, 43 (2020).
468. Kim, S. & Coulombe, P. A. Intermediate filament scaffolds fulfill mechanical, organizational, and signaling functions in the cytoplasm. *Genes Dev.* **21**, 1581–1597 (2007).
469. Coulombe, P. A., Kerns, M. L. & Fuchs, E. Epidermolysis bullosa simplex: a paradigm for disorders of tissue fragility. *J. Clin. Invest.* **119**, 1784–1793 (2009).
470. Coulombe, P. A. *et al.* Point mutations in human keratin 14 genes of epidermolysis bullosa simplex patients: Genetic and functional analyses. *Cell* **66**, 1301–1311 (1991).
471. Khani, P. *et al.* Keratins and epidermolysis bullosa simplex. *J. Cell. Physiol.* **234**, 289–

297 (2019).
472. Dong, F., Su, H., Huang, Y., Zhong, Y. & Zhong, G. Cleavage of Host Keratin 8 by a Chlamydia-Secreted Protease. *Infect. Immun.* **72**, 3863–3868 (2004).
473. Pedersen, I. S. *et al.* Differential effect of surgical manipulation on gene expression in normal breast tissue and breast tumor tissue. *Mol. Med.* **24**, 57 (2018).
474. Liu, S. & Trapnell, C. Single-cell transcriptome sequencing: recent advances and remaining challenges. *F1000Research* **5**, 182 (2016).
475. Holtmann, H., Shemer-Avni, Y., Wessel, K., Sarov, I. & Wallach, D. Inhibition of growth of Chlamydia trachomatis by tumor necrosis factor is accompanied by increased prostaglandin synthesis. *Infect. Immun.* **58**, 3168–3172 (1990).
476. Fiers, W. Tumor necrosis factor Characterization at the molecular, cellular and in vivo level. *FEBS Lett.* **285**, 199–212 (1991).
477. Conway, D. J. *et al.* Scarring trachoma is associated with polymorphism in the tumor necrosis factor alpha (TNF-alpha) gene promoter and with elevated TNF-alpha levels in tear fluid. *Infect. Immun.* **65**, 1003–1006 (1997).
478. Heinemann, M., Susa, M., Simnacher, U., Marre, R. & Essig, A. Growth of Chlamydia pneumoniae induces cytokine production and expression of CD14 in a human monocytic cell line. *Infect. Immun.* **64**, 4872–4875 (1996).
479. Paland, N. *et al.* Reduced Display of Tumor Necrosis Factor Receptor I at the Host Cell Surface Supports Infection with Chlamydia trachomatis. *J. Biol. Chem.* **283**, 6438–6448 (2008).
480. Dinarello, C. A. Biologic basis for interleukin-1 in disease. *Blood* **87**, 2095–147 (1996).
481. Dinarello, C. A. Overview of the IL-1 family in innate inflammation and acquired immunity. *Immunol. Rev.* **281**, 8–27 (2018).
482. Rothermel, C. D., Schachter, J., Lavrich, P., Lipsitz, E. C. & Francus, T. Chlamydia trachomatis-induced production of interleukin-1 by human monocytes. *Infect. Immun.* **57**, 2705–2711 (1989).
483. Gervassi, A. *et al.* Differential Regulation of Inflammatory Cytokine Secretion by Human Dendritic Cells upon Chlamydia trachomatis Infection. *Infect. Immun.* **72**, 7231–7239 (2004).
484. Rothman, J. E. & Wieland, F. T. Protein Sorting by Transport Vesicles. *Science* **272**, 227–234 (1996).
485. Rzomp, K. A., Scholtes, L. D., Briggs, B. J., Whittaker, G. R. & Scidmore, M. A. Rab GTPases Are Recruited to Chlamydial Inclusions in Both a Species-Dependent and Species-Independent Manner. *Infect. Immun.* **71**, 5855–5870 (2003).
486. Archer, N. K., Dilolli, M. N. & Miller, L. S. Pushing the Envelope in Psoriasis: Late Cornified Envelope Proteins Possess Antimicrobial Activity. *J. Invest. Dermatol.* **137**, 2257–2259 (2017).
487. Ohmer, M. *et al.* Infection of HeLa cells with <scp> *Chlamydia trachomatis* </scp> inhibits protein synthesis and causes multiple changes to host cell pathways. *Cell. Microbiol.* **21**, (2019).
488. Hayward, R. J., Marsh, J. W., Humphrys, M. S., Huston, W. M. & Myers, G. S. A. Chromatin accessibility dynamics of Chlamydia-infected epithelial cells. *Epigenetics Chromatin* **13**, 45 (2020).

489. Bierne, H., Hamon, M. & Cossart, P. Epigenetics and Bacterial Infections. *Cold Spring Harb. Perspect. Med.* **2**, a010272–a010272 (2012).
490. Hamon, M. A. & Cossart, P. Histone Modifications and Chromatin Remodeling during Bacterial Infections. *Cell Host Microbe* **4**, 100–109 (2008).
491. Haidl, G. & Allam, J.-P. Chlamydia trachomatis infection of the male genital tract: what seems to be the trouble? *Asian J. Androl.* **24**, 121 (2022).
492. Nogueira, A. T., Braun, K. M. & Carabeo, R. A. Characterization of the Growth of Chlamydia trachomatis in In Vitro-Generated Stratified Epithelium. *Front. Cell. Infect. Microbiol.* **7**, (2017).
493. Faller, E. M., McVey, M. J., Kakal, J. A. & MacPherson, P. A. Interleukin-7 Receptor Expression on CD8 T-Cells Is Downregulated by the HIV Tat Protein. *JAIDS J. Acquir. Immune Defic. Syndr.* **43**, 257–269 (2006).
494. Kim, D. Y. *et al.* CBFβ Stabilizes HIV Vif to Counteract APOBEC3 at the Expense of RUNX1 Target Gene Expression. *Mol. Cell* **49**, 632–644 (2013).
495. Beatty, W. L. Trafficking from CD63-positive late endocytic multivesicular bodies is essential for intracellular development of Chlamydia trachomatis. *J. Cell Sci.* **119**, 350–359 (2006).
496. Pedersen, I. S. *et al.* Differential effect of surgical manipulation on gene expression in normal breast tissue and breast tumor tissue. *Mol. Med.* **24**, 57–57 (2018).
497. De Cecco, L. *et al.* Impact of biospecimens handling on biomarker research in breast cancer. *BMC Cancer* **9**, 409–409 (2009).
498. Borgan, E. *et al.* Ischemia caused by time to freezing induces systematic microRNA and mRNA responses in cancer tissue. *Mol. Oncol.* **5**, 564–576 (2011).
499. UNAIDS, 2022. Unaids, 2022. *Urban Aff. Q.* **25**, 200–211 (2022).
500. Boily, M.-C. *et al.* Heterosexual risk of HIV-1 infection per sexual act: systematic review and meta-analysis of observational studies. *Lancet Infect. Dis.* **9**, 118–129 (2009).
501. Gray, R. H. *et al.* Male circumcision for HIV prevention in men in Rakai, Uganda: a randomised trial. *The Lancet* **369**, 657–666 (2007).
502. WHO/UNAIDS. Uneven progress on the voluntary medical male circumcision. **2022**, 1–6 (2022).
503. Baeten, J. M. *et al.* Antiretroviral Prophylaxis for HIV Prevention in Heterosexual Men and Women. *N. Engl. J. Med.* **367**, 399–410 (2012).
504. Kibengo, F. M. *et al.* Safety, Adherence and Acceptability of Intermittent Tenofovir/Emtricitabine as HIV Pre-Exposure Prophylaxis (PrEP) among HIV-Uninfected Ugandan Volunteers Living in HIV-Serodiscordant Relationships: A Randomized, Clinical Trial. *PLoS ONE* **8**, e74314 (2013).
505. Baeten, J. M. *et al.* Single-agent tenofovir versus combination emtricitabine plus tenofovir for pre-exposure prophylaxis for HIV-1 acquisition: an update of data from a randomised, double-blind, phase 3 trial. *Lancet Infect. Dis.* **14**, 1055–1064 (2014).
506. Grulich, A. E. *et al.* Population-level effectiveness of rapid, targeted, high-coverage roll-out of HIV pre-exposure prophylaxis in men who have sex with men: the EPIC-NSW prospective cohort study. *Lancet HIV* **5**, e629–e637 (2018).
507. Hladik, F. *et al.* Mucosal effects of tenofovir 1% gel. *eLife* **4**, (2015).
508. Herrera, C. *et al.* Dose finding study for on-demand HIV pre-exposure prophylaxis for

insertive sex in sub-Saharan Africa: results from the CHAPS open label randomised controlled trial. *eBioMedicine* **93**, 104648 (2023).
509. Gray, C. M. *et al.* Impact of chemokine C–C ligand 27, foreskin anatomy and sexually transmitted infections on HIV-1 target cell availability in adolescent South African males. *Mucosal Immunol.* **13**, 118–127 (2020).
510. Fischetti, L., Barry, S. M., Hope, T. J. & Shattock, R. J. HIV-1 infection of human penile explant tissue and protection by candidate microbicides. *AIDS* **23**, 319–328 (2009).
511. Else, L. *et al.* Pre-Clinical Evaluation of Tenofovir and Tenofovir Alafenamide for HIV-1 Pre-Exposure Prophylaxis in Foreskin Tissue. *Pharmaceutics* **14**, 1285 (2022).
512. Petkov, S. *et al.* Short-term oral pre-exposure prophylaxis against HIV-1 modulates the transcriptome of foreskin tissue in young men in Africa. *Front. Immunol.* **13**, (2022).
513. Grivel, J.-C., Shattock, R. J. & Margolis, L. B. Selective transmission of R5 HIV-1 variants: where is the gatekeeper? *J. Transl. Med.* **9**, S6 (2011).
514. Salazar-Gonzalez, J. F. *et al.* Genetic identity, biological phenotype, and evolutionary pathways of transmitted/founder viruses in acute and early HIV-1 infection. *J. Exp. Med.* **206**, 1273–1289 (2009).
515. Cernadas, M., Lu, J., Watts, G. & Brenner, M. B. CD1a expression defines an interleukin-12 producing population of human dendritic cells. *Clin. Exp. Immunol.* **155**, 523–533 (2009).
516. Hardman, C. S. *et al.* CD1a promotes systemic manifestations of skin inflammation. *Nat. Commun.* **13**, 7535 (2022).
517. Monnot, G. C. *et al.* Staphylococcal phosphatidylglycerol antigens activate human T cells via CD1a. *Nat. Immunol.* **24**, 110–122 (2023).
518. Ahmed, Z., Kawamura, T., Shimada, S. & Piguet, V. The Role of Human Dendritic Cells in HIV-1 Infection. *J. Invest. Dermatol.* **135**, 1225–1233 (2015).
519. Tebbe, B. *et al.* Tight junction proteins: a novel class of integral membrane proteins. *Arch. Dermatol. Res.* **294**, 14–18 (2002).
520. Lemos, M. P. *et al.* The Inner Foreskin of Healthy Males at Risk of HIV Infection Harbors Epithelial CD4+ CCR5+ Cells and Has Features of an Inflamed Epidermal Barrier. *PLoS ONE* **9**, e108954 (2014).
521. Nash, S. *et al.* Combined HIV Adolescent Prevention Study (CHAPS): comparison of HIV pre-exposure prophylaxis regimens for adolescents in sub-Saharan Africa—study protocol for a mixed-methods study including a randomised controlled trial. *Trials* **21**, 900 (2020).
522. Furuse, M. *et al.* Claudin-based tight junctions are crucial for the mammalian epidermal barrier. *J. Cell Biol.* **156**, 1099–1111 (2002).
523. Juffermans, N. P. *et al.* Up-regulation of HIV coreceptors CXCR4 and CCR5 on CD4(+) T cells during human endotoxemia and after stimulation with (myco)bacterial antigens: the role of cytokines. *Blood* **96**, 2649–54 (2000).
524. Ebert, L. M. & McColl, S. R. Up-Regulation of CCR5 and CCR6 on Distinct Subpopulations of Antigen-Activated CD4+ T Lymphocytes. *J. Immunol.* **168**, 65–72 (2002).
525. Liebenberg, L. J. P. *et al.* Genital Immune Cell Activation and Tenofovir Gel Efficacy: A Case-Control Study. *Clin. Infect. Dis.* **75**, 1088–1091 (2022).

526. Pena-Cruz, V. *et al.* HIV-1 replicates and persists in vaginal epithelial dendritic cells. *J. Clin. Invest.* **128**, 3439–3444 (2018).
527. Deckers, J., Hammad, H. & Hoste, E. Langerhans Cells: Sensing the Environment in Health and Disease. *Front. Immunol.* **9**, (2018).
528. Naik, S. *et al.* Commensal–dendritic-cell interaction specifies a unique protective skin immune signature. *Nature* **520**, 104–108 (2015).
529. Soyka, M. B. *et al.* Defective epithelial barrier in chronic rhinosinusitis: The regulation of tight junctions by IFN-γ and IL-4. *J. Allergy Clin. Immunol.* **130**, 1087-1096.e10 (2012).
530. Sugita, K. *et al.* Human type 2 innate lymphoid cells disrupt skin keratinocyte tight junction barrier by IL-13. *Allergy* **74**, 2534–2537 (2019).
531. Dinh, M. H., McRaven, M. D., Kelley, Z., Penugonda, S. & Hope, T. J. Keratinization of the adult male foreskin and implications for male circumcision. *AIDS* **24**, 899–906 (2010).
532. Prodger, J. L. *et al.* Impact of asymptomatic Herpes simplex virus-2 infection on T cell phenotype and function in the foreskin. *AIDS* **26**, 1319–1322 (2012).

APPENDIX I

Case Report Form

(https://drive.google.com/drive/folders/1Ehg2PWwfcKpd7N68jXTFPzUxxM_eAbPG?usp=sharing)

Meter readings and environmental factors

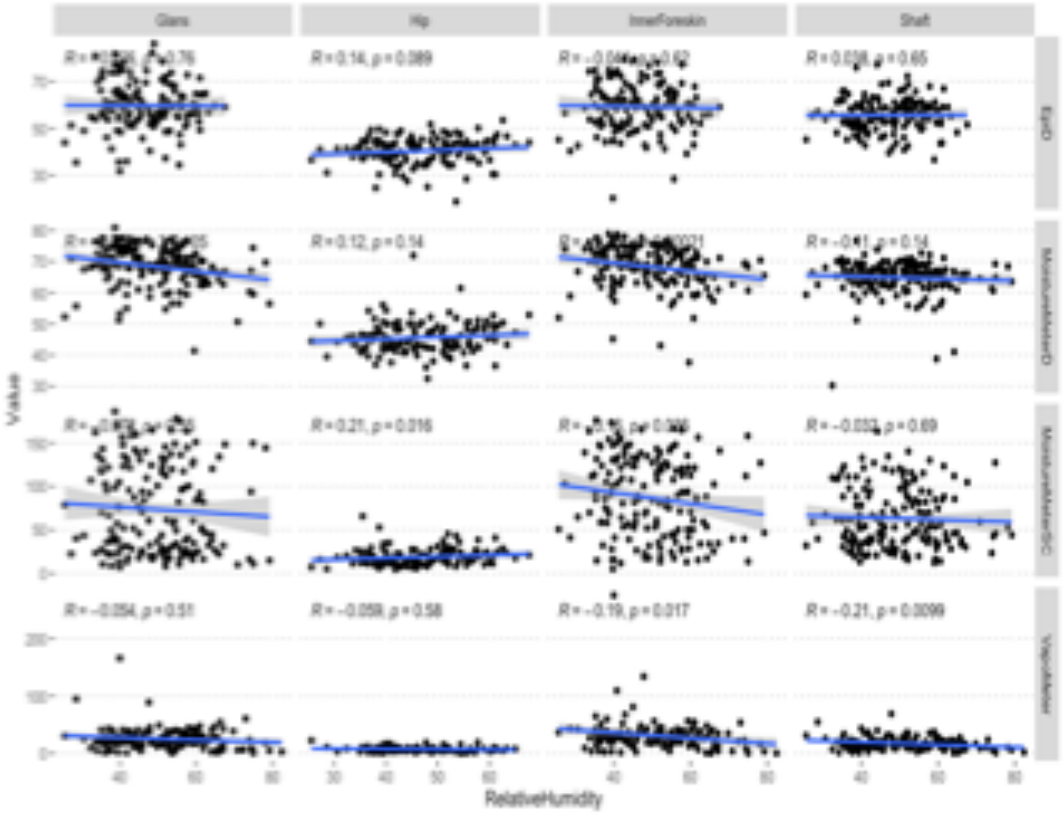

Figure 1: Environmental climate conditions strongly correlate with meter readings

This demonstrates readings taken with the four various meters across the various sites in correlation (Pairewise) with the relative humidity taken at the time of measurements.

Cleaning methods

Four cleaning methods were employed on the forearm skin of 5 volunteers: none (no cleaning method employed before applying meters on the skin for reading), dry cotton, saline, ethanol. Following this, after consistent time exposure to the air (60 seconds), triplicate readings were measured using two of the meter machines – Vapometer and MoistureSC. These were then

analyzed to examine if there were any significant differences across the different cleaning methods. Transepithelial water loss readings using the handheld vapometer taken from the forearm skin of five volunteers are shown in table 1A, figure 5. Triple readings for each cleaning method were not significantly different from each other methods (vapometer; p=0.96 & mositureSc; p=0.53). What was noted however, was the inherent biologically variability in the readings across different individuals as opposed to across methods. For example, the median reading for participant one (1) 5.1 $g/m^2/h$ (IQR 4.5:5.6) in the "no cleaning method" versus 15 $g/m^2/h$ (IQR 12.1:15.8) in participant 4. Finally, there was also slight intraindividual variability in readings within the same cleaning method. The vapometer displayed more variability in its measurements compared to the MositureSC meter, as shown by the higher CV values range (>50% for the vapometer) and < 50% CV values for the MoistureSC (Table 1). As a result of these findings, we proceeded to move forward with using dry method for cleaning in our main cohort measurements.

(a)

Cleaning method	None			Dry			Saline			Ethanol		
Participant 1	5.6	5.1	4.5	4.3	4.4	4.4	4.2	6.6	4.8	5.6	5.8	6.4
Participant 2	9.5	9.1	9.2	8.2	7.9	8.0	10.4	12.9	10.7	13.3	11.0	10.0
Participant 3	7.8	8.2	7.0	4.6	5.5	6.1	18.6	16.8	9.9	14.1	11.5	7.2
Participant 4	19.6	19.5	19.7	18.1	18.4	19.4	20.3	20.5	19.8	18.6	18.8	17.2
Participant 5	15.8	12.1	15.0	17.4	23.7	19.5	17.5	19.6	24.4	24.0	24.0	23.7

Vapometer

(b)

Cleaning method	None			Dry			Saline			Ethanol		
Participant 1	36.5	29.4	36.7	28.1	28.1	34.7	24.7	19.6	21.4	17.7	19.3	21.3
Participant 2	19.7	22.9	21.2	22.9	24.3	22.9	26.1	19.4	17.7	34.6	27.5	26.1
Participant 3	14.8	11.6	13.2	11.4	11.1	11.3	17.6	12.9	12.8	15.5	12.8	10.6
Participant 4	21.3	19.6	19.5	17.8	19.7	17.7	21.1	21.3	22.9	21.3	24.6	24.4
Participant 5	14.7	14.4	12.6	6.4	9.3	9.6	12.8	12.8	14.2	19.7	19.6	19.5

MoistureSC

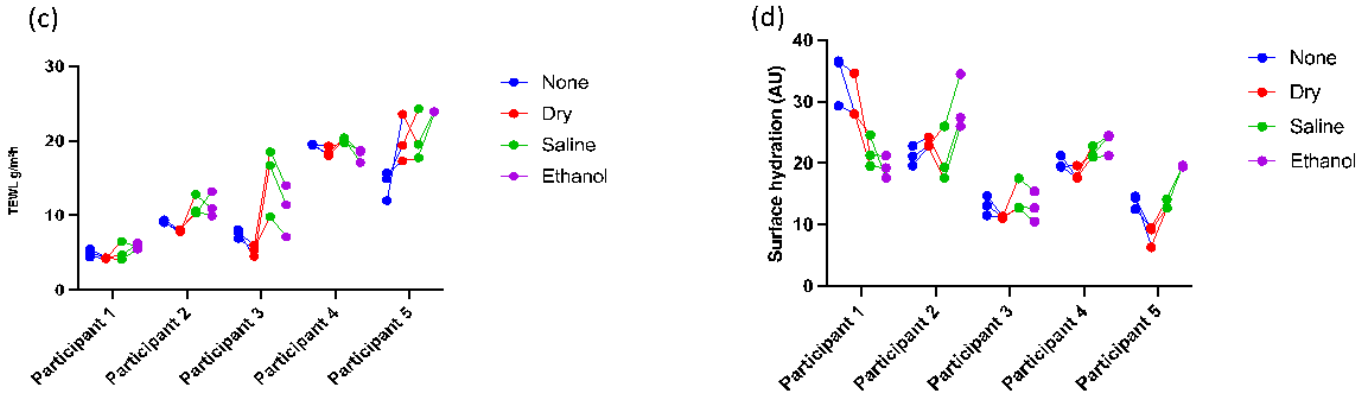

Figure 2: Cleaning methods. Absolute triplicate TEWL values measured in 5 participants following four different types of cleaning methods prior to measuring using the (A) Vapometer and (B) MoistureSC Absolute values of surface hydration values using (C) Vapometer showing median & IQR across different methods from all the five volunteers and (D) moistureSC showing median & IQR across different methods.

Pilot meter readings

To optimize the use of meter machines for the characterization of penile skin barrier function, hand-held meter machines were used to measure transepithelial water loss (TEWL), surface hydration and % water content in triplicate using vapometer and moistureSC respectively on thefirst 30 participants who were recruited across the various clinical sites described in chapter 1. The objective of this was to assess the variation of meter readings across various anatomical sites of the penis and to assess if the choice of the control site (i.e. shaft) is adequate. Measurements were taken with Vapometer and MoistureMeterSC, on the glans, inner foreskin and penile shaft prior to medical penile circumcision. No participants had no overt signs of STIs as determined by the dermatologist who examined them nor symptoms according to self-report. After 15 minutes in a hospital gown to acclimatize to the examination room, readings were taken in triplicate.

Figure 6 demonstrates TEWL and surface hydration readings from the 30 participants included in the pilot study.. The shaft was included to serve as a control site whilst the glans and inner foreskin were the regions of interest due to their proven susceptibility to HIV infection. Figure 6A shows the TEWL readings from the vapometer. The shaft demonstrated the lowest and least variable TEWL (median, 10.97 [IQR 6.35:18.67] g/m^2/h. The glans had a median TEWL of 20.22 [IQR 5.56:38.57] g/m^2/h, and the inner foreskin median was 22.35 [IQR4.19:35.08] g/m^2/h. Comparison between the three anatomical sites showed that only the glans and shaft were significantly different (p=0.0135). Consistent with vapometer reading patterns, surface hydration readings using the mositureSC on the shaft also had the least variability (CV 51.3%), with the glans and inner foreskin (80.2 & 68.5% respectively) having the most variability. The shaft surface hydration median readings were 43.48 [IQR 34.19:61.65] au, the glans 46.82 [IQR 20.53:119.9] au, and the inner foreskin 52.15 IQR [28.20:113.3] au (Figure 6B). Comparison with multiple testing corrections showed no significant difference in the surface hydration between the 3 sites.

Initially, the hypothesis was that the shaft would be the more conserved penile anatomical site compared to the other sites (inner foreskin and glans). However, the variability in shaft readings too high, and this high variability shown by high CV values led to the decision to use five instead of three repeat readings and use a more conservative control site than the shaft as it also showed variability. Therefore, from this, it was decided to choose a site that is outside the penile genital tract (as we hypothesized it would be less variable), thus we used the hip site as a control site in the main cohort.

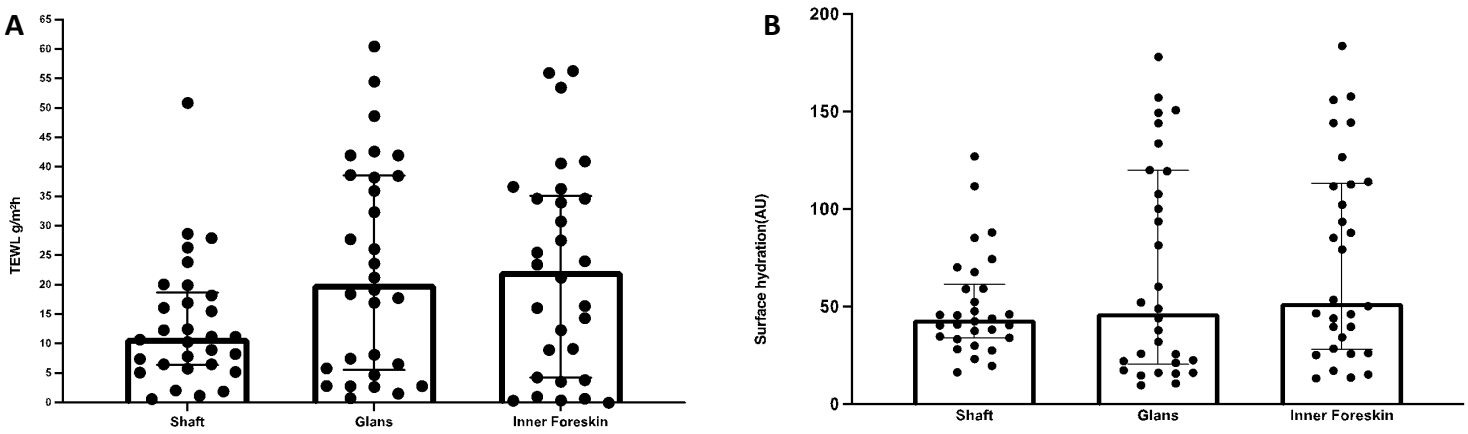

Figure 3: Pilot Meter data readings. A TEWL readings And B, surface hydration readings measured from the penile shaft, glans and inner foreskin using Vapometer in 30 male participants.

Primer Annealing Temperature (Ta) optimization

A range of annealing temperatures (55.3-65.3°C) were tested using multiple qPCR experiments in separate 384-well plates (Table 3). Each assay in each plate was run in triplicate with each sample consisting of pooled cDNA (from all the study samples) diluted 20-fold, forward and reverse primers at 500nM, 5µL 2X PowerUp SYBR Green Mastermix (Thermo Fisher) in a total reaction volume of 10µL. NTC and NRT were included as controls for each assay. To avoid variations introduced by reaction set-up, all reaction mixes for each gene were prepared as a mastermix for all six plates and aliquoted into the individual plates. The plates were sealed and stored at room temperature in the dark before they were run on the QuantStudio 12K Flex (Applied Biosystems) and analyzed within 24 hours using the following cycling parameters: UDG activation at 50°C for 2 min; initial denaturation at 95°C for 2 min followed by 40 cycles of 95°C for 15 sec, 54-64°C for 15 sec and 72°C for 1 min. A dissociation step was included at the end of the PCR run. The choice of optimal temperature was based on not having non-specific amplification.

Gene	Primer Name	Primer Sequence (5'---------3')	Tm (°C)	Amplicon Size (bp) cDNA	gDNA	Source
cadherin 1	CDH1F CDH1R	CTGCTGCTCTTGCTGTTTCTTC CTCCGCCTCCTTCTTCATCATA	56.7 56.1	112		Pendaries et al. 2015
Claudin 1	Claudin 1F2 Claudin 1R2	AGGTGCAGAAGATGAGGATGGC CCTGACCAAATTCGTACCTGGC		156	2618	This study
Claudin 2	Claudin 2F Claudin 2R	CCCAAACCCACTAATCACATC GCCACTGCTTCTCCTTCC	53.5 55.9	112		
Claudin 3	Claudin 3F2 Claudin 3R2	CACGCGAGAAGAAGTACACGG TAGACGTAGTCCTTGCGGTCG		106	106	This study
Claudin 4	Claudin 4F Claudin 4R	GGCGTGGTGTTCCTGTTG AGCGGATTGTAGAAGTCTTGG	56.9 54.5	89		
Claudin 5	Claudin 5F2 Claudin 5R2	TCTTTACTCCATCGGCAGGGC TTCTTAGCCTTCCCACTCCCG		137	137	This study
filaggrin (FLG)	FLG 1F FLG 1R	CATCAAAAGAAACTCAGTAAA CCCTCGGTTTCCACTGTCTC	57.0 57.5	123		
filaggrin 2 (FLG2)	FLG2F FLG2R	TCTGAAGAACCCAGATGATCCA CATCAAAAGAAACTCAGTAAAGTCC AA	55.4 54.0	100		Pendaries et al. 2015
glyceraldehyde-3-phosphate	GAPDH F GAPDH R	TCTCTGCTCCTCCTGTTC CTCCGACCTTCACCTTCC	53.4 54.9	96		

dehydrogenase (GAPDH)	GAPDH F2 GAPDH R2	CGGAGTCAACGGATTTGGTCGTAT AGCCTTCTCCATGGTGGTGAAGAC	58.9 60.8		
involucrin (IVL)	IVLF IVLR	GGGTGGTTATTTATGTTTGGGTGG GCCAGGTCCAAGACATTCAAC	56.3 56.3	116	Pendaries et al. 2015
TATA-box binding protein (TBP)	TBPF TBPR	TCAAACCCAGAATTGTTCTCCTTAT CCTGAATCCCTTTAGAATAGGGTAGA	54.4 55.3	122	Pendaries et al. 2015

Table 1 : qPCR Primer List

A1

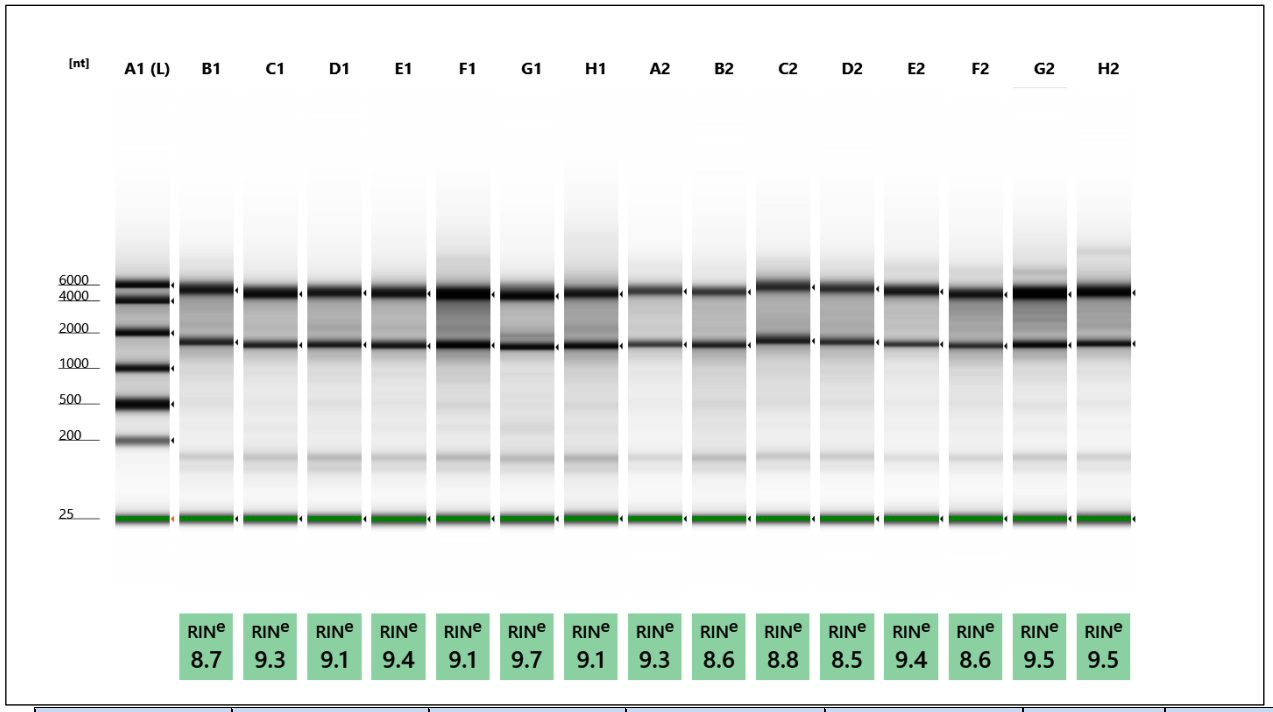

A2

A1	-	-	285	Ladder		Ladder
B1	8.7	1.2	161	1666PCR020		
C1	9.3	1.8	155	1666PCR039		
D1	9.1	1.5	157	1666PCR040		
E1	9.4	1.6	147	1666PCR049		
F1	9.1	1.7	238	1666PCR050		
G1	9.7	1.6	170	1666PCR051		
H1	9.1	1.1	178	1666PCR052		
A2	9.3	1.4	114	1666PCR053		
B2	8.6	0.8	157	1666PCR054		
C2	8.8	1.0	171	1666PCR055		
D2	8.5	1.3	145	1666PCR056		
E2	9.4	2.0	124	1666PCR057		
F2	8.6	1.9	145	1666PCR058		
G2	9.5	2.2	208	1666PCR059		
H2	9.5	2.0	159	1666PCR060		

B1

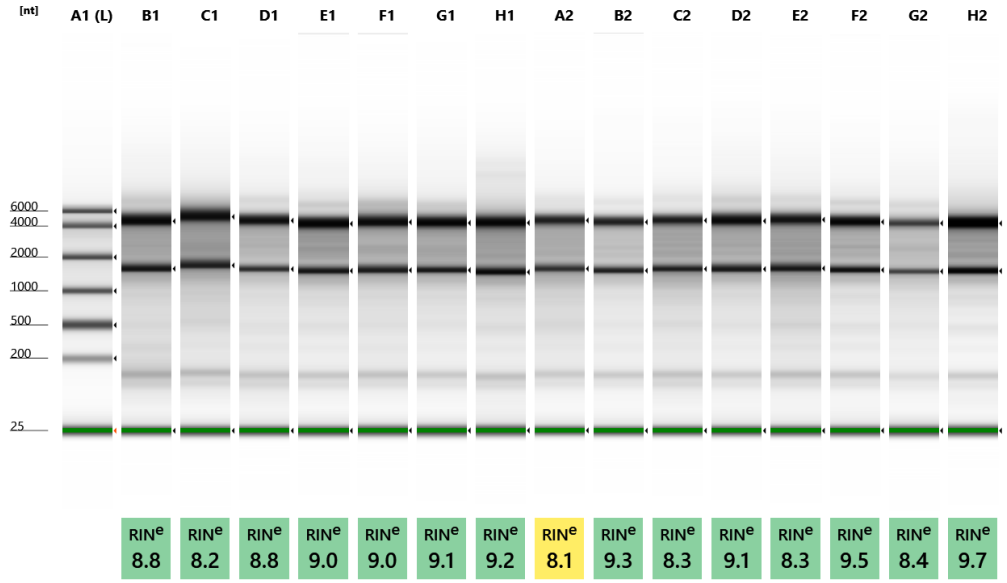

B2

Well	RINe	28S/18S (Area)	Conc. [ng/µl]	Sample Description	Alert	Observations
A1	-	-	124	Ladder		Ladder
B1	8.8	1.3	221	1666PCR033		
C1	8.2	1.3	202	1666PCR034		
D1	8.8	1.9	157	1666PCR021		
E1	9.0	1.8	183	1666PCR022		
F1	9.0	1.5	172	1666PCR035		
G1	9.1	1.8	161	1666PCR036		
H1	9.2	1.6	191	1666PCR041		
A2	8.1	1.1	168	1666PCR042		
B2	9.3	1.3	140	1666PCR043		
C2	8.3	1.0	172	1666PCR044		
D2	9.1	1.6	181	1666PCR045		
E2	8.3	1.0	191	1666PCR046		
F2	9.5	1.7	166	1666PCR047		
G2	8.4	1.2	108	1666PCR048		
H2	9.7	2.0	202	1666PCR019		

C1

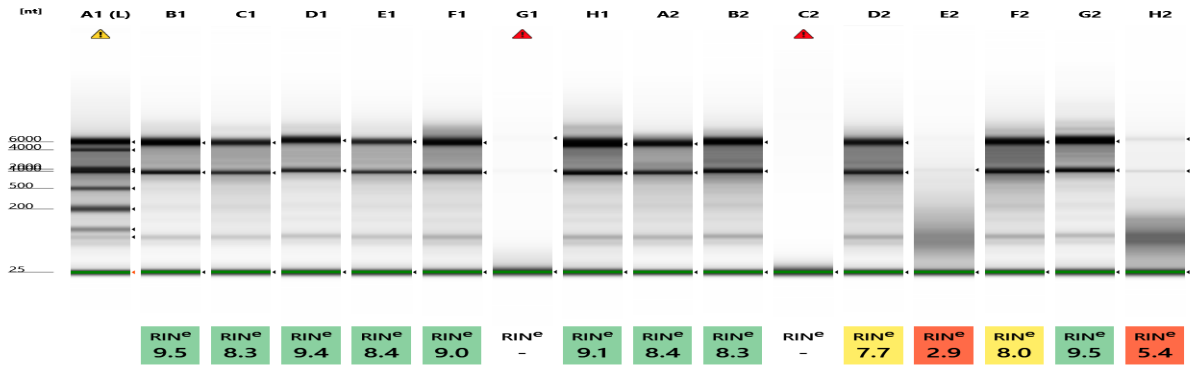

C2

Well	RINe	28S/18S (Area)	Conc. [ng/µl]	Sample Description	Alert	Observations
A1	-	-	288	Ladder	⚠	Issue with ladder peak detection (too many peaks detected); Ladder
B1	9.5	2.1	169	1666PCR018		
C1	8.3	1.5	143	1666PCR037		
D1	9.4	1.9	135	1666PCR038		
E1	8.4	1.5	122	1666PCR063		
F1	9.0	1.6	180	1666PCR064		
G1	-	-	8.40	1666PCR011	⚠	Sample concentration outside functional range for RINe and the assay
H1	9.1	1.9	206	1666PCR012		
A2	8.4	1.4	188	1666PCR025		
B2	8.3	1.3	229	1666PCR026		
C2	-	-	5.14	1666PCR027	⚠	Sample concentration outside functional range for RINe and the assay
D2	7.7	1.0	196	1666PCR028		
E2	2.9	-	89.4	1666PCR029		The upper ribosomal fragment has degraded
F2	8.0	1.1	222	1666PCR030		
G2	9.5	2.2	181	1666PCR031		
H2	5.4	1.1	93.4	1666PCR032		

D1

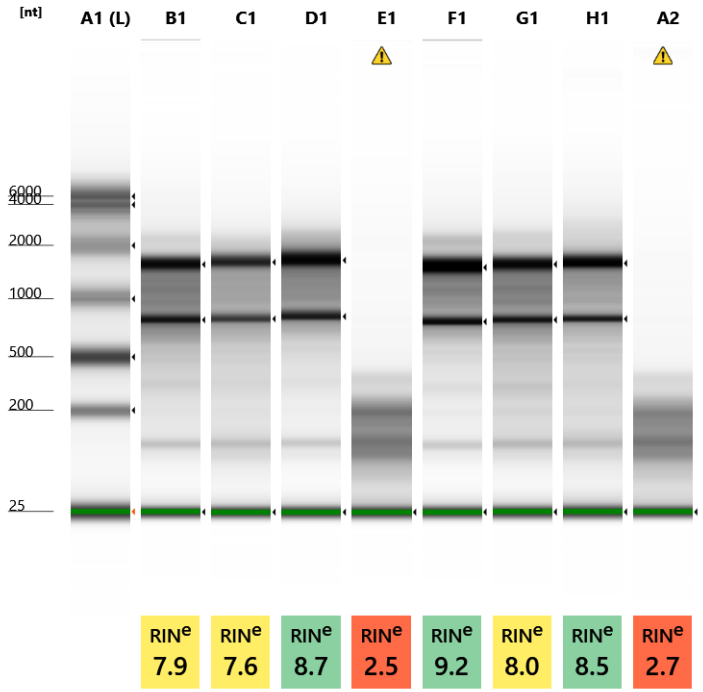

D2

Well	RINe	28S/18S (Area)	Conc. [ng/µl]	Sample Description	Alert	Observations
A1	-	-	119	Ladder		Ladder
B1	7.9	1.2	195	1666PCR061		
C1	7.6	1.3	150	1666PCR062		
D1	8.7	1.9	179	1666PCR065		
E1	2.5	-	90.5	1666PCR066	⚠	The lower ribosomal fragment is missing
F1	9.2	2.2	196	1666PCR067		
G1	8.0	1.4	186	1666PCR068		
H1	8.5	1.7	156	1666PCR071		
A2	2.7	-	88.1	1666PCR072	⚠	The lower ribosomal fragment is missing

Figure 3: RNA extraction QC. The concentration and purity of the total RNA were determined using a NanoDrop ND8000 spectrophotometer. Absolute Quantification of RNA was done on the Qubit 4.0 Fluorometer with the Qubit® RNA HS Assay Kit and the Agilent Tapestation. A-D show all results from all the inner and outer foreskin samples used. Colors: Green samples have high quality, yellow samples also good quality but RIN values fall below the software's default 8.3 cut-off. The orange and red samples are poor quality, which were not used but rather re-extracted for better quality samples.

									Reference Genes			
Annealing Temperature (°C)	**CHD1**	**Claudin 1**	**Claudin 2**	**Claudin 4**	**Claudin 5**	**FLG pimer set 1**	**FLG primer set 2**	**IVLF**	**GAPDH primer set 1**	**GAPDH primer set 2**	**TBP**	
55.3	21.70	22.12	28.61	22.69	28.45	16.78	19.68	21.65	19.14	17.96	27.31	
57.3	21.39	22.68	28.26	22.51	27.87	16.24	19.41	21.666	18.6	17.07	26.48	
59,3	21.69	22.835	28.35	22.66	28,4	16.3	19.45	21.73	18.63	17.41	26.78	
61,3	21.72	22.032	28.46	22.60	27,3	16.05	19.20	21.80	18.33	17.36	26.43	
63,3	22.02	21.88	29.09	22.80	27,5	17.73	19.71	20.93	19.95	17.32	26.20	
65,3	22.35	22.052	29.88	23.08	27,9	18.24	26.81	21.96	35.05	17.41	26.37	

Table 2 : Primer Ta optimization For each gene, the annealing temperature that resulted in the lowest CT value was selected as the optimal temp (highlighted in green).

Determination of optimal primer concentration

Varying amounts of the forward and reverse primer of 300, 500 and 800nM were mixed with 2µl pooled cDNA (pre-diluted 1:20), 5µL 2X PowerUp SYBR Green Mastermix (Thermo Fisher) in a total reaction volume of 10µL. Each primer concentration combination was analyzed in triplicate using the cycling parameters with the optimized annealing temperature mentioned above .

		Forward Primer (nM)					
		300		500		800	
Reverse Primer (nM)	300						
	500						
	800						

Table 3: Primer Concentration optimizations – test a range of concentrations for the forward primer against different concentrations of the reverse primer.

For each gene, the primer concentration combination that resulted in the lowest CT value was selected as the optimal primer concentration (summarized in the table below). Primer concentration combinations tested were 300nM, 500nM and 800nM for both forward (F) and reverse (R) primers (Table 5).

Primer Combination	Target Name	C_T Mean	C_T SD
500F, 300R	CDH1	20.8	0.053
500F, 500R	Claudin 2	27.3	0.136
800F, 800R	Claudin 4	21.9	0.046
500F, 500R	FLG1 (1)	16.3	0.074
300F, 500R	FLG2 (2)	17.2	0.145
800F, 500R	GAPDH (1)	16.7	0.092
800F, 500R	GAPDH (2)	16.3	0.018
300F, 500R	IVLF	20.5	0.101
300F, 500R	TBP	24.6	0.381

Table 4: Determination of optimal primer concentrations

Calculating qPCR primer Efficiencies using slopes of Standard Curves

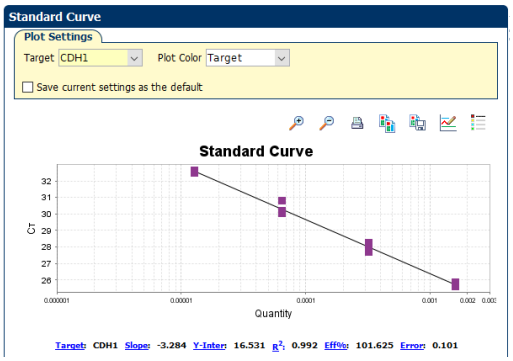

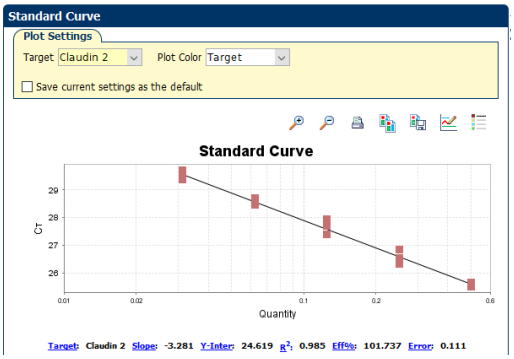

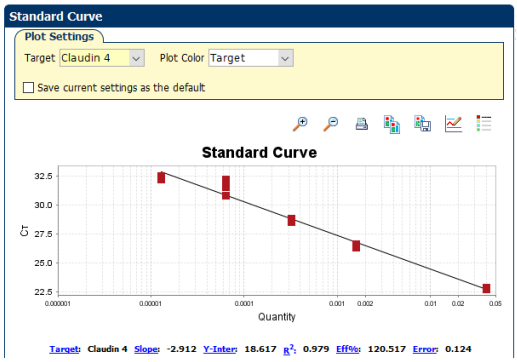

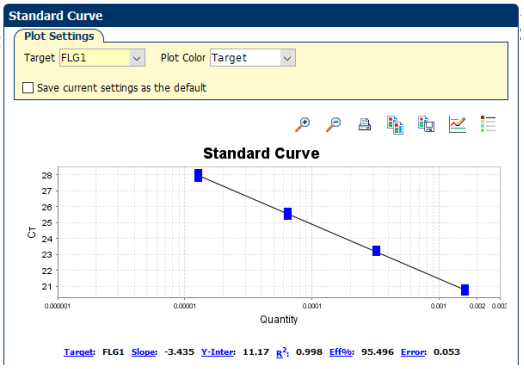

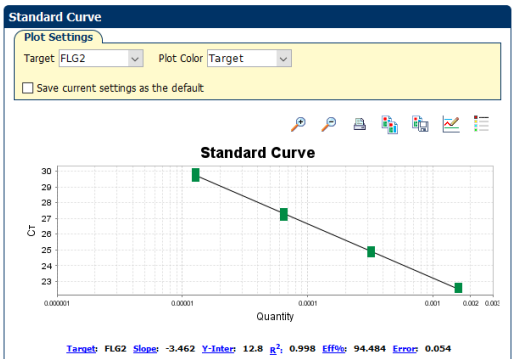

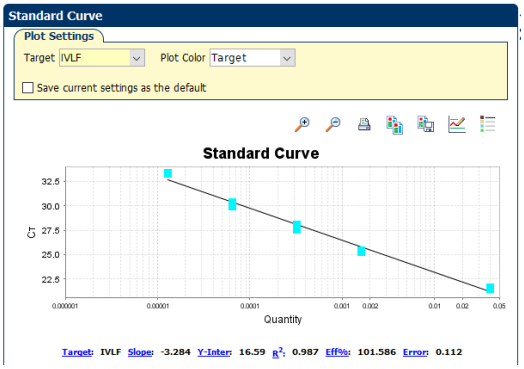

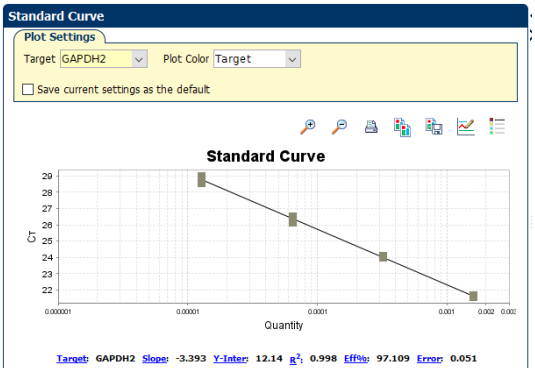

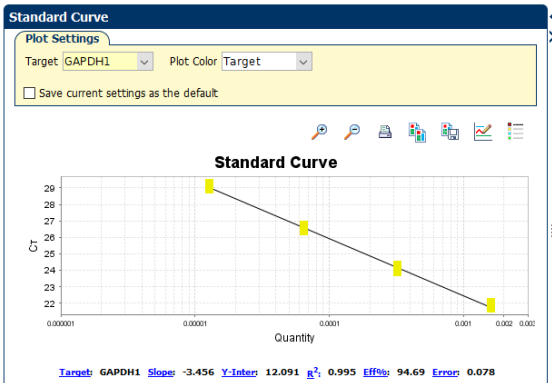

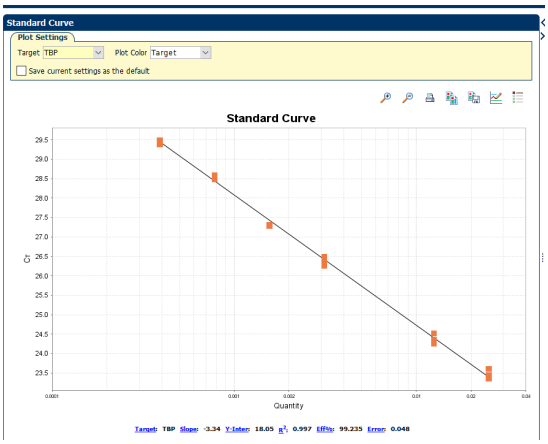

Figure 4: Individual standard curves (for each gene) used to assess qPCR primer efficiencies.

APPENDIX II

Table 1: List of antibodies used in immunophenotyping

Antibody Specificity	Fluorochrome	Catalog number	Company	Clone	Dilution(in 50µl)
CD45	BV786	563716	BD Biosciences	HI30	1.25µl
CD3	APC/Cy7	300426	Biolegend	UCHT1	1.25µl
CD4	AF700	344622	Biolegend	SK3	1.5µl
CD8a	BV570	301038	BD Biosciences	RPA-T8	1.25µl
Live/dead fixable Violet dead cell stain kit		L34955	Life Technologies		stock diluted at 1:40 then 1 µl to 49 µl

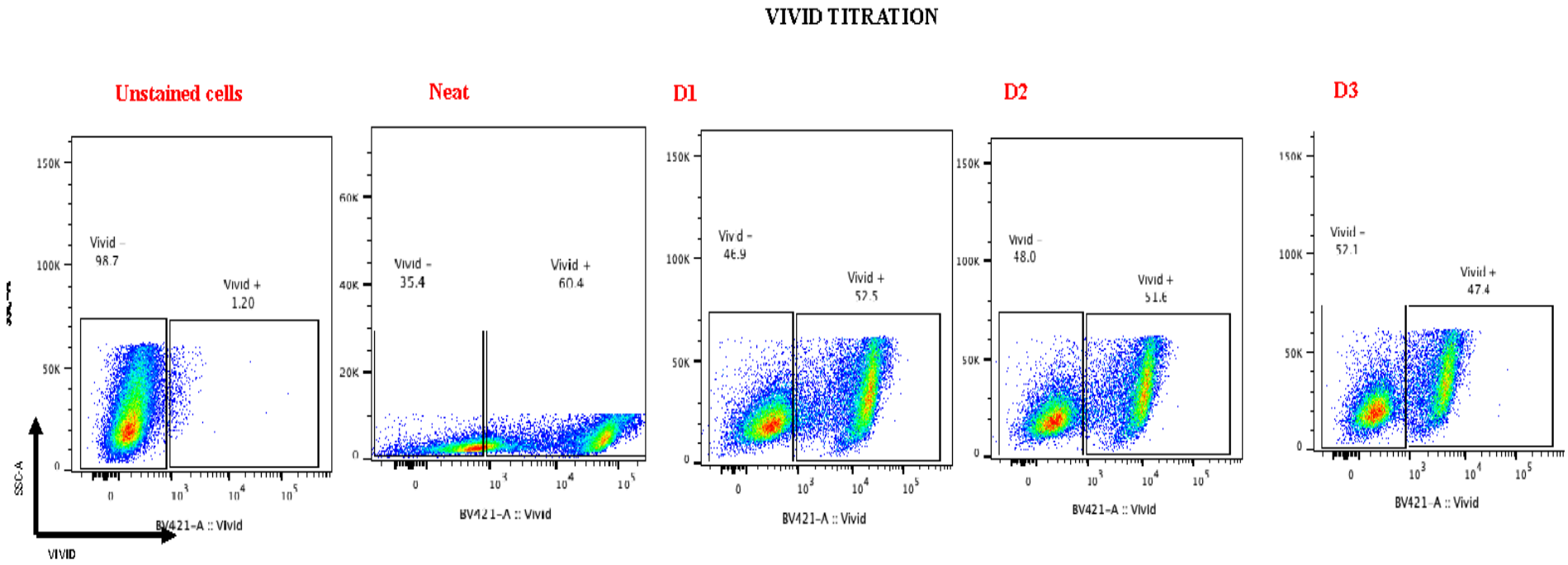

Figure 1.1 Vivid Titrations

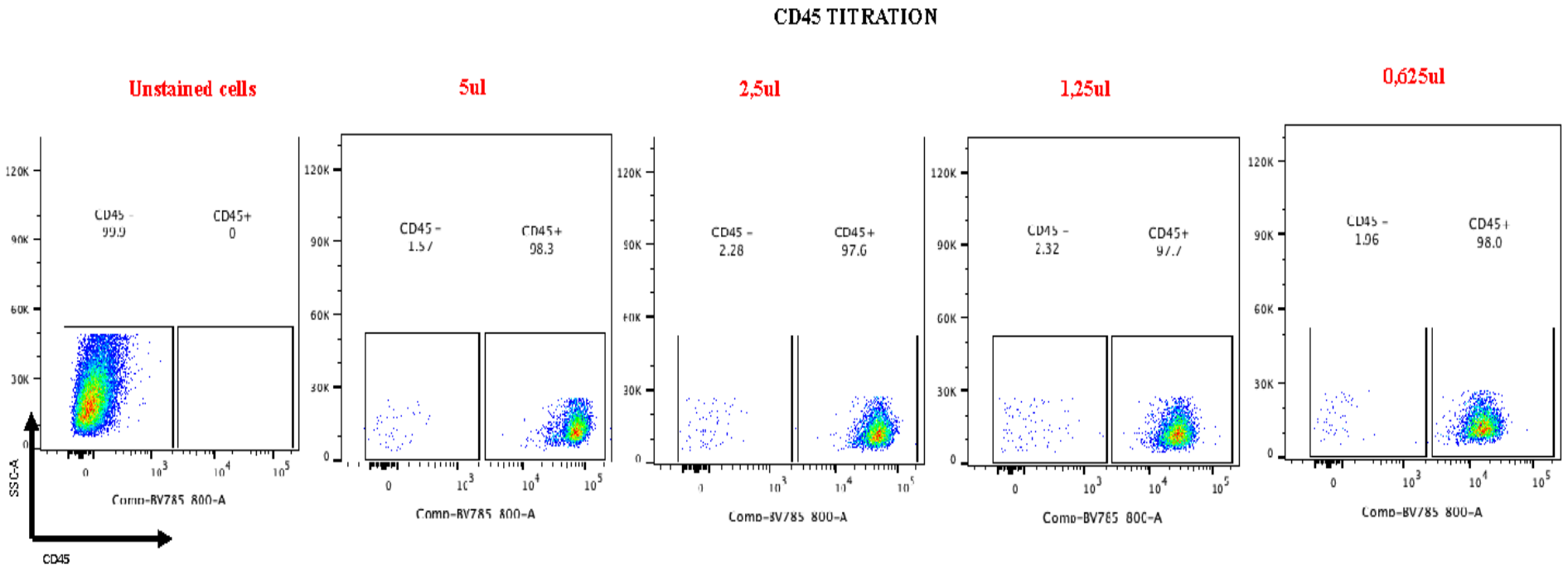

Figure 1.2 CD45 Titrations

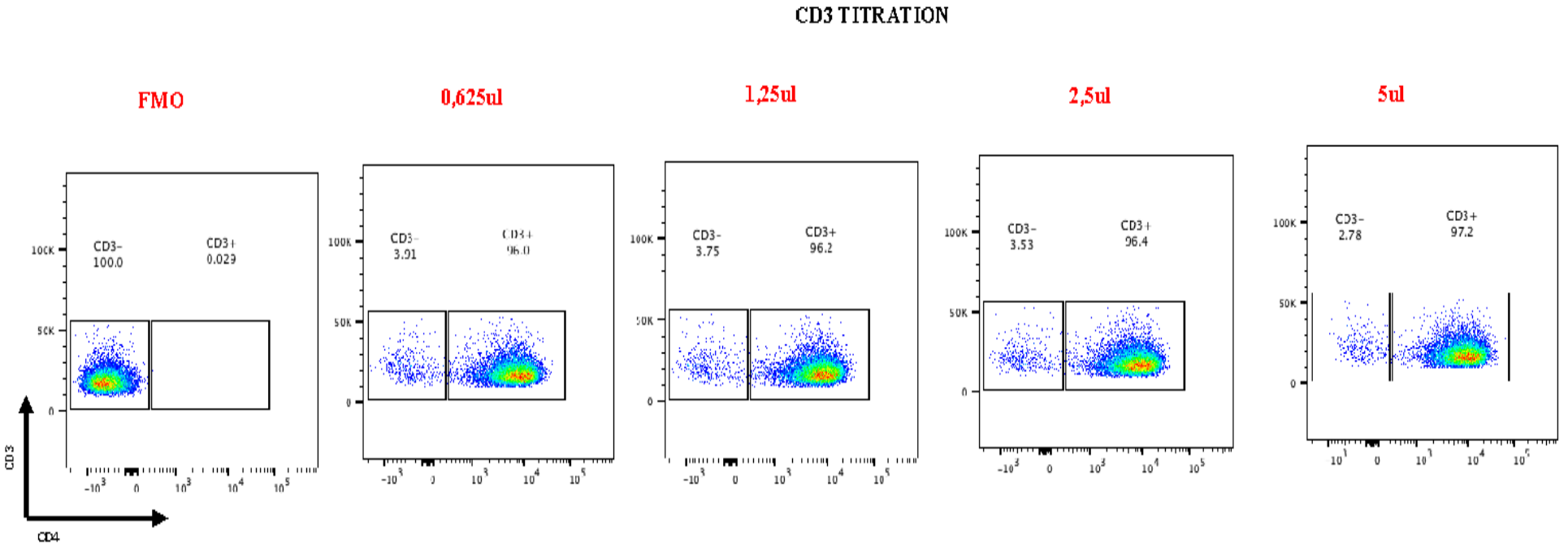

Figure 1.3 CD3 Titration

CD4 TITRATION

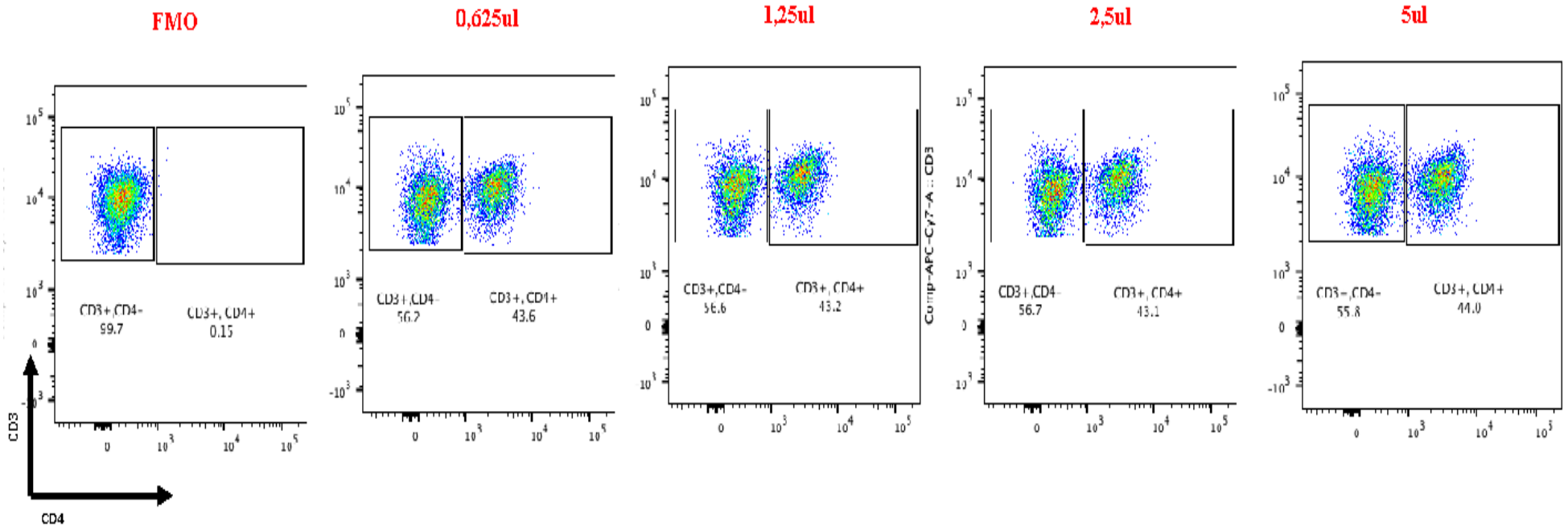

Figure 1.4 CD4 Titration

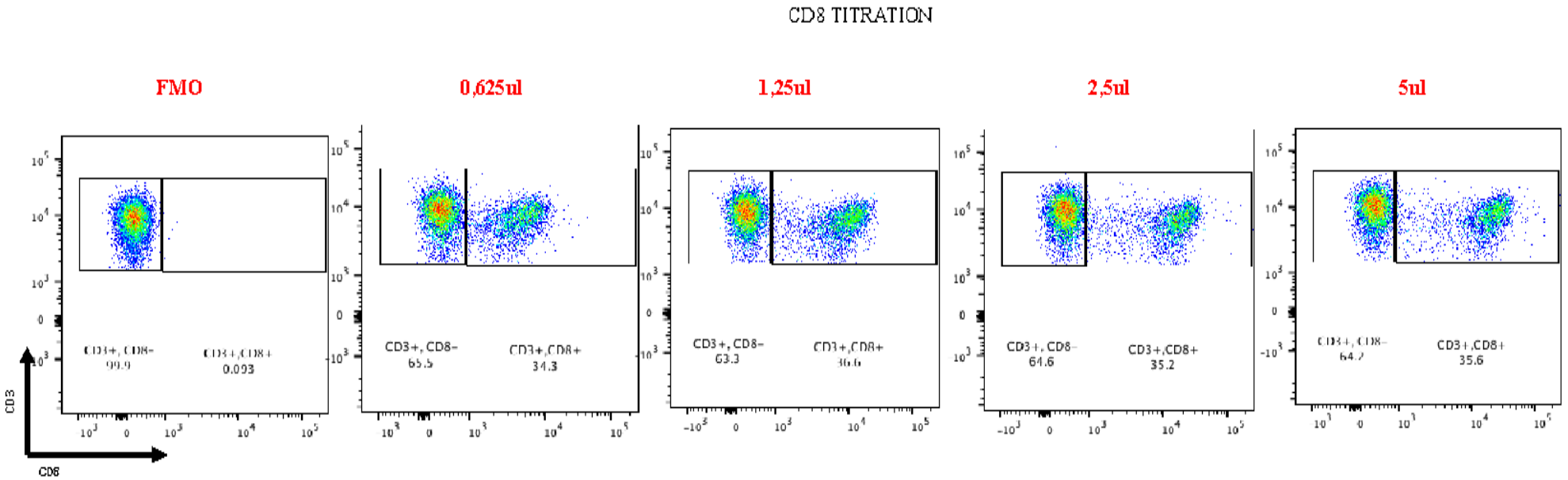

Figure 1.5 CD8 Titration

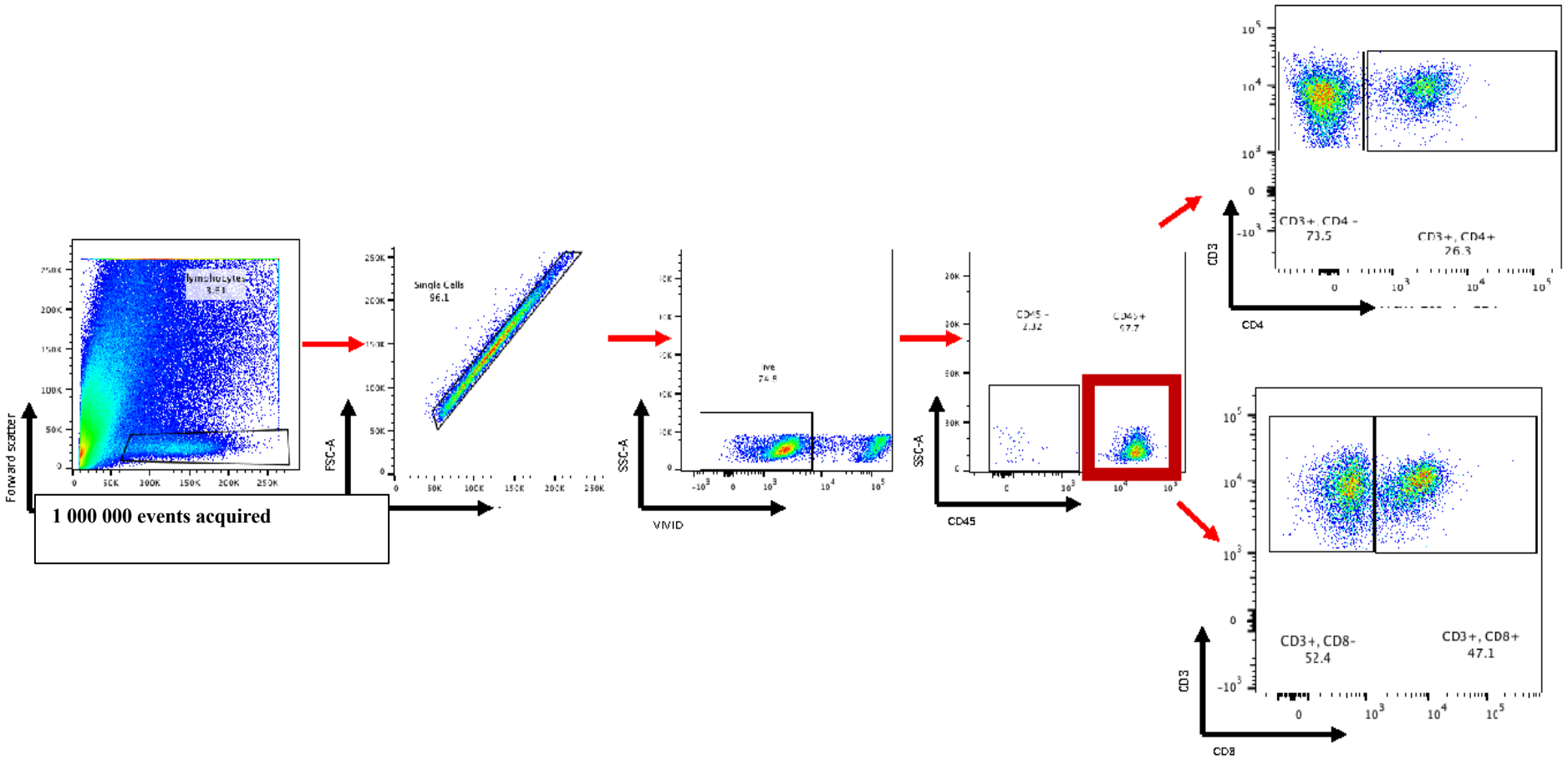

Figure 2 : Gating Strategy

APPENDIX III

Antibody titrations

The protocol GeoMx used in this study was optimized using a different tissue, we still conducted optimization experiments for the key steps for using foreskin tissue samples shown below:

- placed the slides overnight in the incubator at 37C prior to baking
- Bake the slides for 4 hrs instead of 3hrs in the incubator at 60C.This improved in that less tissue fell off on the slides
- Changed slides to apex adhesive slides(Leica)-recommended by nanostring. This improved tissue adherence following baking, however, after the retrieval step for 20 minutes, tissue loss still occurred
- For the target retrieval step, the protocol had various recommendations for various tissues. We trialed boiling for 5, 15 and 20 minutes, and the 5 minutes retravel time resulted in all tissues. The best outcome was 5 minutes.
- This 5-minute antigen retrieval time was then validated to ensure it did not dampen the morphology marker staining.
- Morphology markers: CD68and PanCK were titrated as follows and the final optimsed markers were for CD68 and for PanCK,

Antibody	Titre 1	Titre 2	Titre 3	Titre 4
CD68 [200ug/ml]	**1.25ul**	2.5ul	5.5ul	7ul
PanCK []	1,25ul	**2.5ul**	5.5ul	7ul

Table 1 antibody titrations

https://drive.google.com/drive/folders/1qwvzKtmpTXx-

SNWEGEIe7ICGmiHWDwmv?usp=drive_link

Table 2: DEGs in CD68+Cells (Inner and Outer Foreskin)

Table 3: Enriched Pathways in CD68+ Cells inner foreskin

Table 4: Enriched Pathways in CD68+ Cells Outer foreskin

Table 5: DEGs in PanCK+Cells (Inner and Outer Foreskin)

Table 6: Enriched Pathways in PanCK+ Cells inner foreskin

Table 7: Enriched Pathways in PanCK+ Cells Outer foreskin

APPENDIX IV

Supplementary Figure 1: Consort flow chart showing the number of participants screened and how many were analysed in each of the 8 treatment arms versus the control arm (no PrEP).

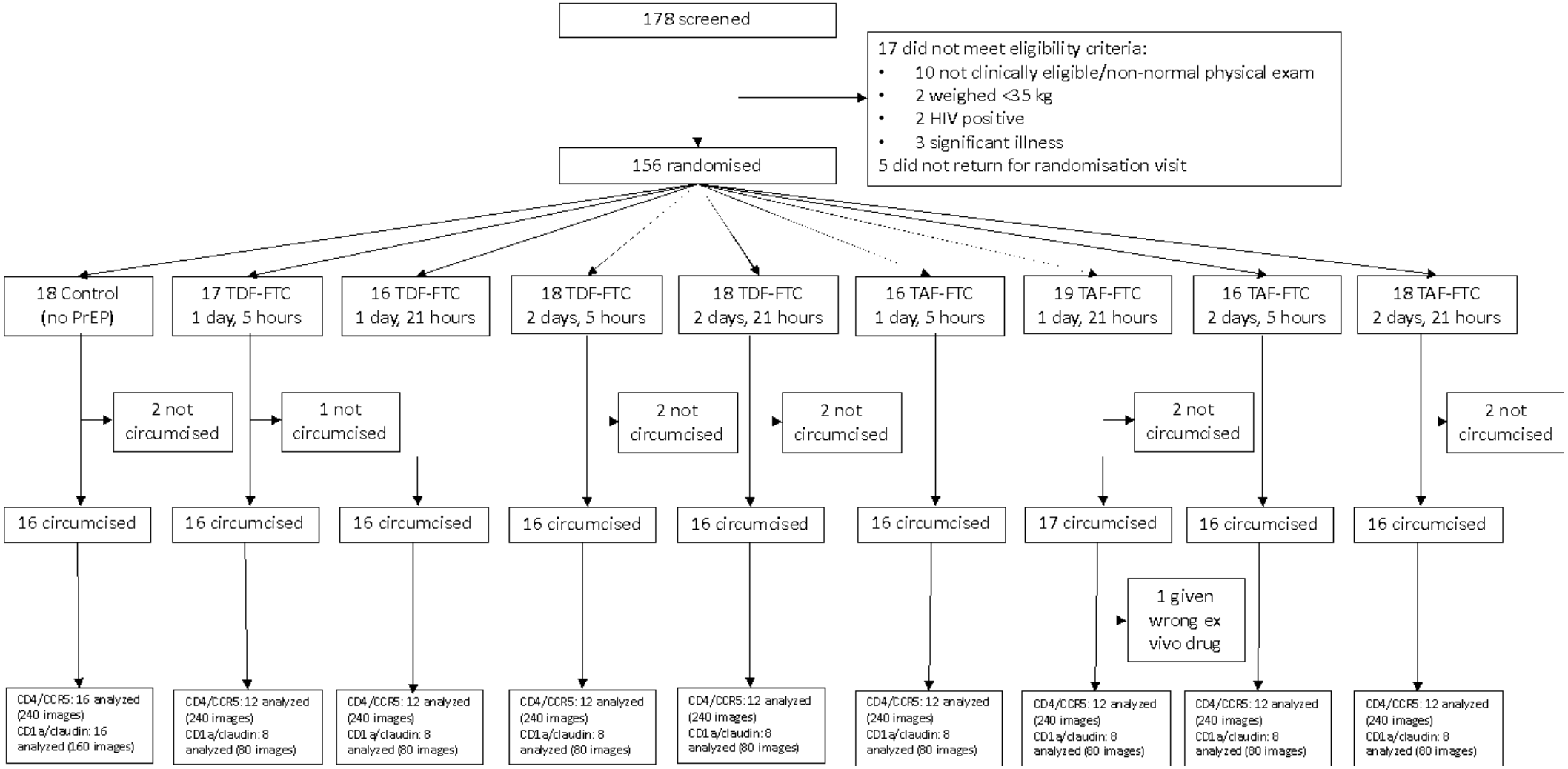
178 screened
17 did not meet eligibility criteria:
• 10 not clinically eligible/non-normal physical exam
• 2 weighed <3.5 kg
• 2 HIV positive
• 3 significant illness
5 did not return for randomisation visit
156 randomised
18 Control (no PrEP)
17 TDF-FTC 1 day, 5 hours
16 TDF-FTC 1 day, 21 hours
18 TDF-FTC 2 days, 5 hours
18 TDF-FTC 2 days, 21 hours
16 TAF-FTC 1 day, 5 hours
19 TAF-FTC 1 day, 21 hours
16 TAF-FTC 2 days, 5 hours
18 TAF-FTC 2 days, 21 hours
2 not circumcised
1 not circumcised
2 not circumcised
2 not circumcised
2 not circumcised
2 not circumcised
16 circumcised
16 circumcised
16 circumcised
16 circumcised
16 circumcised
16 circumcised
17 circumcised
16 circumcised
16 circumcised
1 given wrong ex vivo drug
CD4/CCR5: 16 analyzed (240 images) CD1a/claudin: 16 analyzed (160 images)
CD4/CCR5: 12 analyzed (240 images) CD1a/claudin: 8 analyzed (80 images)
CD4/CCR5: 12 analyzed (240 images) CD1a/claudin: 8 analyzed (80 images)
CD4/CCR5: 12 analyzed (240 images) CD1a/claudin: 8 analyzed (80 images)
CD4/CCR5: 12 analyzed (240 images) CD1a/claudin: 8 analyzed (80 images)
CD4/CCR5: 12 analyzed (240 images) CD1a/claudin: 8 analyzed (80 images)
CD4/CCR5: 12 analyzed (240 images) CD1a/claudin: 8 analyzed (80 images)
CD4/CCR5: 12 analyzed (240 images) CD1a/claudin: 8 analyzed (80 images)
CD4/CCR5: 12 analyzed (240 images) CD1a/claudin: 8 analyzed (80 images)

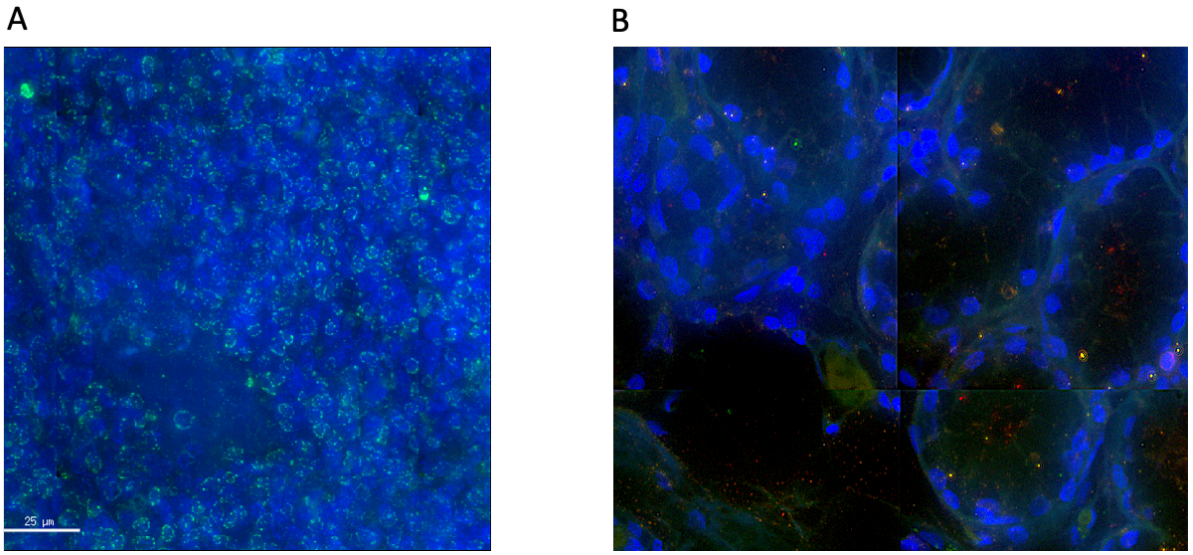

Supplementary Figure 2. CCR5 positive and negative controls stainings: A) Shows tonsillar tissue stained by with CCR5 antibody (green) and B) illustrated CCR5 staining of human renal tissue, which did not stain with the CCR5 antibody , both show nuclei staining in blue .

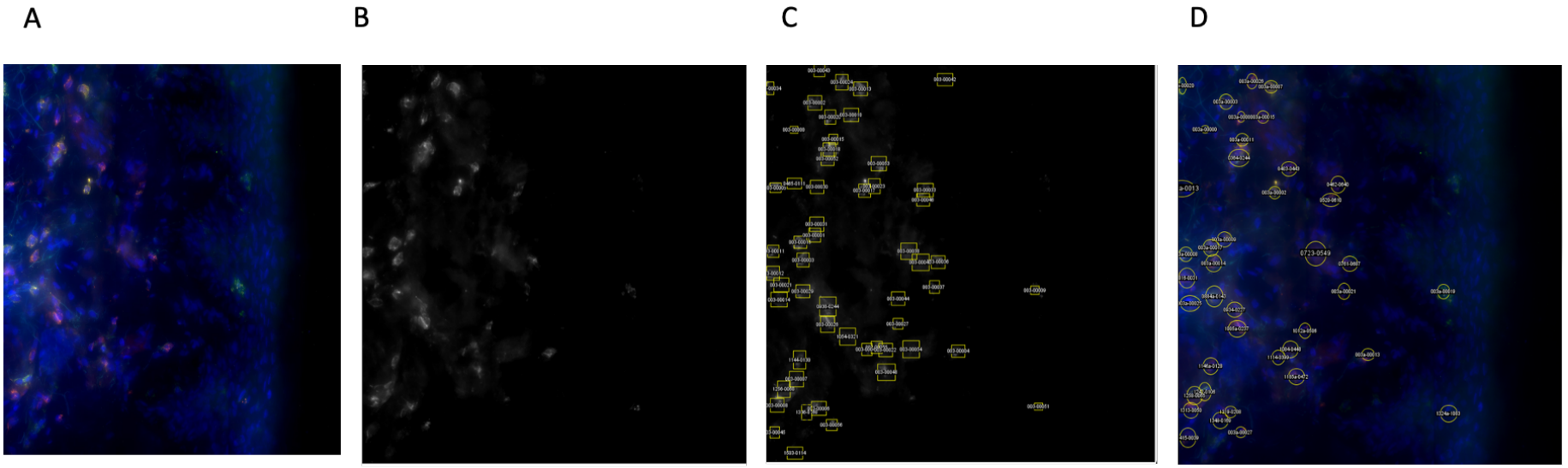

Supplementary Figure 3. quantification of immune cells. (A) acquired image with single(green or red) and double positive cells9(yellow),(B) ImageJ split images by channels, shown is the red channel –CD4 on the split grey scale,(C) automated quantification of CD4 cells on grayscale by pipsqueak software and finally, (D) quantified CD4 cells superimposed on the original color image. These are used to objectively quantify each marker.

		CD4		CCR5		CD4+CCR5		Distance from epidermis		Percent CCR5 on CD4	
Reference group	**Comparator group**	**Geometric mean ratio (95% CI)**	**p-value**	**Geometric mean ratio (95% CI)**	**p-value**	**Geometric mean ratio (95% CI)**	**p-value**	**Geometric mean ratio (95% CI)**	**p-value**	**Mean difference (95% CI)**	**p-value**
Effect of any PrEP versus no PrEP											
Control arm	Any PrEP	0.92 (0.73, 1.18)	0.53	0.91 (0.70, 1.17)	0.44	0.84 (0.50, 1.41)	0.51	1.04 (0.92, 1.18)	0.51	-2.9 (-10.6, 4.8)	0.46
Overall effects of drug, dosage and interval											
F/TDF (all)	F/TAF (all)	0.93 (0.77, 1.12)	0.45	0.91 (0.75, 1.10)	0.33	0.82 (0.55, 1.22)	0.33	0.95 (0.87, 1.03)	0.20	-2.1 (-7.8, 3.6)	0.46
2 tabs (both drugs)	2+1 tabs (both drugs)	0.91 (0.76, 1.10)	0.35	0.89 (0.73, 1.08)	0.23	0.80 (0.54, 1.19)	0.28	1.02 (0.94, 1.11)	0.58	0.7 (-5.0, 6.4)	0.81
5 hours (all regimens)	21 hours (all regimens)	1.06 (0.88, 1.28)	0.53	1.05 (0.86, 1.27)	0.64	1.09 (0.74, 1.63)	0.66	0.95 (0.87, 1.03)	0.20	0.1 (-5.6, 5.8)	0.97
Effects of dosage, separately for each drug											
F/TDF, 2 tabs	F/TDF, 2+1 tabs	0.94 (0.72, 1.21)	0.61	0.94 (0.71, 1.23)	0.64	0.92 (0.55, 1.53)	0.75	1.01 (0.91, 1.13)	0.81	3.7 (-4.8, 12.2)	0.39
F/TAF, 2 tabs	F/TAF, 2+1 tabs	0.90 (0.68, 1.19)	0.44	0.84 (0.64, 1.11)	0.23	0.71 (0.38, 1.30)	0.26	1.04 (0.91, 1.18)	0.60	-2.3 (-10.0, 5.4)	0.56
Effects of interval, separately for each drug and dosage											
F/TDF, 2 tabs (5h)	F/TDF, 2 tabs (21h)	0.85 (0.59, 1.24)	0.40	0.87 (0.58, 1.31)	0.51	0.82 (0.40, 1.68)	0.60	1.07 (0.92, 1.24)	0.37	-0.8 (-12.0, 10.3)	0.89
F/TDF, 2+1 tabs (5h)	F/TDF, 2+1 tabs (5h)	1.12 (0.79, 1.60)	0.53	1.12 (0.76, 1.65)	0.56	1.35 (0.64, 2.86)	0.43	0.88 (0.76, 1.01)	0.08	5.1 (-8.0, 18.2)	0.45
F/TAF, 2 tabs (5h)	F/TAF, 2 tabs (21h)	1.31 (0.83, 2.07)	0.24	1.13 (0.72, 1.78)	0.59	1.20 (0.52, 2.75)	0.67	0.84 (0.68, 1.03)	0.10	-2.7 (-14.2, 8.9)	0.65
F/TAF, 2+1 tabs (5h)	F/TAF, 2+1 tabs (21h)	1.02 (0.73, 1.43)	0.89	1.09 (0.78, 1.52)	0.61	1.07 (0.43, 2.69)	0.88	1.02 (0.86, 1.20)	0.84	-1.3 (-12.0, 9.3)	0.81

Supplementary Table 1.Comparisons between trial arms, all samples combined, both countries. Results from mixed effects models (each image measurement is included in the model and clustering of measurements within each participant is accounted for by including a random effect). Geometric mean ratios are shown for all outcomes apart from percent CCR5 on CD4, as they were skewed.

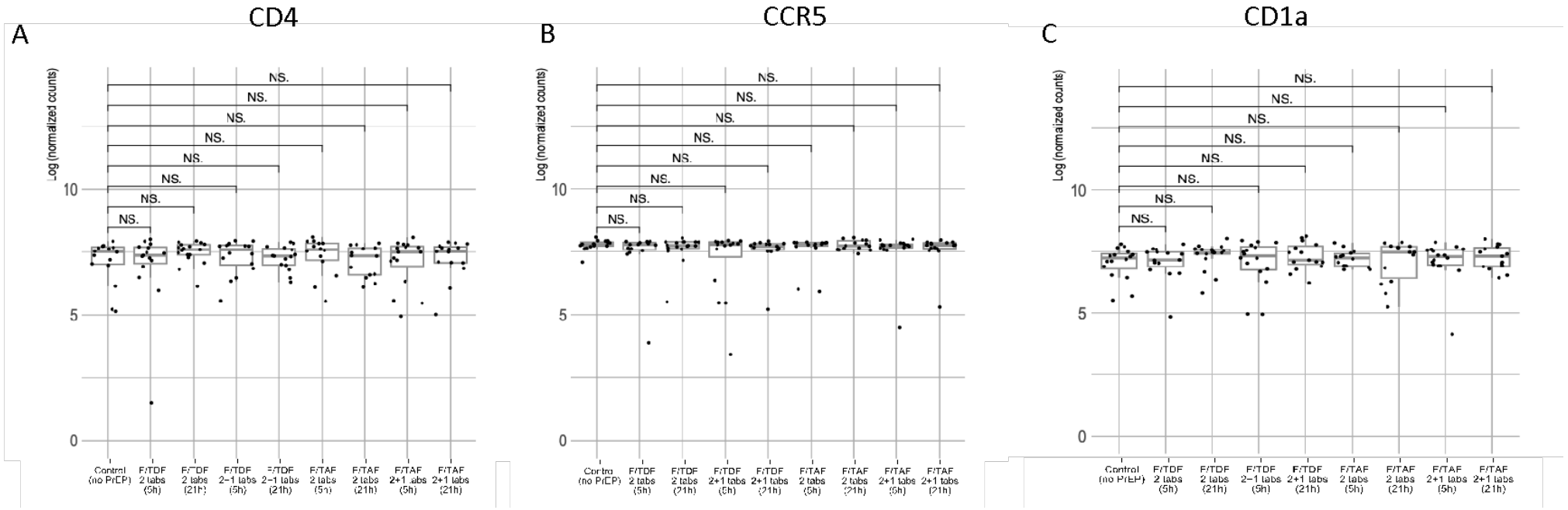

Supplementary Figure 4

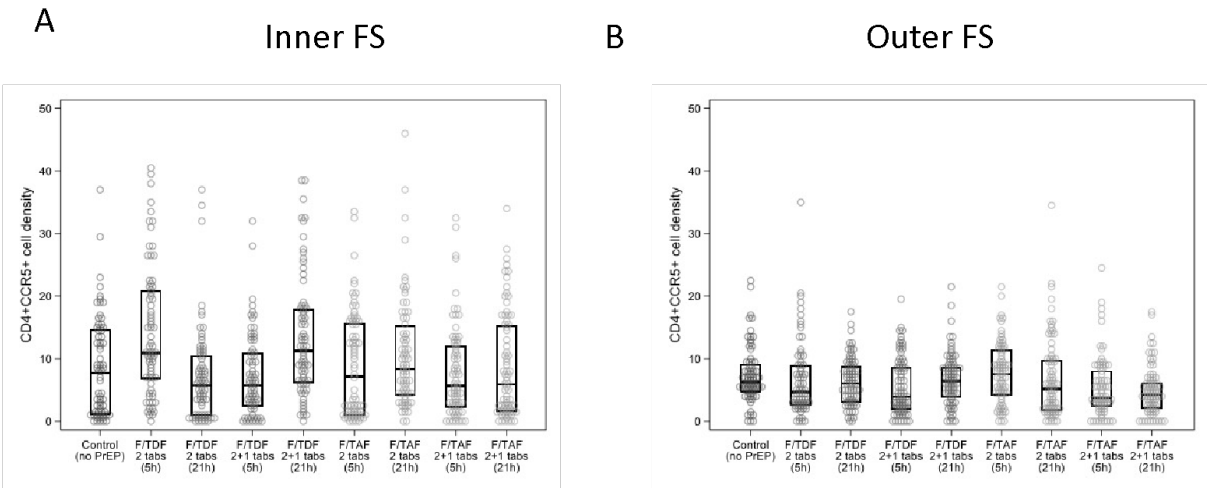

Supplementary Figure 5. Density of CD4+CCR5+ in the inner and outer foreskins (FS) (A) Combined density of CD4+CCR5+ cells in FS across the different trial arms in the inner FS from the SA site; (B) Combined density of CD4+CCR5+ cells in foreskins across the different trial arms in the outer FS from the SA site.

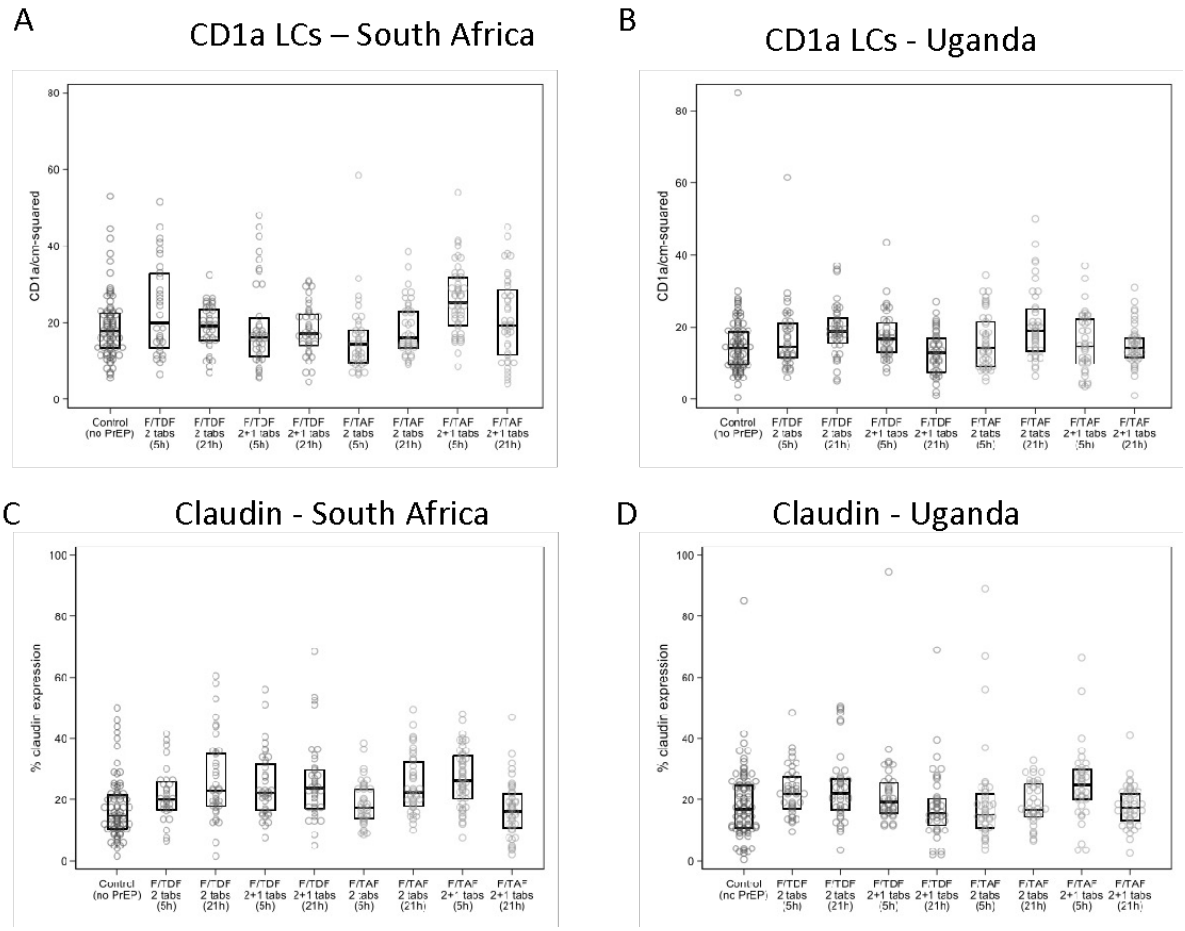

Supplementary Figure 6: Density of CD1a and claudin 1 expression in foreskins across treatment arms from two CHAPS sites in Africa. (A) Density of CD1a (cells/cm2) in foreskins across treatment arms from South Africa participants (n=40); (B) Density of CD1a (cells/cm2) in foreskins across treatment arms from Uganda participants (n=40); (C) Percent expression of claudin-1 in foreskin tissue across treatment arms from South Africa participants (n=40); (D) Percent expression of claudin-1 in foreskin tissue across treatment arms from Uganda participants (n=40).

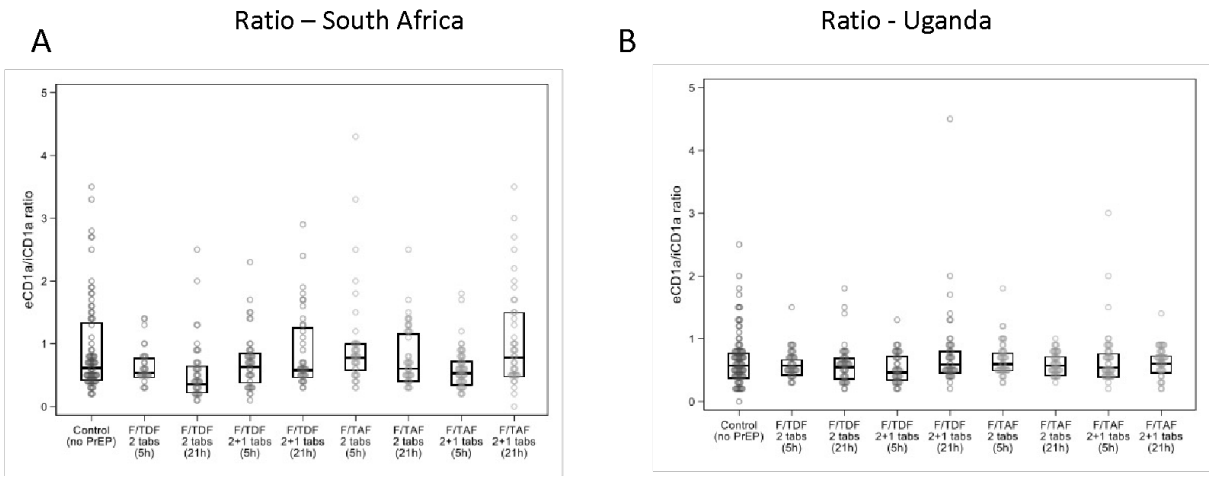

Supplementary Figure 7: Ratio of eCD1a/iCD1a Langerhans cells in the foreskin (FS) from South Africa and Uganda participants. (A) Ratio's of CD1a/claudin across different treatment arms in participants from South Africa (n=40); (B) Ratio's of CD1a/claudin across different treatment arms in participants from Uganda (n=40).